Cosmological and Astrophysical Probes of Physics Beyond the Standard Model

by

Subir Sabharwal

A Dissertation Presented in Partial Fulfillment
of the Requirement for the Degree
Doctor of Philosophy

Approved May 2015 by the
Graduate Supervisory Committee:

Lawrence Maxwell Krauss, Co-Chair
Tanmay Vachaspati, Co-Chair
Philip Daniel Mauskopf
Cecilia Lunardini

ARIZONA STATE UNIVERSITY

August 2015

ABSTRACT

Cosmology, carrying imprints from the entire history of the universe, has emerged as a precise observational science over the past 30 years. It can probe physics beyond the Standard Model at energy scales much higher than the weak scale. This thesis reports on some important probes of beyond standard model physics derived in a cosmological setting - (I) It is shown that primordial gravitational waves left over from inflation carry unique detectable CMB signatures for neutrino masses, axions and any other relativistic species that may have been present. (II) Higgs Inflation, the most popular and compelling inflation model with a higgs boson is studied next and it is shown that quantum effects have so far been incorrectly incorporated. A spurious gauge ambiguity arising from quantum effects enters the canonical prediction for observables in Higgs Inflation that must be addressed. (III) A new novel mechanism for generating the observed baryon asymmetry of the universe via decaying gravitinos is proposed. If the Supersymmetry (SUSY) breaking scale is high, then in the presence of R-parity violation, gravitinos can successfully reproduce the baryon asymmetry and evade all low energy constraints. (IV) The final chapter reports on a new completely general analysis of simplified models used in direct detection of dark matter. This is useful to explore what high energy physics constraints can be obtained from direct detection experiments.

To my parents, Manju & Sudhir

ACKNOWLEDGEMENTS

TABLE OF CONTENTS

LIST OF TABLES

LIST OF FIGURES

Chapter 1

INTRODUCTION

The Standard Model of particle physics is a remarkable theory and one of the towering and most significant scientific achievements of the 20th century. It is a precise quantum mechanical theory of the fundamental particles that make up all matter and the interactions among them. The existence of these particles and interactions have been verified to a high degree of accuracy. The last important piece, the Higgs Boson, a particle which gives mass to all the other particles in the standard model (including itself) and which eluded detection for many decades was recently discovered, effectively closing the chapter on the validity of this theory.

However, this wonderful theory isn't complete. The most glaring inadequacy of the standard model is the absence of a description of gravity. Einstein's General Relativity (GR) is a classical field theory of gravity, described by the warping of the spacetime metric as a function of matter energy-momentum. It provides a description of gravity at the macroscopic scale, however the microphysical laws of gravity still elude us. It is hoped that a microphysical theory of gravity would provide resolutions to the singularity puzzles of the big bang and black holes.

Besides the exclusion of gravity, there are other cosmological and experimental observations that can't be explained by the contents of the standard model alone. Over the past 30 years, cosmological observations have given us a detailed picture of the contents of the universe. This is shown schematically in Fig. (1.1). Only 4.1% of the matter-energy budget of the universe today is made up of ordinary baryonic

matter, that is described by the Standard Model. Most (95.1%) of the universe isn't in the form of matter described by the standard model. Since Dark Matter redshifts just like ordinary matter (a^{-3}), it is expected that it is a new kind of particle, that interacts perhaps very weakly (if at all, besides gravitationally) with the standard model particles. Dark Energy, on the other hand is best modeled by a cosmological constant (vacuum energy) in Einstein's equations which causes repulsive gravity. However, its value isn't explained by the standard model, which predicts a vacuum energy which is off from the cosmological observations by $\mathcal{O}(10^{120})$!
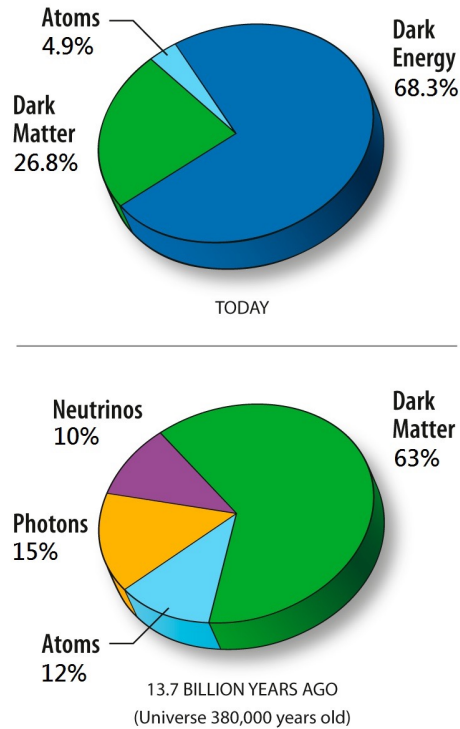
Figure 1.1: Matter-Energy content of the Universe as determined by the Planck satellite.

Cosmological parameters like the energy budget of the universe are measured by observations of the Cosmic Microwave Background (CMB) radiation, which is the remnant afterglow of the Big Bang. The radiation has a predicted blackbody spectrum and this was verified by NASA's COBE satellite in 1992. The imprints of

fundamental physics are most readily captured by studying the anisotropies in the CMB, shown in Fig (1.2). Planck's observations show an incredibly smooth universe with small anisotropies, the temperature fluctuating only $\mathcal{O}(10^{-5})$K from the mean, $T_{CMB} = 2.725$K across the sky.
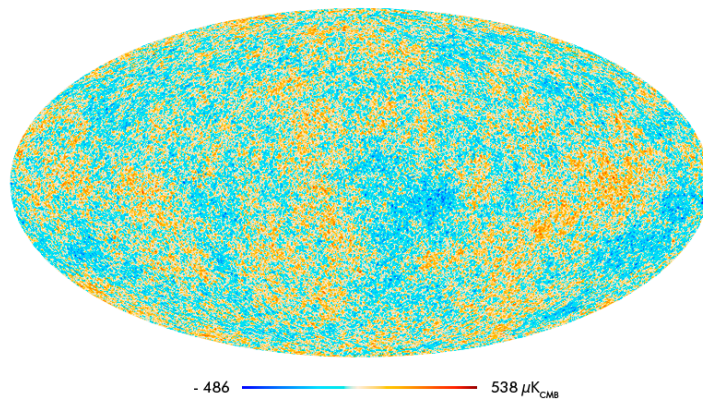
Figure 1.2: Anisotropies in the CMB radiation, measured by the Planck satellite.

An important feature of the anisotropic sky is the extreme homogeneity and isotropy of the universe. Why did the Universe start in a state that is so isotropic and homogenous? The Standard Model doesn't make any prediction to explain this observation. Whats even more troubling is there are superhorizon correlations in the CMB, that is, correlations which are larger than the horizon scale at photon decoupling. These parts of the sky never had a chance to communicate in the evolution of the universe up to that point. How could perturbations on patches of which were causally disconnected be correlated? Inflation provides a possible explanation. It introduces the possibility that the universe went through a phase of exponential expansion just after the big bang. This tearing of space smoothed out a small patch, which was initially causally connected that grew to be our observable universe. The repulsive gravity needed to cause this expansion involves beyond standard model physics.

An important prediction of inflation is the existence of primordial tensor perturbations or gravity waves. An inflating universe excites (via quantum fluctuations) all possible modes of the metric. The scalar mode is the density fluctuation (hot and cold patches in the CMB), which provides the primordial seeds for structure. They also fix the amplitude of quantum fluctuations. The excited tensor perturbations, imprint themselves as curl-like patterns on the CMB and they instead determine the energy scale of inflation. Because we expect that inflation happened at a relatively high scale, the CMB can potentially give us information about physics at energy scales much larger than those probed by typical astrophysical processes and particle accelerators. Moreover, as these gravitational waves travel, they are damped (or amplified) by other decoupled species like photons, neutrinos etc. Thus, studying their impact on the CMB can potentially give us valuable information about additional neutrino species or axions.

Another shortcoming of the standard model which manifests itself only in the cosmological context is the baryon asymmetry of the universe. The universe has more particles than anti-particles. The strongest evidence comes from big bang nucleosynthesis (BBN) - a highly successful theory that correctly predicts the abundance of light elements like ^2H, ^3H, ^3He, ^4He, ^6Li, ^7Li and ^7Be. However, the calculation requires the essential input of baryon asymmetry, $(n_B - n_{\bar{B}})/n_\gamma \sim \mathcal{O}(10^{-10})$ where n_γ is the number of photons. The Standard Model does indeed predict that the universe should be baryon asymmetric but its predicted asymmetry is smaller than that required by BBN. To explain this asymmetry, we again need some physics beyond the standard model.

In the past couple of decades then, cosmological observations have emerged as the most important probe for investigating physics beyond the standard model. The CMB can tell us about the physics of inflation and via primordial tensors provide us with valuable information about physics at energy scales higher than the weak scale (which is the highest scale to which the standard model has yet been tested). The statistical features of the CMB are also sensitive to the specifics of inflation. From BBN constraints on baryon asymmetry, we can infer the amount of CP violation and baryon number violation that must exist in the universe. Finally, the presence of dark matter definitively tells us that there must be particle species beyond the standard model.

This thesis investigates, in detail, cosmological probes of beyond standard model physics, specifically focusing on primordial tensor perturbations, baryon asymmetry and discernibility of dark matter models via direct detection. A brief outline of this thesis is as follows. The propagation of tensor perturbations in the presence of new particles, not present in the standard model is studied in Ch 2. We take a careful look at the classical and quantum predictions of the most well motivated inflation model, Higgs Inflation in Ch 3. Supersymmetry (SUSY) being the most important prevailing beyond standard model theory that provides viable dark matter candidates, coupling constant unification and keeps the higgs mass light (weak scale). With LHC searches for SUSY currently underway, cosmology can provide an alternative probe into the nature of SUSY interactions. It is shown in Ch 4 that SUSY with R-parity violation, and high scale SUSY breaking can successfully create the observed baryon asymmetry of the universe and avoid any serious observational constraints. Direct detection of Dark Matter is an active area of observational research in astroparticle physics, with number of experiments currently underway and more coming online in

the future. Ch 5 investigates what could be learned about underlying microphysical interactions of dark matter, were a detection be made. This study is based on the recently developed non-relativistic effective theory of dark matter direct detection. A new catalog of nuclear detector responses directly arising from a general set of fundamental dark matter interactions is derived and presented.

Chapter 2

COSMOLOGICAL DAMPING OF PRIMORDIAL TENSORS

2.1   Introduction

A generic prediction of cosmological perturbation theory in an inflating background of the early universe [2, 3, 4] is the production of gravitational waves (GW) with a nearly flat spectrum [5, 6]. There are ongoing observational efforts to detect such a spectrum [7, 8]. The dominant signature in the near term involves the effect that long-wavelength gravitational waves can have on the cosmic microwave background (CMB) through the generation of B-mode polarization (*e.g.*, [9, 10, 11, 12, 13, 14, 15]). The amplitude of the gravitational waves can be related to the energy scale at which inflation occurred, and the ratio of the power spectrum of gravitational waves to that of the scalar power spectrum, also known as the "tensor-to-scalar ratio", r, can give vital information into the nature of the inflaton – the field which drives inflation – via the Lyth bound [16, 17]. Additionally, primordial gravitational wave spectra produced by various non-inflationary mechanisms have been suggested [18, 19, 20, 21]. Therefore any observation of a primordial gravitational wave spectrum would be an immensely powerful tool in the study of the very early universe.

A question naturally arises - are there any effects that can intervene and alter the nature of the GW spectrum from the time of its production until the time of observation? If the answer is yes, then one must account for such effects in order to accurately describe the primordial spectrum. As is well known, just such an intervening effect does arise due to the fact that an anisotropic stress from free streaming particles can

7

damp the amplitude of GWs from their primordial value. Weinberg showed in [22] that the damping effect of free-streaming neutrinos on the GW spectrum can be quite significant with up to 35.6% loss in amplitude, and following this work, the issue has been the subject of some attention [23, 24, 25, 26, 27, 28, 29, 30, 31, 32, 33].

The original study of Weinberg, and much of the following work has been focused on the effects of three massless neutrinos of the Standard Model. However, recent cosmological observations have shown hints of deviations from the standard cosmological value of three effective neutrino degrees of freedom [34, 35, 36, 37, 38]. Due to neutrino oscillation experiments, it is also known that neutrinos are not massless, as described in a recent global analysis of neutrino properties [39]). There are also some, albeit statistically insignificant presently, hints that the addition of extra neutrino species can improve fits to short baseline neutrino oscillation data [40]. Recently issues regarding light sterile neutrinos and cosmology have been addressed in [41, 42, 43, 44].

In this chapter, we broaden the scope of this calculation to include beyond standard model species. The most relevant are massive neutrinos, additional (beyond three) massive and massless neutrino species, extra *bosonic* degrees of freedom and axions (an extensive introduction to axions is given in Appendix C). The important step in including the effect of these species is to derive a general expression for the anisotropic stress caused by any massive particle species. We present a general treatment below and then apply it to study the effect of these beyond standard model species on primordial gravity waves. Introductions to Cosmological Perturbation Theory (deriving the general evolution equation for tensor perturbations) and Inflation are given in Appendices A & B respectively.

2.2   Generalized Anisotropic Stress

We have already seen in cosmological perturbation theory, to first order, a perturbed FRW metric with scale factor $a(t)$ can be written as

$$
\begin{aligned}
ds^2 &= -(1+2\phi)dt^2 + 2a(\partial_i B + S_i)dx^i dt \\
&\quad + a^2(t)[\delta_{ij}(1-2\psi) - h_{ij} - 2\partial_i\partial_j E - \partial_j F_i - \partial_i F_j]dx^i dx^j
\end{aligned}
\tag{2.1}
$$

Gravitational waves or tensor perturbations arise as the transverse, traceless components of the metric fluctuations, which are characterized by h_{ij},

$$
\partial^i h_{ij} = 0 \quad ; \quad h_{ii} = 0
\tag{2.2}
$$

They satisfy the tensor equation which in fourier transformed k-space is,

$$
h_k'' + 2\mathcal{H}h_k' + k^2 h_k = 16\pi G_N a^2(\tau)\Pi_k
\tag{2.3}
$$

where the prime denotes differentiation with respect to conformal time $d\tau = dt/a(t)$, and Π_k is the anisotropic stress i.e., the off-diagonal elements of the stress-energy tensor.

In order to solve this equation, we first need an expression for the anisotropic stress for different species like decoupled neutrinos or bosons or axions. To do this, we turn to the Boltzmann equation, which determines the evolution of the phase space density of the particles, $F(x, P)$. It is in general a function of the four-momentum P which has components $P^\mu = dx^\mu/d\lambda$. The anisotropic stress can be determined by perturbing the distribution function about the equilibrium background distribution, $F(x, P) = \bar{F}(P^0) + \delta F(x, P)$, and employing the collisionless Boltzmann equation $dF(x, P)/dt = 0$. In general, the RHS has a collision term, but in this project we only consider free-streaming species. This is because such particles have the highest

anisotropic stress which means they have the most significant effect on tensor pertur-
bations. We generalize the situation of three massless neutrinos which already exists
in literature to include massive neutrinos, extra neutrinos beyond three, bosonic de-
gree of freedom, as well as the novel case of relativistic axions produced by axion
strings. As we have already seen these relativistic axions have a non-thermal spec-
trum.

For particles with a thermal distribution, the background phase space density is
given by

$$\bar{F}(P^0) = \frac{g}{e^{P^0/T_\nu} \pm 1} \tag{2.4}$$

where the plus sign is for fermions while the minus sign is for bosons, and g gives the
number of degrees of freedom. For the two cases of interest in this work: $g = g_\nu = 2$ for
a single neutrino, and $g = g_B = 1$ for a real scalar. T_ν is the temperature of neutrinos
which is related to the photon temperature at times after neutrinos decoupling as
$T_\nu = (4/11)^{1/3} T_\gamma$. We begin with the energy-momentum relationship,

$$g_{\mu\nu} P^\mu P^\nu = -(P^0)^2 + g_{ij} P^i P^j = -m^2 \tag{2.5}$$

We write this as

$$\tilde{p}_0^2 = g_{ij} P^i P^j \tag{2.6}$$

where we have defined a new variable through a shift

$$P^0 \equiv \sqrt{m^2 + \tilde{p}_0^2}. \tag{2.7}$$

10

2.2.1 Damping from Neutrinos

Neutrinos decouple early in the history of the universe. Their distribution function then satisfies the relativistic collisionless Boltzmann equation,

$$\frac{dF(t, x^i, \gamma^i, \tilde{p}_0)}{dt} = \frac{\partial F}{\partial t} + \frac{dx^i}{dt}\frac{\partial F}{\partial x^i} + \frac{d\tilde{p}_0}{dt}\frac{\partial F}{\partial \tilde{p}_0} + \frac{d\gamma^i}{dt}\frac{\partial F}{\partial \gamma^i} = 0 \qquad (2.8)$$

Using the variable $\tilde{p}$, one finds that to first order that Eq. (2.8) becomes the Einstein-Vlasov equation

$$\left(\frac{\partial F}{\partial t}\right)_{first\ order} = \frac{\partial \delta F}{\partial t} + \frac{\gamma_i \tilde{p}_0}{a\sqrt{m^2 + \tilde{p}_0^2}}\frac{\partial \delta F}{\partial x^i} - \frac{\dot{a}}{a}\frac{(m^2 + \tilde{p}_0^2)}{\tilde{p}_0}\frac{\partial \delta F}{\partial \tilde{p}_0} - \frac{1}{2}\frac{\partial \bar{F}}{\partial \tilde{p}_0}\tilde{p}_0\frac{\partial h_{ij}}{\partial t}\gamma^i\gamma^j$$
$$= 0 \qquad (2.9)$$

and $\gamma_i = \gamma^i$ are directional cosines. Defining $\mu \equiv \gamma^i k_i/k$ and using the mode decomposition of h_{ij} and δF

$$h_{ij} = \sum_{\lambda=+,\times} \int \frac{d^3k}{(2\pi)^3} h_{\lambda,k}(t) Q_{ij}^\lambda(\vec{x}) \qquad (2.10)$$

$$\delta F = \sum_{\lambda=+,\times} \int \frac{d^3k}{(2\pi)^3} f_{\lambda,k}(t, \tilde{p}_0, \mu)\gamma^i\gamma^j Q_{ij}^\lambda(\vec{x}) \qquad (2.11)$$

where Q_{ij}^λ are symmetric, traceless and divergenceless tensors that satisfy: $Q_{ij}^\lambda = Q_{ji}^\lambda$, $Q_{ij;a}^{\lambda\ ;a}(\vec{x}) + k^2 Q_{ij}^\lambda(\vec{x}) = 0$ and $Q_{ij}^{\lambda\ ;j} = 0$. The covariant derivative is with respect to the unperturbed spatial FRW metric. Thus, the first order Einstein-Vlasov equation in terms of the decomposed modes becomes

$$\frac{\partial f_k}{\partial t} + \frac{ik\mu}{a}\left(\frac{\tilde{p}_0}{\sqrt{m^2 + \tilde{p}_0^2}}\right) f_k - \frac{\dot{a}}{a}\left(\frac{m^2 + \tilde{p}_0^2}{\tilde{p}_0}\right)\frac{\partial f_k}{\partial \tilde{p}_0} = \frac{1}{2}\tilde{p}_0\frac{\partial \bar{F}}{\partial \tilde{p}_0}\frac{\partial h_k}{\partial t} \qquad (2.12)$$

Once again, following [26] we define new variables $q^\mu = aP^\mu$ and $q^0 = aP^0 \equiv q$ and conformal time, $d\tau = dt/a(t)$. Then Eq. (2.12) can be written as

$$\frac{\partial f_k}{\partial \tau} + \frac{ik\mu\tilde{p}_0}{\sqrt{m^2 + \tilde{p}_0^2}} f_k = \left(\frac{q^2 - a^2m^2}{q}\right)\frac{\partial \bar{F}}{\partial q}\frac{1}{2}\frac{\partial h_k}{\partial \tau} \qquad (2.13)$$

11

This equation determines the time evolution of the perturbation of distribution function δF which in turn determines the anisotropic stress part of the perturbed energy-momentum tensor that goes into the RHS of Eq. (2.3).

$$\delta \mathcal{T}_{ij} = a^2 \sum_{\lambda=+,\times} \int \frac{d^3k}{(2\pi)^3} \Pi_{\lambda,k} Q_{ij}^{\lambda}(\vec{x}) \tag{2.14}$$

and

$$\mathcal{T}_{ij} = \frac{1}{\sqrt{-g}} \int \frac{d^3q}{(2\pi)^3 q} q_i q_j F(q) \implies \delta \mathcal{T}_{ij} = \frac{1}{\sqrt{-g}} \int \frac{d^3q}{(2\pi)^3 q} q_i q_j \delta F(q) \tag{2.15}$$

Using Eqs.(2.11), (2.14) and (2.15), one finds that the anisotropic stress is

$$\Pi_{\lambda,k} Q_{ij}^{\lambda}(\vec{x}) = a^{-4} \int \frac{d^3q}{(2\pi)^3 q} q^2 \gamma^i \gamma^j \gamma^l \gamma^m f_{\lambda,k} Q_{lm}^{\lambda}(\vec{x}) \tag{2.16}$$

where $f_{\lambda,k} \equiv f_{\lambda,k}(\tau, q, \mu)$. On the other hand, Eq. (2.13), which is a first order differential equation, has the following solution

$$f_k(\tau, q, m, \mu) = \frac{q^2}{2} \frac{\partial \bar{F}}{\partial q} \int_{\tau_{dec}}^{\tau} d\tau' h'_k(\tau') \alpha(m, \tau', q)^2 e^{-i\mu\alpha^2 k(\tau-\tau')} \tag{2.17}$$

where we have defined

$$\alpha(\tau, m, q)^2 = 1 - \frac{m^2 a(\tau)^2}{q^2} \tag{2.18}$$

and

$$\mu = \frac{\gamma^i k_i}{k} \implies \mu = \hat{\gamma} \cdot \hat{k} \tag{2.19}$$

and used the fact that $f_k(\tau_{dec}, q, m, \mu) = 0$ because there is no anisotropic stress at neutrino decoupling since the neutrinos just start to free-stream at decoupling. The polarization index λ is suppressed on both sides of Eqs.(2.17). Finally using the identity

$$\int d\Omega_q \gamma^i \gamma^j \gamma^l \gamma^m e^{-i\gamma_i k^i u} Q_{lm}^{\lambda} = \frac{1}{8} (\delta^{il} \delta^{jm} + \delta^{im} \delta^{jl}) \int d\Omega_q e^{-i\mu u}; \quad d^3q = q^2 dq \, d\Omega_q \tag{2.20}$$

12

one can write the anisotropic stress in momentum space (again the polarization index λ is suppressed)

$$\Pi_k = \frac{1}{8a(\tau)^4} \int d\tau' \frac{d^3q}{(2\pi)^3} (1-\mu^2)^2 e^{-i\mu b} h'_k(\tau') \frac{\partial \bar{F}(q)}{\partial q} q^2 \alpha^2 \qquad (2.21)$$

where

$$b \equiv k(\tau - \tau')\alpha^2 \qquad (2.22)$$

$$\alpha^2 \equiv 1 - \frac{m^2 a(\tau')^2}{q^2} \qquad (2.23)$$

$$\mu = \hat{\gamma} \cdot \hat{k} = \cos\theta_q \qquad (2.24)$$

where we have taken $\hat{k}^i$ to be in the z-direction in q-space. We also define

$$u \equiv k\tau \qquad (2.25)$$

$$s \equiv k\tau' \qquad (2.26)$$

We can perform the integrations over $d\Omega_q = d\phi_q d(\cos\theta_q)$ and find that anisotropic stress is then given by

$$\begin{aligned}
\Pi_k &= \frac{\pi}{2a(u)^4} \int_{u_{dec}}^{u} ds\, dq \frac{dh_k(s)}{ds} \frac{\partial \bar{F}(q)}{\partial q} q^4 \alpha^2 \left[\frac{\sin b}{b} + 2\alpha^2 \left(-\frac{\sin b}{b} - 2\frac{\cos b}{b^2} + 2\frac{\sin b}{b^3} \right) \right. \\
&+ \left. \alpha^4 \left(\frac{\sin b}{b} + 4\frac{\cos b}{b^2} - 12\frac{\sin b}{b^3} - 24\frac{\cos b}{b^4} + 24\frac{\sin b}{b^5} \right) \right]
\end{aligned} \qquad (2.27)$$

Furhermore we define

$$x \equiv \frac{q}{aT} = \frac{q}{a_0 T_0} = \frac{q}{T_0} \qquad (2.28)$$

where the second equality holds for our normalization that the present day scale factor is $a_0 = 1$. This allows us to write the distribution $\bar{F}(q)$ and the function α as

$$\bar{F}(x) = \frac{g_\nu}{e^x + 1} \qquad (2.29)$$

$$\alpha^2(m, x) = 1 - \frac{m^2 a^2}{T_0^2 x^2} \qquad (2.30)$$

13

With this we find

$$
\begin{aligned}
\Pi_k &= \frac{1}{16\pi^2 a(u)^4} \int_{u_{dec}}^{u} ds \; dx \frac{dh_k(s)}{ds} \frac{\partial \bar{F}(x)}{\partial x} x^4 T_0^4 \alpha^2(m,x) \left[\frac{\sin((u-s)\alpha^2(m,x))}{(u-s)\alpha^2(m,x)} \right. \\
&+ 2\alpha^2(m,x) \left(-\frac{\sin((u-s)\alpha^2(m,x))}{(u-s)\alpha^2(m,x)} - 2\frac{\cos((u-s)\alpha^2(m,x))}{((u-s)\alpha^2(m,x))^2} \right. \\
&\left. + 2\frac{\sin((u-s)\alpha^2(m,x))}{((u-s)\alpha^2(m,x))^3} \right) + \alpha^4(m,x) \left(\frac{\sin((u-s)\alpha^2(m,x))}{(u-s)\alpha^2(m,x)} \right. \\
&+ 4\frac{\cos((u-s)\alpha^2(m,x))}{((u-s)\alpha^2(m,x))^2} - 12\frac{\sin((u-s)\alpha^2(m,x))}{((u-s)\alpha^2(m,x))^3} - 24\frac{\cos((u-s)\alpha^2(m,x))}{((u-s)\alpha^2(m,x))^4} \\
&\left.\left. + 24\frac{\sin((u-s)\alpha^2(m,x))}{((u-s)\alpha^2(m,x))^5} \right) \right]
\end{aligned}
\tag{2.31}
$$

The full gravitational wave equation is

$$
\begin{aligned}
\frac{d^2 h_k(u)}{du^2} + 2\left(\frac{da(u)/du}{a(u)} \right) \frac{dh_k(u)}{du} + h_k(u) &= \frac{16\pi G_N a^2(u)}{k^2} \Pi_k \\
&= \frac{6}{\rho(u)} \left(\frac{da(u)/du}{a(u)} \right)^2 \Pi_k
\end{aligned}
\tag{2.32}
$$

This gives an equation for the transverse-traceless tensor modes as a general function of the mass of the particle creating the anisotropic stress for a general phase space distribution $\bar{F}(x)$. It can be seen to reduce to the standard form for three massless neutrinos when $g_\nu = 6$ and $m = 0$ [26].

From the relation Eq. (2.31), one can then include additional degrees of freedom by simply using $g_\nu = 8$ (10) for four (five) massless neutrino species. We use the simplifying assumption that the neutrinos all have the same decoupling temperature. (To generalize to arbitrary decoupling temperatures we would change the lower integration limit of the anisotropic stress for that species). For a mixed scenario where particles of different masses contribute, one can use Eq. (2.31) for the anisotropic stress, $\Pi_{k,i}$, generated by a single species of mass $m = m_i$ with $g_\nu = g_i$ degrees of

14

freedom, and then add another anisotropic stress term of this form for any additional species of mass m_j with degrees of freedom g_j. In other words, the total anisotropic stress due to i particles is given by the sum $\Pi_{k,tot} = \sum_i \Pi_{k,i}$.

To graphically display the effect of adding non-zero neutrino masses we adopt the simple analytic form for the scale factor $a(\tau)$ in a matter plus radiation universe given by

$$a(\tau) = \left(\frac{\tau}{\tau_0}\right)^2 + 2\left(\frac{\tau}{\tau_0}\right)\sqrt{a_{\text{eq}}}; \ \tau_0 = \frac{2}{\sqrt{\Omega_M}H_0}. \tag{2.33}$$

Note that today, the relation between radiation and matter densities is given by

$$\Omega_r = a_{\text{eq}}\Omega_M \tag{2.34}$$

For the standard cosmological scenario with $N_{\text{eff}} = 3$, *i.e.*, three effective neutrino degrees of freedom, we have $a_{\text{eq}} = 1/3600$, $\Omega_M = 0.3$ and $\Omega_r = \Omega_\gamma + \Omega_\nu$ since the free-streaming neutrinos are relativistic. Further it can be shown that [26]

$$\frac{\Omega_\nu}{\Omega_\nu + \Omega_\gamma} = 0.40523; \quad g_\nu = 6 \tag{2.35}$$

When adding extra neutrino species, we use the above relation and keep Ω_M fixed but change the ratio in Eq. (2.35) accordingly to get a new redshift for matter-radiation equality [45]. So, for $N_{\text{eff}} = 4$, $a_{\text{eq}} = 1/3172$ and for $N_{\text{eff}} = 5$, $a_{\text{eq}} = 1/2834$.

One sees that Eq. (2.32) is an integro-differential equation since the source term on the right-hand-side is the integral in Eq. (2.31). To put the equation into a suitable form for a numerical solution, we adopt the method in Appendix A of [46], which consists of rewriting the single, second order integro-differential equation as a

system of coupled first-order Volterra type integro-differential equations. This can then be solved by standard methods of numerical integration [47]. There is a slight difference in our method of solution from that in [26] and [46] due to the form of the integral kernel. Namely, we do not have the simplifying option of integrating out the distribution function (which would give the energy density in the standard case of massless neutrinos) due to the additional x-dependence of other factors in the integrand. We therefore were forced to generate numerical values for the integrand at each value of u and s, after which the procedure of [46] could be implemented.

2.2.2 Damping from Axions

The fine tuning of θ_{QCD} can be avoided in models of particle physics that contain an extra $U(1)$ Peccei-Quinn (PQ) symmetry. A consequence of these models is a light pseudo-scalar particle, the axion. In a cosmological setting, the axion is massless above the QCD temperature but gains a small mass below this temperature. Even though the axion is very light, with a typical mass $m_a = \mathcal{O}(10^{-3}\ \mathrm{eV})$, it can be non-relativistic because it is produced coherently throughout the cosmological horizon and has momenta given by $\sim t^{-1}$ at cosmic time t. This argument, however, ignores the topology that accompanies the breaking of the PQ symmetry, which is relevant if the PQ symmetry breaking scale occurs below the scale of inflation. In this case, the spontaneous breaking of the PQ symmetry leads to the production of axionic cosmic strings with energy density set by the PQ energy scale. As the strings oscillate, they radiate relativistic axions. At the QCD temperature scale, the strings get connected by axionic domain walls, and the whole network of strings and walls collapses, dissipating energy again into *relativistic* axions. Hence the axion density in the universe contains two separate components: the non-relativistic component due to coherent oscillations of the axion field, and the relativistic component due to the

radiation from topological defects. The latter component can be significant, and may even dominate the non-relativistic component for large values of the Peccei-Quinn symmetry breaking scale. Relativistic axions can also have anisotropic stress and hence they can couple to gravitational waves just as neutrinos do.

In Appendix C, we present an extended introduction to Axions as well as derive the spectral energy density of relativistic axions which is presented here again,

$$\rho_a(t) = \frac{4\pi f_a^2}{t^2} \int_{\Omega^{2/3}/\tilde{t}}^{\Omega^{5/6}/\sqrt{\tilde{t}t^*}} \left(\frac{q^2 + (t/\tilde{t})m_a^2}{q^2 + \tilde{m}^2} \right)^{1/2} \left[\ln\left(\frac{\Omega^{5/3}}{\tilde{t}q^2\delta} \right) - \frac{1}{2} \right] \frac{dq}{q} \tag{2.36}$$

where, as previously defined, q is the comoving momentum, $f_a \leq 2 \times 10^{10}$ GeV is the PQ symmetry breaking scale, $\delta = 1/f_a$, $\Omega = 2\pi$, $\tilde{m} \equiv 1/\tilde{t} = 10^{-9} - 10^{-8}$ eV and t^* is the time at which the axions decoupled. The mass of the axion m_a and the decoupling temperature T_d^* of axions is related to the scale f_a through [48]

$$m_a = 6 \times 10^{-6}\text{eV} \left(\frac{10^{12}\text{GeV}}{f_a} \right) = \frac{6 \times 10^{15}\text{eV}^2}{f_a} \tag{2.37}$$

$$T_d^* = 5 \times 10^{11} \text{ GeV } \left(\frac{f_a}{10^{12} \text{ GeV}} \right)^2 \tag{2.38}$$

Since $T \propto 1/a(t)$, we can find t^* using T_d^* and the scale factor $a(t)$ in (2.33). We will consider damping from relativistic axions with the spectrum (2.36) for three different f_a values 10^8, 10^9 and 10^{10} GeV. This lies within the range $10^7\text{GeV} < f_a < 2 \times 10^{10}\text{GeV}$ where the lower bound on f_a comes from astrophysical constraints [49] and the upper bound which comes from the requirement that the energy density in relativistic axions remain below critical energy density to avoid overclosing the universe. To calculate the anisotropic stress Π_k, we need the unperturbed phase space distribution function $\bar{F}(q)$ of these relativistic axions which we can read off from (2.36)

$$\bar{F}^{\text{axion}}(q) = \frac{f_a^2 a(t)^4}{t^2 q^3 (q^2 + a(t)^2 m_a^2)^{1/2}} \left(\frac{q^2 + (t/\tilde{t})m_a^2}{q^2 + \tilde{m}^2} \right)^{1/2} \left[\ln\left(\frac{\Omega^{5/3}}{\tilde{t}q^2\delta} \right) - \frac{1}{2} \right] \tag{2.39}$$

17

However, there are few differences from the neutrino case of (2.31). Since axions have a non-thermal spectrum, we don't do the substitution of (2.28) and retain the expression for α^2 in (2.18). Thus, the expression for Π_k for axions becomes

$$\Pi_k^{\text{axion}} = \Pi_k(\bar{F} \to \bar{F}^{\text{axion}}) \tag{2.40}$$

where Π_k is defined in Eq. (2.31) and $\alpha(m, q, \tau)^2$ is the same as in Eq. (2.18)

2.3   Results and Analysis

For massless neutrinos, the effects of damping are determined solely by the neutrino energy density contribution, (which falls as a^{-4}) once one enters the matter-dominated era, and will thus be most significant for $k \gtrsim k_{\text{eq}} = a_{\text{eq}} H_{\text{eq}} \approx 170/\tau_0$. The effect of non-zero neutrino masses will be to add an extra k-dependence to damping, as free streaming, and hence damping, will be reduced when the temperature is of order of the mass. k-modes that come inside the horizon while neutrinos are relativistic, and contribute significantly to the overall energy density, will be damped more. On the other hand, those modes that come inside the horizon at later times, either when neutrino masses become significant, or during matter domination, when the neutrino energy density fraction may have been reduced considerably due to red-shifting will be damped less. This heuristic behavior is validated by our detailed calculations, which quantitatively explore this effect. For demonstrations purposes here, we display the damping as a function of neutrino mass for three different values of $k\tau_0 = 100, 200, 1000$.

In Fig. 2.1, we plot the damping from 3 massless and a 1 eV neutrino and compare it to the case of 4 massless neutrinos. In doing so, we have adjusted a_{eq} to $N_{\text{eff}} = 4$ for both cases, which is a good approximation since neutrino masses of
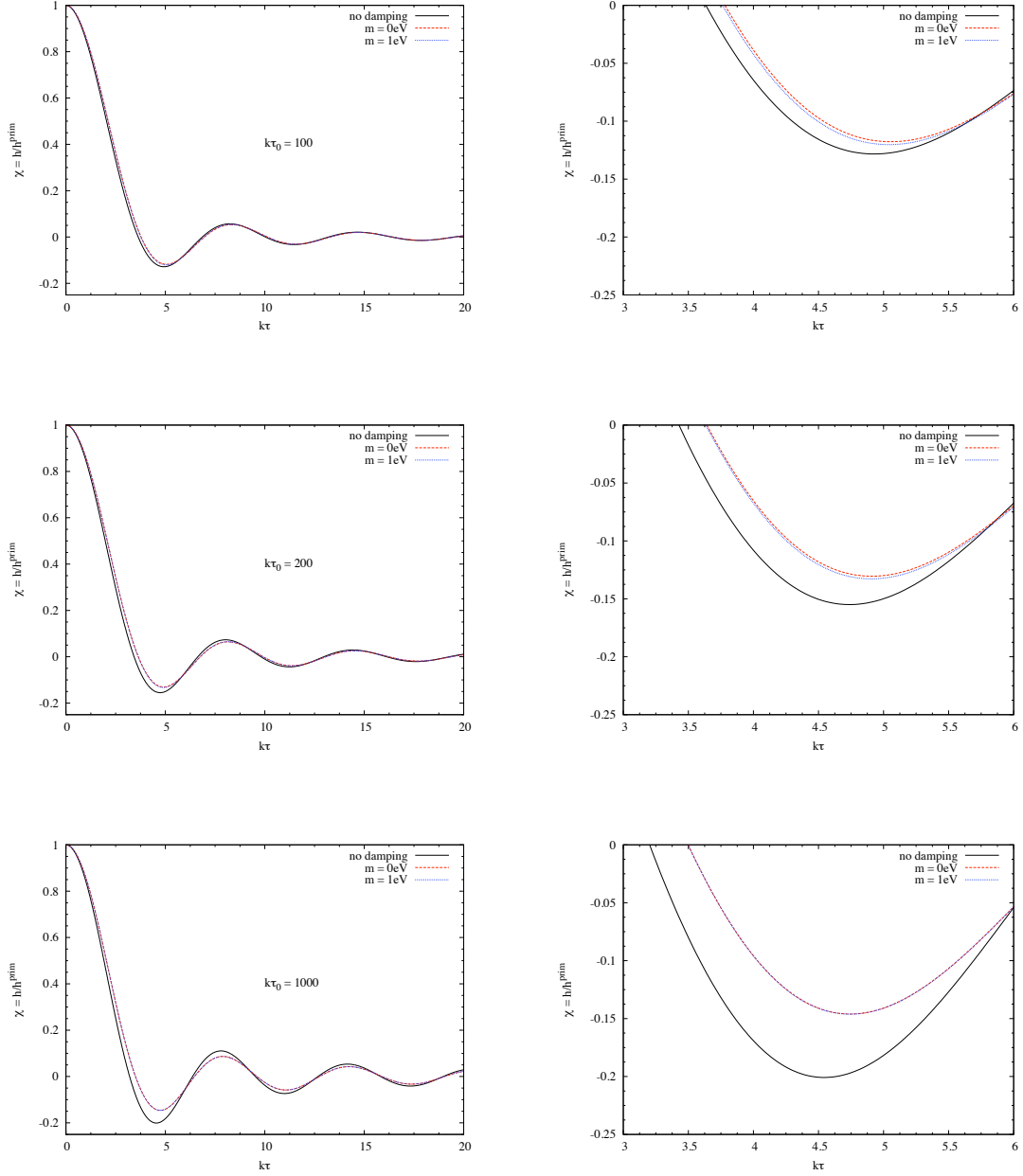
Figure 2.1: The k-dependence of the damping of an extra massive neutrino is demonstrated. The plots show that the damping is reduced for gravitational wave modes that enter the horizon as neutrinos are beginning to become non-relativistic. The damping is also less at later times when the neutrino energy fraction has been reduced due to redshifting. The region in each plot on the left around the first minima is zoomed in the adjacent plot on the right. For the $k\tau_0 = 1000$, the red and blue lines are overlapping, implying a negligible effect of mass.

19

$O(1)$ eV are largely relativistic at matter-radiation equality. Note that a cosmological scenario with a 1 eV neutrino and $N_{\text{eff}} = 4$ is consistent with the current Planck data [50]. For $k\tau_0 = 100$, the ratio between the minima of 3 massless plus 1 eV and homogeneous (*undamped*) case is 0.94, and for the 4 massless vs homogeneous case is 0.92, a difference of order 2%. For $k\tau_0 = 200$, the difference in damping is of order 1.5%. And finally, for $k\tau_0 = 1000$ the difference in damping is now only 0.7%.
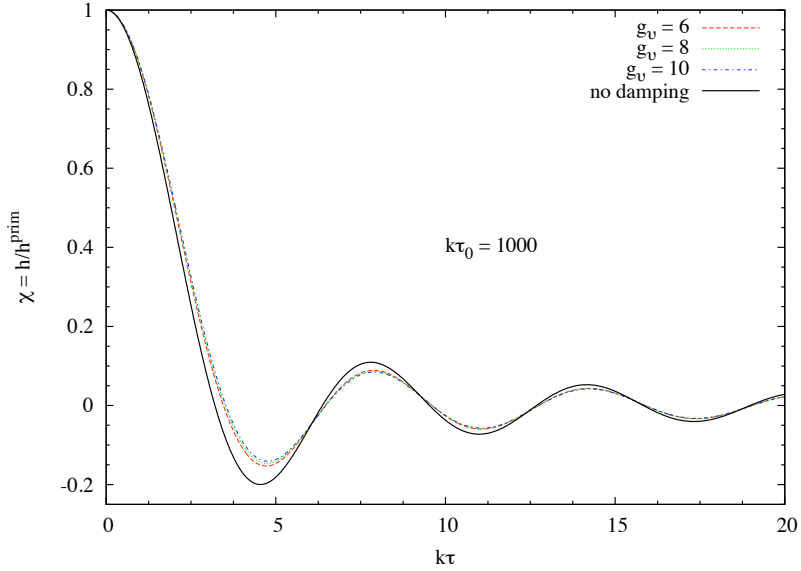
Figure 2.2: The damping effect of extra massless neutrino species is shown. Each neutrino species has 2 degrees of freedom, thus $g_\nu = 6$, 8, and 10 correspond to 3, 4, and 5 neutrinos.

Similarly the effect of additional massless degrees of freedom is to increase the damping of gravitational waves. As seen in Fig. 2.2 this effect varies slightly with conformal time, τ. We can compare the effect of extra species for example at the first minima. For the undamped case, this minima occurs at $u = 4.54$ independent of N_{eff}. However, including GW damping through free-streaming, this minima shifts

to $u = 4.72$, 4.74, 4.76 ($N_{\text{eff}} = 3$, 4, 5 respectively). With respect to homogenous case, the mode amplitude at the minima is 76.5%, 73.1% and 70.5% as large for $N_{\text{eff}} = 3$, 4, 5, respectively. Thus, tensor modes are damped more, with increasing N_{eff}, as expected. Since the identity of the source of any possible extra degrees of freedom is currently unknown, one may want to expand the realm of possibilities to include bosonic degrees of freedom. As expected on the basis of number of degrees of freedom, and hence N_{eff}, the damping due to a single boson is less by about 19%, than for that of a single, massless neutrino species. Two bosonic degrees of freedom are virtually indistinguishable from a single neutrino.
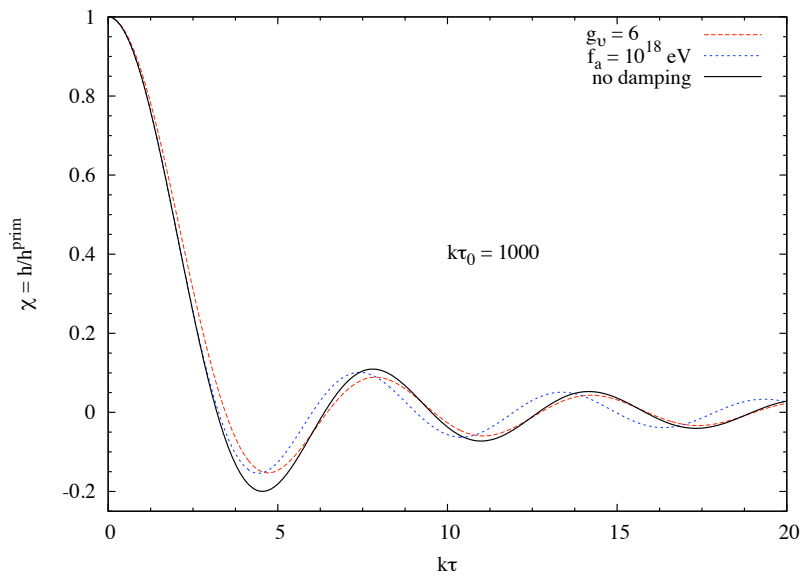
Figure 2.3: The effect of axions produced by axionic strings.

In Fig. 2.3, we examine the damping of gravitational waves caused by relativistic axions. We compare the results for axions with $f_a = 10^9$ GeV versus 3 massless neutrinos since relativistic axions have 26% and 3 massless neutrinos constitute 10%

of critical density at last scattering. With respect to the no-damping case, the mode amplitudes at the minima are damped by 76.5% for 3 neutrinos versus 77% for axions. However, note that the minima for neutrinos is at $u = 4.72$ but for axions it is at $u = 4.42$. And as can be seen this phase shift persists throughout the time evolution. Thus, although axions damp the amplitudes by the same amount as neutrinos for these parameters, their phase shift is an important distinguishing feature. We can understand this effect on physical grounds. The axion phase space distribution, Eq. (2.39), has an explicit time dependence that is not present in the thermal neutrino distribution function. As a result the integral over time of the anisotropic stress, which produces the damping, is modulated compared to the neutrino case, and hence modulates the resulting k-dependent damping of gravitational waves. This phase difference will have an observational impact on the damping of CMB B-modes. Recall that it is $\dot{\chi}$ that enters into the Boltzmann equation for the temperature perturbations [51]. Following [22], we expect all tensor multipole coefficients to depend on $\chi(u)$ only through a factor of $|\chi'(u_{\mathrm{LSS}})|^2$, where $u_{\mathrm{LSS}} = (1 + z_{\mathrm{EQ}})/(1 + z_{\mathrm{LSS}})$ is the value of u at the last scattering surface (LSS). We take $z_{\mathrm{LSS}} = 1089$ and convert into u_{LSS} using Eq. (2.33) and $\Omega_M = 0.3$. Moreover, we expect the dominant contribution to multipole l in the CMB will come from wavenumber, $k \approx a_{\mathrm{LSS}} l / d_{\mathrm{LSS}}$ [22] where a_{LSS} is the scale factor at the surface of last scattering and d_{LSS} is the angular diameter distance of the surface of last scattering. Using numerical values of a_{LSS} and d_{LSS} we get

$$l = 0.878 u_{\mathrm{LSS}}. \tag{2.41}$$

In Fig. 2.4 we show the ratio of χ'^2 for damped to undamped gravitational waves for axions and different numbers of massless neutrinos. We have extracted this ratio at the surface of last scattering for several different low l values. We expect the graph
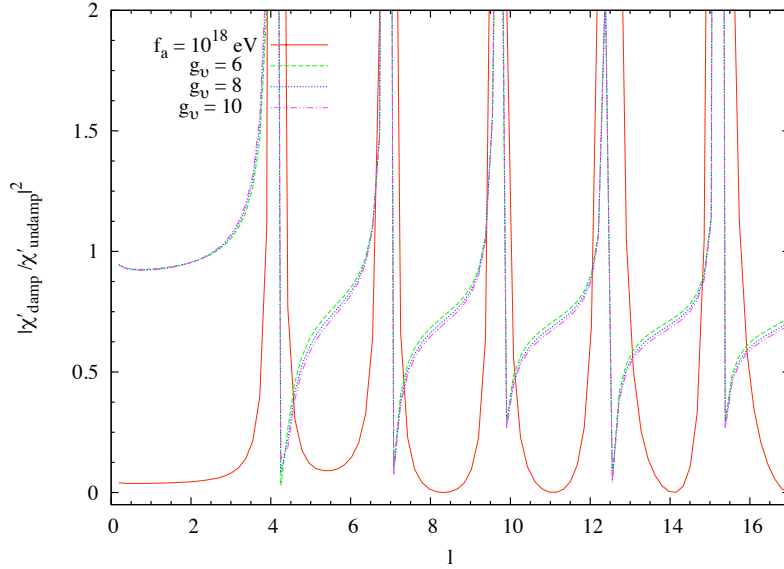
Figure 2.4: The square of the ratio of the time derivative of damped modes to undamped modes which is useful for calculating the B mode correlation function C_l^{BB}.

to look similar at higher l values but the computations at high l become prohibitively expensive. Both neutrinos and axions produce an oscillatory pattern in the damping but there is a phase shift between them. It is important to note that at certain l, "damped" gravitational waves can actually produce a larger signal than undamped waves by a factor of 2 or more. This surprising effect is due to the fact that for some $k\tau$ values there is actually a relative amplification caused by anisotropic stress, as can be seen from Figs. 2.1 and 2.2, where the mode amplitude does not decrease as rapidly as in the undamped case.

2.4   Conclusions

The observation of a primordial gravitational wave spectrum would provide a direct window on physics of the very early universe and possibly beyond standard

model physics. In order to extract as much cosmological information as possible from such a signal, one must be mindful of any phenomena which may alter the primordial signal. One example of such a process is the damping of gravitational waves by free-streaming particles such as neutrinos. In this chapter, we have generalized the formalism for deriving the effects of damping of gravitational waves due to anisotropic stress caused by free-streaming by deriving a general formula for the anisotropic stress as a function of mass and number of degrees of freedom, which should be useful for calculating the cosmological signature of possible additional non-standard model relativistic species. We find that for additional neutrino masses of current cosmological interest, the effects of non-zero mass on damping in comparison to the massless case is most pronounced for $k\tau_0 \approx 100 - 200$. For longer wavelength modes, that enter the horizon later, the damping is suppressed for all cases because the neutrino energy density is less significant. In addition we have explored the possible impact of a relativistic axion background, as might be present due to radiation from axion strings. While the overall damping produced by such a background could perhaps be comparable to that due to three standard model neutrinos, we find that their non-thermal phase space distribution will produce a possibly measurable phase shift in the damping signature. If a non-zero tensor B-mode contribution is observed in future CMB experiments, one might hope to use these results to help constrain new physics beyond the standard model.

Chapter 3

INFLATING WITH THE HIGGS BOSON

3.1 Introduction

Inflation [52, 2, 3] successfully addresses the greatest puzzles of theoretical cosmology. Over the past 20 years, increasingly precise measurements of the temperature fluctuations of the cosmic microwave background radiation (CMB) have confirmed the nearly scale invariant power spectrum of scalar perturbations, a relatively generic inflationary prediction. These many successes, however, underscored the inability to probe perhaps the most robust and unambiguous prediction of inflation, the generation of a stochastic background of gravity waves associated with what are likely enormous energy densities concomitant with inflation (*e.g.*, [53]).

Higgs Inflation (HI) postulates that the Standard Model Higgs field and the inflaton are one in the same [54]. This powerful assumption allows HI to be, in principle much more predictive than many other models of inflation, as by measuring the masses of the Higgs boson and the top quark at the electroweak scale (100 GeV), one might predict observables at much larger energy scales associated with inflation ($V_{\mathrm{inf}}^{1/4} \lesssim 10^{16}$ GeV).

However, in practice this enhanced predictive power is elusive due to a strong sensitivity to quantum effects, unknown physics, and other technical subtleties in the model. Specifically, one connects observables at the electroweak and inflationary scales using the renormalization group flow (RG) of the SM couplings [55, 56, 57, 58,

59, 60]. It is reasonable however to expect that there is new beyond standard model physics at intermediate scales, and even if the SM is extended only minimally to include a dark matter candidate [61] or neutrino masses [62, 63, 64, 65] this new physics can qualitatively affect the connection between electroweak and inflationary observables. Moreover, perturbative unitarity arguments require new physics just above the scale of inflation [66, 67], and in addition the unknown coefficients of dimension six operators can significantly limit the predictive power of HI [68]. The HI calculation also runs into various technical subtleties that arise from the requisite non-minimal gravitational coupling and quantization in a curved spacetime [69, 70, 71]. Finally, it is worth noting that HI is also at tension with the measured Higgs boson and top quark masses, and an $O(2\sigma)$ heavier Higgs or lighter top is required to evade vacuum stability problems [72].

Besides these issues that impair the predictivity of HI, we discuss in this chapter an important additional source of ambiguity in calculations of HI that had not been fully explored before. Since the quantum corrections are significant when connecting the low energy and high energy observables, one should not work with the classical (tree-level) scalar potential, as is done in may models of inflation, but one must calculate the quantum effective potential. It is well-known that in a gauge theory the effective potential explicitly depends upon the choice of gauge in which the calculation is performed [73, 74], and care must be taken to extract gauge-invariant observables from it [75, 76, 77, 78] (see also [79, 80]). This fact can perhaps be understood most directly by recalling that the effective action is the generating functional for one-particle irreducible Green's functions, which themselves are gauge dependent [74]. In practice one often neglects this subtlety, fixes the gauge at the start of the calculation, and calculates observables with the effective potential as if it were a classical poten-

tial. In the context of finite temperature phase transitions, it is known that when calculated naively in this way, the predictions for observables depend on the choice of gauge used [81, 82, 83, 80, 84, 85, 86]. Because of the extreme tension between HI models and the data, we assess here the degree to which this gauge uncertainty might affect the observables in Higgs Inflation. We found that the gauge ambiguity introduces uncertainties that are comparable to the variation of the physical parameters, *i.e.* the Higgs mass. As a result, this ambiguity alone cannot resuscitate moribund models.

This chapter is organized as follows - we first present the canonical theory of HI in Section 3.2. Next, we briefly discuss the modifications to Standard Model effective potential when working with HI in Section 3.3. In Section 3.4 we present the results of gauge dependence of physical observables predicted from HI. Finally, we conclude in Section 3.5. A thorough introduction to the concept of Effective Potential is relegated to Appendix D.

3.2 Fundamentals of Higgs Inflation

Since the most common models of inflation are driven by a scalar field, it is most interesting to see if the Higgs could be that field. The higgs field potential is quartic, so to flatten it, higgs inflation relies on a non-minimal gravitational coupling. Let $\Phi = (\phi^+, \phi^0)^T$ be the Standard Model (SM) Higgs doublet. Its gauge interactions are determined from the gauge covariant derivative,

$$D_\mu \Phi = \left(\nabla_\mu - ig t^a W_\mu^a - \frac{ig'}{2} B_\mu \right) \Phi \tag{3.1}$$

where ∇_μ is the metric covariant derivative and $t^a = \sigma^a/2$ are the $SU(2)$ generators. After adding the non-minimal coupling term, $\Phi^\dagger \Phi R$ with R the Ricci scalar, the

action for the Higgs sector becomes

$$S_J[g_{\mu\nu}, \Phi] = \int d^4x \sqrt{-g} \left\{ (D_\mu\Phi)^\dagger D^\mu\Phi - V(\Phi^\dagger\Phi) - \xi\Phi^\dagger\Phi R - \frac{1}{2}M_p^2 R \right\} \qquad (3.2)$$

where

$$V(\Phi^\dagger\Phi) = m^2\Phi^\dagger\Phi + \lambda(\Phi^\dagger\Phi)^2 \qquad (3.3)$$

is the scalar potential. Taking $m^2 < 0$ causes the Higgs to acquire a vacuum expectation value $\langle\Phi\rangle = (0,\ v\sqrt{2})^T$. To prevent the theory from containing ghosts, we must require $M_p^2 + \xi v^2 > 0$.

The action in Eqn (3.2), known as the Jordan frame action, yields field equations with an undesirable coupling between the Higgs field and the metric. We can remove the non-minimal coupling term and move to the Einstein frame by performing a Weyl transformation

$$g_{\mu\nu} = \frac{1}{\Omega^2(x)}\hat{g}_{\mu\nu}(x) \qquad (3.4)$$

where

$$\Omega^2(x) \equiv 1 + \frac{2\xi\Phi^\dagger\Phi}{M_p^2} \qquad (3.5)$$

Under this transformation,

$$g^{\mu\nu} = \Omega^2\hat{g}^{\mu\nu} \det g = \Omega^{-8}\det\hat{g} \qquad (3.6)$$

and thus the action becomes

$$S_E[\hat{g}_{\mu\nu}, \Phi] = \int d^4x \sqrt{-g} \left\{ \frac{(D_\mu\Phi)^\dagger D^\mu\Phi}{\Omega^2} - \frac{V(\Phi^\dagger\Phi)}{\Omega^4} + \frac{3M_p^2}{4}\frac{\nabla_\mu\Omega^2}{\Omega^2}\frac{\nabla^\mu\Omega^2}{\Omega^2} - \frac{1}{2}M_p^2\hat{R} \right\}$$
$$(3.7)$$

28

However, the kinetic term is no longer canonically normalized. For a theory with one real scalar field, it is always possible to perform a field redefinition and return the kinetic term to its canonical form. But when the theory contains multiple scalar fields with non-minimal couplings this is not possible in general. The Standard Model Higgs doublet, for example, contains four real scalar degrees of freedom. However, for the SM Higgs we can make use of the SU(2) symmetry by writing,

$$\Phi(x) = \mathcal{U} \begin{pmatrix} 0 \\ h(x)/\sqrt{2} \end{pmatrix} \quad \text{where} \quad \mathcal{U} = exp\left[2i\pi^a(x)t^a\right] \tag{3.8}$$

Here $h(x)$ and $\pi^a(x)$ are real scalars. And in this frame (Einstein) the action becomes,

$$S_E[\hat{g}_{\mu\nu}, h, \pi^a] = \int d^4x \sqrt{-\hat{g}} \left\{ \frac{1}{2} \frac{\nabla_\mu h \nabla^\mu h}{\Omega^2} + \frac{h^2}{\Omega^2} \text{Tr}[V_\mu V^\mu] - U(h) - \frac{1}{2} M_p^2 \hat{R} \right. $$
$$\left. + \frac{3 M_p^2}{4} \frac{\nabla_\mu \Omega^2}{\Omega^2} \frac{\nabla^\mu \Omega^2}{\Omega^2} \right\} \tag{3.9}$$

where importantly,

$$U(h) \equiv \frac{V(h^2/2)}{\Omega^2} = \frac{2m^2 h^2 + \lambda h^4}{4 \left(1 + \frac{\xi h^2}{M_p^2}\right)^2} \tag{3.10}$$

and V_μ is defined as

$$V_\mu \equiv (\partial_\mu \mathcal{U}) \mathcal{U}^\dagger + i W_\mu^a t^a - i \mathcal{U} B_\mu t^3 \mathcal{U}^\dagger \tag{3.11}$$

The second term in Eqn (3.9) represents interactions between the physical Higgs field and the gauge and Goldstone boson fields. These interactions are important for reheating and for loop-corrections to inflation, but for the moment we will drop them. Finally, we put the action in its canonical form by introducing a new field $\chi(h)$ which satisfies,

$$\frac{d\chi}{dh} = \sqrt{\frac{1}{\Omega^2} + \frac{3}{2} \frac{M_p^2}{\Omega^4} \left(\frac{d\Omega^2}{dh}\right)^2} \tag{3.12}$$

29

We can solve this explicitly to obtain $\chi(h)$,

$$
\begin{aligned}
\chi(h) \ &= \chi(0) + \sqrt{6}M_p\sqrt{1 + \tfrac{1}{6\xi}} \ \mathrm{arcsinh}\left[\tfrac{\xi h}{M_p}\sqrt{6 + \tfrac{1}{\xi}}\right] \\
&\quad - \sqrt{6}M_p \ \mathrm{arctanh}\left[\frac{1}{\sqrt{1 + \tfrac{1}{6\xi} + \tfrac{m_p^2}{6\xi^2 h^2}}}\right]
\end{aligned}
\tag{3.13}
$$

The solution can be broken up into three district regimes:

$$
\chi(h) \approx \begin{cases} h \ \text{if} \ h < \tfrac{M_p}{\xi} \\[2mm] \sqrt{\tfrac{3}{2}}M_p \ln\left[1 = \tfrac{\xi h^2}{M_p^2}\right] \approx \begin{cases} \sqrt{\tfrac{3}{2}}M_p\tfrac{\xi h^2}{M_p^2} & \text{for} \ \tfrac{M_p}{\xi} < h < \tfrac{M_p}{\sqrt{\xi}} \\[2mm] \sqrt{\tfrac{3}{2}}M_p\ln\tfrac{\xi h^2}{M_p^2} & \text{for} \ \tfrac{M_p}{\sqrt{\xi}} < h \end{cases} \end{cases}
\tag{3.14}
$$

where we have also assumed $\xi \gg 1$ and dropped higher order terms in ξ^{-1}. These solutions (taking $\chi(0) = 0$) are shown in Fig. 3.1. Since $\chi(h)$ is monotonically increasing, it is generally possible to invert and obtain $h(\chi)$, but a closed form, exact expression does not exist.
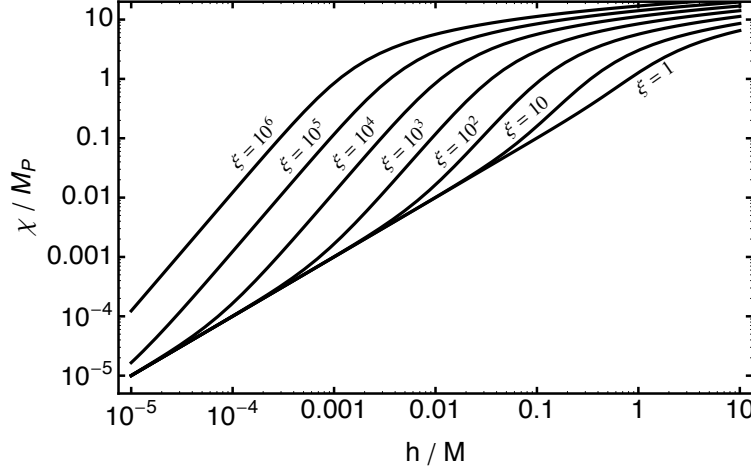
Figure 3.1: The canonically normalized field χ as a function of the higgs field, h.

In terms of the rescaled field ξ, the action becomes

$$
S_E[\hat{g}_{\mu\nu}, \chi] = \int d^4x \sqrt{-\hat{g}}\left\{\frac{1}{2}\nabla_\mu\chi\nabla^\mu\chi - U(\chi) - \frac{1}{2}M_p^2\hat{R}\right\}
\tag{3.15}
$$

where the scalar potential $U(\chi)$ is given by

$$U(\chi) = \frac{2m^2 h(\chi)^2 + \lambda h(\chi)^4}{4 \left(1 + \frac{\xi h(\chi)}{M_p^2}\right)^2} \tag{3.16}$$

For the purposes of studying Higgs inflation, the $O(h^4)$ term dominates and we can neglect the terms of order $O(m^2 h^2)$. Using the approximations for $h(\chi)$, Eq. (14), we can obtain $U(\chi)$ in the three regimes:

$$U(\chi) \approx \begin{cases} \frac{\lambda}{4}\chi^4 \ , \ \chi < \frac{M_p}{\xi} \\ \\ \frac{\lambda}{4}\frac{M_p^4}{\xi^2}\left(1 - e^{-\sqrt{2/3}\chi/M_p}\right)^2 \approx \begin{cases} \frac{\lambda}{6}\frac{\chi^2 M_p^2}{\xi^2} \quad \text{for} \quad \frac{M_p}{\xi} < \chi < M_p \\ \\ \frac{\lambda}{4}\frac{M_p^4}{\xi^2}\left[1 - 2e^{-\sqrt{2/3}\chi/M_p}\right] \quad \text{for} \quad M_p < \chi \end{cases} \end{cases} \tag{3.17}$$
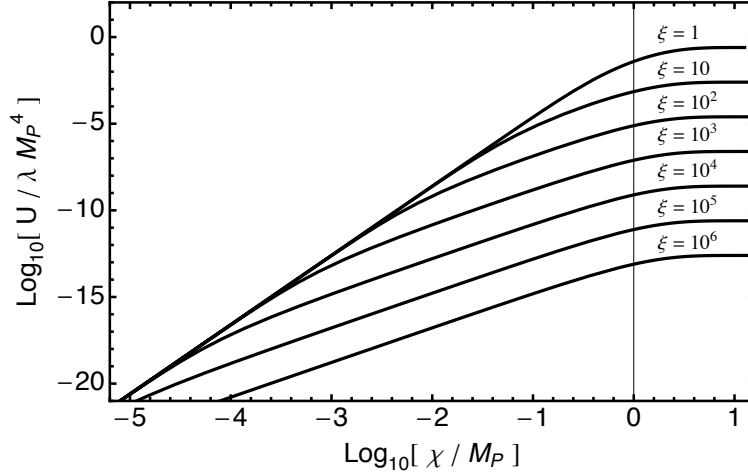
Figure 3.2: The inflationary potential as a function of the canonically normalized scalar field χ.

We show a plot of $U(\chi)$ in Fig. 3.2. As seen in the figure, and confirmed in Eq (3.17), the potential becomes exponentially close to flat above $\chi \gtrsim M_p$. This is the regime in which we get slow-roll inflation.

Inflation occurs in the large field region of the potential where $h \gg M_p/\sqrt{\xi}$ and $\chi \gg M_p$ and ends in the transition region $\chi \sim M_p$, and it is not a good approximation

to assume $\chi \gg M_p$ always. Therefore we will use the lower expression in Eq (3.17) which is valid for all $\chi > M_p/\xi$. That is, the inflationary potential is given by

$$U(\chi) = \frac{\lambda}{4} \frac{M_p^4}{\xi^2} \left(1 - e^{-\sqrt{2/3}\chi/M_p}\right)^2 \quad \text{with} \quad \chi = \frac{3}{2} M_p \ln\left[1 + \frac{\xi h^2}{M_p^2}\right] \qquad (3.18)$$

If we are only working with the tree-level theory, then λ is a constant parameter. Since we would eventually like to consider the loop corrections, we will anticipate the RG scale dependence now by writing $\lambda = \lambda(h(\chi))$. The slow roll parameters are defined by

$$\epsilon \equiv \left(\frac{dU/d\chi}{U}\right)^2, \quad \eta \equiv M_p^2 \frac{d^2U/d\chi^2}{U} \qquad (3.19)$$

and so for the Higgs Inflation potential given above it can be simply calculated as

$$\begin{aligned}
\epsilon &= \frac{4}{3} \frac{1}{(1+\theta^2)^2} \left[\theta^2 + \frac{1}{4} \frac{d\ln\lambda}{d\ln h}(1+\theta^2)\right]^2 \\
\eta &= -\frac{4}{3}\theta^2(1-\theta^2) + \theta^2(1+\theta^2)\left(\frac{d\ln\lambda}{d\ln h}\right) + \frac{1}{6}(1+\theta^2)^2\left[\frac{d^2\ln\lambda}{d(\ln h)^2} + \left(\frac{d\ln\lambda}{d\ln h}\right)^2\right]
\end{aligned}$$

$$(3.20)$$

where $\theta = M_p/(\sqrt{\xi}h)$ and during inflation $\theta \ll 1$. If we are only working to tree level, then λ is just a constant, and we find $\epsilon \propto \theta^4$, $\eta \propto \theta^2$. Then as long as the Higgs field begins at large field values, $h \gg M_p/\sqrt{\xi}$, we are in the slow roll regime. At the one-loop level, quantum corrections cause λ to run, and in this case we find, for instance, $\epsilon \propto (d\ln\lambda/d\ln h)^2$. Assuming that the initial conditions provide $\epsilon, \eta \ll 1$ inflation will continue until $\epsilon = O(1)$. For the tree-level higgs potential in which $d\ln\lambda/d\ln h = 0$, we find the inflationary observables,

$$\epsilon = 1 \implies \frac{h_{end}}{M_p/\sqrt{\xi}} = \left(\frac{4}{3}\right)^{1/3} \approx 1.07 \ , \ \frac{\chi_{end}}{M_p} = \sqrt{\frac{3}{2}}\ln\left(\frac{2}{\sqrt{3}} + 1\right) \approx 0.940 \quad (3.21)$$

As we anticipated in the previous section, at the end of inflation we have $\chi = \mathcal{O}(M_p)$ and we are in the transition region, see Fig. (3.17). The number of e-foldings as the

field rolls from χ_i to $\chi_f < \chi_i$ is given by

$$\mathcal{N} = \ln \frac{a_f}{a_i} = \int_{\chi_i}^{\chi_f} \frac{U(\chi)}{U'(\chi)M_p^2}d\chi \approx \frac{3}{4}\left(\frac{\xi h_i^2}{M_p^2} - \frac{\xi h_f^2}{M_p^2}\right) - \frac{3}{4}\ln\frac{1+\frac{\xi h_i^2}{M_p^2}}{1+\frac{\xi h_f^2}{M_p^2}} \tag{3.22}$$

The CMB scale perturbations were set up approximately $\mathcal{N} = 60$ e-foldings before the end of inflation. By requiring $\mathcal{N} = 60$ and $\chi_f = \chi_{end}$ we can solve for $\chi_i = \chi_{cmb}$ to be

$$\chi_{cmb} \simeq 5.45 M_p \tag{3.23}$$

Equivalently $h_{cmb} \simeq 9.21 M_p/\sqrt{\xi}$. Note that $\mathcal{N}$ and χ_{cmb} are independent of ξ. In the slow roll limit, it is straightforward to calculate the scalar spectral index n_s, its running $d\ln n_s/d\ln k$, and the tensor-to-scalar ratio r. These are given by the standard formulae

$$\begin{aligned}
n_s - 1 &= -6\epsilon + 2\eta = -\frac{8}{3}\theta^2(1 + 2\theta^2) \\
r &= 16\epsilon = \frac{64}{3}\theta^4 \\
\alpha_s = \frac{d\ln n_s}{d\ln k} &= -2\zeta + 16\epsilon\eta - 24\epsilon^2 = -\frac{32}{9}\theta^4(1 + 4\theta^2 + 4\theta^4)
\end{aligned} \tag{3.24}$$

where $\theta = M_p/(\sqrt{\xi}h_{cmb})$ and its clear from above that the spectrum is red-tilted meaning $n_s < 1$. Using χ_{comb} obtained above, we can write these observables down immediately in terms of the higgs self coupling λ

$$\begin{aligned}
n_s - 1 &\approx 0.9678 - 0.0239\frac{d\ln\lambda}{d\ln h} - 0.1706\left(\frac{d\ln\lambda}{d\ln h}\right)^2 + 0.3412\frac{d^2\ln\lambda}{d(\ln h)^2} \\
r &\approx 0.00296 + 0.1272\frac{d\ln\lambda}{d\ln h} + 1.365\left(\frac{d\ln\lambda}{d\ln h}\right)^2 \\
\alpha_s &\approx -0.0005233 - 0.0116\frac{d\ln\lambda}{d\ln h}
\end{aligned} \tag{3.25}$$

The amplitude of curvature perturbations is given by

$$\Delta_{\mathcal{R}}^2 = \frac{1}{24\pi^2 M_p^2}\frac{U(h_{cmb})}{\epsilon(h_{cmb})} \simeq 2.359\frac{\sqrt{\lambda}M_p}{\xi}\frac{1}{1 + 21.46\; d\ln\lambda/d\ln h} \tag{3.26}$$

33

From CMB observations, we know that $\Delta_\mathcal{R} \approx 5 \times 10^{-5} M_p$ and so we finally obtain an expression for the non-minimal coupling

$$\xi \approx \frac{47183\sqrt{\lambda}}{1 + 21.46 \ d\ln\lambda/d\ln h} \tag{3.27}$$

and thus Higgs inflation requires $\xi \approx 17000$ for $\lambda \approx 0.13$. The energy scale of inflation is then predicted to be

$$V_0 \approx (0.79 \times 10^{16} \text{ GeV})^4 \tag{3.28}$$

leading to a tensor-to-scalar ratio, assume scalar density perturbations fixed by CMB observations, $r \approx 0.0036$. To obtain a large value of r in Higgs inflationary models isn't generally possible because HI potential asymptotes to a constant at large field values where inflation occurs. This flat potential then results in relatively large density perturbations, which, in order to then match observations, constrain the magnitude of the potential, resulting in a small tensor contribution.

3.3   Standard Model Effective Potential in Higgs Inflation

The Standard model effective potential, (as discussed in the Appendix D) requires modifications in the context of HI. The canonical Standard Model effective potential is calculated (i) to the one-loop order, (ii) working in the $\overline{\text{MS}}$ renormalization scheme with renormalization scale μ, and (iii) in the renormalizable class of gauges (R_ξ) as follows:

$$V_{\text{eff}}(h) = V^{(0)}(h) + V^{(1)}(h) \ . \tag{3.29}$$

The tree-level potential is

$$V^{(0)}(h) = \frac{\lambda}{4} h^4 \ , \tag{3.30}$$

and we can neglect the $O(h^0)$ and $O(h^2)$ terms for the purposes of studying HI where the field value is large. The one-loop correction is [87] (see also [80] for gauge dependent factors)

$$
\begin{aligned}
V^{(1)}(h) = {} & -\frac{12}{4}\frac{\tilde{m}_t^4}{16\pi^2}\left(\ln\frac{\tilde{m}_t^2}{\mu^2} - \frac{3}{2}\right) + \frac{6}{4}\frac{\tilde{m}_W^4}{16\pi^2}\left(\ln\frac{\tilde{m}_W^2}{\mu^2} - \frac{5}{6}\right) + \frac{3}{4}\frac{\tilde{m}_Z^4}{16\pi^2}\left(\ln\frac{\tilde{m}_Z^2}{\mu^2} - \frac{5}{6}\right) \\
& + \frac{1}{4}\frac{\tilde{m}_G^4}{16\pi^2}\left(\ln\frac{\tilde{m}_G^2}{\mu^2} - \frac{3}{2}\right) + \frac{2}{4}\frac{\tilde{m}_{G^\pm}^4}{16\pi^2}\left(\ln\frac{\tilde{m}_{G^\pm}^2}{\mu^2} - \frac{3}{2}\right) \\
& - \frac{2}{4}\frac{\tilde{m}_{cW}^4}{16\pi^2}\left(\ln\frac{\tilde{m}_{cW}^2}{\mu^2} - \frac{3}{2}\right) - \frac{1}{4}\frac{\tilde{m}_{cZ}^4}{16\pi^2}\left(\ln\frac{\tilde{m}_{cZ}^2}{\mu^2} - \frac{3}{2}\right)
\end{aligned}
\tag{3.31}
$$

where we have neglected the light fermions. We also neglect the contribution from the Higgs mass term. During inflation, the potential is very flat and this contribution is subdominant. The remaining SM fields, the massless photon and gluons, do not enter the effective potential at the one-loop order. The effective masses are

$$
\begin{aligned}
\text{Top Quark} && \tilde{m}_t^2 &= \frac{y_t^2}{2\Omega^2}h^2 \\
\text{W-Bosons} && \tilde{m}_W^2 &= \frac{g^2}{4\Omega^2}h^2 \\
\text{Z-Bosons} && \tilde{m}_Z^2 &= \frac{g^2+g'^2}{4\Omega^2}h^2 \\
\text{Higgs Boson} && \tilde{m}_H^2 &= \frac{3\lambda}{\Omega^4}h^2\frac{1-\xi h^2/M_P^2}{\Omega^2+6\xi^2 h^2/M_P^2} \\
\text{Neutral Goldstone} && \tilde{m}_G^2 &= \frac{\lambda}{\Omega^4}h^2 + \tilde{m}_{cZ}^2 \\
\text{Charged Goldstones} && \tilde{m}_{G^\pm}^2 &= \frac{\lambda}{\Omega^4}h^2 + \tilde{m}_{cW}^2 \\
\text{Ghosts} && \tilde{m}_{cZ}^2 &= \xi_{\text{gf}}\tilde{m}_Z^2 \\
\text{Ghosts} && \tilde{m}_{cW}^2 &= \xi_{\text{gf}}\tilde{m}_W^2
\end{aligned}
\tag{3.32}
$$

where $\Omega^2 = 1+\xi h^2/M_P^2$ was given by Eq. (3.5). We denote the gauge fixing parameter by ξ_{gf} to distinguish it from the non-minimal gravitational coupling parameter, ξ. We implement the RG improvement as per [88, 89, 90]. (See also the reviews [87, 91]). This consists of (1) solving the RG equations (RGEs) to determine the running parameters as functions of the RG flow parameter t, (2) replacing the various coupling constants in V_{eff} with the corresponding running parameter, and (3) evaluating the

RG flow parameter at the appropriate value $t = t_*$ so as to minimize the would-be large logarithms.

For the sake of discussion, let us denote the running parameters collectively as $\hat{c}_i(t) = \left\{ \hat{g}_3(t), \hat{g}_2(t), \hat{g}_1(t), \hat{\lambda}(t), \hat{y}_t(t), \hat{\xi}(t) \right\}$ where $g_2 = g$ and $g_1 = g'$. Then the RGEs take the form $\beta_{\hat{c}_i}/(1+\gamma) = d\hat{c}_i/dt$ with the boundary condition $\hat{c}_i(t = 0) = c_{i,0}$. Here γ is the anomalous dimension of the Higgs field. We neglect the running of the gauge-fixing parameter, ξ_{gf}, since it is self-renormalized. This approximation is reasonable since we focus on $\xi_{\text{gf}} < 4\pi$; for larger values of ξ_{gf}, perturbativity becomes an issue. The Higgs field runs according to $-\gamma\hat{h} = d\hat{h}/dt$ where the anomalous dimension $\gamma(t)$ is given as [92]

$$
\begin{aligned}
\gamma = \ & \frac{1}{(4\pi)^2} \left[-\frac{9}{4}\left(1 - \frac{\xi_{\text{gf}}}{3}\right)g_2^2 - \frac{3}{4}\left(1 - \frac{\xi_{\text{gf}}}{3}\right)g_1^2 + 3y_t^2 \right] \\
& - \frac{1}{(4\pi)^4} \left[\left(\frac{271}{32} - 3\xi_{\text{gf}} - \frac{3}{8}\xi_{\text{gf}}^2\right)g_2^4 - \frac{9}{16}g_1^2 g_2^2 - 6\lambda^2 - \frac{431}{96}g_1^4 \right. \\
& \left. - \frac{5}{2}\left(\frac{9}{4}g_2^2 + \frac{17}{12}g_1^2 + 8g_3^2\right)y_t^2 + \frac{27}{4}y_t^4 \right]
\end{aligned}
\tag{3.33}
$$

This last equation may be solved immediately along with the boundary condition $\hat{h}(t = 0) = h_c$ to obtain

$$
\hat{h}(t) = h_c\, e^{\hat{\Gamma}(t)}
\tag{3.34}
$$

where $\hat{\Gamma}(t) = -\int_0^t \gamma(t')/(1+\gamma(t'))\, dt'$, and we seek to calculate the effective potential as a function of h_c. The beta functions are independent of ξ_{gf}, but the anomalous dimension is gauge-variant since the Higgs field is a gauge-variant operator. Finally, the renormalization scale runs according to $\hat{\mu} = d\hat{\mu}/dt$, which may be solved along with $\hat{\mu}(t = 0) = \mu_0$ to obtain $\hat{\mu}(t) = \mu_0 e^t$. We solve the one-loop beta functions using the Mathematica code made publicly available by Fedor Bezrukov at `http://www.inr.ac.ru/~fedor/SM/` . The code implements the matching at the electroweak

36

scale to determine the couplings, $c_{i,0}$, at the scale $\mu_0 = M_t$ in terms of the physical masses and parameters. The code was extended (1) by generalizing the anomalous dimension to the R_ξ gauge as in Eq. (3.33), and (2) by including the field-dependent factors of

$$s = \frac{1 + \frac{\hat{\xi}(t)\hat{h}(t)^2}{M_P^2}}{1 + (1 + 6\hat{\xi}(t))\frac{\hat{\xi}(t)\hat{h}(t)^2}{M_P^2}} \tag{3.35}$$

in the two-loop beta functions, as indicated by [59]. The factor of s arises because of the non-canonical Higgs kinetic term, and it appears in the commutator of the Higgs field with its conjugate momentum [55]. Finally the RG-improved effective potential is evaluated as in Eq. (D.39) after making the replacements $\lambda \to \hat{\lambda}(t_*)$, $g \to \hat{g}(t_*)$, $h \to \hat{h}(t_*)$, $\mu \to \hat{\mu}(t_*)$, and so on. The RG flow parameter, t_*, is chosen to minimize the would-be large logarithm arising from the top quark. This is accomplished by solving

$$\left.\frac{\hat{y}_t(t)^2\hat{h}(t)^2}{2(1 + \frac{\hat{\xi}(t)\hat{h}(t)^2}{M_P^2})\hat{\mu}(t)^2}\right|_{t=t_*} = 1 \;, \tag{3.36}$$

which must be done numerically. Note that t_* is an implicit function of the field variable, h_c. This can be seen by writing

$$t_* = \frac{1}{2}\ln\left[\frac{\hat{y}_t(t_*)^2 e^{2\hat{\Gamma}(t_*)}h_c^2}{2\mu_0^2}\right] \approx \frac{1}{2}\ln\left[\frac{y_0^2 h_c^2}{2\mu_0^2}\right] \;. \tag{3.37}$$

Using Eq. (3.36), the commutator factor in Eq. (3.35) is written as

$$s = \left[1 + 12\frac{\hat{\xi}(t)^2\hat{\mu}(t)^2}{\hat{y}_t^2 M_P^2}\right]^{-1} \;, \tag{3.38}$$

and the field dependence drops out.

3.4 Gauge Dependence Ambiguities

When working with a gauge theory, such as the Standard Model electroweak sector, calculations typically involve spurious gauge dependence that cancels when

physical observable are calculated. For example, in a spontaneously broken Yang-Mills theory one may work in the renormalizable class of gauges (R_ξ) upon augmenting the Lagrangian with a gauge fixing term $\mathcal{L}_{gf} = -G^a G^a/2$ where $G^a = (1/\sqrt{\xi_{\mathrm{gf}}})(\partial_\mu A^{a\,\mu} - \xi g F^a_{\;i} \chi_i)$ where χ_i are the would-be Goldstone boson fields and $F^a_{\;i} = T^a_{ij} v_j$ with T^a_{ij} the symmetry generators and v_j the symmetry-breaking vacuum expectation value. (See, *e.g.*, [79]). A corresponding Fadeev-Popov ghost term is also added. Physical or "on-shell" quantities, such as cross sections and decay rates, may be calculated perturbatively, and any dependence on the gauge fixing parameter, ξ_{gf}, cancels order-by-order. Unphysical or "off-shell" quantities, such as propagators or one-particle irreducible Green's functions, may harmlessly retain the spurious gauge dependence.

The Coleman-Weinberg effective action Γ_{eff} and effective potential V_{eff} [93] have become standard tools in the study of vacuum structure, phase transitions, and inflation. The effective action is the generating functional of one-particle irreducible Green's functions, and therefore it is important to recognize that both Γ_{eff} and V_{eff} are off-shell quantities, which will carry spurious gauge dependence [74]. When applying the effective potential to a problem, special care must be taken to extract gauge-invariant information. In particular, the Nielsen identities express the gauge invariance of the effective potential at its stationary points, but derivatives of the effective potential are not generally gauge invariant [77]. This suggests that inflationary observables, e.g. n_S, r, and $dn_S/d\ln k$, naively extracted directly from the slow roll parameters will acquire a spurious gauge dependence.

Ideally one would like to determine the "correct" procedure for calculating physical quantities like n_S from a given model in such a way that the spurious gauge

dependence is canceled. There have been significant efforts made in this direction [69, 70], but a full gauge invariant formalism is yet to be developed. Here we will take a different approach that is more aligned with recent work on the gauge dependence of phase transition calculations [80, 84, 85]. Specifically, we numerically perform the "naive" HI calculation using the R_ξ gauge effective potential and RG-improvement to assess the sensitivity of the inflationary observables to the spurious gauge dependence.

After performing the RG improvement, the parameter λ that appears in Eq. (3.18) should be understood as the running coupling evaluated at the scale of inflation. Generally, $\lambda < 0.1$ and its value depends upon the physical Higgs boson and top quark masses at the input scale. For the best fit observed values, $M_H \approx 125$ GeV and $M_t \approx 173$ GeV, the coupling runs negative at $h \approx 10^{10} - 10^{12}$ GeV; this is the well-known vacuum stability problem of the Standard Model [72]. Successful HI requires an $O(2\sigma)$ deviation from central values toward either larger Higgs boson mass or smaller top quark mass.

Gauge dependence enters the calculation at two places: explicitly in the one-loop correction to the effective potential and implicitly through the Higgs anomalous dimension upon performing the RG improvement. To calculate the slow roll parameters, *e.g.*

$$\epsilon = \frac{M_P^2}{2}\left(V'/V\right)^2\Big|_{h_{\mathrm{cmb}}} \tag{3.39}$$

the derivatives are taken with respect to χ, *i.e.*, $V'(h(\chi)) = (\partial V/\partial h)(d\chi/dh)^{-1}$. The potential and its derivatives are evaluated at the field value, h_{cmb}, for which the number of e-foldings, given by

$$\mathcal{N} = \int_{h_{\mathrm{end}}}^{h_{\mathrm{cmb}}} dh\, \frac{V(h)}{V'(h)M_P^2}\,, \tag{3.40}$$

39

is $\mathcal{N} = 60$. Inflation terminates at $h = h_{\mathrm{end}}$ where $(M_P^2/2)(V'/V)^2 = 1$. In Fig. 3.3 we show the energy scale of inflation,

$$V_{\mathrm{inf}} = V(h_{\mathrm{cmb}}) , \tag{3.41}$$

as the the Higgs boson and top quark masses are varied, and the non-minimal coupling, $\xi \approx \mathrm{few} \times 10^3$, is determined to match the observed amplitude of scalar perturbations. This demonstrates that the scale of inflation is insensitive to M_H, varying only at the $O(10^{-4})$ level.

To illustrate the gauge dependence, we show in Fig. 3.4 how V_{inf} varies with ξ_{gf}. We find that V_{inf} also changes at a level comparable to its sensitivity to M_H or M_t as the gauge parameter deviates from the Landau gauge ($\xi_{\mathrm{gf}} = 0$). It is therefore important to consider this ambiguity for model building purposes. Note that at larger vales of ξ_{gf} the scale of inflation appears to continue to decrease, but in this limit the perturbative validity of the calculation begins to break down. To resolve this issue, the unphysical degrees of freedom, the Goldstone bosons and ghosts, should be decoupled as the unitary gauge is approached.

Our numerical results appear consistent with the Nielsen identities [77, 78] which capture the gauge dependence of the effective potential. The relevant identity is

$$\left[\xi \frac{\partial}{\partial \xi} + C(\phi, \xi) \frac{\partial}{\partial \phi} \right] V_{\mathrm{eff}}(\phi, \xi) = 0 . \tag{3.42}$$

In the slow roll regime, the gradient of the effective potential is small, and the gauge dependence is proportionally suppressed. We note that a rigorous gauge invariant calculation could perhaps take Eq. (3.42) as a starting point. This might be an interesting avenue for future work, either in the context of HI or other, potentially more viable models of inflation that are embedded in gauge theories.
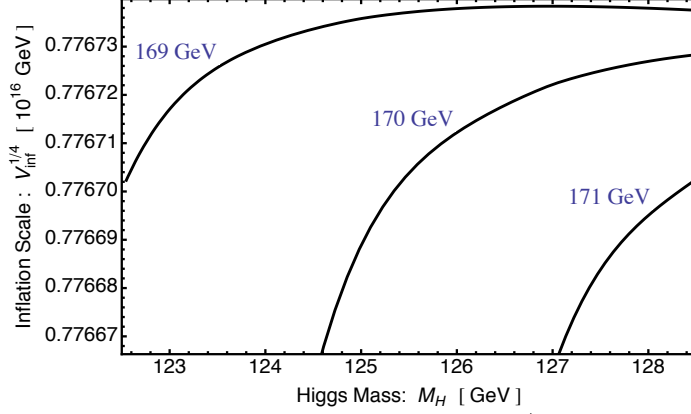
Figure 3.3: The predicted energy scale of inflation, $V_{\text{inf}}^{1/4}$, over a range of Higgs boson masses (M_H), for three values of the top quark mass (M_t), and in the Landau gauge, $\xi_{\text{gf}} = 0$.
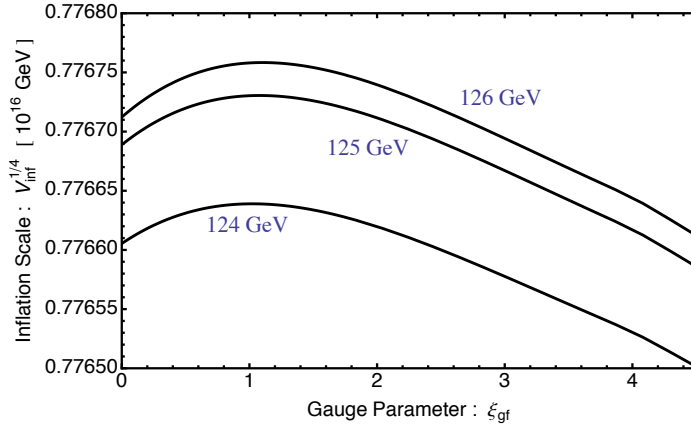
Figure 3.4: The energy scale of inflation, V_{inf}, as the gauge parameter, ξ_{gf}, varies. We fix $M_t = 170$ GeV and show three values of M_H.

3.5   Conclusions

This chapter draws attention to the issue of gauge dependence in the Higgs Infla-tion calculation. We find that observables like the energy scale of inflation acquires an artificial dependence on the gauge fixing parameter by virtue of the gauge dependence of the effective potential from it is extracted. However, we find this gauge dependence of the scale of inflation is comparable to the dependence on other physical parameter uncertainties, which are themselves small.

Chapter 4

LEPTOGENESIS VIA GRAVITINO DECAYS

4.1   Introduction

The Standard Model is a precise theory backed by strong experimental experience and a tight mathematical structure. It is a quantum field theory based on relativistic invariance and one of the consequences of that is CPT invariance - that is, invariance under the combined shift of discrete transformations of charge conjugation, parity and time reversal. Practically, this means that for any particle species X with mass m_X, charge Q_X and (say) decay width Γ_X, there exists an anti-particle with the same mass and decay width but opposite quantum number Q_{-X} where in general $Q_X = 0$ is possible (implying the particle is charge neutral like the Higgs boson is neutral under electric charge). Therefore, we expect this symmetry to be around us, meaning equal numbers of particles and anti-particles not only in our local patch but also the universe at large.

However, this conclusion isn't borne out by observations of either our local neighborhood or even the universe at large. For example, there is no evidence of anti-matter in the solar system and the observational bounds on anti-helium is

$$\frac{\overline{n}_{He}}{n_{He}} < 3.1 \times 10^{-6} \tag{4.1}$$

If on the other hand matter and anti-matter exist in equal amounts, they must be spatially well separated so that they can't annihilate. If regions of equal protons and anti-protons existed in the primordial universe for example, they would annihilate

42

into pions which decay into photons, $\pi \to 2\gamma$ and this injection of photons would significantly distort the CMB, kind of distortion (μ) we don't observe. Based on this we can put bounds on the separation length between matter and anti-matter $l_B \gtrsim 10$ kpc. Further, the abundances of light elements from big bang nucleosynthesis which matches observations well requires as input matter asymmetry.

The matter/anti-matter asymmetry is quantified simply as the difference in the number density of matter vs anti-matter. However, this scales with cosmological expansion as $a(t)^{-3}$ and we can divide this factor out by the number density of photons,

$$\eta \equiv \frac{n_B}{n_\gamma} = \frac{n_b - n_{\bar{b}}}{n_\gamma} \tag{4.2}$$

The number density of photons is related by thermodynamical relation to its temperature simply as

$$n_\gamma = 2 \frac{\zeta(3)}{\pi^2} T_\gamma^3 \tag{4.3}$$

where the temperature of the CMB, $T_\gamma = 2.725$K and thus

$$n_\gamma \approx 411 \text{ cm}^{-3} \tag{4.4}$$

The current experimentally determined value of $\eta = 6.2 \times 10^{-10}$. The ratio of baryon to entropy is also used frequently. This is because the entropy density also scales as a^{-3} and mostly relativistic species contribute to entropy density. With photons being the largest component of relativistic energy density, these two are easily related.

The fact that $\eta \neq 0$ and is a time independent measure of the baryon asymmetry implies the existence of some mechanism that must have been operable in the early

universe which could have created this asymmetry. Any cosmological mechanism that generates this asymmetry is generically called Baryogenesis. However, the exact model of baryogenesis is one of the central open questions in modern cosmology. In the Appendix E, we describe conditions required for successful baryogenesis including some common models. In this chapter, we propose a new mechanism of baryogenesis, which relies on the decay of the spin-3/2 partner of the graviton that arises in Supergravity theories called the gravitino. An introduction to Supersymmetry is also provided in Appendix F.

4.2 Unique Role of Gravitinos

The gravitino has two features that, taken together, make it unique among the particles of the Minimal Supersymmetric Standard Model (MSSM): the gravitino mass is directly related to the scale of supersymmetry breaking, and its interactions are fixed to be uniform and of gravitational strength. Together these properties imply that if it is kinematically allowed for the gravitino to decay, then its decay will necessarily be out of equilibrium. That is to say, the inverse decay process occurs with a rate $\Gamma_{inv} \sim T^3/M_P^2$, which is always smaller than the Hubble expansion rate $H \sim T^2/M_P$. A departure from thermal equilibrium is one of the three necessary conditions for the creation of the baryon asymmetry of the universe (BAU) [94]. The two remaining conditions, the violation of CP and the violation of baryon number (B), are already present in the MSSM through SUSY-breaking and R-parity violating operators. This makes the gravitino a prime candidate with which to study the origin of the cosmological baryon asymmetry.

A possible connection between the gravitino and the cosmic baryon asymmetry was first identified by Cline and Raby [95], hereafter denoted as CR, who recognized

that the so-called 'gravitino problem' and the problem of the cosmic baryon asymmetry could have a common solution. If the gravitino decays prior to the onset of Big Bang Nucelosynthesis (BBN) at $T_{BBN} \approx 1$ MeV, then the abundance of light elements is not disrupted and the gravitino problem is avoided [96, 97, 98, 99]. The gravitino decays with a rate [100]

$$\Gamma_{3/2} = \frac{N_{\mathrm{eff}}}{2\pi} \frac{m_{3/2}^3}{M_P^2} \tag{4.5}$$

where N_{eff} is the effective number of decay channels, $m_{3/2}$ is the gravitino mass, and $M_P \approx 2.4 \times 10^{18}$ GeV is the reduced Planck mass. Therefore, a gravitino with mass $m_{3/2} \geq O(10 \text{ TeV})$ will safely decay at a temperature $T_d \geq T_{BBN}$. CR supposed that these gravitinos decay into a quark / anti-squark pair and that the anti-squark subsequently decays through the MSSM's B-violating operator

$$W_{\mathrm{BV}} = \frac{1}{2} \lambda'' \hat{U}^c \hat{D}^c \hat{D}^c , \tag{4.6}$$

(see, e.g., [101] for a review of R-parity violation), and showed that such a decay could give rise to the cosmological baryon asymmetry.

The present work explores how a baryon asymmetry can be generated from gravitino decays at a different scale, without the aid of the MSSM's B-violating operator. If gravitino decay gives rise to a lepton asymmetry, this asymmetry can be transferred to the baryons by the weak sphaleron process [102], which violates the anomalous $B + L$ charge conservation and rapidly coverts L-number into B-number, as in the by now standard leptogenesis scenario in which the lepton asymmetry arises from the out of equilibrium decay of the Majorana neutrino [103] (see also [104] for a review).

In some sense, gravitino leptogenesis is more general than either the case considered by CR, or standard leptogenesis, as the gravitino can decay through one of the

MSSM's three lepton number violating operators:

$$W_{\mathrm{LV}} = \frac{1}{2}\lambda\hat{L}\hat{L}\hat{E}^c + \frac{1}{2}\lambda'\hat{L}\hat{Q}\hat{D}^c + \mu'\hat{H}_u\hat{L} \ . \tag{4.7}$$

Since weak sphalerons go out of equiliburm after electroweak symmetry breaking occurs at $T_{ew} \approx 100$ GeV [102], to ensure that the gravitino decays prior to this time, we obtain a lower bound on the gravitino mass: $m_{3/2} \gtrsim 10^8$ GeV (see Sec. 4.3 for details). Therefore, a gravitino leptogenesis mechanism can be operative for models with a high SUSY-breaking scale, $M_S \gtrsim 10^{13}$ GeV.

The organization of this chapter is as follows. In Sec. 4.3, we discuss the cosmological context of gravitino leptogenesis, and specifically we derive bounds on the gravitino mass and reheat temperature which are imposed by requiring that gravitinos decay prior to electroweak symmetry breaking. Sec. 4.4 describes the CR gravitino baryogenesis scenario [95] because it forms a useful template for our leptogenesis model. In Sec. 4.5, we consider each of the MSSM R-parity violating operators in turn, including a brief review of the B-violating operator that was previously studied by CR. For the other operators, we determine the parameter ranges required to generate the baryon asymmetry of the universe through a gravitino leptogenesis mechanism. In Sec. 4.6 we summarize our conclusions.

4.3 Cosmological Context of Gravitino Decays

In this section, we will derive an expression for the baryon asymmetry of the universe in terms of i) the gravitino mass, ii) the reheat temperature after inflation, and iii) a parameter β which controls the branching fraction of gravitino decays into L-number. In the following section we then present detailed estimates of β for each of the MSSM's R-parity violating operators.

4.3.1 Gravitino Production

Inflation dilutes any primordial gravitino abundance, but during reheating gravitinos are regenerated by interactions in the hot plasma. This regeneration occurs at $T \approx T_{RH}$, which is generically much earlier than gravitino decay. During adiabatic expansion following inflation, the gravitino to entropy ratio $Y_{3/2} \equiv n_{3/2}/s$ is conserved. We denote the number density of gravitinos by $n_{3/2}$ and $s = \frac{2\pi^2}{45} g_*(T) T^3$ is the entropy density of the plasma, where g_* is the number of helicity states with equilibrium number density in the relativistic gas at temperature T. At the (later) time of gravitino decay, when all of the SM species are light and all but a few of the superpartners are heavy and decoupled, we have $g_* \gtrsim 100$. By summing the various production processes and solving the thermally averaged Boltzmann equation the gravitino relic abundance has been estimated to be [98, 99]

$$Y_{3/2} = \left(\frac{45\zeta(3)}{2\pi^4} \frac{1}{g_*(T_{RH})} \right)^2 \frac{s(T_{RH}) \langle \sigma_{3/2} v \rangle}{H(T_{RH})} . \tag{4.8}$$

In making this estimate the universe is assumed to be radiation dominated with a Hubble parameter $H(T) \approx \sqrt{\pi^2 g_*(T)/90} \, T^2/M_P$.

The thermally averaged gravitino production cross section can be written as $\langle \sigma_{3/2} v \rangle = C_i g_i^2 M_P^{-2}$, where g_i represent gauge couplings and the sum runs over gauge groups, and $C_i = O(1 - 10)$ [99]. This result reflects the fact that gravitinos only interact with a gravitational strength and that the higher-spin gauge fields are required to build up the spin-3/2 gravitino. The largest contribution comes from the $SU3$ group for which $C_3 \approx 10$ and $g_3 \approx 1$, and therefore we will conservatively assume $\langle \sigma_{3/2} v \rangle = 10 M_P^{-2}$. This gives the gravitino relic abundance estimate

$$Y_{3/2} \approx 10^{-10} \frac{T_{RH}}{10^{12} \text{ GeV}}. \tag{4.9}$$

In order for gravitinos to be sufficiently abundant to account for the baryon asymme-

try, $Y_B \sim 10^{-10}$, the reheat temperature must be sufficiently high, $T_{RH} \gtrsim 10^{12}$ GeV. On the other hand, if the gravitinos could be produced from a direct coupling to the inflaton, then it may be possible to relax the bound on T_{RH} due to preheating. Such a scenario, however, would depend on the nature of the gravitino–inflaton coupling and thereby introduce additional model dependent questions.

4.3.2   Gravitino Decay

As can be seen from Eq. (4.9), the relic gravitino abundance is generally low, and therefore presumably the gravitinos can decay before they come to dominate the energy density of the universe. We can confirm this expectation by comparing the energy density of radiation, $\rho = \frac{3}{4} sT$, with the energy density in gravitinos, $\rho_{3/2} = m_{3/2} n_{3/2}$. Imposing $\rho_{3/2} = \rho$ gives

$$T_{\text{eq}} = \frac{4}{3} Y_{3/2} m_{3/2} \approx 0.1 \text{ MeV} \frac{T_{RH}}{10^{10} \text{ GeV}} \frac{m_{3/2}}{10^8 \text{ GeV}} \ . \tag{4.10}$$

Since successful gravitino leptogenesis requires the gravitino to decay prior to electroweak symmetry breaking at $T_{ew} \sim 10^2$ GeV, it is clear in light of Eq. (4.10) that the universe will be radiation dominated at the time of gravitino decay.

The couplings of the gravitino are only gravitational strength, and its decay rate is given by [100]

$$\Gamma_{3/2} \approx \frac{N_{\text{eff}}}{2\pi} \frac{m_{3/2}^3}{M_P^2} \ . \tag{4.11}$$

where N_{eff} is the effective number of decay channels. If all the decay products are much lighter than the gravitino, then N_{eff} just counts the total number of kinematically allowed channels with relative weighting between the chiral superfield and vector superfield final states due to helicity:

$$N_{\text{eff}} = N_V + \frac{1}{12} N_\chi \tag{4.12}$$

where N_V is the number of vector superfields and N_χ is the number of chiral superfields into which the gravitino can decay. If the entire MSSM particle content is light compared to the gravitino, then $N_V = 1 + 3 + 8 = 12$ and $N_\chi = 36 + 9 + 4 = 49$, which give $N_{\text{eff}} \simeq 16$.

We will work in an instantaneous decay approximation with a gravitino lifetime is $\tau_{3/2} = \Gamma_{3/2}^{-1}$. The temperature T_d at which gravitino decays take place is given by

$$\tau = t_{\text{age}}(T_d) \tag{4.13}$$

where $t_{\text{age}}(T)$ is the age of the universe as a function of temperature. During the radiation dominated era

$$t_{\text{age}}(T) = \frac{1}{2}\frac{1}{H} = \sqrt{\frac{45}{2\pi^2 g_*}}\frac{M_P}{T^2} \tag{4.14}$$

where we have used $H = \sqrt{\rho/3M_P^2}$. Solving for T_d one finds

$$T_d = m_{3/2}\left(\frac{3}{2}\frac{N_{\text{eff}}}{\pi^2}\sqrt{\frac{5}{2g_*}}\frac{m_{3/2}}{M_P}\right)^{1/2} \simeq 400 \text{ GeV} \left(\frac{m_{3/2}}{10^8 \text{ GeV}}\right)^{3/2}. \tag{4.15}$$

Let us now discuss the constraints on $m_{3/2}$ and T_{RH}. Typically these parameters are constrained by the requirement that stable gravitinos do not overclose the universe [96, 97] or the requirement that late decaying gravitinos do not disrupt the abundance of light elements or distort the cosmic microwave background [98, 99]. In our model, the gravitino must satisfy an even more stringent requirement. It must decay before the electroweak phase transition takes place when the electroweak sphalerons are still in equilibrium. Imposing $T_d \gtrsim 100$ GeV, we then obtain a lower bound on the gravitino mass

$$m_{3/2} \gtrsim 10^8 \text{ GeV} . \tag{4.16}$$

It is evident that successful gravitino leptogenesis requires an especially heavy gravitino. Since the gravitino mass is set directly by the scale of SUSY breaking, M_S,

through the relationship

$$m_{3/2} \approx \frac{M_S^2}{M_P} \, , \tag{4.17}$$

the bound Eq. (4.16) implies

$$M_S \gtrsim 10^{13} \text{ GeV} \, . \tag{4.18}$$

Such a large scale of SUSY-breaking is less theoretically attractive than connecting it to the weak scale in order to resolve the hierarchy problem, but not only is such a scenario is not ruled out on empirical grounds [96, 97], weak scale SUSY breaking models are becoming more tightly constrained due to the absence of SUSY-induced effects at colliders, including the LHC. High scale SUSY breaking models have in fact already been considered as interesting alternatives to weak scale SUSY for other reasons[105, 106, 107].

There is no direct empirical probe of the reheat temperature, and the only hard bound is $T_{RH} > T_{BBN} \approx 1$ MeV. However, energy conservation arguments relate the reheat temperature to the energy scale of inflation $V_{\mathrm{inf}} = 3M_P^2 H_{\mathrm{inf}}^2 \sim T_{RH}^4$. The scale of inflation, in turn, is probed by tensor perturbations in the cosmic microwave background (CMB) radiation power spectrum. In particular, the ratio of the amplitudes of tensor and scalar perturbations, $r = \Delta_h^2/\Delta_{\mathcal{R}}^2$, is, for single field inflation models, generally proportional to the energy scale of inflation $V_{\mathrm{inf}} \approx (10^{16} \text{ GeV})^4(r/.01)$ [53] [108] [8]. Precisions measurements of the CMB by the Planck satellite yield the bound $r < 0.11$ at 95 % CL [109]. This translates into an upper bound on the reheat temperature,

$$T_{RH} \lesssim O(10^{16} \text{ GeV}) \, , \tag{4.19}$$

which in turn implies an upper bound on the gravitino relic abundance, $Y_{3/2} \lesssim O(10^{-6})$, via Eq. (4.9).

4.3.3 Lepton Number Generation

The gravitino decay rate, described earlier, is estimated through its dominant, standard decay channels. We now suppose that the gravitino has a number of sub-dominant decay channels which are mediated by CP- and L-number-violating interactions. This will provide the conditions necessary for the creation of a lepton asymmetry n_L, which will be proportional to the number density of gravitinos before they decay multiplied by the branching ratio for the decays which lead to the asymmetry. We can therefore write:

$$n_L(T_a) = \beta\, n_{3/2}(T_d) \tag{4.20}$$

where $T_a > T_d$ is the temperature immediately after gravitino decays, assumed to be instantaneous, and the parameter β is defined as the weighted branching fraction

$$\beta = \sum_i L\left[\{f_i\}\right] \mathrm{BR}\left(\tilde{G} \to \{f_i\}\right) \tag{4.21}$$

where the sum runs over all possible final states labeled by $\{f_i\}$, and $L[\{f_i\}]$ is the lepton number of a given final state (possibly negative). In Sec. 4.5 we will evaluate Eq. (4.21) in terms of the model parameters. For now, we will simply treat β as a free parameter.

Since presumably the L-violating decays are rare, we expect $\beta \ll 1$. In the instantaneous decay approximation, the energy density is conserved, and all of the energy in the gravitinos is transferred to radiation. Since the number of thermalized species remains unchanged (since $M_{SUSY} \gg T_d \gg M_{EW}$), the plasma heats up as a result of the energy injection [110]. The energy density after decay ρ is given by

$$\rho(T_a) = \rho^{(0)}(T_d) + \rho_{3/2}(T_d) \tag{4.22}$$

where T_a is the temperature after the gravitinos decay and we use the superscript "(0)"

to denote the era prior to gravitino decay. The lepton asymmetry is parametrized by

$$Y_L = \frac{n_L}{s} \ . \tag{4.23}$$

Using Eqns. (4.20) and (4.22) and $s = (4/3)\rho/T$, we can evaluate the lepton asymmetry as

$$Y_L = \frac{\beta\,Y_{3/2}}{\left(1 + \frac{4}{3}\frac{m_{3/2}}{T_d}Y_{3/2}\right)^{3/4}} \ . \tag{4.24}$$

Using Eqns. (4.9) and (4.15), we see that Y_L is a function of the free parameters $m_{3/2}$, T_{RH}, and β. For the allowed range of parameters, $m_{3/2} \gtrsim 10^8$ GeV and $T_{RH} \lesssim 10^{16}$ GeV, the ratio $m_{3/2}Y_{3/2}/T_d \ll 1$ and the entropy injection is negligible. Also, provided that $T_a \gg T_{EW}$, the EW sphalerons will then efficiently convert L-number into B-number. The final baryon asymmetry is obtained from Y_L after multiplying by a factor of $-8/23$ [111] to obtain

$$Y_B \approx -\frac{8}{23}\beta Y_{3/2} \ . \tag{4.25}$$

Note that $Y_B > 0$ requires $\beta < 0$.

The observed value of the baryon asymmetry is $(Y_B)_{\mathrm{phys}} \approx 0.89 \times 10^{-10}$ [109]. Since the effective parameter β is independent of $m_{3/2}$ and T_{RH}, we can plot the the value of β which is required to give $Y_B = (Y_B)_{\mathrm{phys}}$, shown in Fig. 4.1. If β is larger (smaller) than the value shown at a given $m_{3/2}$ and T_{RH} then B-number is overabundant (underabundant). Inspecting the figure reveals that if we hope to satisfy both constraints Eq. (4.16) and Eq. (4.19), then we must have $\beta > \beta_{\mathrm{min}}$ with

$$\beta_{\mathrm{min}} \approx 10^{-4} \tag{4.26}$$

in order for gravitino leptogenesis to be successful. Alternatively, requiring $\beta < 1$ yields a lower bound on the reheat temperature $T_{RH} > 10^{12}$ GeV, which then provides a firm limit on gravitino leptogenesis scenarios of the type we consider here.
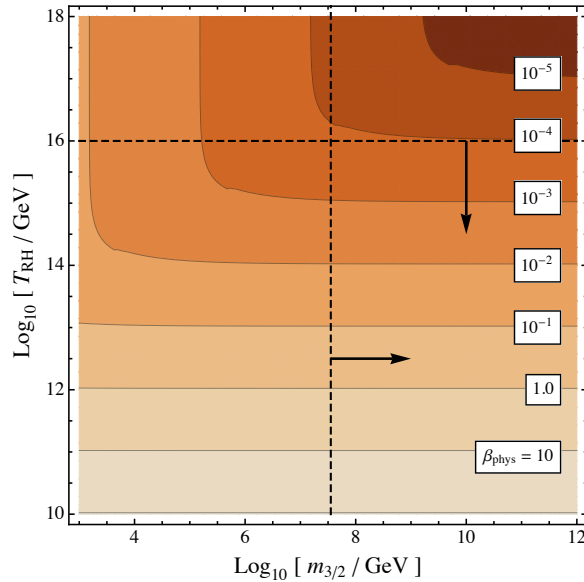
Figure 4.1: The value of β required to ensure $Y_B = (Y_B)_{\text{phys}}$ as $m_{3/2}$ and T_{RH} are varied. See text for further discussion.

4.4 Gravitino Baryogenesis Details

We review here details of the gravitino decay calculation of Ref. [95] that are relevant for our leptogenesis analysis. The baryon asymmetry parameter is given by:

$$\beta = \text{BR}[\bar{\tilde{q}} \to qq] \times \sum_{q,\tilde{q}} \left\{ \left(\text{BR}[\tilde{G} \to q\bar{\tilde{q}}] - \text{BR}[\tilde{G} \to \bar{q}\tilde{q}] \right) \right. \tag{4.27}$$

$$\left. + \sum_{\tilde{X}=\tilde{g},\tilde{Z},\tilde{\gamma}} \text{BR}[\tilde{G} \to X\tilde{X}] \left(\text{BR}[\tilde{X} \to q\bar{\tilde{q}}] - \text{BR}[\tilde{X} \to \bar{q}\tilde{q}] \right) \right\}$$

In principle the sum runs over all quark and squark species, but in light of the interactions in Eq. (4.38), CP violation is only carried by quanta of the fields $s^c, b^c, t^c, \tilde{s}^c, \tilde{b}^c$, and $\tilde{t}^c$. Since these fields carry B-number of $-1/3$, the sum is over $q = \overline{s^c}, \overline{b^c}, \overline{t^c}$ and $\tilde{q} = \bar{\tilde{s}}^c, \bar{\tilde{b}}^c, \bar{\tilde{t}}^c$. The expression Eq. (4.39) assumes that $\text{BR}[\bar{\tilde{q}} \to qq] = \text{BR}[\tilde{q} \to \bar{q}\bar{q}] \equiv \text{BR}_{\text{BV}}$ since any difference must be proportional to the CP violating parameter, which would yield a higher order correction to β.

These various branching ratios in Eq. (4.39) can be calculated exactly [95], but

since we are primarily interested in exploring the possibility of obtaining the correct order of magnitude for the resulting baryon asymmetry here, we will assume the hierarchy of mass scales $m_{3/2} > m_{\tilde{X}} > m_{\tilde{q}} > m_q$. In this limit, the branching ratios can be estimated from dimensional analysis up to undetermined $O(1)$ prefactors. Since the gravitino has a universal gravitational strength coupling, it decays with equal probability into every light species. Then, the branching fraction into the vector supermultiplets can be estimated as

$$\mathrm{BR}[G \to X\tilde{X}] \approx \frac{\mathcal{C}_{\tilde{X}}}{N_{\mathrm{eff}}} \tag{4.28}$$

where $\mathcal{C}_{\tilde{X}}$ is the dimension of the adjoint representation of the gauge group corresponding to the gaugino $\tilde{X}$, i.e.,

$$\mathcal{C}_{\tilde{B}} = \mathcal{C}_{\tilde{Z}} = \mathcal{C}_{\tilde{\gamma}} = 1 \quad , \quad \mathcal{C}_{\tilde{W}} = 3 \quad , \quad \mathcal{C}_{\tilde{g}} = 8 , \tag{4.29}$$

and $N_{\mathrm{eff}} \simeq 16$ is given by Eq. (4.12).

The differential branching fractions into the quark – squark final states are nonzero due to an interference between graphs of the form shown in Fig. 4.2. The CP violation arises from the relative phase of the coupling A''_{332} and the gravitino or gaugino mass parameter. Up to factors of $O(1)$, the interference can be estimated as

$$\left(\mathrm{BR}[\tilde{V} \to q\bar{\tilde{q}}] - \mathrm{BR}[\tilde{V} \to \bar{q}\tilde{q}]\right) \sim \alpha''_{332} \frac{\mathrm{Im}\left[A''_{332}m_{\tilde{V}}\right]}{|m_{\tilde{V}}|^2} \times \begin{cases} 1 & \tilde{V} = \tilde{g}, \tilde{Z}, \tilde{\gamma} \\ \frac{1}{N_{\mathrm{eff}}} & \tilde{V} = \tilde{G} \end{cases} \tag{4.30}$$

where $\alpha''_{332} \equiv |\lambda''_{332}|^2 / 4\pi$. For simplicity one can assume that there is a universal CP-violating parameter $\theta_{\mathrm{CP}} = \mathrm{Arg}[A''_{332}m_{\tilde{V}}]$ for both the gravitino and gaugino masses, and therefore

$$\frac{\mathrm{Im}[A''_{332}m_{\tilde{V}}]}{|m_{\tilde{V}}|^2} = \frac{|A''_{332}|}{|m_{\tilde{V}}|} \sin\theta_{\mathrm{CP}} . \tag{4.31}$$

One can also assume that there is a universal gaugino mass $m_{\tilde{X}} = m_{\tilde{\gamma}} = m_{\tilde{Z}} = m_{\tilde{g}}$. In this case to evaluate Eq. (4.39) one need only sum the possible decay channels. The gravitino, photino, and zino each have 9 decay channels, given by summing over the combinations of three flavors (s^c, t^c, b^c) and three colors. Since the gluino is colored, it has only 3 channels, given by the sum over flavors alone. After these simplifications, Eq. (4.39) becomes

$$\beta \sim \alpha''_{332} \sin\theta_{\mathrm{CP}} \frac{1}{N_{\mathrm{eff}}} \mathrm{Max}\left[9\frac{|A''_{332}|}{|m_{3/2}|}, \ 42\frac{|A''_{332}|}{|m_{\tilde{X}}|}\right] \mathrm{BR}_{\mathrm{BV}} \ . \tag{4.32}$$

Since the relative $O(1)$ factors between the gravitino and gaugino contributions have been left unspecified in Eq. (4.30) one cannot precisely sum the two contributions, and instead one can simply estimate β by taking the larger of the two. The numerical factors of 9 and $42 = 9 + 9 + 8 \cdot 3$ arise from counting the decay channels. Making the further assumption $m_{\tilde{X}} \approx m_{3/2}$ one obtains Eq. (4.40).

One may worry that strong constraints on the RPV coupling λ''_{332} would cause $\mathrm{BR}_{\mathrm{BV}}$, and therefore β, to be too small for baryogenesis to succeed. However, if alternate decay channels are kinematically blocked by spectral constraints then the branching fraction can be $O(1)$. For instance, if the squark is the LSP then $\mathrm{BR}_{\mathrm{BV}} = 1$. More generally, one can suppose that the gluinos are light and the other gauginos are heavy, and in this case the branching fraction is estimated as

$$\epsilon_{\mathrm{BV}} \approx 1 - O\left(\alpha_s/\alpha_{332}\right) \ . \tag{4.33}$$

This helps to evade strong constraints on B-number violation.

4.5   L-number Violating Gravitino Decay Channels

The MSSM admits four operators in the superpotential that violate R-parity. One of these four violates baryon number and the remaining three violate lepton number

(see [101] for a review):

$$W_{\mathrm{RPV}} = W_{\mathrm{BV}} + W_{\mathrm{LV}} \tag{4.34}$$

$$W_{\mathrm{BV}} = \frac{1}{2}\lambda''_{ijk}\hat{U}^c_i\hat{D}^c_j\hat{D}^c_k \tag{4.35}$$

$$W_{\mathrm{LV}} = \frac{1}{2}\lambda_{ijk}\hat{L}_i\hat{L}_j\hat{E}^c_k + \lambda'_{ijk}\hat{L}_i\hat{Q}_j\hat{D}^c_k + \mu'_i\hat{H}_u\hat{L}_i \; . \tag{4.36}$$

In this section, we will focus on each of the three L-number violating operators, in order to calculate the parameter $\beta = n_L/n_{3/2}$, defined by Eq. (4.21), and to assess whether the critical value $\beta_{\min} = 10^{-4}$ can be reached given constraints on the models.

The single B-number violating operator, W_{BV}, has already been shown by CR to be able to give rise to the baryon asymmetry of the universe through gravitino decays [95] (see also [112]). In order to draw a contrast between the CR mechanism and gravitino leptogenesis we briefly review the CR gravitino baryogenesis calculation here.

The B-number violating operator, given by Eq. (4.35), contains 9 distinct terms after the sum over flavor indices has been performed. One may take a conservative approach and assume that only one of these terms is nonzero. In particular, the MSSM superpotential may be extended to include the operator

$$W_{\mathrm{BV}} = \frac{1}{2}\lambda''_{332}\hat{T}^c\hat{B}^c\hat{S}^c \; , \tag{4.37}$$

which violates B-number by one unit. Since this operator does not involve any first generation quarks, it is not strongly constrained by bounds on neutron oscillations and heavy nuclei decay. The other components of λ''_{ijk} are generated at one-loop order due to flavor violation in the quark mass matrix, but the smallness of the quark mixing angles renders these contributions negligible [112].

In this scenario, the baryon asymmetry is generated directly by gravitino decays after weak sphalerons go out of equilibrium. Then, the gravitino need only decay before the onset of BBN at $T_d \approx T_{BBN} \simeq$ MeV, which imposes $m_{3/2} \gtrsim 10$ TeV [97]. The superpotential $W_{\rm BV}$ gives rises to the trilinear interactions

$$\mathcal{L}_{\rm BV} = -\frac{1}{2}\lambda''_{332}\left(t^c b^c \tilde{s}^c + b^c s^c \tilde{t}^c + s^c t^c \tilde{b}^c\right) - \frac{1}{2}A''_{332}\lambda''_{332}\tilde{t}^c \tilde{b}^c \tilde{s}^c + {\rm h.c.} , \qquad (4.38)$$

where the corresponding soft SUSY-breaking term is also included. Quadrilinear B-number violating operators also arise, but these scalar interactions only contribute to gravitino decay at the two loop order.

In the CR scenario, baryogenesis can be divided into two stages. First, CP-violation biases gravitino decays into anti-squarks $(\bar{\tilde{q}})$ over squarks $(\tilde{q})$, and second, B-number is violated when the anti-squarks decay into quark (q) pairs and the squarks decay into anti-quark $(\bar{q})$ pairs. In the first stage, the gravitino can decay into the squark directly or by way of a gaugino $(\tilde{X})$. In the second stage, the squarks decay through the channels $\tilde{q} \to \bar{q}\bar{q}$ and $\bar{\tilde{q}} \to qq$. Thus the two decay chains $\tilde{G} \to q_i\bar{\tilde{q}}_i \to q_i q_j q_k$ and $\tilde{G} \to X\tilde{X} \to Xq_i\bar{\tilde{q}}_i \to Xq_i q_j q_k$ are responsible for generation of the B-number asymmetry. The parameter $\beta = n_B/n_{3/2}$ may be calculated from Eq. (4.21) with the modification that B-number is counted instead of L-number:

$$\beta = {\rm BR}[\bar{\tilde{q}} \to qq] \times \sum_{q,\tilde{q}}\left\{\left({\rm BR}[\tilde{G} \to q\bar{\tilde{q}}] - {\rm BR}[\tilde{G} \to \bar{q}\tilde{q}]\right)\right. \qquad (4.39)$$

$$\left. + \sum_{\tilde{X}=\tilde{g},\tilde{Z},\tilde{\gamma}} {\rm BR}[\tilde{G} \to X\tilde{X}]\left({\rm BR}[\tilde{X} \to q\bar{\tilde{q}}] - {\rm BR}[\tilde{X} \to \bar{q}\tilde{q}]\right)\right\}$$

where BR is the branching ratio of the associated process. The gravitino and gaugino decays violate CP due to an interference between graphs of the form shown in Fig. 4.2.
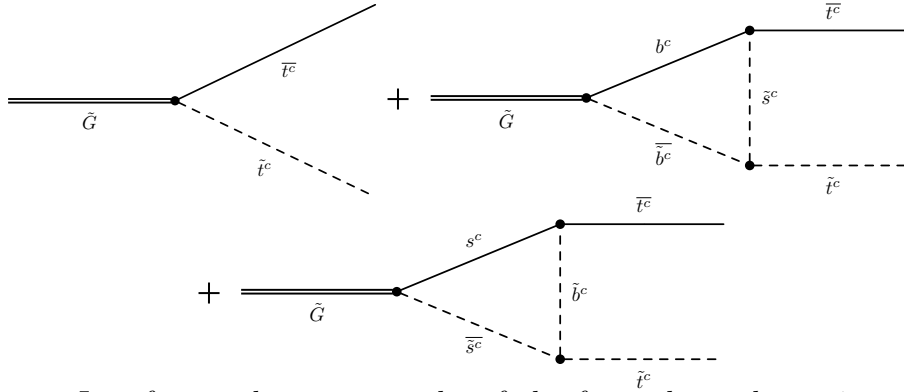
Figure 4.2: Interference between graphs of the form shown here give rise to CP violation via the $\hat{U}^c\hat{D}^c\hat{D}^c$ operator. Additionally graphs with the $\bar{b}^c\tilde{b}^c$ and $\bar{s}^c\tilde{s}^c$ final states are also included.

The parameter β is estimated up to $O(1)$ factors as

$$\beta \sim \alpha''_{332} \sin\theta_{CP} \frac{|A''_{332}|}{|m_{3/2}|} \frac{42}{N_{\text{eff}}} \text{BR}_{BV} \; , \tag{4.40}$$

where $\alpha''_{332} \equiv |\lambda''_{332}|^2/4\pi$ and N_{eff} was given by Eq. (4.12), and $\text{BR}_{\text{BV}} \equiv \text{BR}[\tilde{\bar{q}} \to qq]$, which may be $O(1)$ if the squark is the LSP. The phase $\theta_{\text{CP}} = \text{Arg}[A''_{332}m_{3/2}]$ quantifies the degree of CP violation, which is constrained by the bound on the neutron electric dipole moment (EDM), $d_n \lesssim 2.9 \times 10^{-26}$ cm [113]. For typical values,

$$\left|m_{3/2}\right| = 20 \text{ TeV} \quad , \quad |A''_{332}| = 10 \text{ TeV} \quad , \quad \alpha''_{332} = 0.1 \quad , \quad \sin\theta_{\text{CP}} = 0.3 \tag{4.41}$$

one finds [95]

$$\beta \simeq 0.03 \quad \text{and} \quad d_n \simeq 10^{-26} \text{ cm} \; . \tag{4.42}$$

In this way, a sufficient baryon asymmetry is generated while evading constraints on CP violation from low energy observables.

Successful baryogenesis requires both the generated baryon asymmetry and CP asymmetry to survive potential washout processes. The baryon asymmetry could be

washed out by the inverse decay processes $qq \to \bar{\tilde{q}}$ and $\bar{q}\bar{q} \to \tilde{q}$, but these processes are suppressed kinematically since $T \approx T_d \ll m_{\tilde{q}}$. The CP asymmetry may be washed out by the s-channel scattering with quarks in the plasma, $\tilde{q}\bar{q} \to \tilde{X} \to \bar{\tilde{q}}q$, where a Majorana mass operator is inserted in the gaugino propagator. If this process occurs on a time scale shorter than the lifetime of the squarks, then the CP asymmetry would be washed out before they have a chance to decay. However, since the CP asymmetry is only carried by the second and third generation squarks, these processes are suppressed by the exponentially low abundances of heavy second and third generation quarks in the MeV-scale plasma.

We now describe how gravitino leptogenesis, which operates prior to electroweak symmetry breaking, involves qualitatively different constraints in order to remain cosmologically viable and consistent with low energy phenomenology.

4.5.1 Decay through $\hat{L}\hat{L}\hat{E}^c$

We now consider the first of the three L-number violating operators which give rise to a lepton asymmetry through gravitino decay through a violation of L-number and R-parity

$$W_{\text{LV}} = \frac{1}{2}\lambda_{233}\hat{L}_2 \cdot \hat{L}_3\hat{E}_3^c \tag{4.43}$$

The notation "$\cdot$" stands for a contraction of $SU2$ indices with the antisymmetric tensor. We have focused on the 233 component of the tensor λ_{ijk} primarily for simplicity. As we will discuss below, the high scale of SUSY breaking renders the constraints on λ_{ijk} to be very weak. The Lagrangian-level interactions are

$$\mathcal{L}_{\text{LV}} = -\frac{1}{2}\lambda_{233}\left(l_2 \cdot l_3\tilde{\tau}^c + \tilde{l}_2 \cdot l_3\tau^c + l_2 \cdot \tilde{l}_3\tau^c\right) - \frac{1}{2}A_{233}\lambda_{233}\tilde{l}_2 \cdot \tilde{l}_3\tilde{\tau}^c + \text{h.c.} , \tag{4.44}$$
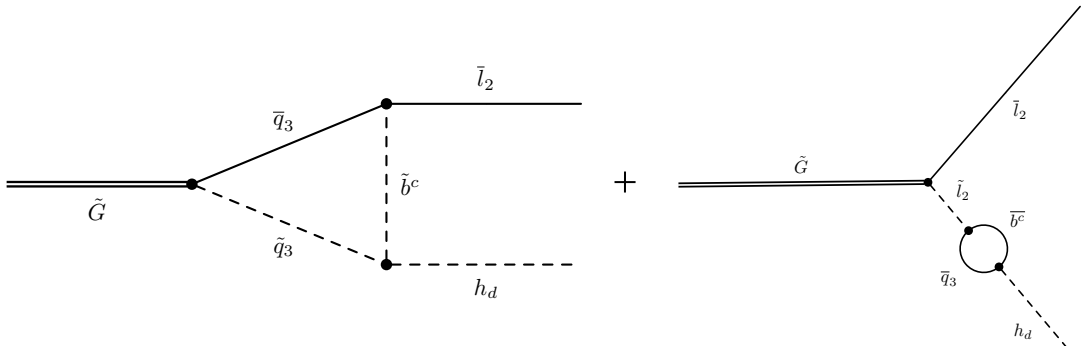
Figure 4.3: Lepton asymmetry generated directly from a gravitino decay through a loop process. Interference between the two graphs gives rise to CP violation.

which may be compared with Eq. (4.38). Since the electroweak symmetry is still unbroken at the time of gravitino decays, the presence of isospin doublets in Eq. (4.44) simply provides a multiplicative prefactor.

In standard leptogenesis, the Majorana neutrino decays into a lepton and a Higgs in a CP violating manner [104]. Based on kinematic arguments one would expect the corresponding supersymmetric decay channels, $\tilde{G} \to \bar{h}_d l_i, \tilde{\bar{h}}_d \tilde{l}_i, h_u l_i$ and $\tilde{h}_u \tilde{l}_i$, with 2-body final states to yield the dominant contribution to the lepton asymmetry. However, the absence of a direct gravitino–lepton–Higgs vertex requires these decays to be loop suppressed. Specifically, graphs of the form shown in Fig. 4.3 are responsible for mediating these decays. Not only are these decays doubly-loop suppressed, but additionally they require factors of the lepton Yukawa couplings. Even the largest Yukawa coupling gives $O(m_\tau^2/v^2) \sim O(10^{-4})$. This suppresses these channels compared to the three-body final states that we consider below, and moreover makes them irrelevant for leptogenesis in light of the requirement $\beta_{\min} \approx 10^{-4}$, Eq. (4.26).

The calculation of the appropriate gravitino decay channels then runs parallel to

the B-number violating decay that was discussed in Sec. 4.5.1. We generate the lepton asymmetry in two stages. First, the gravitino decays out of equilibrium through the channels $\tilde{G} \rightarrow l\bar{\tilde{l}}$ and $\bar{l}\tilde{l}$ where $l(\bar{l})$ is a (anti-)lepton and $\tilde{l}(\bar{\tilde{l}})$ is an (anti-)slepton. This creates equal and opposite CP asymmetries in the leptons and sleptons. The heavy sleptons then decay through L-number violating interaction as $\tilde{l} \rightarrow ll$ and $\bar{\tilde{l}} \rightarrow \bar{l}\bar{l}$, thereby creating the lepton asymmetry. We calculate β by summing over the final states

$$\beta = \epsilon_{l_2} + \epsilon_{l_3} + \epsilon_{\tau^c} \tag{4.45}$$

where

$$
\begin{aligned}
\epsilon_{l_2} &= \mathrm{BR}[\bar{\tilde{l}}_2 \rightarrow l_3\tau^c]\left\{\left(\mathrm{BR}[\tilde{G} \rightarrow l_2\bar{\tilde{l}}_2] - \mathrm{BR}[\tilde{G} \rightarrow \bar{l}_2\tilde{l}_2]\right) + \sum_{\tilde{X}=\tilde{B},\tilde{W}} \mathrm{BR}[\tilde{G} \rightarrow X\tilde{X}]\right.\\
&\qquad\left.\left(\mathrm{BR}[\tilde{X} \rightarrow l_2\bar{\tilde{l}}_2] - \mathrm{BR}[\tilde{X} \rightarrow \bar{l}_2\tilde{l}_2]\right)\right\}, \\
\epsilon_{l_3} &= \mathrm{BR}[\bar{\tilde{l}}_3 \rightarrow l_2\tau^c]\left\{\left(\mathrm{BR}[\tilde{G} \rightarrow l_3\bar{\tilde{l}}_3] - \mathrm{BR}[\tilde{G} \rightarrow \bar{l}_3\tilde{l}_3]\right) + \sum_{\tilde{X}=\tilde{B},\tilde{W}} \mathrm{BR}[\tilde{G} \rightarrow X\tilde{X}]\right.\\
&\qquad\left.\left(\mathrm{BR}[\tilde{X} \rightarrow l_3\bar{\tilde{l}}_3] - \mathrm{BR}[\tilde{X} \rightarrow \bar{l}_3\tilde{l}_3]\right)\right\} \\
\epsilon_{\tau^c} &= \mathrm{BR}[\bar{\tilde{\tau}}^c \rightarrow l_2l_3]\left\{\left(\mathrm{BR}[\tilde{G} \rightarrow \tau^c\bar{\tilde{\tau}}^c] - \mathrm{BR}[\tilde{G} \rightarrow \bar{\tau}^c\tilde{\tau}^c]\right) + \sum_{\tilde{X}=\tilde{B}} \mathrm{BR}[\tilde{G} \rightarrow X\tilde{X}]\right.\\
&\qquad\left.\left(\mathrm{BR}[\tilde{X} \rightarrow \tau^c\bar{\tilde{\tau}}^c] - \mathrm{BR}[\tilde{X} \rightarrow \bar{\tau}^c\tilde{\tau}^c]\right)\right\}
\end{aligned}
\tag{4.46}
$$

CP violation arises in the standard way from the interference of tree level and one loop graphs as shown in Fig. 4.4. Then, following a similar calculational strategy to that employed in CR, we can estimate the branching fractions and obtain

$$\beta \sim \alpha_{233} \sin\theta_{\mathrm{CP}} \frac{1}{N_{\mathrm{eff}}} \mathrm{Max}\left[5\frac{|A_{233}|}{|m_{3/2}|} , 11\frac{|A_{233}|}{|m_{\tilde{X}}|}\right] \mathrm{BR}_{\mathrm{LV}} , \tag{4.47}$$

where $\alpha_{233} \equiv |\lambda_{233}|^2/4\pi$, and where we have assumed a common mass $m_{\tilde{X}} = m_{\tilde{B}} = m_{\tilde{W}}$ for the binos and winos, and also for simplicity, we assume a comparable amount

61

of CP violation arises in the gravitino and gaugino decays, i.e., $\theta_{\text{CP}} = \text{Arg}[A_{233}m_{3/2}] = \text{Arg}[A_{233}m_{\tilde{X}}]$. If it is kinematically forbidden for the sleptons to decay into gauginos or higgsinos, then the branching ratio for the L-number violating decay can be large:

$$\text{BR}_{\text{LV}} = \text{BR}[\bar{\tilde{l}}_2 \to l_3\tau^c] \approx \text{BR}[\bar{\tilde{l}}_3 \to l_2\tau^c] \approx \text{BR}[\bar{\tilde{\tau}}^c \to l_2l_3] = O(1) \ . \tag{4.48}$$

The CP asymmetry in squarks may be washed out by scatterings with leptons in the plasma mediated by a gaugino, i.e., $\tilde{l}\bar{l} \to \tilde{X} \to l\bar{\tilde{l}}$ where $\tilde{X}$ is a bino or a wino. In the model of gravitino baryogenesis [95] reviewed above, such scattering processes were negligible due to the exponential Boltzmann suppression of heavy quarks in the $T \sim$ MeV scale plasma. In the case of leptogenesis, all of the leptons are relativistic at the time of gravitino decay at $T \sim 10^3$ GeV, and we must verify that this scattering is out of equilibrium. The cross-section for the CP washout process may be estimated as

$$\sigma_{\tilde{l}\bar{l}\to l\bar{\tilde{l}}} \approx \frac{\alpha^2}{m_{\tilde{X}}^2} \tag{4.49}$$

where $m_{\tilde{X}}$ is the gaugino mass and α is the fine structure constant. Since all leptons are relativistic at this time their equilibrium number density is $n_l \sim T^3$ and the CP washout rate is

$$\Gamma_{\tilde{l}\bar{l}\to l\bar{\tilde{l}}} \approx \frac{\alpha^2}{m_{\tilde{X}}^2}T^3 \ . \tag{4.50}$$

This must be compared against the slepton decay rate

$$\Gamma_{\tilde{l}\to ll} \approx \alpha_{233}m_{\tilde{l}} \tag{4.51}$$

where $m_{\tilde{l}}$ is the slepton mass. The requirement that slepton decay is more rapid than the CP washout imposes a lower bound on the gaugino mass

$$m_{\tilde{X}} > \sqrt{\frac{\alpha^2 T^3}{\alpha_{233}m_{\tilde{l}}}} \ . \tag{4.52}$$

Taking $T \sim 10^3$ GeV to be the temperature at which gravitinos decay, $\alpha \sim 10^{-2}$, $\alpha_{233} = O(1)$, and $m_{\tilde{l}} \sim m_{3/2} \sim 10^8$ GeV we obtain the weak bound $m_{\tilde{X}} \gtrsim O(1 \text{ GeV})$. For the scale that we are considering however, we expect $m_{\tilde{X}} \sim 10^8$ GeV, so wash out is not a problem.

Low energy observables can be used to constrain CP violation in baryogenesis models. In the decoupling limit, in which the SUSY breaking scale is taken to infinity, these constraints disappear. Since the SUSY breaking scale that we consider is high, we do not expect strong constraints, which we will explicitly confirm below.

The trilinear R-parity violating operators in Eq. (4.44) can radiatively give the neutrinos a mass with a lepton-slepton in the loop. For example, the term with coefficient λ_{233} yields a mass for the muon neutrino: [114, 115]

$$m_{\nu_\mu} \simeq \frac{\lambda_{233}^2}{8\pi^2} \frac{m_\tau^2}{m_{\tilde{l}}} \tag{4.53}$$

where m_τ is the τ lepton mass and $m_{\tilde{l}}$ is the slepton mass. The current neutrino mass constraints of $\sum m_\nu < 1$ eV therefore imply a bound on the R_p-violating coupling λ_{ijk}. For example, $\alpha_{233} \equiv \lambda_{233}^2/4\pi < 0.2$ for $m_{\tilde{l}} \sim 10^8$ GeV. Phenomenologically acceptable neutrino masses might result from the same operator responsible for leptogenesis.

CP violation in the lepton sector generates an electron EDM, d_e. The contribution to d_e in the MSSM may be estimated as [116]

$$d_e \approx \frac{m_e}{m_{\tilde{l}}^2} \sin \theta_{\text{CP}} \tag{4.54}$$

where $m_{\tilde{l}}$ is the slepton mass, m_e is the electron mass, and θ_{CP} is the CP violating phase. The current bound, $d_e < 5 \times 10^{-14}$ GeV^{-1} [117], imposes a constraint on the slepton mass $m_{\tilde{l}} \gtrsim 10^5$ GeV, which is easily accommodated for our fiducial superpartner mass scale $m_{3/2} \sim 10^8$ GeV. The interactions in Eq. (4.44) also violate lepton flavor, which is constrained by bounds on the decay $\mu \to e\gamma$. The branching ratio
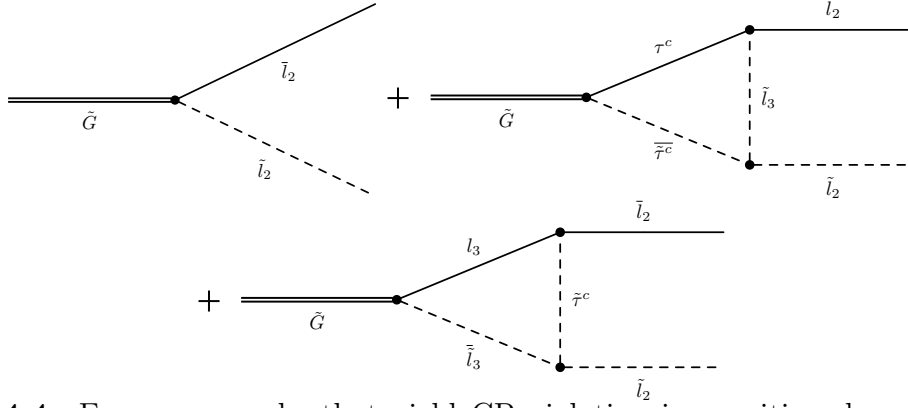
Figure 4.4: Feynman graphs that yield CP violation in gravitino decays via the $\hat{L}\hat{L}\hat{E}^c$ operator. Other graphs with $\bar{l}_3\tilde{l}_3$ and $\tilde{\tau}^c\overline{\tau^c}$ on the external lines are not shown.

may be estimated as

$$\text{BR}[\mu^- \to e^- \gamma] \sim \alpha_{233} \frac{m_\mu^2}{m_{\tilde{l}}^2} \; . \tag{4.55}$$

The current bound, $\text{BR}[\mu^- \to e^- \gamma] \lesssim 2.4 \times 10^{-12}$ [117], imposes a lower bound on the slepton mass, $m_{\tilde{l}} \gtrsim O(10^4 \text{ GeV})$, which is also easy to accommodate.

4.5.2   Decay through $\hat{L}\hat{Q}\hat{D}^c$

The symmetries and field content of the MSSM admit just one other trilinear R-parity and L-number violating operator. Once again we will focus on a single element of the flavor tensor and write the R-parity violating superpotential as

$$W_{\text{LV}} = \frac{1}{2}\lambda'_{233}\hat{L}_2 \cdot \hat{Q}_3\hat{D}_3^c \; , \tag{4.56}$$

which violates L-number but preserves B-number. The interaction Lagrangian contains the following terms

$$\mathcal{L}_{\text{LV}} = -\frac{1}{2}\lambda'_{233}\left(l_2 \cdot q_3\tilde{b}^c + \tilde{l}_2 \cdot q_3 b^c + l_2 \cdot \tilde{q}_3 b^c\right) - \frac{1}{2}A_{233}\lambda'_{233}\tilde{l}_2 \cdot \tilde{q}_3\tilde{b}^c + \text{h.c.} \; . \tag{4.57}$$

which may be compared with Eq. (4.44).

The calculation of β parallels the discussion in Sec. 4.5.1. The qualitative difference is that in the first stage of leptogenesis, the gravitino can decay into either a lepton–slepton pair or a quark–squark pair. Subsequently, both the slepton and the squark decay violating L-number. Summing over the various decay channels, we obtain

$$\beta \equiv \epsilon_{l_2} + \epsilon_{q_3} + \epsilon_{b^c} \tag{4.58}$$

where

$$\epsilon_{l_2} = \mathrm{BR}[\bar{\tilde{l}}_2 \to q_3 b^c]\left\{ \left(\mathrm{BR}[\tilde{G} \to l_2\bar{\tilde{l}}_2] - \mathrm{BR}[\tilde{G} \to \bar{l}_2\tilde{l}_2] \right) + \sum_{\tilde{X}=\tilde{B},\tilde{W}} \mathrm{BR}[\tilde{G} \to X\tilde{X}] \right.$$
$$\left. \left(\mathrm{BR}[\tilde{X} \to l_2\bar{\tilde{l}}_2] - \mathrm{BR}[\tilde{X} \to \bar{l}_2\tilde{l}_2] \right) \right\},$$

$$\epsilon_{q_3} = \mathrm{BR}[\bar{\tilde{q}}_3 \to l_2 b^c]\left\{ \left(\mathrm{BR}[\tilde{G} \to q_3\bar{\tilde{q}}_3] - \mathrm{BR}[\tilde{G} \to \bar{q}_3\tilde{q}_3] \right) + \sum_{\tilde{X}=\tilde{B},\tilde{W},\tilde{g}} \mathrm{BR}[\tilde{G} \to X\tilde{X}] \right.$$
$$\left. \left(\mathrm{BR}[\tilde{X} \to q_3\bar{\tilde{q}}_3] - \mathrm{BR}[\tilde{X} \to \bar{q}_3\tilde{q}_3] \right) \right\}, \tag{4.59}$$

$$\epsilon_{b^c} = \mathrm{BR}[\bar{\tilde{b}}^c \to l_2 q_3]\left\{ \left(\mathrm{BR}[\tilde{G} \to b^c\bar{\tilde{b}}^c] - \mathrm{BR}[\tilde{G} \to \bar{b}^c\tilde{b}^c] \right) + \sum_{\tilde{X}=\tilde{B},\tilde{g}} \mathrm{BR}[\tilde{G} \to X\tilde{X}] \right.$$
$$\left. \left(\mathrm{BR}[\tilde{X} \to b^c\bar{\tilde{b}}^c] - \mathrm{BR}[\tilde{X} \to \bar{b}^c\tilde{b}^c] \right) \right\}.$$

Once again, we estimate

$$\beta \sim \alpha'_{233} \sin\theta_{\mathrm{CP}} \frac{1}{N_{\mathrm{eff}}} \mathrm{Max}\left[11\frac{|A_{233}|}{|m_{3/2}|}, \ 27\frac{|A_{233}|}{|m_{\tilde{X}}|} \right] \mathrm{BR}_{\mathrm{LV}}, \tag{4.60}$$

where $\alpha'_{233} \equiv |\lambda'_{233}|^2/4\pi$. With the appropriate spectral constraints we can obtain

$$\mathrm{BR}_{\mathrm{LV}} = \mathrm{BR}[\bar{\tilde{l}}_2 \to q_3 b^c] \approx \mathrm{BR}[\bar{\tilde{q}}_3 \to l_2 b^c] \approx \mathrm{BR}[\bar{\tilde{b}}^c \to l_2 q_3] \approx O(1), \tag{4.61}$$

as in the previous cases.
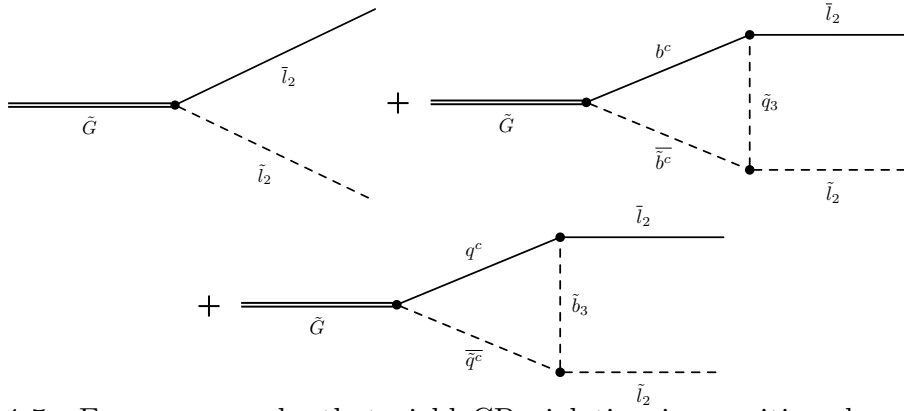
Figure 4.5: Feynman graphs that yield CP violation in gravitino decays via the $\hat{L}\hat{Q}\hat{D}^c$ operator. Other graphs with $\bar{q}_3\tilde{q}_3$ and $\tilde{b}^c\overline{b^c}$ in the final state are not shown.

Apart from the distinctions discussed thus far, the remainder of the analysis of this case follows similarly to Sec. 4.5.1. Washout is possible due to s-channel scatterings through gauginos, but the avoidance of washout imposes only a very weak bound on the gaugino mass. Empirical constraints, arising from electron and neutron EDMs and lepton flavor violation, have little constraining power on the R-parity violating couplings, λ'_{233} and A'_{223}, due to the high scale of SUSY breaking. Neutrinos again acquire a radiatively generated mass with a quark-squark in the loop and the expression for muon neutrino mass in this case involves a bottom-sbottom loop [114, 115],

$$m_{\nu_\mu} \simeq \frac{3\lambda'^2_{233}}{8\pi^2} \frac{m_b^2}{m_{\tilde{b}}} \tag{4.62}$$

which gives an upper bound on $\alpha'_{233} \equiv \lambda'^2_{233}/4\pi$.

4.5.3 Decay through $\hat{H}_u\hat{L}$

As a last case we will consider the bilinear R-parity and L-number violating operator,

$$W_{\text{LV}} = \mu'_i \hat{H}_u \cdot \hat{L}_i \ . \tag{4.63}$$

This operator supplements the R-parity symmetric terms from the MSSM

$$W_{\text{MSSM}} = \mu \hat{H}_u \cdot \hat{H}_d + (\lambda^e)_{ij} \hat{H}_d \cdot \hat{L}_i \hat{E}_j^c - (\lambda^u)_{ij} \hat{H}_u \cdot \hat{Q}_i \hat{U}_j^c + (\lambda^d)_{ij} \hat{H}_d \cdot \hat{Q}_i \hat{D}_j^c . \quad (4.64)$$

The full superpotential $W = W_{\text{MSSM}} + W_{\text{LV}}$ yields the Lagrangian $\mathcal{L} = \mathcal{L}_{\text{LV}}^{\text{bi}} + \mathcal{L}_{\text{LV}}^{\text{tri}} + \mathcal{L}_{\text{LV}}^{\text{quad}} + \mathcal{L}_{\text{LP}} + \mathcal{L}_{\text{MSSM}}$ where

$$-\mathcal{L}_{\text{LV}}^{\text{bi}} = \mu_i' \tilde{h}_u \cdot l_i + B_i^u h_u \cdot \tilde{l}_i + \left(B_i^d + \mu^* \mu_i'\right) h_d^\dagger \tilde{l}_i + \text{h.c.} , \quad (4.65)$$

$$-\mathcal{L}_{\text{LV}}^{\text{tri}} = -\mu_i'^*(\lambda^u)_{jk} \tilde{l}_i^\dagger \tilde{q}_j \tilde{u}^c{}_k + \mu_i'^*(\lambda^e)_{ij} h_u^\dagger h_d \tilde{e}^c{}_j + \text{h.c.} , \qquad \text{and} \qquad (4.66)$$

$$-\mathcal{L}_{\text{LP}} = |\mu_i'|^2 h_u^\dagger h_u + (\mu_i'^* \mu_j') \tilde{l}_i^\dagger \tilde{l}_j \qquad (4.67)$$

are the bilinear L-violating, trilinear L-violating, and L-preserving contributions that are in addition to the MSSM Lagrangian, $\mathcal{L}_{\text{MSSM}}$. We will not need the quadrilinear terms, $\mathcal{L}_{\text{LV}}^{\text{quad}}$, since they only contribute to gravitino decay at the two loop order. As we have done in the previous sections, we will suppose that W_{LV} is the only source of R-parity violation at tree-level.

We will see that bilinear L-number violation provides various gravitino decay channels that generate a lepton asymmetry. This scenario, however, is significantly constrained, because the mixings in Eq. (4.65) allow L-number violation to enter into low energy observables, specifically the neutrino mass, at tree level. This is in contrast to the previous cases of trilinear R-parity violation in which L-number violating effects were loop suppressed. If the mass scale of the sleptons and neutralinos is comparable to the fiducial gravitino mass that we have considered in the previous sections, $m_{3/2} \sim 10^8$ GeV, then the neutrino mass constraints bound the mixings so as to forbid the generation of a sufficiently large lepton asymmetry. Only if the mass scale is lifted to the somewhat more uncomfortable scale, $m_{3/2} \gtrsim O(10^{10} - 10^{11}$ GeV), can the low energy constraints be evaded. While it makes this leptogenesis scenario

less attractive, for completeness we review the parameter ranges that remain viable for this case as well.

In this scenario, the lepton asymmetry is created by the decays of the gravitino or gaugino into a lepton and a Higgs boson. Depending on the spectrum, the gravitino could also decay into a slepton and a Higgsino through the R-parity violating mixing. However, the slepton and Higgsino would eventually decay back through the R-parity violating operator into SM particles, and this may lead to significant washout of the lepton asymmetry. Therefore, we assume the spectrum

$$m_{\tilde{l}} \sim m_{\tilde{h}} \sim m_{\tilde{q}} \gtrsim m_{3/2} \gtrsim m_{\tilde{X}} \sim m_h \gg m_l \,,\, m_q \,, \tag{4.68}$$

and we focus on the two decay channels (and their CP conjugates), $\tilde{V} \rightarrow l_i \bar{h}_d$ and $l_i h_u$, where $\tilde{V} = \tilde{G}, \tilde{B}$, or $\tilde{W}$. In the case of trilinear L-number violation, we had dismissed these two-body final states as subdominant (see Sec. 4.5.1) because they arose from an interference of two one-loop graphs, but for bilinear L-number violation the decays can proceed due to the tree level mixing.

For this scenario, the lepton asymmetry is given by summing over the two final states

$$\beta = (\epsilon_{l_i \bar{h}_d} + \epsilon_{l_i h_u}) f_{wo} \tag{4.69}$$

where

$$\epsilon_{l_i \bar{h}_d} \equiv \sum_i \Big\{ \big(\mathrm{BR}[\tilde{G} \to l_i \bar{h}_d] - \mathrm{BR}[\tilde{G} \to \bar{l}_i h_d] \big) \tag{4.70a}$$

$$+ \sum_{\tilde{X}=\tilde{B},\tilde{W}} \mathrm{BR}[\tilde{G} \to X\tilde{X}] \big(\mathrm{BR}[\tilde{X} \to l_i \bar{h}_d] - \mathrm{BR}[\tilde{X} \to \bar{l}_i h_d] \big) \Big\}$$

$$\epsilon_{l_i h_u} \equiv \sum_i \Big\{ \big(\mathrm{BR}[\tilde{G} \to l_i h_u] - \mathrm{BR}[\tilde{G} \to \bar{l}_i \bar{h}_u] \big) \tag{4.70b}$$

$$+ \sum_{\tilde{X}=\tilde{B},\tilde{W}} \mathrm{BR}[\tilde{G} \to X\tilde{X}] \big(\mathrm{BR}[\tilde{X} \to l_i h_u] - \mathrm{BR}[\tilde{X} \to \bar{l}_i \bar{h}_u] \big) \Big\}$$

and $f_{wo} \leq 1$ is a suppression factor to account for washout effects (see below). CP violation arises from the interference of graphs such as the ones shown in Fig. 4.6. We could include additional graphs with more insertions of the mixing operators, but as we will see below the mixing induced by the parameters μ_i', B_i^d, and B_i^u must be small compared to the superpartner mass scale, and the higher order graphs can be neglected from a perturbative standpoint. Additionally, graphs containing factors of the electron and down-type quark Yukawa coupling are subdominant. Taking $|B^u| \sim |B^d| \sim |\mu'|^2$ and the spectrum in Eq. (4.68) for simplicity, we obtain the order of magnitude estimate

$$\beta \sim |\lambda^u|^2 \sin\theta_{\mathrm{CP}} \frac{1}{N_{\mathrm{eff}}} \frac{|B^d| |\mu'|}{|m_{3/2}|^3} f_{wo} \tag{4.71}$$

where $\theta_{\mathrm{CP}} = \mathrm{Arg}[B^d \mu'^* m_{3/2}]$.

The magnitude of the washout depends critically on the spectrum of the superpartners. For instance, if the gravitino can decay into squarks, then these will scatter on quarks in the plasma and potentially violate R-parity and L-number. It is also possible for two SM particles to scatter violating R-parity, but since the energy of the plasma ($\sim$ TeV) is insufficient to produce a heavy superpartner on shell, such a scattering must contain two factors of the mixing, which is highly suppressed. Thus,
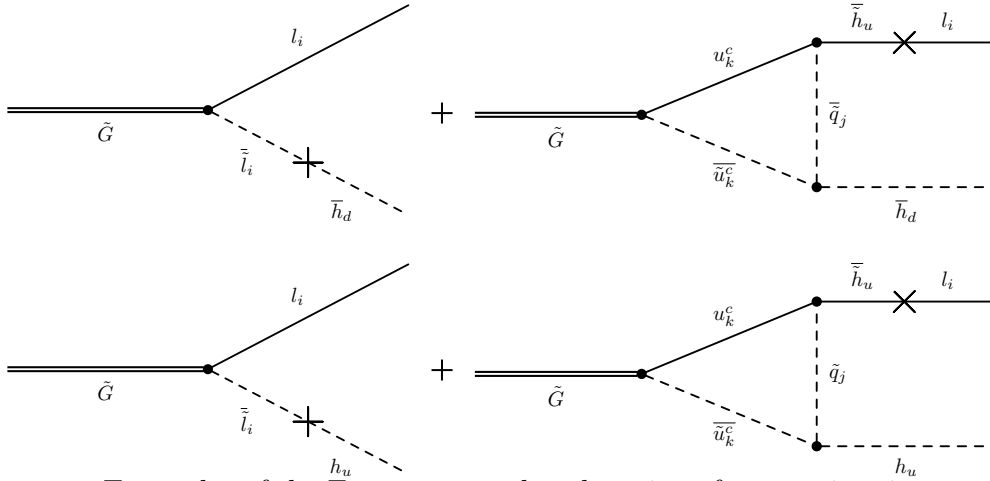
Figure 4.6: Examples of the Feynman graphs whose interference give rise to a lepton asymmetry via bilinear R-parity and L-number violation.

if we assume that the gravitino cannot decay into on shell squarks and sleptons, then washout can be negligible.

Let us now turn to the low energy constraints on this model. The neutrinos mix with the up-type Higgsino through the bilinear operator $\mathcal{L}_{\text{LV}}^{\text{bi}} \ni \mu_i' \tilde{h}_u^0 \nu_i$. This mixing causes the neutrinos to acquire a mass, and therefore neutrino mass constraints impose an upper bound on the mixing [114, 118]. The neutralinos can be integrated out to yield a neutrino mass [119]

$$ m_\nu \sim \frac{m_Z^2 \, |\mu'|^2}{m_{\tilde{\chi}}^3} \frac{1}{1 + t_\beta^2} \, . \tag{4.72} $$

where $m_{\tilde{\chi}} \gg m_Z, m_\nu$ is the neutralino mass and $t_\beta = \langle h_u \rangle / \langle h_d \rangle \sim O(1)$. Taking $m_\nu \lesssim 1$ eV and the fiducial reference $m_{\tilde{\chi}} \sim m_{3/2}$, we obtain the bound

$$ \frac{|\mu'|}{m_{3/2}} \lesssim 10^{-3} \sqrt{\frac{m_{3/2}}{10^8 \text{ GeV}}} \sqrt{\frac{1}{1 + t_\beta^2}} \, . \tag{4.73} $$

Despite the high scale of SUSY breaking, a strong constraint is obtained because the neutrino mass arises at tree level, unlike in the cases of the trilinear operators.

70

After electroweak symmetry breaking the Higgs fields acquire vacuum expectation values and the mixings in Eq. (4.65) induce tadpole terms for the sneutrino fields

$$t_{\tilde{\nu}_i} = \left(B_i^d + \mu^* \mu_i'\right) v_d - B_i^u\, v_u \ .$$
(4.74)

This causes the sneutrinos to acquires VEVs, which may be estimated as

$$v_{\tilde{\nu}} \approx \frac{\left(B^d + \mu^* \mu'\right)\cos\beta - B^u \sin\beta}{M_{\tilde{l}}^2 + |\mu'|^2}\, v$$
(4.75)

where $M_{\tilde{l}}^2$ is the soft SUSY-breaking slepton mass parameter. The charged slepton VEVs are protected by the residual electromagnetic symmetry. The VEV $v_{\tilde{\nu}}$ causes the gauginos and neutrinos to mix and gives rise to a neutrino mass [120]

$$m_\nu \sim \frac{m_Z^2}{v^2}\frac{v_{\tilde{\nu}}^2}{m_{\tilde{X}}}$$
(4.76)

where $m_{\tilde{X}}$ is the gaugino mass. Once again taking $m_{\tilde{X}} \sim m_{3/2}$, the observed neutrino mass scale implies the bound

$$\frac{v_{\tilde{\nu}}}{m_{3/2}} \lesssim 10^{-8}\sqrt{\frac{10^8 \text{ GeV}}{m_{3/2}}} \ .$$
(4.77)

Provided that there is not an unnatural tuning in Eq. (4.75) which would give $v_{\tilde{\nu}} \ll O(B^d) \sim O(B^u)$, the bound in Eq. (4.77) imposes

$$\frac{B^d}{m_{3/2}^2} \sim \frac{B^u}{m_{3/2}^2} \lesssim 10^{-3}\sqrt{\frac{m_{3/2}}{10^8 \text{ GeV}}} \ .$$
(4.78)

The lepton asymmetry, estimated by Eq. (4.71), requires two factors of the mixing, and in light of the constraints Eqs. (4.73) and (4.78), it is not possible to achieve $\beta \gtrsim 10^{-4}$, which is required for successful gravitino leptogenesis (see Eq. (4.26)). The gravitino mass scale must be lifted to at least $m_{3/2} \gtrsim O(10^{10} - 10^{11} \text{ GeV})$ in order for the bounds to be evaded, unless we also impose artificial tuning to lift the masses of the sleptons and neutralinos.

Finally, one may wonder why we have not considered L-number violation entering directly in the the Kähler potential instead of the superpotential. The term $K_{\mathrm{LV}} = \alpha_i \hat{H}_d^\dagger \hat{L}_i$ may be added to the Kähler potential without violating any gauge symmetries or supersymmetry. This term leads to the desired tree level gravitino – lepton – Higgs vertex. However, since the addition of this term makes the Kähler potential non-diagonal, it will also result in non-canonical kinetic terms. A basis may be found in which the kinetic terms are diagonal by rotating away the bilinear coupling, but this also removes the tree level gravitino–lepton–Higgs vertex.

4.6   Conclusions

We have considered in this chapter a possible mechanism for the creation of the baryon asymmetry of the universe via gravitino decays in the MSSM. In this scenario, the out of equilibrium decay of the gravitino gives rise to a lepton asymmetry that is subsequently converted into a baryon asymmetry by weak sphalerons. The requirements of CP and L-number violation are then provided by three of the MSSM's possible R-parity violating operators: $W = \hat{L}\hat{L}\hat{E}^c, \hat{L}\hat{Q}\hat{D}^c$, and $\hat{H}_u\hat{L}$. For the case of the two trilinear operators, the gravitino decay channels responsible for L-number creation are similar to the B-number creation gravitino decays discussed by Ref. [95] for the operator $W = \hat{U}^c\hat{D}^c\hat{D}^c$, and the analysis of the subsequent generation of lepton number asymmetry follows a similar line of analysis, with some key changes due to the differing presumed scale of gravitino mass.

For comparison purposes and to demonstrate the viability of these scenarios, we provide in, Table 4.1 some sample parameter sets which may produce the correct order of magnitude of the observed baryon asymmetry, without coming into conflict with low energy observables such as EDMs and $\mu \to e\gamma$.

In the case of the bilinear operator $W = \hat{H}_u \hat{L}$, a lepton asymmetry can be generated through mixing between leptons and Higgsinos and between sleptons and Higgs bosons. In the particular case where the gravitino decays into a Higgs boson and a lepton via the R-parity violating mixing, the neutrino also acquires a mass by virtue of this mixing. As a result, bounds on the neutrino mass constrain the mixing to the point that an insufficient baryon asymmetry is generated unless the mass scale of the gravitino is increased to $m_{3/2} \gtrsim 10^{10-12}$ GeV, as demonstrated in Table 4.2.

The $\cancel{R}_p$ operators used to generate a baryon asymmetry in this chapter via gravitino decay can also, radiatively, give neutrinos mass. For example, the trilinear $\cancel{R}_p$ interactions LLE^c generates a muon mass given by $m_{\nu_\mu} \sim (1 \text{ eV})(\alpha_{233}/0.2)(M_{\tilde{l}}/10^8 \text{ GeV})^{-1}$. Note that there are values that give successful leptogenesis and the correct neutrino mass. This fact is interesting as it provides a possible new connection between neutrino mass generation and the origin of the baryon asymmetry.

All of these mechanisms of gravitino leptogenesis require an unconventional spectrum of superpartners to the SM fields, or equivalently, a restriction on the mechanism of SUSY breaking. The gravitino must be heavy, $m_{3/2} \gtrsim 10^8$ GeV, to ensure that it decays while the weak sphalerons are still in equilibrium, and this corresponds to a SUSY breaking scale $M_S \gtrsim 10^{13}$ GeV. There is no *a priori* reason to think that the scale of SUSY-breaking cannot be so high, and in fact, the cosmological consequence of high-scale SUSY breaking have been studied [96, 97]. However, if $M_S \gg$ TeV then supersymmetry does not provide a natural solution to the Higgs hierarchy problem. Nevertheless, the lack of evidence for supersymmetry at the LHC already implies that the scale of SUSY breaking is higher than naturalness arguments would suggest, and

$|m_{3/2}|$	$M_{\tilde{X}}$	$M_{\tilde{l}} \sim M_{\tilde{q}}$	$|A|$	$\theta_{\rm CP}$	α	$\rm BR_{LV}$	T_{RH}	$\beta(10^{-3})$	$\frac{Y_B^*}{Y_B^{\rm (obs)}}$	$\frac{d_e}{d_e^{\rm (lim)}}$	$\frac{\rm BR_{\mu \to e\gamma}}{\rm BR_{\mu \to e\gamma}^{\rm (lim)}}$	$\frac{m_\nu}{m_\nu^{\rm (obs)}}$
1	0.1	0.5	0.01	0.4	0.1	0.9	10^{15}	2	1.0	$2 \cdot 10^{-6}$	$2 \cdot 10^{-7}$	1.0
1	0.01	0.2	0.01	0.9	0.05	0.1	10^{15}	2.6	1.0	$2 \cdot 10^{-5}$	$5 \cdot 10^{-7}$	1.3
1	0.01	0.001	0.03	0.9	0.001	0.9	10^{15}	1.5	0.6	$8 \cdot 10^{-1}$	$4 \cdot 10^{-3}$	5.0
1	0.01	0.1	0.03	0.05	0.02	0.6	10^{15}	1.2	0.5	$5 \cdot 10^{-6}$	$8 \cdot 10^{-7}$	1.0
5	1	0.1	0.05	1	0.4	0.8	10^{14}	10	0.4	$8 \cdot 10^{-5}$	$2 \cdot 10^{-5}$	20
5	0.05	2.0	0.05	1	0.4	0.8	10^{13}	185	0.7	$82 \cdot 10^{-7}$	$4 \cdot 10^{-8}$	1.0
10	1	0.5	3.0	0.1	0.1	0.1	10^{15}	2	0.8	$4 \cdot 10^{-7}$	$2 \cdot 10^{-7}$	1.0
10^4	0.1	10	1	0.05	0.1	0.5	10^{14}	17	0.7	$5 \cdot 10^{-10}$	$4 \cdot 10^{-10}$	$5 \cdot 10^{-2}$

Table 4.1: Typical parameter sets for the model $W_{\rm LV} = \hat{L}\hat{L}\hat{E}^c$. The input parameters are the gravitino mass $|m_{3/2}|$, the gaugino mass ($M_{\tilde{X}}$), the squark or slepton mass ($M_{\tilde{l}} \sim M_{\tilde{q}}$), the A parameter $|A|$, the CP-violating phase ($\theta_{\rm CP} = \mathrm{Arg}[Am_{3/2}]$), the R-parity violating Yukawa coupling ($\alpha = |\lambda|^2/4\pi$), the L-number violating branching ratio ($\rm BR_{LV}$), and the reheat temperature (T_{RH}). Dimensionful parameters are expressed in units of 10^8 GeV except T_{RH} which is in GeV, $\theta_{\rm CP}$ is in radians. We estimate the baron asymmetry, Y_B^* using Eq. (4.25) along with the approximate estimate for β given by Eq. (4.47), as well as estimate the ratio of the electron EDM (d_e) to the observed upper limit upper limit, he branching ratio for $\mu \to e\gamma$ with respect to its observed upper limit and the ratio of the neutrino mass m_ν to the observational upper bound, $\sum m_\nu^{\rm (obs)} \lesssim 1$ eV, by Eq. (4.53). The results for $\hat{L}\hat{Q}\hat{D}^c$ would be very similar, differing only by an O(1) factor.

it is therefore worth exploring the possibility that it could be *much* higher as, for example, in the case of split supersymmetry [105, 106, 107]. Also, if the gravitino is to be responsible for leptogenesis, it must decay and therefore cannot be the LSP. Since the latter possibility is a generic prediction of gauge mediated models of SUSY breaking [121], therefore gauge mediation seems incompatible with gravitino leptogenesis. Finally, although we typically assume that the squark and slepton masses are comparable to the gravitino mass, they could be much lighter. It is difficult to imagine a SUSY breaking mechanism that yields $m_{3/2} \gg m_{\tilde{q}}, m_{\tilde{l}}$, but it may be possible that such a scenario is consistent with gravitino leptogenesis and would put SUSY within reach of the LHC.

While our consideration of gravitino leptogenesis is motivated in part by neutrino moderated leptogenesis, there are a number of key differences. The gravitino always decays out of equilibrium by virtue of its universal gravitational strength coupling, whereas the Majorana neutrino decay will be accompanied by some washout factor due to inverse decays [104]. In gravitino decay, the violation of L-number and CP are a consequence of the MSSM's R-parity violating operators. On the other hand, the Majorana neutrino mass operator violates L-number and the mass matrix carries the CP-violating phases. Successful gravitino leptogenesis requires a high SUSY-breaking scale, $M_S \gtrsim 10^{13}$ GeV, while Majorana neutrino leptogenesis (motivated by a Type I seesaw with $O(0.01 - 1)$ Yukawa couplings) requires a high Majorana mass scale, $M_{N_R} \gtrsim 10^{10}$ GeV. Since these scales are much higher than the energies accessible in the laboratory today, conventional low energy tests of CP-violation do not probe the high energy CP-violating parameters that may be responsible for generation of the lepton asymmetry (with few exceptions in cases of standard neutrino leptogenesis [122] [123]). Similarly, bounds on lepton flavor violation in the form of the process $\mu \to e\gamma$ are insensitive to the L-number violation that is responsible for leptogenesis.

Finally, gravitino leptogenesis requires a firm lower bound on the reheat temperature $T_{RH}^{\min} \approx 10^{12}$ GeV in order to generate a sufficiently large population of gravitinos to account for the observed baryon asymmetry in their decays. At present, constraints on the CMB tensor-to-scalar ratio, $r \propto T_{RH}^{1/4}$, give an upper bound on the reheat temperature, $T_{RH}^{\max} \approx 10^{16}$ GeV, so that significant improvements in sensitivity beyond those likely in the near future would be required to use this limit to probe this scenario.

$\lvert m_{3/2}\rvert$	$\lvert\mu'\rvert$	$M_{\tilde l}$	θ_{CP}	f_{wo}	$\mathrm{T_{RH}}$	β	$\dfrac{Y_B^*}{Y_B^{(\mathrm{obs})}}$	$\dfrac{m_\nu}{m_\nu^{(\mathrm{obs})}}$
10^8	$9\cdot10^7$	$8\cdot10^8$	0.1	0.1	10^{16}	$1\cdot10^{-4}$	0.4	1.0
10^{10}	$3\cdot10^9$	10^{10}	1	1.0	10^{16}	$7\cdot10^{-4}$	3	40
10^{12}	$3\cdot10^{11}$	10^{12}	0.5	0.7	10^{16}	$3\cdot10^{-4}$	1	0.4
10^{13}	10^{13}	10^{13}	0.1	0.05	10^{15}	$2\cdot10^{-4}$	0.1	0.4
10^{14}	$9\cdot10^{13}$	10^{14}	0.1	0.1	10^{16}	$2\cdot10^{-4}$	1	$4\cdot10^{-2}$

Table 4.2: Typical parameter sets for the model with $W_{\mathrm{LV}} = \hat{H}_u\hat{L}$ that produce the observed baryon asymmetry. The input parameters are the gravitino mass $\lvert m_{3/2}\rvert$, the mixing mass scale ($\mu' \sim \sqrt{B^u} \sim \sqrt{B^d}$), the CP-violating phase (θ_{CP}) in radians, the washout factor (f_{wo}), and the reheat temperature (T_{RH}). Dimensionful parameters are expressed in units of GeV. We estimate the baron asymmetry, Y_B^* using Eq. (4.25) along with the approximate estimate for β given by Eq. (4.71), and the ratio of the neutrino mass m_ν to the observed value, $m_\nu^{(\mathrm{obs})} \lesssim 1$ eV, by Eq. (4.72), setting $m_{\tilde{X}} \sim m_{3/2}$ and $t_\beta = 1$.

Chapter 5

GENERAL ANALYSIS OF DIRECT DARK MATTER DETECTION

5.1   Introduction

The existence of non-baryonic dark matter has been inferred from measurements including galactic rotation curves [124], large scale structure surveys [125, 126, 127], X-ray observations [128], gravitational lensing [129, 130], and cosmic microwave background anisotropy measurements [50], spanning cosmological eras from the present day to the remote past. This widespread and robust data has led to cold dark matter models with a cosmological constant, labeled ΛCDM becoming entrenched as the standard cosmological model.

Nevertheless, this impressive array of observations has only been sensitive to the *gravitational* influence of dark matter and constrained its relic abundance, leaving its particle nature as one of the most important open questions in physics. The search for dark matter includes indirect astrophysical searches ([131, 132, 133, 134, 135]), collider production efforts (for some examples of dark matter searches at the LHC, see [136, 137, 138, 139, 140]) which will examine new territory soon with LHC run 2 which will commence this year, and attempts to observe dark matter interactions with Standard Model (SM) particles via dark matter-nucleus scattering processes in direct detection experiments, to which we now turn.

The search for dark matter via direct detection goes back at least three decades [141, 142] and has been particularly vigorous over the last decade or so with experi-

ments such as LUX [143], Xenon100 [144], CDMS II (Ge) [145], CDMS I (Si) [146], DAMA/LIBRA [147], COGENT [148], and CRESST [149] pushing ever deeper into weakly interacting dark matter mass and scattering cross-section parameter space, but has thus far failed to yield a convincing signal. In the near future detectors such as Super CDMS [150] (which has recently released its first results on low mass dark matter searches [151, 152]), XENON1T [153], and DARWIN [154] are expected to push the limits of direct detection orders of magnitude below the current levels.

In order to connect observations to microphysical models one needs a general framework within which to interpret the observations of direct detection experiments. For quite some time the prevailing method of analyzing dark matter-nucleus interactions has been to assume that dark matter is a weakly interacting massive particle (WIMP), and then to categorize the interactions as elastic and isospin conserving and either spin-independent or spin-dependent [155, 156]. For some well studied models of dark matter, such as the weakly interacting Majorana neutralino found in super-symmetry models, this assumption is reasonable.

With an absence of observed dark matter signals, there has of late been a surge in interest in exploring more general types of interactions between dark matter and nuclei. Generalizations include inelastic and momentum dependent interactions, which may arise due to additional structure in the dark sector including excited dark matter states, or dark gauge bosons giving rise to electric and magnetic form factors [157, 158, 159, 160, 161, 162, 163, 164].

The formalism of choice for many of these investigations is relativistic effective field theory, which provides a model independent framework to analyse dark matter-SM

interactions [165, 166, 167]. It has been shown that these effective theories break down when applied to high-momentum transfer experiments, such as the LHC [168]. Therefore analyses moved beyond this framework and have moved to what are labeled as 'simplified models' instead [169, 170, 171]. Simplified models are field theories which extend the SM by a single dark matter particle and a single mediator particle which allows the WIMP to communicate with quarks and/or leptons. The newly added dark matter content is assumed to be a singlet under the SM gauge groups (we will consider some cases where the particles mediating the interaction have SM charge). In this context it is then possible to calculate collider amplitudes valid at the high energies of interest in such experiments. Given this simple dark sector, one can write down an exhaustive list of every combination of WIMP and mediator spins, and all possible tree level interactions. These simplified models have now gained popularity for analyzing indirect detection signals [172, 173], allowing connections to be made with the growing body of literature which make use of them.

Another step towards placing dark matter-nucleus interactions on a general footing has been accomplished recently by utilizing a non-relativistic effective field theory (EFT) approach [174, 1, 175, 176]. Since the interactions in direct detection scenarios are assumed to take place due to an incoming dark matter particle with a typical velocity $\mathcal{O}(100\text{km/s})$, the recoil momenta in such an interaction will be $\mathcal{O}(\lesssim 100\text{keV})$. The particle masses involved, including the nucleons of roughly GeV scale, the dark matter particles, which typically range from the GeV region to several orders of magnitude above, and mediators that can also be quite heavy compared to the typical interaction momenta, produce a situation where an EFT treatment is quite natural.

In order to circumvent as much model dependence as possible, one can construct

general interactions which obey Galilean invariance, T-symmetry, and Hermiticity. These operators will take the standard effective four-particle interaction form, reminiscent of Fermi's original model of weak interactions. The non-relativistic interactions can be shown to be functions of only four parameters including the nucleon spin S_N, the dark matter spin S_χ, the momentum transfer, $\vec{q}$, and a kinematic variable $\vec{v}^\perp$ which is a function of the relative incoming $(\vec{v}_{\chi,in} - \vec{v}_{N,in})$ and outgoing velocities $\vec{v}_{\chi,out} - \vec{v}_{N,out}$

$$\vec{v}^\perp = \frac{1}{2} \left(\vec{v}_{\chi,in} - \vec{v}_{N,in} + \vec{v}_{\chi,out} - \vec{v}_{N,out} \right) = \vec{v}_{\chi,in} - \vec{v}_{N,in} + \frac{\vec{q}}{2\mu_N} \tag{5.1}$$

which obeys $\vec{v}^\perp \cdot \vec{q} = 0$. It was demonstrated in [1] that there exist fifteen such non-relativistic interactions which arise from twenty possible bi-linear combinations of dark matter and nucleons.

The formalism developed in [1] is unique in being the only analysis to comprehensively develop the nuclear physics of direct detection experiments. From this general framework it is now apparent that there are interactions beyond the standard spin independent/dependent type. The origins of these 'new' interactions are not necessarily exotic and it has been shown, in the context of relativistic EFT, how many of them can be generated [177].

What has been lacking to date however, is a completely general and comprehensive treatment that connects high energy microphysics with low-energy effective nuclear matrix elements in a model independent way. It is possible, for example, that the various interactions listed in [1] can give rise to degeneracies where different fundamental dark matter Lagrangians, describing dark matter and interaction mediators of various spins, can produce the same interaction types. This will obviously pose

80

problems for attempts to discern the properties of dark matter when interpreting the results of experimental data. Furthermore, dark matter may not be spin-$\frac{1}{2}$, which creates a need for extending the parametric framework from the four descriptors listed above. In particular, as we shall show in this chapter, this allows the existence of new non-relativistic operators to appear in the low energy effective theory.

Motivated by the above we present in this chapter a general analysis covering a broad spectrum of particle and interaction types, starting from the microphysics, which will enable one to link experiment with fundamental theory while incorporating the new nuclear responses described in [1].

We build upon the NR-EFT description by examining simplified models which incorporate the most general renormalizable Lagrangians for scalar, spinor, and vector dark matter interacting with nucleons via scalar, spinor, and vector mediators, consistent with Lorentz invariance and hermiticity while imposing stability of the dark matter candidates. We integrate out the heavy mediator and obtain effective relativistic interaction Lagrangians. Next, we take the non-relativistic limit of these Lagrangians, and identify them with the NR operators from [1], which are reproduced below, in Table 5.1. Using these, we identify which electroweak nuclear responses are excited by a given fundamental interaction model and determine the relative importance of various models within the context of direct detection experiments consisting of xenon and germanium targets by exploring the relative magnitude of coefficients of these operators, and also their energy dependence.

This chapter is organized as follows; in section 5.2 the EFT formalism of [1] is summarized, in section 5.3 we build the generalized relativistic Lagrangians and in section 5.4, we outline the signatures and distinguishability of these models in the con-

text of direct detection experiments, providing a framework for both experimentalists and theorists to base their future analyses.

5.2 Non-Relativistic Effective Field Theory of Direct Detection

Conventionally, coherent WIMP-nucleus scattering has been considered to come from two types of interactions; spin-independent (SI) and spin-dependent (SD). SI interactions couple to the charge/mass of the nucleus while SD couples to the spin. The nuclear cross section is generally written in terms of the nucleon cross section at zero momentum transfer, σ_0, and a form factor, $F(q)$, to take into account the loss of coherence over the finite size of the nucleus,

$$\frac{d\sigma}{dE_r} = \frac{M}{2\pi\mu_{\chi M}v^2}\left(\sigma_0^{SI}F_{SI}^2(q) + \sigma_0^{SD}F_{SD}^2(q)\right). \tag{5.2}$$

where M is the mass of the target nucleus and $\mu_{\chi M}$ is the WIMP-nucleus reduced mass. This picture has recently been shown to be incomplete, as it is also possible for the WIMP to couple to the nucleus through additional nuclear responses [1]. Working in the language of a non-relativistic (NR) effective field theory Fitzpatrick et al. identified 15 operators to characterize the ways in which a WIMP can couple to the various nuclear responses. These operators are constructed from combinations of non-relativistic vectors which respect Galilean invariance, T symmetry and which are Hermitian. We list them in table 5.1. The Hermitian vectors are:

$$i\frac{\vec{q}}{m_N}, \ \vec{v}^\perp = \vec{v} + \frac{\vec{q}}{2\mu_N}, \ \vec{S}_\chi, \ \vec{S}_N, \tag{5.3}$$

where $\vec{q} = \vec{p'} - \vec{p} = \vec{k} - \vec{k'}$ is the momentum transfer, $\vec{v}$ is the velocity of WIMP with respect to the nucleus of the detector, μ_N is the reduced mass of the system and $\vec{S}_\chi$ and $\vec{S}_N$ are the WIMP and nuclear spins respectively. Throughout the chapter, we denote by $\vec{p}$ and $\vec{p'}$ the incoming and outgoing WIMP momenta and by $\vec{k}$ and $\vec{k'}$ the

incoming and outgoing nuclear momenta respectively. Energy-momentum conservation implies the orthogonality condition $\vec{q} \cdot \vec{v}^\perp = 0$. Here we will briefly outline the procedure employed in [1] in going from the NR operators to the final differential WIMP-nucleus cross section.

Table 5.1: List of NR effective operators described in [1]

$$\mathcal{O}_1 \qquad 1_\chi 1_N$$

$$\mathcal{O}_2 \qquad (\vec{v}^\perp)^2$$

$$\mathcal{O}_3 \qquad i\vec{S}_N \cdot \left(\frac{\vec{q}}{m_N} \times \vec{v}^\perp\right)$$

$$\mathcal{O}_4 \qquad \vec{S}_\chi \cdot \vec{S}_N$$

$$\mathcal{O}_5 \qquad i\vec{S}_\chi \cdot \left(\frac{\vec{q}}{m_N} \times \vec{v}^\perp\right)$$

$$\mathcal{O}_6 \qquad \left(\frac{\vec{q}}{m_N} \cdot \vec{S}_N\right)\left(\frac{\vec{q}}{m_N} \cdot \vec{S}_\chi\right)$$

$$\mathcal{O}_7 \qquad \vec{S}_N \cdot \vec{v}^\perp$$

$$\mathcal{O}_8 \qquad \vec{S}_\chi \cdot \vec{v}^\perp$$

$$\mathcal{O}_9 \qquad i\vec{S}_\chi \cdot \left(\vec{S}_N \times \frac{\vec{q}}{m_N}\right)$$

$$\mathcal{O}_{10} \qquad i\frac{\vec{q}}{m_N} \cdot \vec{S}_N$$

$$\mathcal{O}_{11} \qquad i\frac{\vec{q}}{m_N} \cdot \vec{S}_\chi$$

$$\mathcal{O}_{12} \qquad \vec{S}_\chi \cdot \left(\vec{S}_N \times \vec{v}^\perp\right)$$

$$\mathcal{O}_{13} \qquad i(\vec{S}_\chi \cdot \vec{v}^\perp)\left(\frac{\vec{q}}{m_N} \cdot \vec{S}_N\right)$$

$$\mathcal{O}_{14} \qquad i(\vec{S}_N \cdot \vec{v}^\perp)\left(\frac{\vec{q}}{m_N} \cdot \vec{S}_\chi\right)$$

$$\mathcal{O}_{15} \qquad -(\vec{S}_\chi \cdot \frac{\vec{q}}{m_N})\left((\vec{S}_N \times \vec{v}^\perp) \cdot \frac{\vec{q}}{m_N}\right)$$

In general one can write down the non-relativistic interaction Lagrangian as

$$\mathcal{L}_{NR} = \sum_{\alpha=n,p} \sum_{i=1}^{15} c_i^\alpha \mathcal{O}_i^\alpha, \tag{5.4}$$

where the coefficients c_i^α are given by the microphysics of the interaction and in general one could allow for isospin violation by having different couplings to neutron

and proton inside the nucleus. This can be rewritten in 2-component isospin space as

$$\mathcal{L}_{NR} = \sum_{\tau=0,1} \sum_{i=1}^{15} c_i^\tau \mathcal{O}_i t^\tau \tag{5.5}$$

where t^0 and t^1 are the identity matrix and the Pauli matrix σ^3 respectively. The nucleus is composed of nucleons, and these can individually interact with the WIMP. This is incorporated by considering the operator $\mathcal{O}(j)$ as an interaction between a single nucleon, j, and the WIMP, and then summing over the nucleons.

$$\sum_{\tau=0,1} \sum_{i=1}^{15} c_i^\tau \mathcal{O}_i t^\tau \rightarrow \sum_{\tau=0,1} \sum_{i=1}^{15} c_i^\tau \sum_{j=1}^{A} \mathcal{O}_i(j) t^\tau(j) \tag{5.6}$$

where A is the atomic mass number given by the total number of neutrons and protons. One can do the same reduction with $\vec{v}^\perp$,

$$
\begin{aligned}
\vec{v}^\perp & \rightarrow & \{\vec{v}_\chi - \vec{v}_N(i), i = 1, ..., A\} \\
& \equiv & \vec{v}_T^\perp - \{\dot{\vec{v}}_N(i), i = 1, ..., A-1\}
\end{aligned} \tag{5.7}
$$

where $\vec{v}_\chi$ and $\vec{v}_N(i)$ are the symmetrized combination of incoming and outgoing velocities for the WIMP and nucleons respectively. $\vec{v}_T^\perp$ (here T stands for target, i.e., the nuclear center-of-mass) is defined as

$$\vec{v}_T^\perp = \vec{v}_\chi - \frac{1}{2A} \sum_{i=1}^{A} [\vec{v}_{N,in}(i) + \vec{v}_{N,out}(i)] \tag{5.8}$$

This allows for a decomposition of the nucleon velocities into internal velocities $\dot{\vec{v}}_N(i)$ that act only on intrinsic nuclear coordinates and 'in' and 'out' velocities that evolve as a WIMP scatters off the detector. As an example, the dot product between $\vec{v}_N^\perp$ and $\vec{S}_N$ can be rewritten as

$$
\begin{aligned}
\vec{v}^\perp \cdot \vec{S}_N & \rightarrow & \sum_{i=1}^{A} \frac{1}{2} [\vec{v}_{\chi,in} + \vec{v}_{\chi,out} - \vec{v}_{N,in}(i) - \vec{v}_{N,out}(i)] \cdot \vec{S}_N(i) \tag{5.9} \\
& = & \vec{v}_T^\perp \cdot \sum_{i=1}^{A} \vec{S}_N(i) - \left\{ \sum_{i=1}^{A} \frac{1}{2} [\vec{v}_{N,in}(i) + \vec{v}_{N,out}(i)] \cdot \vec{S}_N(i) \right\}_{int} \tag{5.10}
\end{aligned}
$$

The second term in the curly brackets is internal to the nucleus and acts as an operator on the 'in' and 'out' nucleon states. $\vec{v}_{N,in}$ can be replaced by $\vec{p}_{N,in}/M$ acting on the incoming state, which can in turn be replaced by $i\overleftarrow{\nabla}/M$, and similarly $\vec{p}_{N,out}/M$ by $-i\overrightarrow{\nabla}/M$ on the outgoing nuclear state. Finally, since the nucleus is non-zero in size and individual nucleons locally interact with the WIMP, nuclear operators built from $\mathcal{O}_i$ are accompanied by an additional spatial operator $e^{-i\vec{q}\cdot\vec{x}(i)}$ where $x(i)$ is the location of the ith nucleon inside the nucleus.

Starting from Eqn. 5.6 and using the substitution rules for $\vec{v}^\perp$ and including a factor of $e^{-i\vec{q}\cdot\vec{x}_i}$, the interaction Lagrangian can be written as a sum of five distinct terms (nuclear electroweak operators) that only act on internal nucleon states. Their coefficients, on the other hand, act on WIMP 'in' and 'out' states. The WIMP-nucleus interaction can then be written as

$$\sum_{\tau=0,1}\left\{l_0^\tau S + l_0^{A\tau} T + \vec{l}_5^\tau \cdot \vec{P} + \vec{l}_M^\tau \cdot \vec{Q} + \vec{l}_E^\tau \cdot \vec{R}\right\} t^\tau(i) \tag{5.11}$$

where

$$S = \sum_{i=1}^{A} e^{-i\vec{q}\cdot\vec{x}_i}$$

$$T = \sum_{i=1}^{A} \frac{1}{2M}\left[-\frac{1}{i}\overleftarrow{\nabla}_i \cdot \vec{\sigma}(i) e^{-i\vec{q}\cdot\vec{x}_i} + e^{-i\vec{q}\cdot\vec{x}_i}\vec{\sigma}(i) \cdot \frac{1}{i}\overrightarrow{\nabla}_i\right]$$

$$\vec{P} = \sum_{i=1}^{A} \vec{\sigma}(i) e^{-i\vec{q}\cdot\vec{x}_i}$$

$$\vec{Q} = \sum_{i=1}^{A} \frac{1}{2M}\left[-\frac{1}{i}\overleftarrow{\nabla}_i e^{-i\vec{q}\cdot\vec{x}_i} + e^{-i\vec{q}\cdot\vec{x}_i}\frac{1}{i}\overrightarrow{\nabla}_i\right]$$

$$\vec{R} = \sum_{i=1}^{A} \frac{1}{2M}\left[\overleftarrow{\nabla}_i \times \vec{\sigma}(i) e^{-i\vec{q}\cdot\vec{x}_i} + e^{-i\vec{q}\cdot\vec{x}_i}\vec{\sigma}(i) \times \overrightarrow{\nabla}_i\right] \tag{5.12}$$

and

$$l_0^\tau = c_1^\tau + ic_5^\tau \vec{S}_\chi \cdot \left(\frac{\vec{q}}{m_N} \times \vec{v}_T^\perp \right) + c_8^\tau (\vec{S}_\chi \cdot \vec{v}_T^\perp) + ic_{11}^\tau \frac{\vec{q} \cdot \vec{S}_\chi}{m_N}$$

$$l_0^{A\tau} = -\frac{1}{2} \left[c_7^\tau + ic_{14}^\tau \left(\vec{S}_\chi \cdot \frac{\vec{q}}{m_N} \right) \right]$$

$$\vec{l}_5 = \frac{1}{2} \left[c_3^\tau i \frac{(\vec{q} \times \vec{v}_T^\perp)}{m_N} + c_4^\tau \vec{S}_\chi + c_6^\tau \frac{(\vec{q} \cdot \vec{S}_\chi)\vec{q}}{m_N^2} + c_7^\tau \vec{v}_T^\perp + ic_9^\tau \frac{(\vec{q} \times \vec{S}_\chi)}{m_N} + ic_{10}^\tau \frac{\vec{q}}{m_N} \right.$$
$$\left. c_{12}^\tau (\vec{v}_T^\perp \times \vec{S}_\chi) + ic_{13}^\tau \frac{(S_\chi \cdot \vec{v}_T^\perp)\vec{q}}{m_N} + ic_{14}^\tau \left(\vec{S}_\chi \cdot \frac{\vec{q}}{m_N} \right) \vec{v}_T^\perp + c_{15}^\tau \frac{(\vec{q} \cdot \vec{S}_\chi)(\vec{q} \times \vec{v}_T^\perp)}{m_N^2} \right]$$

$$\vec{l}_M = c_5^\tau \left(i \frac{\vec{q}}{m_N} \times \vec{S}_\chi \right) - \vec{S}_\chi c_8^\tau$$

$$\vec{l}_E = \frac{1}{2} \left[c_3^\tau \frac{\vec{q}}{m_N} + ic_{12}^\tau \vec{S}_\chi - c_{13}^\tau \frac{(\vec{q} \times \vec{S}_\chi)}{m_N} - ic_{15}^\tau \frac{(\vec{q} \cdot \vec{S}_\chi)\vec{q}}{m_N^2} \right] \tag{5.13}$$

The WIMP-nucleus amplitude, $\mathcal{M}$, can then be succinctly written as

$$\mathcal{M} = \sum_{\tau=0,1} \langle j_\chi, M_\chi; j_N, M_N | \left\{ l_0^\tau S + l_0^{A\tau} T + \vec{l}_5^\tau \cdot \vec{P} + \vec{l}_M^\tau \cdot Q + \vec{l}_E^\tau \cdot \vec{R} \right\}$$
$$t^\tau(i) | j_\chi, M_\chi; j_N, M_N \rangle \tag{5.14}$$

By using spherical decomposition, the internal nuclear operators S, T, P, Q and R can be further rewritten in terms of standard nuclear electroweak responses as follows:

$$\mathcal{M} = \sum_{\tau=0,1} \langle j_\chi, M_{\chi f}; j_N, M_{Nf} | \left(\sum_{J=0} \sqrt{4\pi(2J+1)}(-i)^J \left[l_0^\tau M_{J0;\tau} - il_0^{A\tau} \frac{q}{m_N} \tilde{\Omega}_{J0;\tau}(q) \right] \right.$$
$$+ \sum_{J=1} \sqrt{2\pi(2J+1)}(-i)^J \sum_{\lambda\pm1}(-1)^\lambda \left\{ l_{5\lambda}^\tau [\lambda \Sigma_{J-\lambda;\tau}(q) + i\Sigma'_{J-\lambda;\tau}(q)] \right.$$
$$\left. -i\frac{q}{m_N} l_{M\lambda}^\tau [\lambda \Delta_{J-\lambda;\tau}(q)] - i\frac{q}{m_N} l_{E\lambda}^\tau [\lambda \tilde{\Phi}_{J-\lambda;\tau}(q) + i\tilde{\Phi}'_{J-\lambda;\tau}(q)] \right\} \tag{5.15}$$
$$+ \sum_{J=0}^\infty \sqrt{4\pi(2J+1)}(-i)^J \left[il_{50}^\tau \Sigma''_{J0;\tau}(q) + \frac{q}{m_N} l_{M0}^\tau \tilde{\Delta}''_{J0;\tau}(q) \right.$$
$$\left. \left. + \frac{q}{m_N} l_{E0}^\tau \tilde{\Phi}''_{J0;\tau}(q) \right] \right) | j_\chi, M_{\chi i}; j_N, M_{Ni} \rangle$$

Where there is an implicit sum over the nucleons,

$$\mathcal{O}_{JM;\tau}(q) \equiv \sum_{i=1}^{A} \mathcal{O}_{JM}(q\vec{x}_i)t^\tau(i), \tag{5.16}$$

and the various electroweak responses are defined as

$$
\begin{aligned}
M_{JM}(q\vec{x}) &\equiv j_J(qx)Y_{JM}(\Omega_x) \\
\vec{M}_{JL}^{M} &\equiv j_J(qx)\vec{Y}_{JLM}(\Omega_x) \\
\Delta_{JM} &\equiv \vec{M}_{JJ}^{M}(qx_i) \cdot \frac{1}{q}\vec{\nabla}_i \\
\Sigma'_{JM} &\equiv -i\left\{\frac{1}{q}\vec{\nabla}_i \times \vec{M}_{JJ}^{M}(q\vec{x}_i)\right\} \cdot \vec{\sigma}(i) \\
\Sigma''_{JM} &\equiv \left\{\frac{1}{q}\vec{\nabla}_i M_{JM}(q\vec{x}_i)\right\} \cdot \vec{\sigma}(i) \\
\tilde{\Phi}'_{JM} &\equiv \left[\frac{1}{q}\vec{\nabla}_i \times \vec{M}_{JJ}^{M}(q\vec{x}_i)\right] \cdot \left[\vec{\sigma}(i) \times \frac{1}{q}\vec{\nabla}_i\right] + \frac{1}{2}\vec{M}_{JJ}^{M}(q\vec{x}_i) \cdot \vec{\sigma}(i) \\
\Phi''_{JM} &\equiv i\left[\frac{1}{q}\vec{\nabla}_i M_{JM}(q\vec{x}_i)\right] \cdot \left[\vec{\sigma}(i) \times \frac{1}{q}\vec{\nabla}_i\right] \\
\Sigma_{JM} &\equiv \vec{M}_{JJ}^{M}(q\vec{x}_i) \cdot \vec{\sigma}(i) \\
\tilde{\Omega}_{JM} &\equiv \Omega_{JM}(q\vec{x}_i) + \frac{1}{2}\Sigma''_{JM}(q\vec{x}_i) \\
\tilde{\Phi}_{JM} &\equiv \Phi_{JM}(qx_i) - \frac{1}{2}\Sigma'_{JM}(qx_i) \\
\tilde{\Delta}''_{JM} &\equiv \Delta''_{JM}(qx_i) - \frac{1}{2}M_{JM}(qx_i) \tag{5.17}
\end{aligned}
$$

where Y_{JM} and $\vec{Y}_{JLM}$ are spherical harmonics and vector spherical harmonics respectively. We are only considering elastic transitions, and assuming parity and CP as symmetries of the nuclear ground state. This eliminates some of the responses, and only $M, \Phi'', \Sigma', \Delta, \Sigma'', \tilde{\Phi}'$ survive. To calculate cross-sections, one needs to square the amplitude, average over initial spins and sum over final spins. The matrix element squared for the nuclear portion of the amplitude has been made available by Fitzpatrick et al. [1], and codes have been supplied to calculate the full amplitude and rate [175].

As we shall describe, in the following analysis we discovered that two additional NR operators are required to fully describe the scattering of spin-1 WIMPs off nuclei,

$$\mathcal{O}_{17} \equiv i\frac{\vec{q}}{m_N} \cdot \mathcal{S} \cdot \vec{v}_{\perp},$$

$$\mathcal{O}_{18} \equiv i\frac{\vec{q}}{m_N} \cdot \mathcal{S} \cdot \vec{S}_N, \tag{5.18}$$

where $\mathcal{S}$ is the symmetric combination of polarization vectors.

5.3 Simplified Models for Direct Detection

From a model building perspective, one would like to know how relevant the novel nuclear responses are in interpreting direct detection data. Previous work [177] demonstrated that using only the SI/SD form factors (even with additional momentum dependence taken into account) can lead one to infer wildly incorrect values of the WIMP mass and cross sections.

Here we go further by starting with simplified models at the Lagrangian level, where 'simplified model' means a single WIMP with a single mediator coupling it to the quark sector. This is useful for two reasons; it allows us to better explore which NR operators arise from a broad set of UV complete theories, and also make connection with the growing body of literature which use simplified models for indirect detection and collider searches.

When it comes to interpreting signals, knowing comprehensively how different interactions with different nuclei arise from different UV complete models will allow us to identify degeneracies between competing models. Further, it can also help optimize target selection for maximum discrimination of the UV model parameter space.

In building these simplified models we remain agnostic about the WIMP's spin,

and consider dark matter spins of $0, \frac{1}{2}$ and 1. We do however only consider renormalizable interactions between quarks and WIMPs. To ensure a stable WIMP, we assume that the WIMP is either charged under some internal gauge group or a discrete symmetry group (for example Z_2). However, we assume that this gauge charge is not shared by quarks. We will couple the WIMP to the quarks via a heavy mediator in two distinct ways: charged and uncharged mediators, each with all possible spins consistent with angular momentum conservation. The mediator mass is chosen to be the heaviest scale in the problem (and certainly much greater than the momentum exchange which characterizes the scattering process) so that we can integrate it out (see Appendix G for details). This leads to relativistic effective WIMP-nucleon interactions, whose NR limit can then be examined. In the uncharged mediator case we will consider mediators that are neutral under all SM and WIMP gauge charges, while in the charged case, the mediator must have both WIMP and SM gauge charges. Given the above as a guide, our Lagrangian construction is then constrained only by gauge invariance, Lorentz invariance, renormalizability and hermiticity. In certain cases which follow, the requirement of hermiticity demands coupling constants be complex. Unless explicitly noted, the coupling constants are dimensionless and can be assumed to be real.

A. Uncharged-mediator Lagrangians

1. Scalar Dark Matter

We begin with a spin-0 scalar WIMP, S, which has some internal charge to ensure stability, and $S^\dagger$ is its Hermitian conjugate. To have renormalizable interactions, the neutral mediator can only be a scalar or a vector. We denote the scalar mediator by ϕ and the vector mediator by G^μ with field strength tensor $\mathcal{G}_{\mu\nu}$.

The most general renormailzable Lagrangian for scalar mediation consistent with the above assumptions is given by

$$
\begin{aligned}
\mathcal{L}_{S\phi q} &= \partial_\mu S^\dagger \partial^\mu S - m_S^2 S^\dagger S - \frac{\lambda_S}{2}(S^\dagger S)^2 + \frac{1}{2}\partial_\mu \phi \partial^\mu \phi - \frac{1}{2}m_\phi^2 \phi^2 - \frac{m_\phi \mu_1}{3}\phi^3 - \frac{\mu_2}{4}\phi^4 \\
&\quad + i\bar{q}\slashed{D}q - m_q \bar{q}q - g_1 m_S S^\dagger S \phi - \frac{g_2}{2}S^\dagger S \phi^2 - h_1 \bar{q}q\phi - ih_2 \bar{q}\gamma^5 q\phi \qquad (5.19)
\end{aligned}
$$

where we have suppressed all the SM quark interactions. Similarly, the Lagrangian for vector mediation (up to gauge fixing terms) is

$$
\begin{aligned}
\mathcal{L}_{SGq} &= \partial_\mu S^\dagger \partial^\mu S - m_S^2 S^\dagger S - \frac{\lambda_S}{2}(S^\dagger S)^2 - \frac{1}{4}\mathcal{G}_{\mu\nu}\mathcal{G}^{\mu\nu} + \frac{1}{2}m_G^2 G_\mu G^\mu - \frac{\lambda_G}{4}(G_\mu G^\mu)^2 \\
&\quad + i\bar{q}\slashed{D}q - m_q \bar{q}q - \frac{g_3}{2}S^\dagger S G_\mu G^\mu - ig_4(S^\dagger \partial_\mu S - \partial_\mu S^\dagger S)G^\mu \\
&\quad - h_3(\bar{q}\gamma_\mu q)G^\mu - h_4(\bar{q}\gamma_\mu \gamma^5 q)G^\mu \qquad (5.20)
\end{aligned}
$$

2. Spin-$\frac{1}{2}$ Dark Matter

If the WIMP has spin-$\frac{1}{2}$ (denoted by χ below), then, as in the scalar WIMP case, mediation will only occur via scalar or vector mediators. The most general renormalizable interactions for the scalar (ϕ) and vector mediator (G_μ) cases respectively are given below,

$$
\begin{aligned}
\mathcal{L}_{\chi\phi q} &= i\bar{\chi}\slashed{D}\chi - m_\chi \bar{\chi}\chi + \frac{1}{2}\partial_\mu \phi \partial^\mu \phi - \frac{1}{2}m_\phi^2 \phi^2 - \frac{m_\phi \mu_1}{3}\phi^3 - \frac{\mu_2}{4}\phi^4 \\
&\quad + i\bar{q}\slashed{D}q - m_q \bar{q}q - \lambda_1 \phi \bar{\chi}\chi - i\lambda_2 \phi \bar{\chi}\gamma^5 \chi - h_1 \phi \bar{q}q - ih_2 \phi \bar{q}\gamma^5 q \qquad (5.21)
\end{aligned}
$$

$$
\begin{aligned}
\mathcal{L}_{\chi Gq} &= i\bar{\chi}\slashed{D}\chi - m_\chi \bar{\chi}\chi - \frac{1}{4}\mathcal{G}_{\mu\nu}\mathcal{G}^{\mu\nu} + \frac{1}{2}m_G^2 G_\mu G^\mu + i\bar{q}\slashed{D}q - m_q \bar{q}q \\
&\quad - \lambda_3 \bar{\chi}\gamma^\mu \chi G_\mu - \lambda_4 \bar{\chi}\gamma^\mu \gamma^5 \chi G_\mu - h_3 \bar{q}\gamma_\mu q G^\mu - h_4 \bar{q}\gamma_\mu \gamma^5 q G^\mu \qquad (5.22)
\end{aligned}
$$

3. Spin-1 Dark Matter

If the WIMP is a massive spin-1 particle, uncharged mediation to the quark sector can occur via a heavy scalar or a vector particle. For the case of vector mediation, there are many possible interactions because the Lorentz indices on the vectors afford a more diverse set of terms. The general interaction Lagrangian for the scalar mediation case is

$$
\begin{aligned}
\mathcal{L}_{X\phi q} &= -\frac{1}{2}\mathcal{X}_{\mu\nu}^{\dagger}\mathcal{X}^{\mu\nu} + m_X^2 X_\mu^{\dagger}X^\mu - \frac{\lambda_X}{2}(X_\mu^{\dagger}X^\mu)^2 + \frac{1}{2}(\partial_\mu\phi)^2 - \frac{1}{2}m_\phi^2\phi^2 \\
&\quad - \frac{m_\phi\mu_1}{3}\phi^3 - \frac{\mu_2}{4}\phi^4 + i\bar{q}\slashed{D}q - m_q\bar{q}q - b_1 m_X\phi X_\mu^{\dagger}X^\mu - \frac{b_2}{2}\phi^2 X_\mu^{\dagger}X^\mu \\
&\quad - h_1\phi\bar{q}q - ih_2\phi\bar{q}\gamma^5 q
\end{aligned}
\tag{5.23}
$$

For the case of vector mediation, there are many possible interactions because the Lorentz indices on the vectors afford a more diverse set of terms. The Lagrangian is given by

$$
\begin{aligned}
\mathcal{L}_{XGq} &= -\frac{1}{2}\mathcal{X}_{\mu\nu}^{\dagger}\mathcal{X}^{\mu\nu} + m_X^2 X_\mu^{\dagger}X^\mu - \frac{\lambda_X}{2}(X_\mu^{\dagger}X^\mu)^2 - \frac{1}{4}\mathcal{G}_{\mu\nu}\mathcal{G}^{\mu\nu} + \frac{1}{2}m_G^2 G_\mu^2 \\
&\quad - \frac{\lambda_G}{4}(G_\mu G^\mu)^2 + i\bar{q}\slashed{D}q - m_q\bar{q}q - \frac{b_3}{2}G_\mu^2(X_\nu^{\dagger}X^\nu) - \frac{b_4}{2}(G^\mu G^\nu)(X_\mu^{\dagger}X_\nu) \\
&\quad - \left[ib_5 X_\nu^{\dagger}\partial_\mu X^\nu G^\mu + b_6 X_\mu^{\dagger}\partial^\mu X_\nu G^\nu + b_7\epsilon_{\mu\nu\rho\sigma}(X^{\dagger\mu}\partial^\nu X^\rho)G^\sigma + h.c.\right] \\
&\quad - h_3 G_\mu\bar{q}\gamma^\mu q - h_4 G_\mu\bar{q}\gamma^\mu\gamma^5 q
\end{aligned}
\tag{5.24}
$$

where, for the Lagrangian to be Hermitian, b_6 and b_7 are complex (this implies a new source of CP violation, which will not be considered further here).

5.3.1 Charged-Mediator Lagrangians

Here we consider the simplest case of mediators that are charged under both the DM internal symmetry group and SM gauge groups. This is motivated by the absence of spin-$\frac{1}{2}$ mediators (s-channel processes) in the previous section. Such a mediator, if neutral, is forbidden by simultaneous requirements of gauge invariance

and renormalizability. Dark Matter models with mediators endowed with charges from both DM and SM side have been considered in the literature before [178, 179]. The case of a spin-$\frac{1}{2}$ mediator carrying $SU(3)_c$ is also motivated by studies of heavy quark models. This allows unique interactions as we show below. In particular they necessitate a direct interaction between quarks and WIMPs at the level of the Lagrangian.

1. Scalar Dark Matter

Scalar WIMPs with a charged scalar or vector mediator do not lead to any Lorentz invariant interactions. This is easy to see since both the scalars (or scalar and vector) and the quark are required in the (gauge invariant) interaction, but there is no way to contract the spinor indices consistently if the mediating particle is a scalar or vector. Therefore, the only possibility is that of a spin-1/2 mediator, Q, which acts like a heavy quark. The general renormalizable action is given by

$$
\begin{aligned}
\mathcal{L}_{SQq} = {} & \partial_\mu S^\dagger \partial^\mu S - m_S^2 S^\dagger S - \lambda_S (S^\dagger S)^2 + i\bar{Q}\slashed{D}Q - m_Q \bar{Q}Q \\
& + i\bar{q}\slashed{D}q - m_q \bar{q}q - \left(y_1 S\bar{Q}q + y_2 S\bar{Q}\gamma^5 q + h.c. \right)
\end{aligned}
\tag{5.25}
$$

where y_1 and y_2 are again complex.

2. Spin-$\frac{1}{2}$ Dark Matter

For a spin-1/2 WIMP, both a charged scalar and charged vector mediator exchange can lead to novel interactions. The charged scalar is denoted by Φ and the charged vector by V_μ

$$
\begin{aligned}
\mathcal{L}_{\chi\Phi q} = {} & i\bar{\chi}\slashed{D}\chi - m_\chi \bar{\chi}\chi + (\partial_\mu \Phi^\dagger)(\partial^\mu \Phi) - m_\Phi^2 \Phi^\dagger \Phi - \frac{\lambda_\Phi}{2}(\Phi^\dagger \Phi)^2 + i\bar{q}\slashed{D}q - m_q \bar{q}q \\
& - \left(l_1 \Phi^\dagger \bar{\chi}q + l_2 \Phi^\dagger \bar{\chi}\gamma^5 q + h.c. \right)
\end{aligned}
\tag{5.26}
$$

$$\mathcal{L}_{\chi V q} \;=\; i\bar{\chi}\slashed{D}\chi - m_\chi\bar{\chi}\chi - \frac{1}{2}\mathcal{V}_{\mu\nu}^\dagger\mathcal{V}^{\mu\nu} + m_V^2 V_\mu^\dagger V^\mu + i\bar{q}\slashed{D}q - m_q\bar{q}q$$

$$- \left(d_1\bar{\chi}\gamma^\mu q V_\mu^\dagger + d_2\bar{\chi}\gamma^\mu\gamma^5 q V_\mu^\dagger + h.c.\right), \tag{5.27}$$

where l_1, l_2, d_1 and d_2 are complex.

3. Vector DM

Here again we only have the case of a spin-$\frac{1}{2}$ mediated interaction between vector DM and quarks (again scalar and vector charged mediators aren't possible because they don't lead to Lorentz invariant and renormalizable interactions). The general Lagrangian is given by

$$\mathcal{L}_{XQq} \;=\; -\frac{1}{2}\mathcal{X}_{\mu\nu}^\dagger\mathcal{X}^{\mu\nu} + m_X^2 X_\mu^\dagger X^\mu - \frac{\lambda_X}{2}(X_\mu^\dagger X^\mu)^2 + i\bar{Q}\slashed{D}Q - m_Q\bar{Q}Q + i\bar{q}\slashed{D}q - m_q\bar{q}q$$

$$- \left(y_3 X_\mu\bar{Q}\gamma^\mu q + y_4 X_\mu\bar{Q}\gamma^\mu\gamma^5 q + h.c.\right), \tag{5.28}$$

where y_3 and y_4 are complex.

5.4 Non-Relativistic Reduction of Simplified Models

After integrating out the heavy mediator we replace quark operators with nucleon operators, take the non-relativistic limit, and match onto the operators given in table 5.1. The details of this procedure are given at the end of this section. The results of this calculation are presented in terms of the c_i coefficients from [175], described in section 5.2, facilitating a straightforward computation of amplitudes and rates. The c_i's are given for each of the WIMP spins in tables 5.2, 5.3 and 5.4. With this general framework in place we can now easily find the leading order NR operators for each distinct WIMP-nucleus interaction. One can imagine a series of minimal scenarios in which a combination of two Lagrangian couplings that give rise to a direct detection signal is non-zero with all others set to zero, and then proceeding in this manner for

93

the entire set. Each of these scenarios is listed with its leading operators in table 5.5 and with all operators generated in table 5.10. Note that in the case of a complex coupling constant we consider purely real and purely imaginary values as separate cases since they produce a distinct set of operators.

Table 5.2: Non-zero c_i coefficients for a spin-0 WIMP

	Uncharged Mediator	Charged Mediator
c_1	$\frac{h_1^N g_1}{m_\phi^2}$	$\frac{y_1^\dagger y_1 - y_2^\dagger y_2}{m_Q m_S} f_T^N$
c_{10}	$\frac{-i h_2^N g_1}{m_\phi^2} + \frac{2 i g_4 h_4^N}{m_G^2} \frac{m_N}{m_S}$	$i \frac{y_2^\dagger y_1 - y_1^\dagger y_2}{m_Q m_S} \tilde{\Delta}^N$

Table 5.3: c_i coefficients for a spin-$\frac{1}{2}$ WIMP

	Uncharged Mediator	Charged Mediator
c_1	$\frac{h_1^N \lambda_1}{m_\phi^2} - \frac{h_3^N \lambda_3}{m_G^2}$	$\left(\frac{l_2^\dagger l_2 - l_1^\dagger l_1}{4 m_\Phi^2} + \frac{d_2^\dagger d_2 - d_1^\dagger d_1}{4 m_V^2}\right) f_T^N + \left(-\frac{l_2^\dagger l_2 + l_1^\dagger l_1}{4 m_\Phi^2} + \frac{d_2^\dagger d_2 + d_1^\dagger d_1}{8 m_V^2}\right) \mathcal{N}^N$
c_4	$\frac{4 h_4^N \lambda_4}{m_G^2}$	$\frac{l_2^\dagger l_2 - l_1^\dagger l_1}{m_\Phi^2} \delta^N - \left(\frac{l_1^\dagger l_1 + l_2^\dagger l_2}{m_\Phi^2} + \frac{d_2^\dagger d_2 - d_1^\dagger d_1}{2 m_V^2}\right) \Delta^N$
c_6	$\frac{h_2^N \lambda_2 m_N}{m_\phi^2 m_\chi}$	$\left(\frac{l_1^\dagger l_1 - l_2^\dagger l_2}{4 m_\Phi^2} + \frac{d_2^\dagger d_2 - d_1^\dagger d_1}{4 m_V^2}\right) \frac{m_N}{m_\chi} \tilde{\Delta}^N$
c_7	$\frac{2 h_4^N \lambda_3}{m_G^2}$	$\left(\frac{l_1^\dagger l_2 - l_2^\dagger l_1}{2 m_\Phi^2} + \frac{d_1^\dagger d_2 + d_2^\dagger d_1}{4 m_V^2}\right) \Delta^N$
c_8	$-\frac{2 h_3^N \lambda_4}{m_G^2}$	$\left(\frac{l_1^\dagger l_2 - l_2^\dagger l_1}{2 m_\Phi^2} - \frac{d_1^\dagger d_2 + d_2^\dagger d_1}{4 m_V^2}\right) \mathcal{N}^N$
c_9	$-\frac{2 h_4^N \lambda_3 m_N}{m_\chi m_G^2} - \frac{2 h_3^N \lambda_4}{m_G^2}$	$\left(\frac{l_1^\dagger l_2 - l_2^\dagger l_1}{2 m_\Phi^2} - \frac{d_1^\dagger d_2 + d_2^\dagger d_1}{4 m_V^2}\right) \mathcal{N}^N - \left(\frac{l_1^\dagger l_2 - l_2^\dagger l_1}{2 m_\Phi^2} - \frac{d_1^\dagger d_2 + d_2^\dagger d_1}{4 m_V^2}\right) \frac{m_N}{m_\chi} \Delta^N$
c_{10}	$\frac{h_2^N \lambda_1}{m_\phi^2}$	$i\left(\frac{l_1^\dagger l_2 - l_2^\dagger l_1}{4 m_\Phi^2} + \frac{d_2^\dagger d_1 - d_1^\dagger d_2}{4 m_V^2}\right) \tilde{\Delta}^N - i \frac{l_1^\dagger l_2 - l_2^\dagger l_1}{m_\Phi^2} \delta^N$
c_{11}	$-\frac{h_1^N \lambda_2 m_N}{m_\phi^2 m_\chi}$	$i\left(\frac{l_2^\dagger l_1 - l_1^\dagger l_2}{4 m_\Phi^2} + \frac{d_2^\dagger d_1 - d_1^\dagger d_2}{4 m_V^2}\right) \frac{m_N}{m_\chi} f_T^N + i \frac{l_1^\dagger l_2 - l_2^\dagger l_1}{m_\Phi^2} \frac{m_N}{m_\chi} \delta^N$
c_{12}	0	$\frac{l_2^\dagger l_1 - l_1^\dagger l_2}{m_\Phi^2} \delta^N$

As described earlier, we find that it is important to consider operators beyond those incorporated into the standard spin-independent and spin-dependent formalism, i.e. simple models exist in which one would infer an incorrect rate in current experiments by not including these effects. Also importantly, not all of the NR operators are actually generated at leading order; for example, the operators $\mathcal{O}_2$, $\mathcal{O}_3$, $\mathcal{O}_{13}$

Table 5.4: c_i coefficients for a spin-1 WIMP

	Uncharged Mediator	Charged Mediator
c_1	$\dfrac{b_1 h_1^N}{m_\phi^2}$	$\dfrac{y_3^\dagger y_3 - y_4^\dagger y_4}{m_Q m_X} f_T^N$
c_4	$\dfrac{4\mathrm{Im}(b_7)h_4^N}{m_G^2} + i\dfrac{q^2}{m_X^2}\dfrac{\mathrm{Re}(b_7)h_4^N}{m_G^2} - \dfrac{q^2}{m_X m_N}\dfrac{\mathrm{Re}(b_6)h_3^N}{m_G^2}$	$2\dfrac{y_3^\dagger y_3 - y_4^\dagger y_4}{m_Q m_X}\delta^N$
c_5	$\dfrac{\mathrm{Re}(b_6)h_3^N}{m_G^2}\dfrac{m_N}{m_X}$	0
c_6	$\dfrac{\mathrm{Re}(b_6)h_3^N}{m_G^2}\dfrac{m_N}{m_X} - i\dfrac{\mathrm{Re}(b_7)h_4^N}{m_G^2}\dfrac{m_N^2}{m_X^2}$	0
c_8	$\dfrac{2\mathrm{Im}(b_7)h_3^N}{m_G^2}$	0
c_9	$-\dfrac{2\mathrm{Re}(b_6)h_4^N}{m_G^2}\dfrac{m_N}{m_X} + \dfrac{2\mathrm{Im}(b_7)h_3^N}{m_G^2}$	0
c_{10}	$\dfrac{b_1 h_2^N}{m_\phi^2} - \dfrac{3b_5 h_4^N}{m_G^2}\dfrac{m_N}{m_X}$	$i\dfrac{y_4^\dagger y_3 - y_3^\dagger y_4}{m_Q m_X}\tilde{\Delta}^N$
c_{11}	$\dfrac{\mathrm{Re}(b_7)h_3^N}{m_G^2}\dfrac{m_N}{m_X}$	$i\dfrac{y_4^\dagger y_3 - y_3^\dagger y_4}{m_Q m_X}\delta^N$
c_{12}	0	$2i\dfrac{y_3^\dagger y_4 - y_4^\dagger y_3}{m_Q m_X}\delta^N$
c_{14}	$-\dfrac{2\mathrm{Re}(b_7)h_4^N}{m_G^2}\dfrac{m_N}{m_X}$	0
c_{17}	$-\dfrac{4\mathrm{Im}(b_6)h_3^N}{m_G^2}\dfrac{m_N}{m_X}$	0
c_{18}	$\dfrac{4\mathrm{Im}(b_6)h_4^N}{m_G^2}\dfrac{m_N}{m_X}$	$-2i\dfrac{y_4^\dagger y_3 - y_3^\dagger y_4}{m_Q m_X}\delta^N$

and $\mathcal{O}_{15}$ are missing at leading order. Note that we only consider renormalizable Lagrangians, higher order non-renormalizable operators, which are presumably further suppressed. We have also not considered the case of kinetic mixing, which could be used to generate anapole interactions [177], because the effective interaction doesn't arise from one mediator exchange.

While spin independent interactions are a generic feature of direct couplings to quarks in our charged mediator cases, it is sometimes possbile to suppress them. In the scalar (and vector) WIMP with charged mediator cases, it is possible to suppress the spin independent interaction by ensuring that $|y_1| = |y_2|(|y_3| = |y_4|)$ while keeping their relative phases non-zero (or π). While these non-minimal scenarios require

some fine tuning we include it for completeness and label them y_1, y_2 and y_3, y_4.

Aside from scalar WIMPs, each particular spin produces some non-relativistic operators that are unique to that spin. Also, importantly, the operators $\mathcal{O}_1$ and $\mathcal{O}_{10}$ are generic to all spins. In five cases relativistic operators generate unique non-relativistic operators at leading order. Therefore distinguishing WIMP scenarios in these cases reduces to experimentally discerning between these operators (see also [180]). Given the likely low statistics of any detection in upcoming direct detection experiments, sub-leading operators are not likely to contribute enough to provide any further discriminating power.

5.4.1   Non-Relativistic Reduction

We find effective relativistic interaction Lagrangians by integrating out heavy mediators. We only keep the leading order interactions (suppressed by m or m^2). To the right of each operator is their non-relativistic reduction expressed in terms of the operators in table 5.1 with the coefficient derived from the Lagrangian parameters along with the relevant nucleon form factor. As multiple operators can have the same non-relativistic limit, it is important to include the nucleon form factor at the relativistic level. If this is not performed, erroneous cancellations can occur.

For free spinors we use the Bjorken & Drell [181] normalization and γ matrix

Table 5.5: Leading order operators which can arise from the relativistic Lagrangians considered in this work, the column '$\mathcal{L}$ terms' gives the non-zero couplings for that scenario. Each row represents a possible leading order direct detection signal. A '†' indicates that the mediator is charged. The 'Eqv. M_m' column gives the mediator mass required for each scenario to produce ~ 10 events $t^{-1}yr^{-1}keV^{-1}$ in xenon, with couplings set to 0.1.

WIMP spin	Mediator spin	$\mathcal{L}$ terms	leading NR operator	Eqv. M_m
0	0	h_1, g_1	$\mathcal{O}_1$	13 TeV
0	0	h_2, g_1	$\mathcal{O}_{10}$	14 GeV
0	1	h_4, g_4	$\mathcal{O}_{10}$	8 GeV
0	$\frac{1}{2}^\dagger$	y_1	$\mathcal{O}_1$	3.2 PeV
0	$\frac{1}{2}^\dagger$	y_2	$\mathcal{O}_1$	3.2 PeV
0	$\frac{1}{2}^\dagger$	y_1, y_2	$\mathcal{O}_{10}$	41 GeV
$\frac{1}{2}$	0	h_1, λ_1	$\mathcal{O}_1$	12.7 TeV
$\frac{1}{2}$	0	h_2, λ_1	$\mathcal{O}_{10}$	293 GeV
$\frac{1}{2}$	0	h_1, λ_2	$\mathcal{O}_{11}$	14 GeV
$\frac{1}{2}$	0	h_2, λ_2	$\mathcal{O}_6$	1.9 GeV
$\frac{1}{2}$	1	h_3, λ_3	$\mathcal{O}_1$	6.3 TeV
$\frac{1}{2}$	1	h_4, λ_3	$\mathcal{O}_9$	6.4 GeV
$\frac{1}{2}$	1	h_3, λ_4	$\mathcal{O}_8$	180 GeV
$\frac{1}{2}$	1	h_4, λ_4	$\mathcal{O}_4$	135 GeV
$\frac{1}{2}$	$0^\dagger$	l_1	$\mathcal{O}_1$	7.1 TeV
$\frac{1}{2}$	$0^\dagger$	l_2	$\mathcal{O}_1$	5.5 TeV
$\frac{1}{2}$	$1^\dagger$	d_1	$\mathcal{O}_1$	5.9 TeV
$\frac{1}{2}$	$1^\dagger$	d_2	$\mathcal{O}_1$	6.7 TeV
1	0	h_1, b_1	$\mathcal{O}_1$	13 TeV
1	0	h_2, b_1	$\mathcal{O}_{10}$	10 GeV
1	1	h_4, b_5	$\mathcal{O}_{10}$	5.1 GeV
1	1	$h_3, b_6^{\mathrm{Re}}(b_6^{\mathrm{Im}})$	$\mathcal{O}_5(\mathcal{O}_{17})$	5.5 GeV(23 GeV)
1	1	$h_4, b_6^{\mathrm{Re}}(b_6^{\mathrm{Im}})$	$\mathcal{O}_9(\mathcal{O}_{18})$	3 GeV(4.6 GeV)
1	1	$h_3, b_7^{\mathrm{Re}}(b_7^{\mathrm{Im}})$	$\mathcal{O}_{11}(\mathcal{O}_8)$	186 GeV(228 GeV)
1	1	$h_4, b_7^{\mathrm{Re}}(b_7^{\mathrm{Im}})$	$\mathcal{O}_4(\mathcal{O}_4)$	78 MeV (172 GeV)
1	$\frac{1}{2}^\dagger$	y_3	$\mathcal{O}_1$	3.2 PeV
1	$\frac{1}{2}^\dagger$	y_4	$\mathcal{O}_1$	3.2 PeV
1	$\frac{1}{2}^\dagger$	y_3, y_4	$\mathcal{O}_{11}$	120 TeV

conventions. In the non-relativistic limit we make the following replacements:

$$
\begin{aligned}
S &\rightarrow \frac{1_S}{\sqrt{m_S}} \\
X_\mu &\rightarrow \frac{\epsilon_\mu^s}{\sqrt{m_X}} \\
\chi &\rightarrow \sqrt{\frac{E + m_\chi}{2m_\chi}} \begin{pmatrix} \xi \\ \frac{\vec{\sigma}\cdot\vec{p}}{E+m_\chi}\xi \end{pmatrix}
\end{aligned}
\tag{5.29}
$$

where $s = 1, 2, 3$ are the different polarization states of the vector. $\xi = (1\ 0)^T$ is

the left handed Weyl spinor. The following Fierz transformation and gamma matrix

97

identites were useful in the charged mediator cases, (a sign difference was found in the final identity when compared with [182]):

$$
\begin{aligned}
(\bar{q}\chi)(\bar{\chi}q) &= -\frac{1}{4}\Big[\bar{q}q\bar{\chi}\chi + \bar{q}\gamma^\mu q\bar{\chi}\gamma_\mu\chi + \frac{1}{2}\bar{q}\sigma^{\mu\nu}q\bar{\chi}\sigma_{\mu\nu}\chi - \bar{q}\gamma^\mu\gamma^5 q\bar{\chi}\gamma_\mu\gamma^5\chi \\
&\quad +\bar{q}\gamma^5 q\bar{\chi}\gamma^5\chi\Big] \\
(\bar{q}\gamma^5\chi)(\bar{\chi}\gamma^5 q) &= -\frac{1}{4}\Big[\bar{q}q\bar{\chi}\chi + \bar{q}\gamma^5 q\bar{\chi}\gamma^5\chi - \bar{q}\gamma^\mu q\bar{\chi}\gamma_\mu\chi + \bar{q}\gamma^\mu\gamma^5 q\bar{\chi}\gamma_\mu\gamma^5\chi \\
&\quad +\frac{1}{2}\bar{q}\sigma^{\mu\nu}q\bar{\chi}\sigma_{\mu\nu}\chi\Big] &(5.30) \\
(\bar{q}\chi)(\bar{\chi}\gamma^5 q) &= -\frac{1}{4}\Big[\bar{q}q\bar{\chi}\gamma^5\chi + \bar{q}\gamma^5 q\bar{\chi}\chi - \bar{q}\gamma^\mu q\bar{\chi}\gamma_\mu\gamma^5\chi + \bar{q}\gamma^\mu\gamma^5 q\bar{\chi}\gamma_\mu\chi \\
&\quad +i\epsilon_{\mu\nu\alpha\beta}\bar{q}\sigma^{\mu\nu}q\bar{\chi}\sigma^{\alpha\beta}\chi\Big] \\
(\bar{q}\gamma_\mu\chi)(\bar{\chi}\gamma^\mu q) &= -\Big[\bar{q}q\bar{\chi}\chi - \bar{q}\gamma^5 q\bar{\chi}\gamma^5\chi - \frac{1}{2}\bar{q}\gamma^\mu q\bar{\chi}\gamma_\mu\chi - \frac{1}{2}\bar{q}\gamma^\mu\gamma^5 q\bar{\chi}\gamma_\mu\gamma^5\chi\Big] \\
(\bar{q}\gamma_\mu\gamma^5\chi)(\bar{\chi}\gamma^\mu\gamma^5 q) &= -\Big[-\bar{q}q\bar{\chi}\chi + \bar{q}\gamma^5 q\bar{\chi}\gamma^5\chi - \frac{1}{2}\bar{q}\gamma^\mu q\bar{\chi}\gamma_\mu\chi - \frac{1}{2}\bar{q}\gamma^\mu\gamma^5 q\bar{\chi}\gamma_\mu\gamma^5\chi\Big] \\
(\bar{q}\gamma_\mu\chi)(\bar{\chi}\gamma^\mu\gamma^5 q) &= -\Big[\bar{q}q\bar{\chi}\gamma^5\chi - \bar{q}\gamma^5 q\bar{\chi}\chi + \frac{1}{2}\bar{q}\gamma^\mu q\bar{\chi}\gamma_\mu\gamma^5\chi + \frac{1}{2}\bar{q}\gamma^\mu\gamma^5 q\bar{\chi}\gamma_\mu\chi\Big]
\end{aligned}
$$

$$
\sigma^{\mu\nu}\gamma^5 = \frac{i}{2}\epsilon^{\mu\nu\rho\sigma}\sigma_{\rho\sigma} \qquad (5.31)
$$

All of the following operators are collected in terms of the coefficients of the NR operators, c_i, in tables 5.2, 5.3 and 5.4.

Table 5.6: Non-relativistic reduction of operators for a spin-0 WIMP

Scalar Mediator		
$(S^\dagger S)(\bar{q}q)$	$\longrightarrow$	$\left(\frac{h_1^N g_1}{m_\phi^2}\right)\mathcal{O}_1$
$(S^\dagger S)(\bar{q}\gamma^5 q)$	$\longrightarrow$	$\left(\frac{h_2^N g_1}{m_\phi^2}\right)\mathcal{O}_{10}$

Vector Mediator		
$i(S^\dagger \partial_\mu S - \partial_\mu S^\dagger S)(\bar{q}\gamma^\mu q)$	$\longrightarrow$	0
$i(S^\dagger \partial_\mu S - \partial_\mu S^\dagger S)(\bar{q}\gamma^\mu\gamma^5 q)$	$\longrightarrow$	$\left(\frac{2ig_4 h_4^N}{m_G^2}\frac{m_N}{m_S}\right)\mathcal{O}_{10}$

Charged Spinor Mediator		
$(S^\dagger S)(\bar{q}q)$	$\longrightarrow$	$\frac{y_1^\dagger y_1 - y_2^\dagger y_2}{m_Q m_S} f_T^N \mathcal{O}_1$
$(S^\dagger S)(\bar{q}\gamma^5 q)$	$\longrightarrow$	$i\frac{y_2^\dagger y_1 - y_1^\dagger y_2}{m_Q m_S}\tilde{\Delta}^N \mathcal{O}_{10}$

Table 5.7: Operators for a spin-$\frac{1}{2}$ WIMP via a neutral mediator

Scalar Mediator		
$\bar{\chi}\chi\bar{q}q$	$\longrightarrow$	$\left(\frac{h_1^N \lambda_1}{m_\phi^2}\right)\mathcal{O}_1$
$\bar{\chi}\chi\bar{q}\gamma^5 q$	$\longrightarrow$	$\left(\frac{h_2^N \lambda_1}{m_\phi^2}\right)\mathcal{O}_{10}$
$\bar{\chi}\gamma^5\chi\bar{q}q$	$\longrightarrow$	$\left(-\frac{h_1^N \lambda_2 m_N}{m_\phi^2 m_\chi}\right)\mathcal{O}_{11}$
$\bar{\chi}\gamma^5\chi\bar{q}\gamma^5 q$	$\longrightarrow$	$\left(\frac{h_2^N \lambda_2 m_N}{m_\phi^2 m_\chi}\right)\mathcal{O}_6$

Vector Mediator		
$\bar{\chi}\gamma^\mu\chi\bar{q}\gamma_\mu q$	$\longrightarrow$	$\left(-\frac{h_3^N \lambda_3}{m_G^2}\right)\mathcal{O}_1$
$\bar{\chi}\gamma^\mu\chi\bar{q}\gamma_\mu\gamma^5 q$	$\longrightarrow$	$\left(-\frac{2h_4^N \lambda_3}{m_G^2}\right)\left(-\mathcal{O}_7 + \frac{m_N}{m_\chi}\mathcal{O}_9\right)$
$\bar{\chi}\gamma^\mu\gamma^5\chi\bar{q}\gamma_\mu q$	$\longrightarrow$	$\left(-\frac{2h_3^N \lambda_4}{m_G^2}\right)(\mathcal{O}_8 + \mathcal{O}_9)$
$\bar{\chi}\gamma^\mu\gamma^5\chi\bar{q}\gamma_\mu\gamma^5 q$	$\longrightarrow$	$\left(\frac{4h_4^N \lambda_4}{m_G^2}\right)\mathcal{O}_4$

Table 5.8: Non-relativistic reduction of operators for a spin-$\frac{1}{2}$ WIMP via a charged mediator (after using Fierz identities)

Charged Scalar Mediator		
$\bar{\chi}\chi\bar{q}q$	$\longrightarrow$	$\frac{l_2^\dagger l_2 - l_1^\dagger l_1}{4m_\Phi^2} f_{Tq}^N \mathcal{O}_1$
$\bar{\chi}\chi\bar{q}\gamma^5 q$	$\longrightarrow$	$i\frac{l_1^\dagger l_2 - l_2^\dagger l_1}{4m_\Phi^2} \Delta\tilde{q}^N \mathcal{O}_{10}$
$\bar{\chi}\gamma^5\chi\bar{q}q$	$\longrightarrow$	$i\frac{l_2^\dagger l_1 - l_1^\dagger l_2}{4m_\Phi^2} \frac{m_N}{m_\chi} f_{Tq}^N \mathcal{O}_{11}$
$\bar{\chi}\gamma^5\chi\bar{q}\gamma^5 q$	$\longrightarrow$	$\frac{l_1^\dagger l_1 - l_2^\dagger l_2}{4m_\Phi^2} \frac{m_N}{m_\chi} \Delta\tilde{q}^N \mathcal{O}_6$
$\bar{\chi}\gamma^\mu\chi\bar{q}\gamma_\mu q$	$\longrightarrow$	$-\frac{l_1^\dagger l_1 + l_2^\dagger l_2}{4m_\Phi^2} \mathcal{N}_q^N \mathcal{O}_1$
$\bar{\chi}\gamma^\mu\gamma^5\chi\bar{q}\gamma_\mu q$	$\longrightarrow$	$\frac{l_1^\dagger l_2 + l_2^\dagger l_1}{2m_\Phi^2} \mathcal{N}_q^N (\mathcal{O}_8 + \mathcal{O}_9)$
$\bar{\chi}\gamma^\mu\chi\bar{q}\gamma_\mu\gamma^5 q$	$\longrightarrow$	$\frac{l_1^\dagger l_2 + l_2^\dagger l_1}{2m_\Phi^2} \Delta_q^N (\mathcal{O}_7 - \frac{m_N}{m_\chi}\mathcal{O}_9)$
$\bar{\chi}\gamma^\mu\gamma^5\chi\bar{q}\gamma_\mu\gamma^5 q$	$\longrightarrow$	$-\frac{l_1^\dagger l_1 + l_2^\dagger l_2}{m_\Phi^2} \Delta_q^N \mathcal{O}_4$
$\bar{\chi}\sigma^{\mu\nu}\chi\bar{q}\sigma_{\mu\nu} q$	$\longrightarrow$	$\frac{l_2^\dagger l_2 - l_1^\dagger l_1}{m_\Phi^2} \delta_q^N \mathcal{O}_4$
$\epsilon_{\mu\nu\alpha\beta}\bar{\chi}\sigma^{\mu\nu}\chi\bar{q}\sigma^{\alpha\beta} q$	$\longrightarrow$	$\frac{l_2^\dagger l_1 - l_1^\dagger l_2}{m_\Phi^2} \delta_q^N (i\mathcal{O}_{10} - i\frac{m_N}{m_\chi}\mathcal{O}_{11} + 4\mathcal{O}_{12})$

Charged Vector Mediator		
$\bar{\chi}\chi\bar{q}q$	$\longrightarrow$	$\frac{d_2^\dagger d_2 - d_1^\dagger d_1}{4m_V^2} f_{Tq}^N \mathcal{O}_1$
$\bar{\chi}\chi\bar{q}\gamma^5 q$	$\longrightarrow$	$i\frac{d_2^\dagger d_1 - d_1^\dagger d_2}{4m_V^2} \Delta\tilde{q}^N \mathcal{O}_{10}$
$\bar{\chi}\gamma^5\chi\bar{q}q$	$\longrightarrow$	$i\frac{d_2^\dagger d_1 - d_1^\dagger d_2}{4m_V^2} \frac{m_N}{m_\chi} f_{Tq}^N \mathcal{O}_{11}$
$\bar{\chi}\gamma^5\chi\bar{q}\gamma^5 q$	$\longrightarrow$	$\frac{d_2^\dagger d_2 - d_1^\dagger d_1}{4m_V^2} \frac{m_N}{m_\chi} \Delta\tilde{q}^N \mathcal{O}_6$
$\bar{\chi}\gamma^\mu\chi\bar{q}\gamma_\mu q$	$\longrightarrow$	$\frac{d_2^\dagger d_2 + d_1^\dagger d_1}{8m_V^2} \mathcal{N}_q^N \mathcal{O}_1$
$\bar{\chi}\gamma^\mu\gamma^5\chi\bar{q}\gamma_\mu q$	$\longrightarrow$	$-\frac{d_2^\dagger d_1 + d_1^\dagger d_2}{4m_V^2} \mathcal{N}_q^N [\mathcal{O}_8 + \mathcal{O}_9]$
$\bar{\chi}\gamma^\mu\chi\bar{q}\gamma_\mu\gamma^5 q$	$\longrightarrow$	$\frac{d_2^\dagger d_1 + d_1^\dagger d_2}{4m_V^2} \Delta_q^N \left[\mathcal{O}_7 - \frac{m_N}{m_\chi}\mathcal{O}_9\right]$
$\bar{\chi}\gamma^\mu\gamma^5\chi\bar{q}\gamma_\mu\gamma^5 q$	$\longrightarrow$	$-\frac{d_2^\dagger d_2 + d_1^\dagger d_1}{2m_V^2} \Delta_q^N \mathcal{O}_4$

Table 5.9: Non-relativistic reduction of operators for a spin-1 WIMP

Scalar Mediator		

$X_\mu^\dagger X^\mu \bar{q} q$ $\longrightarrow$ $\left(\frac{b_1 h_1^N}{m_\phi^2}\right) \mathcal{O}_1$

$X_\mu^\dagger X^\mu \bar{q} \gamma^5 q$ $\longrightarrow$ $\left(\frac{b_1 h_2^N}{m_\phi^2}\right) \mathcal{O}_{10}$

Vector Mediator

$(X_\nu^\dagger \partial_\mu X^\nu - \partial_\mu X_\nu^\dagger X^\nu)(\bar{q}\gamma^\mu q)$ $\longrightarrow$ 0

$(X_\nu^\dagger \partial_\mu X^\nu - \partial_\mu X_\nu^\dagger X^\nu)(\bar{q}\gamma^\mu \gamma^5 q)$ $\longrightarrow$ $\left(\frac{-3b_5 h_4^N}{m_G^2} \frac{m_N}{m_X}\right) \mathcal{O}_{10}$

$\partial_\nu (X^{\nu\dagger} X_\mu + X_\mu^\dagger X^\nu)(\bar{q}\gamma^\mu q)$ $\longrightarrow$ $\left(\frac{\mathrm{Re}(b_6) h_3^N}{m_G^2} \frac{m_N}{m_X}\right) \left[\mathcal{O}_5 + \mathcal{O}_6 - \frac{q^2}{m_N^2}\mathcal{O}_4\right]$

$\partial_\nu (X^{\nu\dagger} X_\mu + X_\mu^\dagger X^\nu)(\bar{q}\gamma^\mu \gamma^5 q)$ $\longrightarrow$ $\left(-\frac{2\mathrm{Re}(b_6) h_4^N}{m_G^2} \frac{m_N}{m_X}\right) \mathcal{O}_9$

$\partial_\nu (X^{\nu\dagger} X_\mu - X_\mu^\dagger X^\nu)(\bar{q}\gamma^\mu q)$ $\longrightarrow$ $\left(-\frac{4\mathrm{Im}(b_6) h_3^N}{m_G^2} \frac{m_N}{m_X}\right) \mathcal{O}_{17}$

$\partial_\nu (X^{\nu\dagger} X_\mu - X_\mu^\dagger X^\nu)(\bar{q}\gamma^\mu \gamma^5 q)$ $\longrightarrow$ $\left(\frac{4\mathrm{Im}(b_6) h_4^N}{m_G^2} \frac{m_N}{m_X}\right) \mathcal{O}_{18}$

$\epsilon_{\mu\nu\rho\sigma} \left(X^{\nu\dagger} \partial^\rho X^\sigma + X^\nu \partial^\rho X^{\sigma\dagger}\right) (\bar{q}\gamma^\mu q)$ $\longrightarrow$ $\left(\frac{\mathrm{Re}(b_7) h_3^N}{m_G^2} \frac{m_N}{m_X}\right) \mathcal{O}_{11}$

$\epsilon_{\mu\nu\rho\sigma} \left(X^{\nu\dagger} \partial^\rho X^\sigma + X^\nu \partial^\rho X^{\sigma\dagger}\right) (\bar{q}\gamma^\mu \gamma^5 q)$ $\longrightarrow$ $\left(\frac{\mathrm{Re}(b_7) h_4^N}{m_G^2} \frac{m_N}{m_X}\right) \left[i\frac{q^2}{m_X m_N}\mathcal{O}_4 - i\frac{m_N}{m_X}\mathcal{O}_6 - 2\mathcal{O}_{14}\right]$

$\epsilon_{\mu\nu\rho\sigma} \left(X^{\nu\dagger} \partial^\rho X^\sigma - X^\nu \partial^\rho X^{\sigma\dagger}\right) (\bar{q}\gamma^\mu q)$ $\longrightarrow$ $\left(\frac{2\mathrm{Im}(b_7) h_3^N}{m_G^2}\right) [\mathcal{O}_8 + \mathcal{O}_9]$

$\epsilon_{\mu\nu\rho\sigma} \left(X^{\nu\dagger} \partial^\rho X^\sigma - X^\nu \partial^\rho X^{\sigma\dagger}\right) (\bar{q}\gamma^\mu \gamma^5 q)$ $\longrightarrow$ $\left(\frac{4\mathrm{Im}(b_7) h_4^N}{m_G^2}\right) \mathcal{O}_4$

Charged Spinor Mediator

$(X_\mu^\dagger X_\nu)(\bar{q}\gamma^\mu \gamma^\nu q)$ $\longrightarrow$ $\left(\frac{y_3^\dagger y_3 - y_4^\dagger y_4}{m_Q m_X}\right) \left[f_{Tq}^N \mathcal{O}_1 + 2\delta_q^N \mathcal{O}_4\right]$

$(X_\mu^\dagger X_\nu)(\bar{q}\gamma^\mu \gamma^\nu \gamma^5 q)$ $\longrightarrow$ $\left(\frac{y_4^\dagger y_3 - y_3^\dagger y_4}{m_Q m_X}\right) \left[i\Delta_{\tilde{q}}^N \mathcal{O}_{10} + i\delta_q^N \mathcal{O}_{11} - 2i\delta_q^N \mathcal{O}_{12}\right.$

$$\left. -2i\delta_q^N \mathcal{O}_{18}\right]$$

5.4.2   Quarks to Nucleons

To go from the fundamental interactions of WIMPs with quarks to scattering from point-like nucleons, one must evaluate the quark (parton) bilinears in the nucleons. For a full discussion see the Appendices of [182] and [183]. Here, we write the nucleon couplings in terms of the quark couplings times a form factor (in the limit of zero momentum transfer): The scalar bilinear for light quarks can be evaluated from

$$\langle N_o | m_q \bar{q} q | N_i \rangle \longrightarrow f_{Tq}^N \bar{N} N$$

$$\langle N_o | \bar{q} \gamma^5 q | N_i \rangle \longrightarrow \Delta \tilde{q}^N \bar{N} \gamma^5 N$$

$$\langle N_o | \bar{q} \gamma^\mu q | N_i \rangle \longrightarrow \mathcal{N}_q^N \bar{N} \gamma^\mu N$$

$$\langle N_o | \bar{q} \gamma^\mu \gamma^5 q | N_i \rangle \longrightarrow \Delta_q^N \bar{N} \gamma^\mu \gamma^5 N$$

$$\langle N_o | \bar{q} \sigma^{\mu\nu} q | N_i \rangle \longrightarrow \delta_q^N \bar{N} \sigma^{\mu\nu} N$$

$$\langle N | m_q \bar{q} q | N \rangle = m_N f_{Tq}^N \tag{5.32}$$

while for the heavy quarks

$$\langle N | m_q \bar{q} q | N \rangle = \frac{2}{27} m_N F_{TG}^N = \frac{2}{27} m_N \left(1 - \sum_{q=u,d,s} f_{Tq}^N \right). \tag{5.33}$$

Summing over all the quarks one finds

$$h_1^N = \sum_{q=u,d,s} h_1^q \frac{m_N}{m_q} f_{Tq}^N + \frac{2}{27} f_{TG}^N \sum_{q=c,b,t} h_1^q \frac{m_N}{m_q} \tag{5.34}$$

The pseudo-scalar bilinear was recently revisited in [183]:

$$h_2^N = \sum_{q=u,d,s} h_2^q \Delta \tilde{q}^N - \Delta \tilde{G}^N \sum_{q=c,b,t} \frac{h_2^q}{m_q} \tag{5.35}$$

The vector bilinear essentially gives the number operator:

$$h_3^N = \begin{cases} 2h_3^u + h_3^d & N = p \\ h_3^u + 2h_3^d & N = u \end{cases} \tag{5.36}$$

The psuedo-vector bilinear counts the contributions of spin to the nucleon (note that sometimes this coupling has a G_F factored out to make it dimensionless)

$$h_4^N = \sum_{q=u,d,s} h_4^q \Delta_q^N \tag{5.37}$$

Throughout this chapter the following values are used (it should be noted that

there are large uncertainties in these values) [182, 183]:

$$
\begin{aligned}
f_{Tu}^{n} &= & 0.014 && f_{Tu}^{p} &= 0.02 \\
f_{Td}^{n} &= & 0.036 && f_{Td}^{p} &= 0.026 \\
f_{Ts}^{n} &= & 0.118 && f_{Ts}^{p} &= 0.118 \\
\Delta_{u}^{n} &= & -0.427 && \Delta_{u}^{p} &= 0.842 \\
\Delta_{d}^{n} &= & 0.842 && \Delta_{d}^{p} &= -0.427 \\
\Delta_{s}^{n} &= & -0.085 && \Delta_{s}^{p} &= -0.085 \\
\Delta\tilde{u}^{n} &= & -108.03 && \Delta\tilde{u}^{p} &= 110.55 \\
\Delta\tilde{d}^{n} &= & 108.60 && \Delta\tilde{d}^{p} &= -107.17 \\
\Delta\tilde{s}^{n} &= & -0.57 && \Delta\tilde{s}^{p} &= -3.37 \\
\Delta\tilde{G}^{n} &= & 35.7\text{MeV} && \Delta\tilde{G}^{p} &= 395.2\text{MeV}
\end{aligned}
$$

$$(5.38)$$

Assuming a universal coupling of the mediators to all quarks, the nucleon level couplings can then be written as,

$$
\begin{aligned}
h_{1}^{N} &= f_{T}^{N} h_{1} \\
h_{2}^{N} &= \tilde{\Delta}^{N} h_{2} \\
h_{3}^{N} &= \mathcal{N}^{N} h_{3} \\
h_{4}^{N} &= \Delta^{N} h_{4}
\end{aligned}
$$

$$(5.39)$$

where we have defined,

$$
\begin{aligned}
f_T^n &= 11.93 & f_T^p &= 12.31 \\
\tilde{\Delta}^n &= -0.07 & \tilde{\Delta}^p &= -0.28 \\
\mathcal{N}^n &= 3 & \mathcal{N}^p &= 3 \\
\Delta^n &= 0.33 & \Delta^p &= 0.33 \\
\delta^n &= 0.564 & \delta^p &= 0.564
\end{aligned}
$$

$$. \tag{5.40}$$

This introduces a small amount of isospin violation, and it is known that relaxing the assumption of universal couplings to quarks can lead to interesting isospin violating effects [183, 184].

5.5 Observables

The principle observable in direct detection experiments is the differential event rate. Since the incoming WIMPs originate in the galactic halo, one must average over the WIMP velocity distribution, $f(v)$, which we assume to be Maxwell-Boltzmann,

$$
\frac{dR}{dE_R} = N_T \frac{\rho_\chi M}{2\pi m_\chi} \int_{v_{min}} \frac{f(v)}{v} P_{tot} dv \tag{5.41}
$$

where we use the value $\rho_\chi = 0.3 \mathrm{GeV/cm}^3$ for the local dark matter density, N_T is the number of nuclei in the target and P_{tot} can be calculated from the amplitude $\mathcal{M}$ in Eq. 5.14

$$
P_{tot} = \frac{1}{2j_\chi + 1} \frac{1}{2j_N + 1} \sum_{spins} |\mathcal{M}|^2. \tag{5.42}
$$

Thoughout this work we use the mathematica package supplied in [175] to calculate rates. To determine the leading order operator which arises from a given relativistic scenario we first plot the rate for each of the NR operators in xenon-131. To simply
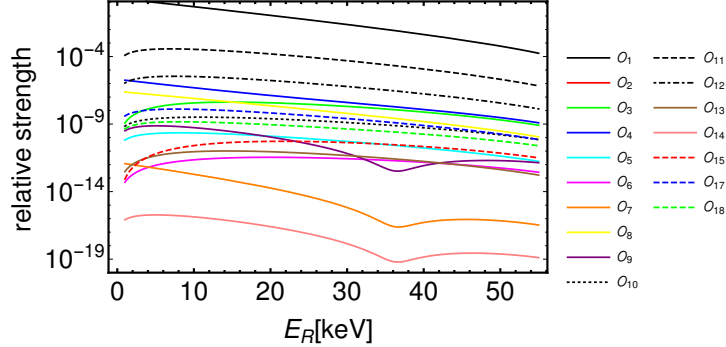
Figure 5.1: The relative strength of event rates for a 50GeV spin-$\frac{1}{2}$ WIMP in xenon for each of the non-relativistic operators in table 5.1, where the coefficients of each operator are set to be equal

compare the operators we set the c_i coefficients to be the same and normalized the overall rate to that of $\mathcal{O}_1$, see Fig. 5.1. Since operators are either zero, first or second order in momentum transfer q or velocity $\vec{v}^\perp$, the relative strengths of the operators span 16 orders of magnitude. This is an important point to keep in mind when finding the leading operator, as sometimes a term which appears to be higher order in q can dominate the non-relativistic reduction. For example in the $b_7^{\mathrm{Re}}h_4$ scenario, one finds that $q^2\mathcal{O}_4$ dominates over the $\mathcal{O}_6$ and $\mathcal{O}_{14}$ which contain powers of q within the operators.

Since the Lagrangians we have considered are not tied to specific complete and consistent particle physics models, the mediator masses are not fixed in advance and thus specific event rates are not predicted in advance. Clearly one requires a rate that is low enough to evade the current experimental constraints. For example, a 50 GeV WIMP producing 10 events per tonne per year is sufficiently low to evade the bounds from LUX [143]. For demonstration purposes we set the couplings to 0.1 (or $0.1i$ for imaginary) in the various Lagrangians and find a mediator mass that will produce 10 events/t/y in the signal region for xenon ($5 - 45$keV). The calculated masses are given in table 5.5. It is perhaps telling that the mediator masses span 6

orders of magnitude, from just a few GeV up to a PeV. While it is unlikely that a full model of thermal relic dark matter could be built around all of these Lagrangians, it is nevertheless a useful metric to estimate the relative strength of the different nuclear responses to each of the operators.

In Figs. 5.2, 5.3, 5.4 and 5.5 we have plotted rates for two common targets. For simplicity and again for demonstration purposes, we only plot the rates for a single isotope of both germanium and xenon. The choice of isotopes, ^{73}Ge and ^{131}Xe, was made to ensure sensitivity to spin-dependent responses. As can be seen in the figures, many operators produce rates with similar recoil energy dependence in the same target, but different nuclei can have very different responses to the various operators [1]. Thus a complementary choice of nuclear targets can provide important discriminating information.

To illustrate this discriminating power we plot the ratio of the rates in xenon and germanium in Fig. 5.5 and 5.6. We choose to only present ratios for the uncharged mediator cases of spinor and vector WIMPs since the other cases produce trival results (all operators being spin independent). To estimate the effect astrophysical uncertainties will have on discriminating between operators, we plot the rate for a range of astrophysical parameters from $v_0 = 200$m/s, and $v_{esc} = 500$m/s (lower) to $v_0 = 240$m/s and $v_{esc} = 600$m/s (upper). The uncertainty in the dark matter density does not appear since we are considering the ratio of rates. Given the vastly different energy dependence of the ratio of rates of each scenario the astrophysical errors do not completely inhibit their identification. Furthermore, operators $\mathcal{O}_9$ and $\mathcal{O}_{14}$, produced in scenarios $h_4 b_7^{\mathrm{Re}}$ and $h_4 b_6^{\mathrm{Re}}$ respectively, remain indistingushable when considering the ratio of rates. While it appears that in principle almost every operator

is discernible, in practice isotopically impure targets and low statistics will further complicate the situation and provide limits on practical discrimination.
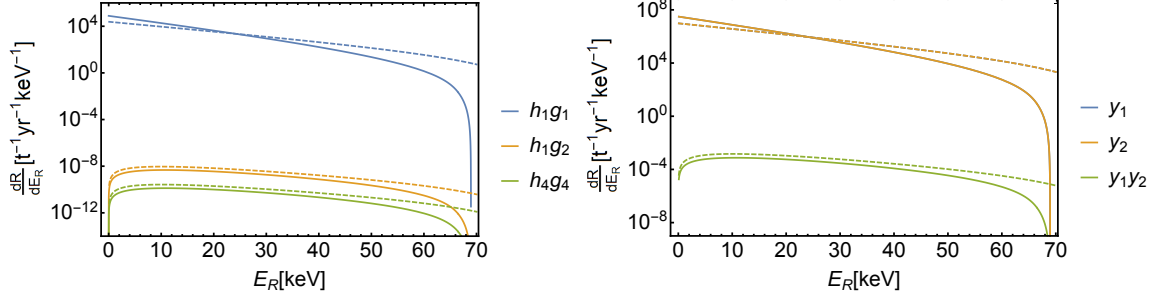
Figure 5.2: Rates for a 50GeV spin-0 WIMP in xenon (solid) and germanium (dashed) with uncharged (left) and charged mediators (right), assuming mediator mass of 1TeV and $\mathcal{O}(1)$ coupling constants.
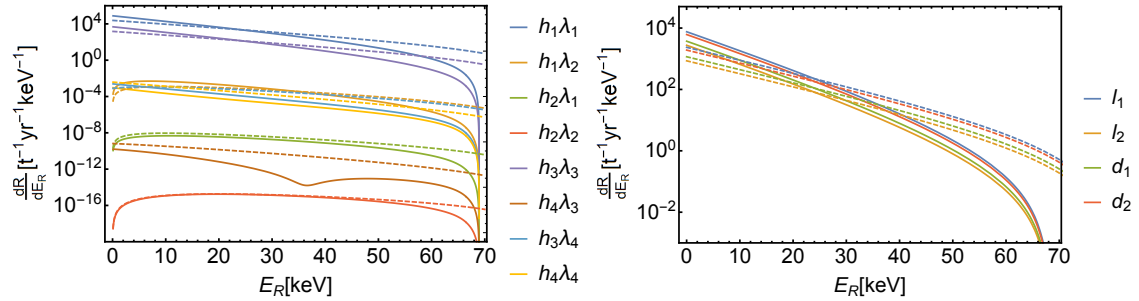
Figure 5.3: Rates for a 50GeV spin-$\frac{1}{2}$ WIMP in xenon (solid) and germanium (dashed) with uncharged (left) and charged mediators (right), assuming mediator mass of 1TeV and $\mathcal{O}(1)$ coupling constants.

5.6 Calculation Details

5.6.1 Vector Dark Matter

If the WIMP has spin 1, we find two extra operators that haven't been considered previously. Specifically, the operators depend on the symmetric combination of polarization vectors, $S_{ij} = \frac{1}{2}\left(\epsilon_i^\dagger \epsilon_j + \epsilon_j^\dagger \epsilon_i\right)$. This necessitates a modification to the WIMP response functions by first modifying the ℓ coefficients given in Eq. 5.13. Based on our non-relativistic reduction for vector dark matter, the Lagrangian for vector dark

107

Figure 5.4: Rates for a 50GeV spin-1 WIMP in xenon (solid) and germanium (dashed) with uncharged (left) and charged mediators (right), assuming mediator mass of 1TeV and $\mathcal{O}(1)$ coupling constants.
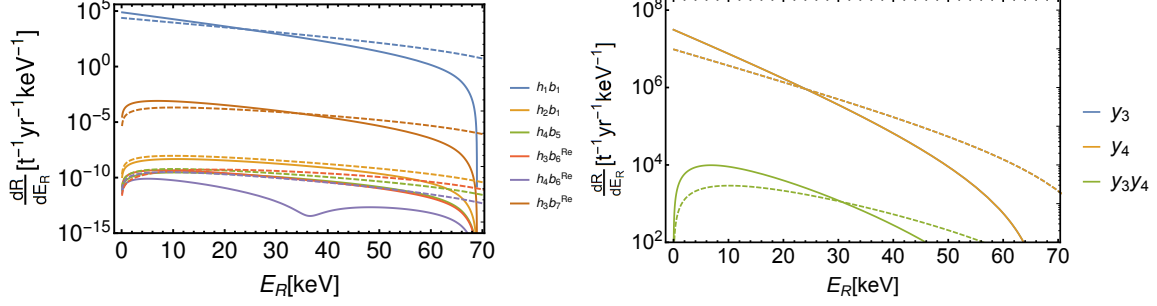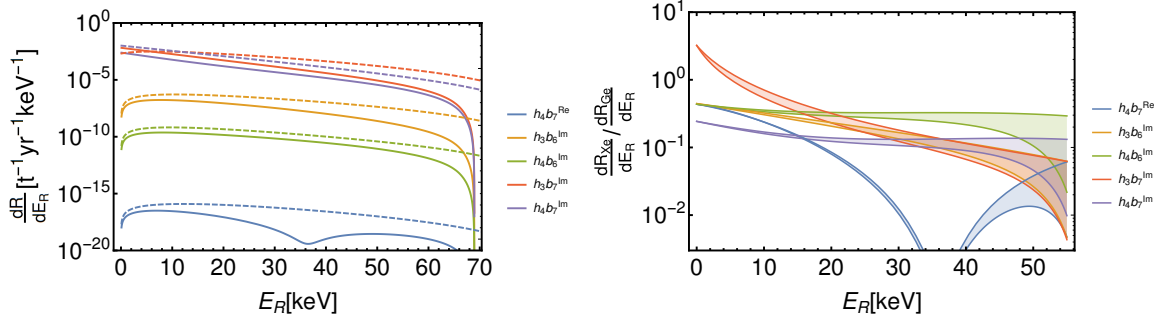

Figure 5.5: Rates (left) for a 50GeV spin-1 WIMP in xenon (solid) and germanium (dashed) with uncharged mediators and imaginary couplings, assuming mediator mass of 1TeV and $\mathcal{O}(1)$ coupling constants. Also shown is the ratio of rates in xenon and germanium (right).

matter and the nucleus, interacting via an uncharged scalar or vector mediator can be written in general as:

$$
\mathcal{L}_{vector} = c_1 \mathcal{O}_1 + c_4 \mathcal{O}_4 + c_5 \mathcal{O}_5 + c_8 \mathcal{O}_8 + c_9 \mathcal{O}_9 + c_{10} \mathcal{O}_{10} + c_{11} \mathcal{O}_{11} + c_{14} \mathcal{O}_{14} + c_{17} \mathcal{O}_{17}
$$
$$
+ c_{18} \mathcal{O}_{18} \tag{5.43}
$$

where we've defined $\mathcal{O}_{17} \equiv \frac{i\vec{q}}{m_N} \cdot \mathcal{S} \cdot \vec{v}_\perp$ and $\mathcal{O}_{18} \equiv \frac{i\vec{q}}{m_N} \cdot \mathcal{S} \cdot \vec{S}_N$ and the c_i's are given in table 5.4. To decompose these new operators we replace $\vec{v}^\perp$ with the target velocity and the internucleon velocities and sum over nucleons. $\mathcal{O}_{17}$ can then be put into the form

$$
\mathcal{O}_{17} \rightarrow \frac{i\vec{q}}{m_N} . \mathcal{S} . \left[\vec{v}_T^\perp e^{-i\vec{q}.\vec{x}_i} - \sum_{i=1}^A \frac{1}{2M} \left(-\frac{1}{i} \overleftarrow{\nabla}_i e^{-i\vec{q}.\vec{x}_i} + e^{-i\vec{q}.\vec{x}_i} \frac{1}{i} \overrightarrow{\nabla}_i \right)_{int} \right] \tag{5.44}
$$
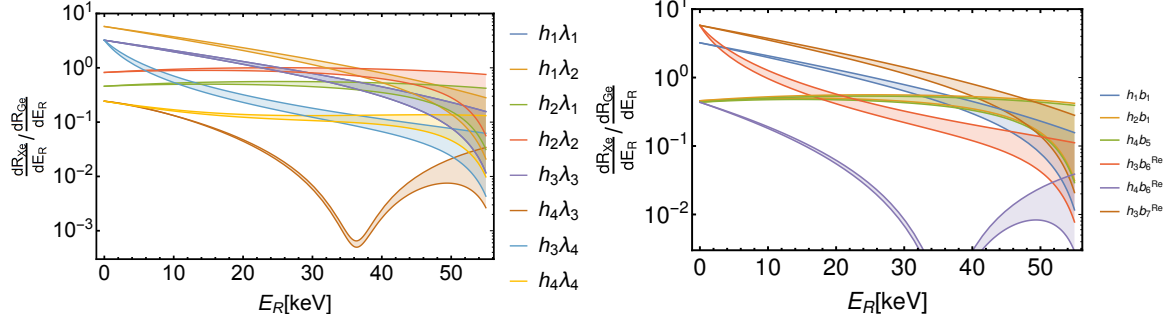
Figure 5.6: Ratio of rates in xenon and germanium, illustrating the discriminating power of having multiple nuclear targets. For a 50GeV spin-$\frac{1}{2}$ WIMP with uncharged mediator (left) and a 50GeV spin-1 WIMP with uncharged mediator (right), the shaded regions show the upper and lower bounds due to the astrophysical parameters

$\mathcal{O}_{18}$ can be expanded as

$$\mathcal{O}_{18} \rightarrow \frac{1}{2}\frac{i\vec{q}}{m_N}\cdot \mathcal{S}\cdot \vec{\sigma} \tag{5.45}$$

Together, all the terms of $\mathcal{L}_{vector}$ give rise to the following ℓ factors from Eq. 5.13,

$$
\begin{aligned}
\ell_0^\tau &= c_1^\tau + i\left(\frac{\vec{q}}{m_N}\times \vec{v}_T^\perp\right)\cdot \vec{S}_\chi c_5^\tau + (\vec{v}_T^\perp\cdot \vec{S}_\chi)c_8^\tau + i\left(\frac{\vec{q}}{m_N}\cdot \vec{S}_\chi\right)c_{11}^\tau \\
&\quad + i\left(\frac{\vec{q}}{m_N}\cdot \mathcal{S}\cdot \vec{v}_\perp^T\right)c_{17}^\tau \\
l_0^{A\tau} &= -i\left(\frac{\vec{q}}{2m_N}\cdot \vec{S}_\chi\right)c_{14}^\tau \\
\vec{l}_E^\tau &= 0 \\
\vec{l}_M^\tau &= i\left(\frac{\vec{q}}{m_N}\times \vec{S}_\chi\right)c_5^\tau - \vec{S}_\chi c_8^\tau - i\left(\frac{\vec{q}}{m_N}\cdot \mathcal{S}\right)c_{17}^\tau \\
\vec{l}_5^\tau &= \frac{1}{2}\vec{S}_\chi c_4^\tau + i\left(\frac{\vec{q}}{m_N}\times \vec{S}_\chi\right)c_9^\tau + \frac{1}{2}\left(i\frac{\vec{q}}{m_N}\right)c_{10}^\tau + \frac{1}{2}\vec{v}_T^\perp\left(\frac{\vec{q}}{2m_N}\cdot \vec{S}_\chi\right)c_{14}^\tau \\
&\quad + \frac{1}{2}\left(i\frac{\vec{q}}{m_N}\cdot \mathcal{S}\right)c_{18}^\tau
\end{aligned}
\tag{5.46}
$$

Based on the ℓ's above, the coefficients of the various nuclear responses are found by squaring the amplitude and then summing over spins. To simplify calculations, we choose a convenient basis for polarization vectors, $\epsilon_i^s = \delta_i^s$. Recall that the spin can then be written as the anti-symmetric combination $iS_k = \epsilon_{ijk}\epsilon_i^\dagger\epsilon_j$. The WIMP

responses unique to the vector case are then given by:

$$
\begin{aligned}
R_M^{\tau\tau'} &= c_1^\tau c_1^{\tau'} + \frac{2}{3}\left(\frac{\vec{q}^2}{m_N^2}v_T^{\perp 2}c_5^\tau c_5^{\tau'} + v_T^{\perp 2}c_8^\tau c_8^{\tau'} + \frac{q^2}{m_N^2}c_{11}^\tau c_{11}^{\tau'} + \frac{q^2 v_T^{\perp 2}}{4m_N^2}c_{17}^\tau c_{17}^{\tau'}\right) \\
R_{\Phi''}^{\tau\tau'} &= 0 \\
R_{\Phi'' M}^{\tau\tau'} &= 0 \\
R_{\tilde{\Phi}'}^{\tau\tau'} &= 0 \\
R_{\Sigma''}^{\tau\tau'} &= \frac{1}{6}c_4^\tau c_4^{\tau'} + \frac{q^2}{4m_N^2}c_{10}^\tau c_{10}^{\tau'} + \frac{q^2}{12m_N^2}c_{18}^\tau c_{18}^{\tau'} \\
R_{\Sigma'}^{\tau\tau'} &= \frac{1}{6}c_4^\tau c_4^{\tau'} + \frac{q^2}{6m_N^2}c_9^\tau c_9^{\tau'} + \frac{q^2 v_T^{\perp 2}}{2m_N^2}c_{14}^\tau c_{14}^{\tau'} + \frac{q^2}{24m_N^2}c_{18}^\tau c_{18}^{\tau'} \\
R_\Delta^{\tau\tau'} &= \frac{2}{3}\left(\frac{\vec{q}^2}{m_N^2}c_5^\tau c_5^{\tau'} + c_8^\tau c_8^{\tau'}\right) + \frac{q^2}{6m_N^2}c_{17}^\tau c_{17}^{\tau'} \\
R_{\Delta\Sigma'}^{\tau\tau'} &= \frac{2}{3}\left(c_5^\tau c_4^{\tau'} - c_8^\tau c_9^{\tau'}\right)
\end{aligned}
\tag{5.47}
$$

5.7   Conclusions

The analysis we have given here builds on previous analyses to provide, in generality, a roadmap to use event rates in direct dark matter detectors to constrain fundamental dark matter models. We have outlined the steps needed to go from fundamental Lagrangians, first to relativistic operators, then to non-relativistic operators, and finally to produce nuclear matrix elements. In the process several significant facts have been elaborated.

- Not all possible non-relativistic operators contributing to nuclear matrix elements in direct detection will arise from simple UV complete dark matter models.

- Aside from scalar WIMPs each particular spin produces some non-relativistic operators that are unique to that spin.

110

- Two non-relativistic operators, $\mathcal{O}_1$ and $\mathcal{O}_{10}$, are ubiquitous and arise for all WIMP spins we have explored.

- In 5 scenarios, relativistic operators generate unique non-relativistic operators at leading order.

- Two new non-relativistic operators not previously considered within the context of the full array of allowed nuclear responses arise at low energies if spin-1 WIMP dark matter is allowed for.

- While the different operators that can contribute to event rates in detectors using specific elements or isotopes cannot be distinguished on the basis of their impact on the differential event rates in these detectors, they can produce radically different energy dependence for scattering off different nuclear targets. Thus, a complementary use of different target materials will be necessary to reliably distinguish between different particle physics model possibilities for WIMP dark matter.

While current detectors have only yielded upper limits, with new generations of larger detectors with greater energy resolution and lower thresholds coming online, the search for WIMP dark matter has never been so vibrant and promising. The tools we have provided here should help experimenters to probe the most useful parameter space, to interpret any non-zero signals in terms of constraints on fundamental models, and should allow theorists who build fundamental models to frame predictions in an accurate and simple way so that they might be directly compared with experiment.

Table 5.10: List of scenarios with leading operators colored by which are distinguishable via the ratio $\left(\frac{dR_{Xe}}{dE}\right) / \left(\frac{dR_{Ge}}{dE}\right)$.

		$\mathcal{O}_1$	$\mathcal{O}_2$	$\mathcal{O}_3$	$\mathcal{O}_4$	$q^2\mathcal{O}_4$	$\mathcal{O}_5$	$\mathcal{O}_6$	$\mathcal{O}_7$	$\mathcal{O}_8$	$\mathcal{O}_9$	$\mathcal{O}_{10}$	$\mathcal{O}_{11}$	$\mathcal{O}_{12}$	$\mathcal{O}_{13}$	$\mathcal{O}_{14}$	$\mathcal{O}_{15}$	$\mathcal{O}_{17}$	$\mathcal{O}_{18}$
Spin-0 WIMP	(h_1, g_1)	✓																	
	(h_2, g_1)											✓							
	(h_4, g_4)											✓							
	(y_1)	✓										✓							
	(y_2)	✓										✓							
	(y_1, y_2)											✓							
Spin-$\frac{1}{2}$ WIMP	(h_1, λ_1)	✓																	
	(h_2, λ_1)											✓							
	(h_1, λ_2)												✓						
	(h_2, λ_2)							✓											
	(h_3, λ_3)	✓																	
	(h_4, λ_3)								✓		✓								
	(h_3, λ_4)									✓	✓								
	(h_4, λ_4)				✓														
	(l_1)	✓			✓			✓											
	(l_2)	✓			✓			✓											
	(d_1)	✓			✓			✓											
	(d_2)	✓			✓			✓											
Spin-1 WIMP	(h_1, b_1)	✓																	
	(h_2, b_1)											✓							
	(h_4, b_5)											✓							
	(h_3, b_6)					✓	✓	✓										✓*	
	(h_4, b_6)										✓								✓*
	(h_3, b_7)									✓*	✓*		✓						
	(h_4, b_7)				✓*	✓		✓								✓			
	(y_3)	✓			✓							✓	✓	✓					✓
	(y_4)	✓			✓							✓	✓	✓					✓
	(y_3, y_4)											✓	✓	✓					✓

112

REFERENCES

[1] A. Liam Fitzpatrick, Wick Haxton, Emanuel Katz, Nicholas Lubbers, and Yiming Xu. The Effective Field Theory of Dark Matter Direct Detection. *JCAP*, 1302:004, 2013.

[2] Alan H. Guth. The Inflationary Universe: A Possible Solution to the Horizon and Flatness Problems. *Phys. Rev.*, D23:347–356, 1981.

[3] Andrei D. Linde. A New Inflationary Universe Scenario: A Possible Solution of the Horizon, Flatness, Homogeneity, Isotropy and Primordial Monopole Problems. *Phys. Lett.*, B108:389–393, 1982.

[4] Andreas Albrecht and Paul J. Steinhardt. Cosmology for Grand Unified Theories with Radiatively Induced Symmetry Breaking. *Phys. Rev. Lett.*, 48:1220–1223, 1982.

[5] L. P. Grishchuk. Amplification of gravitational waves in an istropic universe. *Sov. Phys. JETP*, 40:409–415, 1975. [Zh. Eksp. Teor. Fiz.67,825(1974)].

[6] Alexei A. Starobinsky. Spectrum of relict gravitational radiation and the early state of the universe. *JETP Lett.*, 30:682–685, 1979. [Pisma Zh. Eksp. Teor. Fiz.30,719(1979)].

[7] C. Pryke. The Quest for Gravity Wave B-modes. 2012.

[8] Lawrence Krauss, Scott Dodelson, and Stephan Meyer. Primordial Gravitational Waves and Cosmology. *Science*, 328:989–992, 2010.

[9] Arthur Kosowsky. Cosmic microwave background polarization. *Annals Phys.*, 246:49–85, 1996.

[10] Marc Kamionkowski, Arthur Kosowsky, and Albert Stebbins. Statistics of cosmic microwave background polarization. *Phys. Rev.*, D55:7368–7388, 1997.

[11] Matias Zaldarriaga and Uros Seljak. An all sky analysis of polarization in the microwave background. *Phys. Rev.*, D55:1830–1840, 1997.

[12] Wayne Hu and Martin J. White. CMB anisotropies: Total angular momentum method. *Phys. Rev.*, D56:596–615, 1997.

[13] Wayne Hu and Martin J. White. A CMB polarization primer. *New Astron.*, 2:323, 1997.

[14] Paolo Cabella and Marc Kamionkowski. Theory of cosmic microwave background polarization. 2004.

[15] Daniel Baumann et al. CMBPol Mission Concept Study: Probing Inflation with CMB Polarization. *AIP Conf.Proc.*, 1141:10–120, 2009.

[16] David H. Lyth. What would we learn by detecting a gravitational wave signal in the cosmic microwave background anisotropy? *Phys. Rev. Lett.*, 78:1861–1863, 1997.

[17] Sayantan Choudhury and Anupam Mazumdar. An accurate bound on tensor-to-scalar ratio and the scale of inflation. *Nucl.Phys.*, B882:386–396, 2014.

[18] Lawrence M. Krauss. Gravitational waves from global phase transitions. *Phys. Lett.*, B284:229–233, 1992.

[19] Katherine Jones-Smith, Lawrence M. Krauss, and Harsh Mathur. A Nearly Scale Invariant Spectrum of Gravitational Radiation from Global Phase Transitions. *Phys.Rev.Lett.*, 100:131302, 2008.

[20] Elisa Fenu, Daniel G. Figueroa, Ruth Durrer, and Juan Garcia-Bellido. Gravitational waves from self-ordering scalar fields. *JCAP*, 0910:005, 2009.

[21] Lawrence M. Krauss, Katherine Jones-Smith, Harsh Mathur, and James Dent. Probing the Gravitational Wave Signature from Cosmic Phase Transitions at Different Scales. *Phys.Rev.*, D82:044001, 2010.

[22] Steven Weinberg. Damping of tensor modes in cosmology. *Phys.Rev.*, D69:023503, 2004.

[23] Sergei Bashinsky. Coupled evolution of primordial gravity waves and relic neutrinos. *Phys.Rev.D*, 2005.

[24] Duane A. Dicus and Wayne W. Repko. Comment on damping of tensor modes in cosmology. *Phys.Rev.*, D72:088302, 2005.

[25] Latham A. Boyle and Paul J. Steinhardt. Probing the early universe with inflationary gravitational waves. *Phys.Rev.*, D77:063504, 2008.

[26] Yuki Watanabe and Eiichiro Komatsu. Improved Calculation of the Primordial Gravitational Wave Spectrum in the Standard Model. *Phys.Rev.*, D73:123515, 2006.

[27] H.X. Miao and Yang Zhang. Analytic spectrum of relic gravitational waves modified by neutrino free streaming and dark energy. *Phys.Rev.*, D75:104009, 2007.

[28] Anna Mangilli, Nicola Bartolo, Sabino Matarrese, and Antonio Riotto. The impact of cosmic neutrinos on the gravitational-wave background. *Phys.Rev.*, D78:083517, 2008.

[29] Wen Zhao, Yang Zhang, and Tianyang Xia. New method to constrain the relativistic free-streaming gas in the Universe. *Phys.Lett.*, B677:235–238, 2009.

[30] Riccardo Benini, Massimiliano Lattanzi, and Giovanni Montani. Signatures of the neutrino thermal history in the spectrum of primordial gravitational waves. *Gen.Rel.Grav.*, 43:945–958, 2011.

[31] Ben A. Stefanek and Wayne W. Repko. Analytic description of the damping of gravitational waves by free streaming neutrinos. *Phys.Rev.*, D88(8):083536, 2013.

[32] Gavriil Shchedrin. Infrared divergence of the gravitational wave damping in the early Universe. 2012.

[33] Ryusuke Jinno, Takeo Moroi, and Kazunori Nakayama. Probing dark radiation with inflationary gravitational waves. *Phys.Rev.*, D86:123502, 2012.

[34] Y.I. Izotov and T.X. Thuan. The primordial abundance of 4He: evidence for non-standard big bang nucleosynthesis. *Astrophys.J.*, 710:L67–L71, 2010.

[35] E. Komatsu et al. Seven-Year Wilkinson Microwave Anisotropy Probe (WMAP) Observations: Cosmological Interpretation. *Astrophys.J.Suppl.*, 192:18, 2011.

[36] J. Dunkley, R. Hlozek, J. Sievers, V. Acquaviva, P.A.R. Ade, et al. The Atacama Cosmology Telescope: Cosmological Parameters from the 2008 Power Spectra. *Astrophys.J.*, 739:52, 2011.

[37] R. Keisler, C.L. Reichardt, K.A. Aird, B.A. Benson, L.E. Bleem, et al. A Measurement of the Damping Tail of the Cosmic Microwave Background Power Spectrum with the South Pole Telescope. *Astrophys.J.*, 743:28, 2011.

[38] Maria Archidiacono, Erminia Calabrese, and Alessandro Melchiorri. The Case for Dark Radiation. *Phys.Rev.*, D84:123008, 2011.

[39] G.L. Fogli, E. Lisi, A. Marrone, D. Montanino, A. Palazzo, et al. Global analysis of neutrino masses, mixings and phases: entering the era of leptonic CP violation searches. *Phys.Rev.*, D86:013012, 2012.

[40] J.M. Conrad, C.M. Ignarra, G. Karagiorgi, M.H. Shaevitz, and J. Spitz. Sterile Neutrino Fits to Short Baseline Neutrino Oscillation Measurements. *Adv.High Energy Phys.*, 2013:163897, 2013.

[41] Chiu Man Ho and Robert J. Scherrer. Sterile Neutrinos and Light Dark Matter Save Each Other. *Phys.Rev.*, D87(6):065016, 2013.

[42] Thomas D. Jacques, Lawrence M. Krauss, and Cecilia Lunardini. Additional Light Sterile Neutrinos and Cosmology. *Phys.Rev.*, D87(8):083515, 2013.

[43] Alessandro Mirizzi, Gianpiero Mangano, Ninetta Saviano, Enrico Borriello, Carlo Giunti, et al. The strongest bounds on active-sterile neutrino mixing after Planck data. *Phys.Lett.*, B726:8–14, 2013.

[44] Maria Archidiacono, Elena Giusarma, Steen Hannestad, and Olga Mena. Cosmic dark radiation and neutrinos. *Adv.High Energy Phys.*, 2013:191047, 2013.

[45] E. Komatsu et al. Five-Year Wilkinson Microwave Anisotropy Probe (WMAP) Observations: Cosmological Interpretation. *Astrophys.J.Suppl.*, 180:330–376, 2009.

[46] Jonathan R. Pritchard and Marc Kamionkowski. Cosmic microwave background fluctuations from gravitational waves: An Analytic approach. *Annals Phys.*, 318:2–36, 2005.

[47] William H. Press, Saul A. Teukolsky, William T. Vetterling, and Brian P. Flannery. Numerical Recipes in FORTRAN: The Art of Scientific Computing. 1992.

[48] Pierre Sikivie. Axion Cosmology. *Lect. Notes Phys.*, 741:19–50, 2008. [,19(2006)].

[49] Georg G. Raffelt and David S. P. Dearborn. Bounds on Hadronic Axions From Stellar Evolution. *Phys. Rev.*, D36:2211, 1987.

[50] P.A.R. Ade et al. Planck 2013 results. XVI. Cosmological parameters. *Astron.Astrophys.*, 571:A16, 2014.

[51] Steven Weinberg. *Cosmology*. 2008.

[52] Alexei A. Starobinsky. A New Type of Isotropic Cosmological Models Without Singularity. *Phys.Lett.*, B91:99–102, 1980.

[53] Lawrence M. Krauss and Martin J. White. Grand unification, gravitational waves, and the cosmic microwave background anisotropy. *Phys.Rev.Lett.*, 69:869–872, 1992.

[54] F.L. Bezrukov and Mikhail Shaposhnikov. The Standard Model Higgs boson as the inflaton. *Phys.Lett.*, B659:703–706, 2008.

[55] Andrea De Simone, Mark P. Hertzberg, and Frank Wilczek. Running Inflation in the Standard Model. *Phys.Lett.*, B678:1–8, 2009.

[56] A.O. Barvinsky, A. Yu. Kamenshchik, and A.A. Starobinsky. Inflation scenario via the Standard Model Higgs boson and LHC. *JCAP*, 0811:021, 2008.

[57] F. Bezrukov, A. Magnin, M. Shaposhnikov, and S. Sibiryakov. Higgs inflation: consistency and generalisations. *JHEP*, 1101:016, 2011.

[58] Fedor Bezrukov, Mikhail Yu. Kalmykov, Bernd A. Kniehl, and Mikhail Shaposhnikov. Higgs Boson Mass and New Physics. *JHEP*, 1210:140, 2012.

[59] Kyle Allison. Higgs xi-inflation for the 125-126 GeV Higgs: a two-loop analysis. 2013.

[60] Alberto Salvio. Higgs Inflation at NNLO after the Boson Discovery. *Phys. Lett.*, B727:234–239, 2013.

[61] T.E. Clark, Boyang Liu, S.T. Love, and T. ter Veldhuis. The Standard Model Higgs Boson-Inflaton and Dark Matter. *Phys.Rev.*, D80:075019, 2009.

[62] Nobuchika Okada, Mansoor Ur Rehman, and Qaisar Shafi. Running Standard Model Inflation And Type I Seesaw. 2009.

[63] Bin He, Nobuchika Okada, and Qaisar Shafi. Higgs Boson Mass Bounds in Seesaw Extended Standard Model with Non-Minimal Gravitational Coupling. *Phys.Lett.*, B695:219–224, 2011.

[64] Werner Rodejohann and He Zhang. Impact of massive neutrinos on the Higgs self-coupling and electroweak vacuum stability. *JHEP*, 1206:022, 2012.

[65] Archil Kobakhidze and Alexander Spencer-Smith. Neutrino Masses and Higgs Vacuum Stability. *JHEP*, 1308:036, 2013.

[66] J.L.F. Barbon and J.R. Espinosa. On the Naturalness of Higgs Inflation. *Phys.Rev.*, D79:081302, 2009.

[67] C.P. Burgess, Hyun Min Lee, and Michael Trott. Comment on Higgs Inflation and Naturalness. *JHEP*, 1007:007, 2010.

[68] C.P. Burgess, Subodh P. Patil, and Michael Trott. On the Predictiveness of Single-Field Inflationary Models. 2014.

[69] Damien P. George, Sander Mooij, and Marieke Postma. Effective action for the Abelian Higgs model in FLRW. *JCAP*, 1211:043, 2012.

[70] Damien P. George, Sander Mooij, and Marieke Postma. Quantum corrections in Higgs inflation: the real scalar case. *JCAP*, 1402:024, 2014.

[71] Tomislav Prokopec and Jan Weenink. Naturalness in Higgs inflation in a frame independent formalism. 2014.

[72] Dario Buttazzo, Giuseppe Degrassi, Pier Paolo Giardino, Gian F. Giudice, Filippo Sala, et al. Investigating the near-criticality of the Higgs boson. 2013.

[73] Steven Weinberg. Perturbative Calculations of Symmetry Breaking. *Phys.Rev.*, D7:2887–2910, 1973.

[74] R. Jackiw. Functional evaluation of the effective potential. *Phys. Rev.*, D9:1686, 1974.

[75] L. Dolan and R. Jackiw. Gauge Invariant Signal for Gauge Symmetry Breaking. *Phys.Rev.*, D9:2904, 1974.

[76] J.S. Kang. Gauge Invariance of the Scalar-Vector Mass Ratio in the Coleman-Weinberg Model. *Phys.Rev.*, D10:3455, 1974.

[77] N. K. Nielsen. On the Gauge Dependence of Spontaneous Symmetry Breaking in Gauge Theories. *Nucl. Phys.*, B101:173, 1975.

[78] Reijiro Fukuda and Taichiro Kugo. Gauge Invariance in the Effective Action and Potential. *Phys.Rev.*, D13:3469, 1976.

[79] I. J. R. Aitchison and C. M. Fraser. Gauge Invariance and the Effective Potential. *Ann. Phys.*, 156:1, 1984.

[80] Hiren H. Patel and Michael J. Ramsey-Musolf. Baryon Washout, Electroweak Phase Transition, and Perturbation Theory. 2011.

[81] Steven Weinberg. Gauge and Global Symmetries at High Temperature. *Phys.Rev.*, D9:3357–3378, 1974.

[82] L. Dolan and R. Jackiw. Symmetry Behavior at Finite Temperature. *Phys. Rev.*, D9:3320–3341, 1974.

[83] Claude W. Bernard. Feynman Rules for Gauge Theories at Finite Temperature. *Phys.Rev.*, D9:3312, 1974.

[84] Carroll Wainwright, Stefano Profumo, and Michael J. Ramsey-Musolf. Gravity Waves from a Cosmological Phase Transition: Gauge Artifacts and Daisy Resummations. *Phys.Rev.*, D84:023521, 2011.

[85] Carroll L. Wainwright, Stefano Profumo, and Michael J. Ramsey-Musolf. Phase Transitions and Gauge Artifacts in an Abelian Higgs Plus Singlet Model. *Phys.Rev.*, D86:083537, 2012.

[86] Mathias Garny and Thomas Konstandin. On the gauge dependence of vacuum transitions at finite temperature. *JHEP*, 1207:189, 2012.

[87] Marc Sher. Electroweak Higgs Potentials and Vacuum Stability. *Phys. Rept.*, 179:273–418, 1989.

[88] Boris M. Kastening. Renormalization group improvement of the effective potential in massive phi**4 theory. *Phys.Lett.*, B283:287–292, 1992.

[89] Masako Bando, Taichiro Kugo, Nobuhiro Maekawa, and Hiroaki Nakano. Improving the effective potential. *Phys.Lett.*, B301:83–89, 1993.

[90] Masako Bando, Taichiro Kugo, Nobuhiro Maekawa, and Hiroaki Nakano. Improving the effective potential: Multimass scale case. *Prog.Theor.Phys.*, 90:405–418, 1993.

[91] C. Ford, D.R.T. Jones, P.W. Stephenson, and M.B. Einhorn. The Effective potential and the renormalization group. *Nucl.Phys.*, B395:17–34, 1993.

[92] A.V. Bednyakov, A.F. Pikelner, and V.N. Velizhanin. Higgs self-coupling beta-function in the Standard Model at three loops. *Nucl.Phys.*, B875:552–565, 2013.

[93] Sidney R. Coleman and Erick J. Weinberg. Radiative Corrections as the Origin of Spontaneous Symmetry Breaking. *Phys.Rev.*, D7:1888–1910, 1973.

[94] A. D. Sakharov. Violation of CP Invariance, c Asymmetry, and Baryon Asymmetry of the Universe. *Pisma Zh. Eksp. Teor. Fiz.*, 5:32–35, 1967. [Usp. Fiz. Nauk161,61(1991)].

[95] James M. Cline and Stuart Raby. Gravitino induced baryogenesis: A Problem made a virtue. *Phys. Rev.*, D43:1781–1787, 1991.

[96] Heinz Pagels and Joel R. Primack. Supersymmetry, Cosmology and New TeV Physics. *Phys. Rev. Lett.*, 48:223, 1982.

[97] Steven Weinberg. Cosmological Constraints on the Scale of Supersymmetry Breaking. *Phys. Rev. Lett.*, 48:1303, 1982.

[98] John R. Ellis, Jihn E. Kim, and Dimitri V. Nanopoulos. Cosmological Gravitino Regeneration and Decay. *Phys. Lett.*, B145:181, 1984.

[99] M. Kawasaki and T. Moroi. Gravitino production in the inflationary universe and the effects on big bang nucleosynthesis. *Prog. Theor. Phys.*, 93:879–900, 1995.

[100] Lawrence M. Krauss. New Constraints on Ino Masses from Cosmology. 1. Supersymmetric Inos. *Nucl. Phys.*, B227:556, 1983.

[101] R. Barbier et al. R-parity violating supersymmetry. *Phys. Rept.*, 420:1–202, 2005.

[102] V. A. Kuzmin, V. A. Rubakov, and M. E. Shaposhnikov. On the Anomalous Electroweak Baryon Number Nonconservation in the Early Universe. *Phys. Lett.*, B155:36, 1985.

[103] M. Fukugita and T. Yanagida. Baryogenesis Without Grand Unification. *Phys. Lett.*, B174:45, 1986.

[104] W. Buchmuller, R. D. Peccei, and T. Yanagida. Leptogenesis as the origin of matter. *Ann. Rev. Nucl. Part. Sci.*, 55:311–355, 2005.

[105] Nima Arkani-Hamed and Savas Dimopoulos. Supersymmetric unification without low energy supersymmetry and signatures for fine-tuning at the LHC. *JHEP*, 06:073, 2005.

[106] G. F. Giudice and A. Romanino. Split supersymmetry. *Nucl. Phys.*, B699:65–89, 2004. [Erratum: Nucl. Phys.B706,65(2005)].

[107] Asimina Arvanitaki, Nathaniel Craig, Savas Dimopoulos, and Giovanni Villadoro. Mini-Split. *JHEP*, 02:126, 2013.

[108] Andrew R. Liddle. The Inflationary energy scale. *Phys. Rev.*, D49:739–747, 1994.

[109] P.A.R. Ade et al. Planck 2013 results. XXII. Constraints on inflation. 2013.

[110] Robert J. Scherrer and Michael S. Turner. Decaying Particles Do Not Heat Up the Universe. *Phys. Rev.*, D31:681, 1985.

[111] S. Yu. Khlebnikov and M. E. Shaposhnikov. The Statistical Theory of Anomalous Fermion Number Nonconservation. *Nucl. Phys.*, B308:885–912, 1988.

[112] Savas Dimopoulos and Lawrence J. Hall. Baryogenesis at the MeV Era. *Phys. Lett.*, B196:135, 1987.

[113] K. A. Olive et al. Review of Particle Physics. *Chin. Phys.*, C38:090001, 2014.

[114] Lawrence J. Hall and Mahiko Suzuki. Explicit R-Parity Breaking in Supersymmetric Models. *Nucl. Phys.*, B231:419, 1984.

[115] K. S. Babu and R. N. Mohapatra. Supersymmetry and Large Transition Magnetic Moment of the Neutrino. *Phys. Rev. Lett.*, 64:1705, 1990.

[116] S. A. Abel, A. Dedes, and Herbert K. Dreiner. Dipole moments of the electron, neutrino and neutron in the MSSM without R-parity symmetry. *JHEP*, 05:013, 2000.

[117] J. Beringer et al. Review of Particle Physics (RPP). *Phys. Rev.*, D86:010001, 2012.

[118] David E. Brahm, Lawrence J. Hall, and Stephen D. H. Hsu. Ruling Out Large Sneutrinos VEVs. *Phys. Rev.*, D42:1860–1862, 1990.

[119] Anjan S. Joshipura and Marek Nowakowski. 'Just so' oscillations in supersymmetric standard model. *Phys. Rev.*, D51:2421–2427, 1995.

[120] John R. Ellis, G. Gelmini, C. Jarlskog, Graham G. Ross, and J. W. F. Valle. Phenomenology of Supersymmetry with Broken R-Parity. *Phys. Lett.*, B150:142, 1985.

[121] G. F. Giudice and R. Rattazzi. Theories with gauge mediated supersymmetry breaking. *Phys. Rept.*, 322:419–499, 1999.

[122] P. H. Frampton, S. L. Glashow, and T. Yanagida. Cosmological sign of neutrino CP violation. *Phys. Lett.*, B548:119–121, 2002.

[123] T. Endoh, S. Kaneko, S. K. Kang, T. Morozumi, and M. Tanimoto. CP violation in neutrino oscillation and leptogenesis. *Phys. Rev. Lett.*, 89:231601, 2002.

[124] Yoshiaki Sofue and Vera Rubin. Rotation curves of spiral galaxies. *Ann. Rev. Astron. Astrophys.*, 39:137–174, 2001.

[125] Shaun Cole et al. The 2dF Galaxy Redshift Survey: Power-spectrum analysis of the final dataset and cosmological implications. *Mon. Not. Roy. Astron. Soc.*, 362:505–534, 2005.

[126] Florian Beutler, Chris Blake, Matthew Colless, D. Heath Jones, Lister Staveley-Smith, Lachlan Campbell, Quentin Parker, Will Saunders, and Fred Watson. The 6dF Galaxy Survey: Baryon Acoustic Oscillations and the Local Hubble Constant. *Mon. Not. Roy. Astron. Soc.*, 416:3017–3032, 2011.

[127] Lauren Anderson et al. The clustering of galaxies in the SDSS-III Baryon Oscillation Spectroscopic Survey: Baryon Acoustic Oscillations in the Data Release 9 Spectroscopic Galaxy Sample. *Mon. Not. Roy. Astron. Soc.*, 427(4):3435–3467, 2013.

[128] A. Vikhlinin et al. Chandra Cluster Cosmology Project III: Cosmological Parameter Constraints. *Astrophys. J.*, 692:1060–1074, 2009.

[129] L. Fu et al. Very weak lensing in the CFHTLS Wide: Cosmology from cosmic shear in the linear regime. *Astron. Astrophys.*, 479:9–25, 2008.

[130] Richard Massey et al. COSMOS: 3D weak lensing and the growth of structure. *Astrophys. J. Suppl.*, 172:239–253, 2007.

[131] Oscar Adriani et al. An anomalous positron abundance in cosmic rays with energies 1.5-100 GeV. *Nature*, 458:607–609, 2009.

[132] Meng Su, Tracy R. Slatyer, and Douglas P. Finkbeiner. Giant Gamma-ray Bubbles from Fermi-LAT: AGN Activity or Bipolar Galactic Wind? *Astrophys. J.*, 724:1044–1082, 2010.

[133] Dan Hooper and Lisa Goodenough. Dark Matter Annihilation in The Galactic Center As Seen by the Fermi Gamma Ray Space Telescope. *Phys. Lett.*, B697:412–428, 2011.

[134] Christoph Weniger. A Tentative Gamma-Ray Line from Dark Matter Annihilation at the Fermi Large Area Telescope. *JCAP*, 1208:007, 2012.

[135] Esra Bulbul, Maxim Markevitch, Adam Foster, Randall K. Smith, Michael Loewenstein, et al. Detection of An Unidentified Emission Line in the Stacked X-ray spectrum of Galaxy Clusters. *Astrophys.J.*, 789:13, 2014.

[136] Georges Aad et al. Search for dark matter in events with a Z boson and missing transverse momentum in pp collisions at $\sqrt{s}$=8 TeV with the ATLAS detector. *Phys.Rev.*, D90(1):012004, 2014.

[137] G. Aad et al. Search for dark matter in events with heavy quarks and missing transverse momentum in *pp* collisions with the ATLAS detector. *Eur.Phys.J.*, C75(2):92, 2015.

[138] Georges Aad et al. Search for new phenomena in final states with an energetic jet and large missing transverse momentum in pp collisions at $\sqrt{s} = 8$ TeV with the ATLAS detector. *Eur.Phys.J.*, C75(7):299, 2015.

121

[139] Georges Aad et al. Search for dark matter in events with a hadronically decaying W or Z boson and missing transverse momentum in pp collisions at $\sqrt{s} = 8$ TeV with the ATLAS detector. *Phys.Rev.Lett.*, 112(4):041802, 2014.

[140] Steven Lowette. Search for Dark Matter at CMS. 2014.

[141] Mark W. Goodman and Edward Witten. Detectability of Certain Dark Matter Candidates. *Phys. Rev.*, D31:3059, 1985.

[142] Blas Cabrera, Lawrence M. Krauss, and Frank Wilczek. Bolometric Detection of Neutrinos. *Phys. Rev. Lett.*, 55:25, 1985.

[143] D.S. Akerib et al. First results from the LUX dark matter experiment at the Sanford Underground Research Facility. *Phys.Rev.Lett.*, 112:091303, 2014.

[144] E. Aprile et al. Dark Matter Results from 225 Live Days of XENON100 Data. *Phys. Rev. Lett.*, 109:181301, 2012.

[145] Z. Ahmed et al. Results from a Low-Energy Analysis of the CDMS II Germanium Data. *Phys. Rev. Lett.*, 106:131302, 2011.

[146] R. Agnese et al. Silicon Detector Dark Matter Results from the Final Exposure of CDMS II. *Phys.Rev.Lett.*, 111(25):251301, 2013.

[147] R. Bernabei et al. First results from DAMA/LIBRA and the combined results with DAMA/NaI. *Eur. Phys. J.*, C56:333–355, 2008.

[148] C. E. Aalseth et al. CoGeNT: A Search for Low-Mass Dark Matter using p-type Point Contact Germanium Detectors. *Phys. Rev.*, D88(1):012002, 2013.

[149] G. Angloher et al. Results from 730 kg days of the CRESST-II Dark Matter Search. *Eur. Phys. J.*, C72:1971, 2012.

[150] J. Sander, Z. Ahmed, A.J. Anderson, S. Arrenberg, D. Balakishiyeva, et al. SuperCDMS status from Soudan and plans for SNOLab. *AIP Conf.Proc.*, 1534:129–135, 2012.

[151] R. Agnese et al. Search for Low-Mass Weakly Interacting Massive Particles with SuperCDMS. *Phys.Rev.Lett.*, 112(24):241302, 2014.

[152] R. Agnese et al. Search for Low-Mass Weakly Interacting Massive Particles Using Voltage-Assisted Calorimetric Ionization Detection in the SuperCDMS Experiment. *Phys.Rev.Lett.*, 112(4):041302, 2014.

[153] Elena Aprile. The XENON1T Dark Matter Search Experiment. *Springer Proc. Phys.*, 148:93–96, 2013.

[154] Laura Baudis. DARWIN: dark matter WIMP search with noble liquids. *J. Phys. Conf. Ser.*, 375:012028, 2012.

[155] Miguel Pato, Laura Baudis, Gianfranco Bertone, Roberto Ruiz de Austri, Louis E. Strigari, and Roberto Trotta. Complementarity of Dark Matter Direct Detection Targets. *Phys. Rev.*, D83:083505, 2011.

[156] Jayden L. Newstead, Thomas D. Jacques, Lawrence M. Krauss, James B. Dent, and Francesc Ferrer. Scientific reach of multiton-scale dark matter direct detection experiments. *Phys.Rev.*, D88(7):076011, 2013.

[157] David Tucker-Smith and Neal Weiner. Inelastic dark matter. *Phys. Rev.*, D64:043502, 2001.

[158] Spencer Chang, Graham D. Kribs, David Tucker-Smith, and Neal Weiner. Inelastic Dark Matter in Light of DAMA/LIBRA. *Phys. Rev.*, D79:043513, 2009.

[159] Brian Feldstein, A. Liam Fitzpatrick, and Emanuel Katz. Form Factor Dark Matter. *JCAP*, 1001:020, 2010.

[160] Spencer Chang, Aaron Pierce, and Neal Weiner. Momentum Dependent Dark Matter Scattering. *JCAP*, 1001:006, 2010.

[161] Vernon Barger, Wai-Yee Keung, and Danny Marfatia. Electromagnetic properties of dark matter: Dipole moments and charge form factor. *Phys. Lett.*, B696:74–78, 2011.

[162] Tom Banks, Jean-Francois Fortin, and Scott Thomas. Direct Detection of Dark Matter Electromagnetic Dipole Moments. 2010.

[163] R. Foot. A comprehensive analysis of the dark matter direct detection experiments in the mirror dark matter framework. *Phys. Rev.*, D82:095001, 2010.

[164] Chiu Man Ho and Robert J. Scherrer. Anapole Dark Matter. *Phys. Lett.*, B722:341–346, 2013.

[165] Jessica Goodman, Masahiro Ibe, Arvind Rajaraman, William Shepherd, Tim M. P. Tait, and Hai-Bo Yu. Constraints on Dark Matter from Colliders. *Phys. Rev.*, D82:116010, 2010.

[166] Yang Bai, Patrick J. Fox, and Roni Harnik. The Tevatron at the Frontier of Dark Matter Direct Detection. *JHEP*, 12:048, 2010.

[167] Csaba Balzs, Tong Li, and Jayden L. Newstead. Thermal dark matter implies new physics not far above the weak scale. *JHEP*, 1408:061, 2014.

[168] Giorgio Busoni, Andrea De Simone, Enrico Morgante, and Antonio Riotto. On the Validity of the Effective Field Theory for Dark Matter Searches at the LHC. *Phys.Lett.*, B728:412–421, 2014.

[169] Daniele Alves. Simplified Models for LHC New Physics Searches. *J. Phys.*, G39:105005, 2012.

[170] Arvind Rajaraman, William Shepherd, Tim M. P. Tait, and Alexander M. Wijangco. LHC Bounds on Interactions of Dark Matter. *Phys. Rev.*, D84:095013, 2011.

[171] O. Buchmueller, Matthew J. Dolan, and Christopher McCabe. Beyond Effective Field Theory for Dark Matter Searches at the LHC. *JHEP*, 1401:025, 2014.

[172] Asher Berlin, Dan Hooper, and Samuel D. McDermott. Simplified Dark Matter Models for the Galactic Center Gamma-Ray Excess. *Phys.Rev.*, D89(11):115022, 2014.

[173] Csaba Balzs and Tong Li. Simplified Dark Matter Models Confront the Gamma Ray Excess. *Phys.Rev.*, D90(5):055026, 2014.

[174] JiJi Fan, Matthew Reece, and Lian-Tao Wang. Non-relativistic effective theory of dark matter direct detection. *JCAP*, 1011:042, 2010.

[175] Nikhil Anand, A. Liam Fitzpatrick, and W.C. Haxton. Weakly interacting massive particle-nucleus elastic scattering response. *Phys.Rev.*, C89(6):065501, 2014.

[176] Nikhil Anand, A. Liam Fitzpatrick, and W.C. Haxton. Model-independent Analyses of Dark-Matter Particle Interactions. *Phys.Procedia*, 61:97–106, 2015.

[177] Moira I. Gresham and Kathryn M. Zurek. Effect of nuclear response functions in dark matter direct detection. *Phys.Rev.*, D89(12):123521, 2014.

[178] Junji Hisano, Koji Ishiwata, Natsumi Nagata, and Masato Yamanaka. Direct Detection of Vector Dark Matter. *Prog. Theor. Phys.*, 126:435–456, 2011.

[179] Jonathan L. Feng and Jason Kumar. The WIMPless Miracle: Dark-Matter Particles without Weak-Scale Masses or Weak Interactions. *Phys. Rev. Lett.*, 101:231301, 2008.

[180] Riccardo Catena. Prospects for direct detection of dark matter in an effective theory approach. *JCAP*, 1407:055, 2014.

[181] J. D. Bjorken and S. D. Drell. *Relativistic Quantum Field Theory*. 1979.

[182] Prateek Agrawal, Zackaria Chacko, Can Kilic, and Rashmish K. Mishra. A Classification of Dark Matter Candidates with Primarily Spin-Dependent Interactions with Matter. 2010.

[183] Keith R. Dienes, Jason Kumar, Brooks Thomas, and David Yaylali. Overcoming Velocity Suppression in Dark-Matter Direct-Detection Experiments. *Phys.Rev.*, D90(1):015012, 2014.

[184] Jonathan L. Feng, Jason Kumar, and David Sanford. Xenophobic Dark Matter. *Phys.Rev.*, D88(1):015021, 2013.

[185] V. Mukhanov. *Physical Foundations of Cosmology*. Cambridge University Press, Oxford, 2005.

[186] Daniel Baumann. TASI Lectures on Inflation. In *Physics of the large and the small, TASI 09, proceedings of the Theoretical Advanced Study Institute in Elementary Particle Physics, Boulder, Colorado, USA, 1-26 June 2009*, pages 523–686, 2011.

[187] T. P. Cheng and L. F. Li. *Gauge theory of Elementary Particle Physics*. 1984.

[188] R. D. Peccei and Helen R. Quinn. CP Conservation in the Presence of Instantons. *Phys. Rev. Lett.*, 38:1440–1443, 1977.

[189] R. D. Peccei and Helen R. Quinn. Constraints Imposed by CP Conservation in the Presence of Instantons. *Phys. Rev.*, D16:1791–1797, 1977.

[190] Edward W. Kolb and Michael S. Turner, editors. *The Early Universe, Reprints*. 1988.

[191] Richard Lynn Davis. Cosmic Axions from Cosmic Strings. *Phys. Lett.*, B180:225, 1986.

[192] Mariano Quiros. Finite temperature field theory and phase transitions. In *High energy physics and cosmology. Proceedings, Summer School, Trieste, Italy, June 29-July 17, 1998*, pages 187–259, 1999.

[193] Mu-Chun Chen. TASI 2006 Lectures on Leptogenesis. In *Proceedings of Theoretical Advanced Study Institute in Elementary Particle Physics : Exploring New Frontiers Using Colliders and Neutrinos (TASI 2006)*, pages 123–176, 2007.

[194] P. Binetruy. *Supersymmetry: Theory, experiment and cosmology*. 2006.

[195] C. P. Burgess. Introduction to Effective Field Theory. *Ann. Rev. Nucl. Part. Sci.*, 57:329–362, 2007.

APPENDIX A

COSMOLOGICAL PERTURBATION THEORY

The FRW metric describes a uniform, isotropic and homogenous universe. But such a universe would be exceedingly boring because it would look exactly the same everywhere. And thats of course not our universe at the small scale. So if we want to describe the real universe which has large scale structure like clusters of galaxies, we have to move beyond this zeroth order. Fortunately though, at the very largest scales, the universe is still to a high degree of accuracy homogenous ad isotropic. NASA's COBE satellite which studied anisotropies in the CMB that probe matter over-densities showed in 1992 (these observations have been improved by WMAP and Planck) that universe was indeed extremely homogenous and isotropic. This means that large scale structure is but a small perturbation on top of this homogenous and isotropic background. Perturbation theory is a powerful technique to get accurate quantitative solutions to problems for which an exact closed form analytical solution may not exist. Thus, if we could study perturbations on top of FRW universe, we could describe the evolution of this large scale structure. We now turn to a review of cosmological perturbation theory which was extensively used in our research. The treatment here borrows heavily from Ch.7 of [185].

Einstein's equations connect space-time geometry i.e., metric to energy-momentum tensor of matter in that space-time. To understand the evolution of small perturbations, we need to expand both the LHS and RHS of this equation about the FRW background. To keep the discussion general lets label the background FRW metric as $g_{\mu\nu}^{(0)}$ and the perturbation as $g_{\mu\nu}^{(1)}$.

$$g_{\mu\nu} = g_{\mu\nu}^{(0)} + \delta g_{\mu\nu} \tag{A.1}$$

Now ideally we want this perturbation $\delta g_{\mu\nu}$ to be small. However, there's a difficulty. Einstein's equations are diffeomorphic invariant. So, there exist coordinate transformations under which the perturbation and the background metric can mix and thus there is no unique way of decomposing a metric into a big and small part. Fortunately, this dilemma can be solved by working with gauge invariant quantities.

Diffeomorphic invariance is simply invariance under general coordinate transformations $x^{\alpha} \to \tilde{x}^{\alpha} = f(x^{\alpha})$. Consider infinitesimal transformations so that $\tilde{x}^{\alpha} = x^{\alpha} + \epsilon^{\alpha}(x^{\alpha})$ where $\epsilon^{\alpha}(x^{\alpha}) \ll x^{\alpha}$. Under this transformation the metric will transform as a rank-2 tensor,

$$\tilde{g}_{\mu\nu}(\tilde{x}) = \frac{\partial x^{\alpha}}{\partial \tilde{x}^{\mu}} \frac{\partial x^{\beta}}{\partial \tilde{x}^{\nu}} g_{\alpha\beta}(x) = g_{\mu\nu}(x) - \partial_{\nu}\epsilon_{\mu}(x) - \partial_{\mu}\epsilon_{\nu}(x) \tag{A.2}$$

where the derivatives are w.r.t. x^{α}. The symmetric piece on the right side, $\partial_{\mu}\epsilon_{\nu} + \partial_{\nu}\epsilon_{\mu} = \mathcal{L}_{\epsilon}g_{\mu\nu}(x)$ is the Lie derivative of the metric tensor in the direction of the vector field $\epsilon^{\mu}(x)$.

Using this lets derive the infinitesimal coordinate transformation rule for the perturbation $\delta g_{\mu\nu}$. The key idea in cosmological perturbation theory is that observers in any frame see a FRW background and small perturbations on top. So, we should expand about the same background in both frames. Then the perturbation follows a

gauge transformation law,

$$g^{(0)}_{\mu\nu}(\tilde{x}) + \delta\tilde{g}_{\mu\nu}(\tilde{x}) = g^{(0)}_{\mu\nu}(x) + \delta g_{\mu\nu}(x) - \partial_\nu\epsilon_\mu(x) - \partial_\mu\epsilon_\nu(x)$$

$$\delta\tilde{g}_{\mu\nu}(\tilde{x}) = \delta g_{\mu\nu}(x) - \epsilon^\alpha(x)\partial_\alpha g^{(0)}_{\mu\nu}(x) - \partial_\nu\epsilon_\mu(x) - \partial_\mu\epsilon_\nu(x) \tag{A.3}$$

The indices are raised and lowered w.r.t. the original metric $g^{(0)}_{\mu\nu}$. This coordinate transformation law for the perturbations is used to construct gauge-invariant variables. But before that we want to understand the physical degrees of freedom hidden in this perturbation. Similarly, we can also derive the gauge transformation law for a scalar δq and a vector δu_i. A scalar doesn't change under coordinate transformation. So, $\tilde{q}(\tilde{x}) = q(x)$. Expanding $q(x) = q^0(x) + \delta q(x)$ about a background q^0 and similarly $\tilde{q}(\tilde{x}) = q^0(\tilde{x}) + \delta\tilde{q}$, we immediately have

$$\delta q \to \delta\tilde{q} = \delta q - (\partial_\alpha q^0)\epsilon^\alpha \tag{A.4}$$

We can do a similar expansion for a 4-vector u_α except unlike the metric which changes with two factors of $\partial x/\partial\tilde{x}$, a vector only needs one such factor. Following the same method of expanding about a background, we get

$$\delta u_\alpha \to \delta\tilde{u}_\alpha = \delta u_\alpha - (\partial_\beta u^0_\alpha)\epsilon^\gamma - u^0_\beta\epsilon^\beta_\alpha \tag{A.5}$$

Recall that the background FRW metric $g^{(0)}_{\mu\nu}$ is spatially homogenous and isotropic but time asymmetric.

$$ds^2 = g^{(0)}_{\mu\nu}dx^\mu dx^\nu = dt^2 - a(t)^2 d\vec{x}^2 = a(\eta)^2\left[d\eta^2 - d\vec{x}^2\right] \tag{A.6}$$

where $d\eta = dt/a(t)$ is the conformal time (the derivative w.r.t. η is denoted by a prime $'$). Therefore, it has 3 killing vectors, namely the rotation generators corresponding to the spherically symmetric background. We can thus decompose the perturbations according to their transformation properties under rotations in three dimensions. First we observe that the zeroth component of the perturbation parameter, ϵ^0 is obviously a scalar w.r.t. 3-rotations. And the spatial component ϵ^i is a 3-vector. However, the 3-vector can further be decomposed into a divergenceless pure 3-vector part and a gradient of a scalar by Helmholtz theorem $\to \epsilon_i = \epsilon'^\perp_i + \partial_i\xi$ where $\partial_i\epsilon^i = 0$ is a divergenceless vector field and ξ is a scalar field. Under this decomposition of the infinitesimal gauge parameter, the various components of the metric transform as

$$\begin{aligned}
\delta\tilde{g}_{00} &= \delta g_{00} - 2a(a\epsilon^0)' \\
\delta\tilde{g}_{0i} &= \delta g_{0i} + a^2\left[\epsilon'^\perp_i + \partial_i(\xi' - \epsilon^0)\right] \\
\delta\tilde{g}_{ij} &= \delta g_{ij} + a^2\left[\frac{2a'}{a}\delta_{ij}\epsilon^0 + 2\partial_{ij}\xi + \partial_j\epsilon'^\perp_i + \partial_i\epsilon'^\perp_j\right]
\end{aligned} \tag{A.7}$$

Its now easy to see that the (00) component of the perturbation has one scalar degree of freedom. The (0i) component has one and the (ij) component has two scalar degrees of freedom. So, if we just considered scalar perturbations the metric contain 4 scalars,

$$ds^2 = a(\eta)^2\left[(1 + 2\phi)d\eta^2 + 2\partial_i B dx^i d\eta - ((1 - 2\psi)\delta_{ij} - 2\partial_{ij}E)\,dx^i dx^j\right] \tag{A.8}$$

128

Using (A.7), they would transform as

$$\tilde{\phi} = \phi - \frac{1}{a}(a\epsilon^0)'$$
$$\tilde{B} = B + \xi' - \epsilon^0 \qquad\qquad\qquad\qquad (A.9)$$
$$\tilde{\psi} = \psi + \frac{a'}{a}\epsilon^0$$
$$\tilde{E} = E + \xi$$

We can use the gauge freedom to set two of these four scalars to zero. This means a physical perturbation has only two scalar degrees of freedom. In fact, two simple linear combinations of the above scalars are gauge invariant,

$$\Phi = \phi - \frac{1}{a}[a(B - E')]', \quad \Psi = \psi + \frac{a'}{a}(B - E') \qquad (A.10)$$

We use this representation to describe physical scalar perturbations in a gauge invariant matter. If they are both zero in one frame, they are zero in all frames and in that case there is no physical scalar perturbation and thats a coordinate independent statement.

To describe purely vector perturbations, we again refer back to (A.7) and observe that only the $(0i)$ and (ij) components contain truly vector degrees of freedom. Thus, for vector only perturbations the metric becomes

$$ds^2 = a(\eta)^2 \left[d\eta^2 + 2A_i dx^i d\eta - (\delta_{ij} - \partial_i C_j - \partial_j C_i)dx^i dx^j \right] \qquad (A.11)$$

Under gauge transformation, they transform only via the purely vector part $\epsilon_i^\perp$,

$$\tilde{A}_i = A_i + \epsilon_i'^\perp, \quad \tilde{C}_i = C_i + \epsilon_i^\perp \qquad (A.12)$$

Thus, the combination,

$$V_i = A_i - C_i' \qquad\qquad\qquad\qquad (A.13)$$

is gauge invariant and describes the purely vector perturbation in a gauge invariant fashion. And physically, this has only two degrees of freedom.

Finally, there is no purely tensor part of the gauge parameter, ϵ_μ and thus looking at the (ij) component, we see that if the scalar and vector components of the gauge transformation parameter is zero, then

$$\delta g_{ij} = \delta \tilde{g}_{ij} \qquad\qquad\qquad\qquad (A.14)$$

i.e., there is a part of the (ij) component that is purely gauge invariant. We call this a tensor perturbation and it describes a gravitational wave. And the metric with only tensor perturbations is given as

$$ds^2 = a(\eta)^2 \left[d\eta^2 - (\delta_{ij} - h_{ij})dx^i dx^j \right] \qquad (A.15)$$

129

To describe the dynamics of perturbations, we need to perturb Einstein's equations and we turn our attention to that now.

$$G_{\alpha\beta} = 8\pi G T_{\alpha\beta} \implies \delta G_{\alpha\beta} = 8\pi \delta T_{\alpha\beta} \qquad (A.16)$$

The energy-momentum tensor is a rank-2 tensor object so it transforms under a gauge transformation similar to the metric. We can thus find a suitable gauge invariant combination of its components separately under scalar, vector or tensor perturbations of the metric. For scalar only perturbations,

$$
\begin{aligned}
\delta \bar{T}^0_0 &= \delta T^0_0 - (T^{(0)0}_0)'(B - E') \\
\delta \bar{T}^0_i &= \delta T^0_i - \left(T^{(0)0}_0 - \frac{T^{(0)k}_k}{3} \right) \partial_i (B - E') \\
\delta \bar{T}^i_j &= \delta T^i_j - (T^{(0)i}_j)'(B - E')
\end{aligned}
\qquad (A.17)
$$

are the gauge invariant components of the perturbation in energy-momentum tensor. A superscript (0) denotes the background energy-momentum tensor and $\mathcal{H} = a'(\eta)/a = \dot{a}(t)$ is the 'Hubble' constant in conformal time. And given this, we can write the evolution equations for the gauge-invariant scalar perturbations Φ and Ψ,

$$
\begin{aligned}
\nabla^2 \Psi - 3\mathcal{H}(\Psi' + \mathcal{H}\Phi) &= 4\pi G a^2 \delta \bar{T}^0_0 \\
\partial_i (\Psi' + \mathcal{H}\Phi) &= 4\pi G a^2 \delta \bar{T}^0_i
\end{aligned}
\qquad (A.18)
$$

$$\left[\Psi'' + \mathcal{H}(2\Psi + \Phi)' + (2\mathcal{H}' + \mathcal{H}^2)\Phi + \frac{1}{2}\nabla^2(\Phi - \Psi) \right] \delta^i{}_j - \frac{1}{2}\partial^i \partial_j (\Phi - \Psi) = -4\pi G a^2 \delta \bar{T}^i_j$$

Similarly, the evolution equations for vector perturbations depend only on $\delta \bar{T}^{0V}_i$ and $\delta \bar{T}^{iV}_j$ respectively. For vector only perturbations, they are both gauge invariant when expanded about a FRW background.

$$\nabla^2 V_i = 16\pi G a^2 \delta \bar{T}^{0V}_i$$

$$(V_{i,j} + V_{j,i})' + 2\mathcal{H}(V_{i,j} + V_{j,i}) = -16\pi G a^2 \delta \bar{T}^{iV}_j \qquad (A.19)$$

The tensor perturbation h_{ij} is the remainder in δg_{ij} in (A.7) that can't be factored into a scalar or vector part. It has the simplest evolution equation,

$$h''_{ij} + 2\mathcal{H}h'_{ij} - \nabla^2 h_{ij} = 16\pi G a^2 \delta \bar{T}^T_{ij} \qquad (A.20)$$

where the tensor part of the stress-energy tensor is already gauge invariant. This component of the energy momentum tensor is also called anisotropic stress. Tensor perturbations were extensively studied in this thesis and we now turn our attention exclusively to these perturbations.

A.1 Tensor Perturbations

A simple assumption for the energy-momentum tensor of matter in the universe is a perfect fluid with energy density ρ and pressure p. At the largest scales, the inhomogeneities in the universe are small to first approximation - so a hydrodynamic assumption isn't a bad starting point. In perturbation theory, these inhomogeneities i.e., departures from the perfect fluid approximation are handled as first order corrections to the the perfect fluid energy-momentum tensor T_β^α, which is given as

$$T_\beta^\alpha = (\rho + p)u^\alpha u_\beta - p\delta_\beta^\alpha \tag{A.21}$$

u_α is the normalized 4-velocity field of the fluid and in the case of a perfect fluid at rest is given by $u_\alpha = (a, 0, 0, 0)$. We can find it in any other frame by simply lorentz boosting. This serves as our background energy-momentum tensor $T_\beta^{0\alpha}$. To find the perturbed energy momentum tensor, we perturb each variable ρ, p and u_α and expand to first order,

$$\delta T_\beta^\alpha = (\rho^0 + p^0)(\delta u^\alpha u_\beta^0 + \delta u_\beta u^{0\alpha}) + (\delta\rho + \delta p)u^{0\alpha}u_\beta^0 - \delta p\delta_\beta^\alpha \tag{A.22}$$

The velocity is normalized, $u_\alpha u^\alpha = (u_\alpha^0 + \delta u_\alpha)(u^{0\alpha} + \delta u^\alpha) = 1 \implies u_\alpha^0 \delta u^\alpha = 0$. Thus, if $u_\alpha^0 = (a, 0, 0, 0)$ then $\delta u^\alpha = (0, \delta u^i)$ and so the components of δT_β^α become

$$\delta T_0^0 = \delta\rho, \ \ \delta T_j^i = -\delta p\delta_j^i, \ \ \delta T_i^0 = \left(\frac{\rho^0 + p^0}{a}\right)\delta u_i \tag{A.23}$$

The velocity field can be decomposed again as $\delta u_i = \delta u_i^{||} + \delta u_i^\perp$ where like before $\partial_i \delta u_i^\perp = 0$ and so $\delta u_i^\perp$ is the purely vector part of the velocity field. Using (A.4), (A.5) and (A.17), we can then write the gauge invariant components of the energy-momentum tensor for a perfect fluid,

$$\begin{aligned}
\delta\bar{T}_0^0 &= \delta\bar{\rho} = \delta\rho - \rho^{0\prime}(B - E') \\
\delta\bar{T}_i^0 &= \left(\frac{\rho^0 + p^0}{a}\right)\left(\delta\bar{u}_i^{||} + \delta u_i^\perp\right) \ \ \text{where} \ \ \delta\bar{u}_i^{ll} = \delta u_i - a\partial_i(B - E') \\
\delta T_j^i &= -\delta\bar{p}\,\delta_j^i = -\left[\delta p - p^{0\prime}(B - E')\right]\delta_j^i
\end{aligned} \tag{A.24}$$

Thus, a perfect fluid energy-momentum tensor is invariant under a tensor-only perturbation i.e., there is no anisotropic stress in a perfect fluid. Thus, the RHS of (A.20) is zero,

$$h_{ij}'' + 2\mathcal{H}h_{ij}' - \nabla^2 h_{ij} = 0 \tag{A.25}$$

Recall that the tensor perturbation h_{ij} is the part of metric perturbation that can't be written in terms of a scalar or a vector. There are two scalars in δg_{ij} and one divergence free vector giving a total of 4 degrees of freedom. A symmetric δg_{ij} on the other hand has 6 degrees of freedom. Thus, $6 - 4 = 2$ degrees of freedom are contained in h_{ij}. Specifically, it is the transverse traceless part of δg_{ij}. The trace δg_i^i is excited

solely by scalar perturbations and the transverse part which satisfies $\partial_i \delta g^i_j = 0$ is excited by vector only perturbations $\epsilon^{\perp}_i$. Since h_{ij} is transverse and traceless, we can expand it in fourier space using polarization tensors as follows:

$$h_{ij} = \sum_{\lambda=+,\times} \int \frac{d^3k}{(2\pi)^3} h_\lambda(k,\eta) e^{ik\cdot x} \epsilon^\lambda_{ij} \tag{A.26}$$

where ϵ^λ_{ij} is time-independent, transverse, traceless and depends on k. The two degrees of freedom in h_{ij} are equivalent to two polarizations, denoted $\lambda = +, \times$ in fourier space. And so the polarization tensors are orthogonal i.e.,

$$\sum_{i,j} \epsilon^\lambda_{ij} \cdot \epsilon^{\lambda'}_{ij} = \delta^{\lambda\lambda'} \tag{A.27}$$

Substituting the fourier decomposition in (A.25) and using the orthogonality of the polarization tensors, the two polarization states decouple and evolve similarly but independently and the equation becomes

$$h''_{\lambda,k} + \left(\frac{2a'}{a}\right) h'_{\lambda,k} + k^2 h_{\lambda,k} = 0 \tag{A.28}$$

In a radiation dominated (RD - $a(\eta) \propto \eta$) or matter dominated (MD - $a(\eta) \propto \eta^2$) universe for example, the equation can be solved in general,

$$\begin{aligned} h_\lambda(k) &= \frac{C_1}{k\eta} \sin(k\eta) \to \text{RD} \\ &= \frac{C_1}{k\eta} \left[\frac{\sin(k\eta)}{(k\eta)^2} - \frac{\cos(k\eta)}{(k\eta)}\right] \to \text{MD} \end{aligned} \tag{A.29}$$

where C_1 is related to initial conditions (i.e., primordial tensor amplitude). A plot of this evolution is shown below. It is interesting to note that freely propagating tensor perturbations damp out much faster in a matter dominated universe.
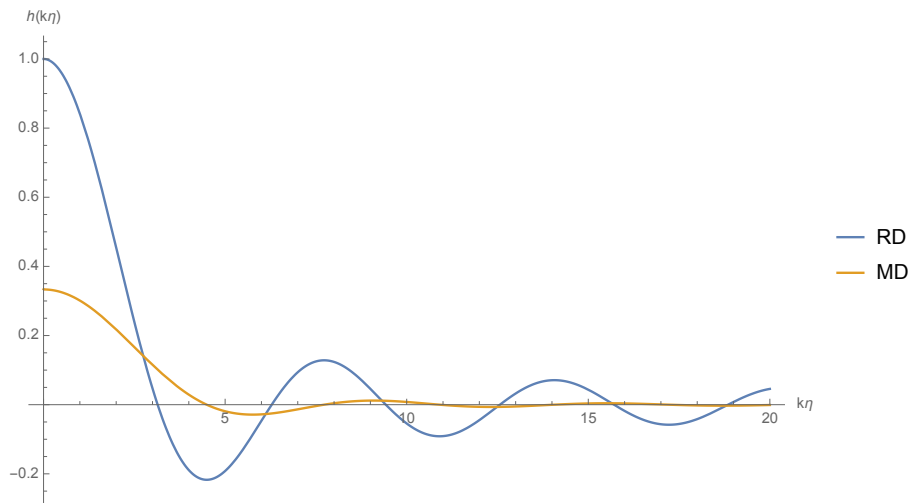
Figure A.1: The two lines show propagation of free tensor perturbations in a radiation or matter dominated universe. The amplitude of oscillations damps out much faster during matter domination.

APPENDIX B

INFLATION

The standard model of Big-Bang cosmology is a wonderful theory. Starting with the FRW metric, it predicts Hubble expansion, a result that was experimental verified in the 1920's. It predicts the existence of the cosmic microwave background, which decoupled 380,000 years after the big bang, at a temperature 2.7K and that was discovered in the 1960's. Next, the theory also correctly predicts the relative abundances of the light nuclei (which happened just 3 mins after the big bang) and this is perhaps one its most triumphant quantitative achievements.

However, this theory suffers from a few fundamental issues -

- <u>Homogeneity & Isotropy</u> At the largest scales, the universe is very homogenous and isotropic. That is it looks the same at every point and in every direction, to a high degree of accuracy. Measurements of the comic microwave background seem to bear this out in explicit detail. The CMB is very uniform with an average temperature of 2.7K and the hot and idol spots on it differ from this mean by only 10^{-5}K as measures most erectly by Planck satellite. Thus, the picture of the universe that the CMB paints is one which is extremely uniform i.e., homogenous and isotropic to a high degree. The standard big bang model doesn't explain why this is so. At first glance, it may seem this may not be a problem since we could argue that the universe was created homogenous and isotropic at the big bang. However, the present universe consists of many regions which were causally disconnected up to the time of recombination of electrons and photons after which the photons we now observe as the cosmic microwave background underwent no further scattering. The puzzle is how these causally disconnected regions could have ended up with the same microwave background temperature.

  To give a quantitative estimate of the scale of this homogeneity problem, consider the present size of the particle horizon, $ct_0 \sim 10^{28}$cm where t_0 is the time today, since the big bang. This is the furthest point that has ever been in causal contact with us i.e., the furthest points from which we can receive a signal. The hubble horizon and particle horizon are slightly different but for the purposes of this discussion, we can take them to be the same, approximately $(aH)^{-1}$. Inhomogeneities can't be diluted away by uniform hubble expansion and our current universe is homogenous over a length scale of 10^{28}cm. Thus, the universe should have been homogenous for about the same length across at some initial time like planck time t_i as it is today t_0, scaled by appropriate ratio of scale factor,

  $$\frac{l_i}{l_0} = \frac{a_i}{a_0} = \frac{T_0}{T_i} \tag{B.1}$$

  where T_0 is the Planck temperature 10^{32}K and T_0 is the temperature today, 2.7K. One more thing to note is that if the scale factor grows as time, then $l_i/l_c \sim \dot{a}_i/\dot{a}_0$. We have used here the formula for CMB redshift while maintaining a thermal spectrum, $aT = $ const.. On the other hand, the particle horizon of the universe at an initial time t_i is ct_i. Thus, extrapolating from today the

homogeneity scale at Planck time versus the particle horizon at that time is

$$\frac{l_i}{l_c} = \frac{t_0}{t_i}\frac{T_0}{T_i} \sim \frac{10^{17}}{10^{-43}}10^{-32} \sim 10^{28} \tag{B.2}$$

Thus the casual scale of the universe at some initial time was 28 orders of magnitude smaller than the size of the universe then. Thus, how could there be uniformity across 10^{28} casually disconnected patches? The universe was homogenous and isotropic on super-horizon scale if it is homogenous today! Back to the CMB spots, this means that their temperature of spots which were widely casually disconnected seem to be the same.

- Initial conditions or flatness As a space-time manifold, the universe can have non-zero curvature. The Friedmann equation for a space-time with curvature is

$$H^2 + \frac{k}{a^2} = \frac{8\pi G_N}{3}\rho \tag{B.3}$$

where k is the curvature and ρ is ratio of energy density in matter and dark energy. Call ρ_{cr} the energy density for a flat universe i.e., $k = 0$. Then we can recast this equation as

$$\Omega(t) - 1 = \frac{k}{(aH)^2} \tag{B.4}$$

where $\Omega = \rho/\rho_{cr}$ and $\rho_{cr} = 3H^2/8\pi G_N$. As before then, we can pick some initial time t_i and calculate how close to one Ω would have to be,

$$\frac{\Omega_i - 1}{\Omega_0 - 1} = \frac{a_0^2 H_0^2}{a_i^2 H_i^2} = \frac{l_i^2}{l_c^2} \sim 10^{-56} \tag{B.5}$$

because the physical horizon size is $\sim (aH)^{-1}$. Thus, if we observe today $\Omega_0 - 1 \approx 0$, then at some initial time the universe would have had to be flatter by 56 more orders of magnitude! That is the universe would have started out exceptionally flat unless we see a huge curvature today. And do we? By measuring the energy density in baryonic matter, dark matter through gravitational lensing and dark energy through high-z supernova survey and independently confirming them from the CMB, we observe that $\Omega_i \approx 1$ and thus the initial universe would most definitely have been extremely flat.

- Unwanted relics The Standard Model is a very successful theory which describes the three forces of nature - the electromagnetic, weak nuclear and strong nuclear forces. They are all described as gauge interactions, $SU(3) \times SU(2) \times U(1)$. The weak and electromagnetic forces unite at a scale above the higgs vev of 246GeV. Its likely then that the strong force unites with the other forces at some higher energy scale. The simplest gauge theory that contains these gauge groups is the $SU(5)$ Grand Unification Theory (GUT). There are other gauge theories like $SO(10)$ or $SO(32)$ GUTs. All these GUTs share a common feature that is when the larger symmetry group breaks into the standard model gauge

groups, there are topological effects like monopoles for example in the case of $SU(5)$ or $SO(10)$. The obvious question then is - do we see these relics of a phase transition of symmetry breaking? A generic relic like a monopole has never been seen but the theory predicts of the order of one for ever nucleon in the universe which is in gross violation of observations and they would carry enough energy to over-close the universe. How do we resolve this issue?

B.1 Exponential Expansion

These problems can be resolved successfully if we imagine a stage of exponential expansion of space in the early universe. This process is called Inflation and the idea was first proposed by Alan Guth in 1981 and since then has gained widespread acceptance and is believed to be the model of the early universe. There have been tantalizing hints recently of unique inflationary signatures and we will study one of them in greater detail later.

Inflation resolves all the three issues in the following manner. First note that in both the case of flatness and horizon problems, the ratio that matters is $\dot{a}_i/\dot{a}_0 = a_i H_i/a_0 H_0$. Consider a period of inflation and replace $a_0 H_0 \rightarrow a_I H_I$ where H_I is the Hubble constant during inflation. Since inflation is a period of exponential expansion, $a(t) = e^{Ht}$ and H is a constant. Thus, we see that inflation leads to exponential suppression in the critical ratio, $a_i H_i/a_I H_I$ before and after inflation. If during inflation the universe grew by N e-folds, then then the curvature and horizon by causal horizon ratios could be down by e^{-N}. Thus, if we started out with $\mathcal{O}(1)$ curvature at the big-bang, after inflation the curvature would be $(a_i H_i)^2/(a_I H_I)^2 = e^{-2N}$. Similarly, for the ratio of causal horizon to hubble or particle horizon after inflation would be down by $(a_i H_i)/(a_I H_I) = e^{-N}$. We have seen that our discrepancy in curvature of horizon size happens to be of 10^{28} between now and some very early time. If inflation happened at the earliest time, right around the time of big bang or around Planck time and if the universe we observe is a patch that inflated, then we see that $(a_i H_i)/(a_0 H_0) = e^{-N}(a_I H_I)/(a_0 H_0)$. If $N \sim 62$ then we have the suppression factor of 28 orders of magnitude we were seeking implying that the universe could have had $\mathcal{O}(1)$ curvature or the particle and causal horizon sizes could have been wildly off at the big-bang or Planck scale, but a patch which was causally connected underwent exponential expansion, becoming our observable universe. Thus, we get rid of curvature or horizon issues. The inflating patch would have also pushed out any unwanted relics like monopoles by diluting them away so that even if a phase transition happened, the relics like monopoles would have been pushed out of the horizon. However, this is only possible if the energy scale associated with inflation is lower than that associated with the phase transition producing these leftover relics.

In the next few sections, we look ay dynamical models which can give rise to early universe inflation and we also study the predictions and observables that arise from Inflation. We will also briefly consider the transition from an inflationary phase to a radiation dominated universe. The treatment in this appendix closely follows [186, 185].

B.2 Slow-Roll Inflation

Inflation is a period of exponential expansion. Such an exponentially expanding maximally symmetric space is also called de Sitter space. That is the scale factor increases exponentially, $a(t) = e^{Ht}$ and H is a constant in de Sitter space. Going back to Friedmann equation,

$$H^2 = \frac{8\pi G_N}{3}\rho \tag{B.6}$$

we immediately see that it implies a constant energy density in the universe which doesn't dilute away much like dark energy. An immediate question then arises - if the universe inflated once and that expansion was exponential, how did it ever get out of that phase and transition to a radiation dominated universe? After all, we don't live in an exponentially expanding universe right now.

The most common model for inflation is single-field slow-roll. It consists of one scalar field (this can be easily generalized to multiple fields). We can figure out how the scalar potential behaves using Friedmann equations. First, (B.6) tells us that if H is constant then ρ should be constant. Now, for a scalar field theory with a potential,

$$H = \text{const.} \implies \rho = \frac{\dot{\phi}^2}{2} + V(\phi) = \text{const.} \tag{B.7}$$

The second Friedmann equation for a perfect fluid filling a universe is

$$\frac{\ddot{a}}{a} = -\frac{4\pi G_N}{3}(\rho + 3p)a \tag{B.8}$$

A scalar field theory with a potential behaves like a perfect fluid in a FRW background. This can be most easily seen from the energy-momentum tensor of the theory,

$$\mathcal{T}_{\mu\nu} = \partial_\mu\phi\partial_\nu\phi - g_{\mu\nu}\left(\frac{1}{2}\partial_\alpha\phi\partial^\alpha\phi - V(\phi)\right) \tag{B.9}$$

For FRW, $g_{00} = 1$, $g_{ij} = -a^2\delta_{ij}$ and $g_{0i} = 0$,

$$\mathcal{T}_{00} = \rho = \frac{1}{2}\dot{\phi}^2 + V(\phi), \ \mathcal{T}_{0i} = 0, \ \mathcal{T}_{ij} = -\delta_{ij}\left(\frac{1}{2}\dot{\phi}^2 - V(\phi)\right) \tag{B.10}$$

Thus, the energy-momentum tensor is diagonal and of the form $\mathcal{T}_{\mu\nu} = (\rho, -p, -p, -p)$. And thus, using above $p = \dot{\phi}^2/2 - V(\phi)$. Using these the second friedmann equation (B.8) becomes,

$$\frac{\ddot{a}}{a} = H^2 + \dot{H} = -\frac{8\pi G_N}{3}(\dot{\phi}^2 - V) = -\frac{8\pi G_N}{3}\left(\frac{3}{2}\dot{\phi}^2 - \rho\right) \tag{B.11}$$

Using $\dot{H} = 0$, we immediately see that $\dot{\phi} = 0$ and thus the energy in the field is potential dominated. But we have already seen that this ideal story would cause eternal

inflation and we would like to have an inflationary scenario where we transition out into radiation dominated universe. However, this modification can be easily accommodated in the context of a scalar field's potential energy driven exponential expansion. We consider a scalar field potential that is slowly sloping downwards. The potential is mostly flat and the field starts out somewhere afar on this flattish potential and slowly rolls down with negligible kinetic energy $\dot{\phi}^2$ so that the energy density is potential energy dominated and we get quasi-deSitter expansion. Ultimately the field rolls down to its minima and it typically oscillates about this minima dumping its energy into particle creation. The field driving inflation (called the inflaton) can couple to other SM particles and thus particle production happens at the end of Inflation and we get a plasma of standard model particles and the universe transitions into the radiation dominated era. This phase is called reheating and we will talk about it in detail later.

Consider a scalar field slowly rolling down its potential such that $\dot{\phi}^2 \ll V(\phi)$ and $\ddot{\phi} \ll 3H\dot{\phi}, V'(\phi)$. That is the kinetic energy in the field rolling down the potential hill is really tiny and even its rate of change i.e., $\ddot{\phi}$ is small compared to potential term so that the field continues to move slowly. The equation of motion for the scalar field is

$$\ddot{\phi} + 3H\dot{\phi} + V_{,\phi} = 0 \tag{B.12}$$

In addition using the two Friedmann equations in (B.6) and (B.8), we see that the condition for slow roll is

$$\boxed{\epsilon \equiv -\frac{\dot{H}}{H^2} = \frac{M_p^2}{2}\left(\frac{V_{,\phi}}{V}\right)^2 \ll 1 \quad \& \quad \eta \equiv -\frac{\ddot{\phi}}{H\dot{\phi}} = M_p^2 \frac{V_{,\phi\phi}}{V} \ll 1} \tag{B.13}$$

and $M_p^2 = 1/8\pi G_N$ is the Planck mass. ϵ and η are called the slow-roll parameters and for successful inflation, they should be much smaller than 1.

139
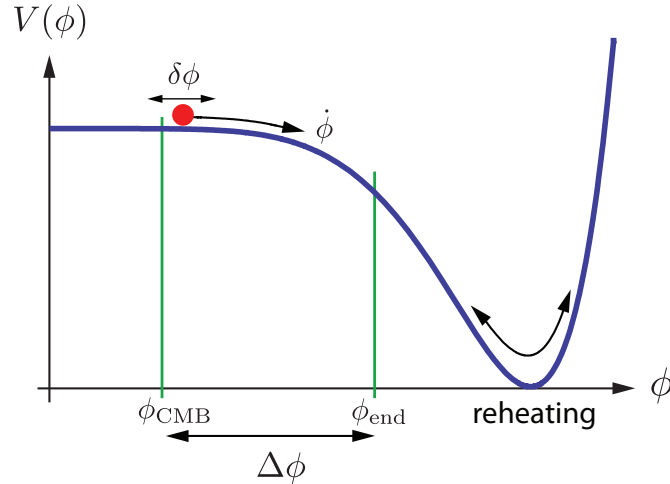
B.3 Observables from Inflation

Inflation solves three important puzzles - horizon, flatness and monopole problem. If that was it, Inflation wouldn't be exciting because many theory can explain puzzles. But a true scientific theory is one that makes reliable predictions which can weighed against existing and future observations. Although inflation is a model-dependent theory which depends not only on the inflaton i.e., the field that drives inflation but also the form of the potential for this field, all models make some generic predictions. In this thesis, we have studied a specific very well motivated model of Inflation driven by the standard model Higgs and there have been tantalizing hints recently that this model might be ruled out based on new observations of tensor perturbations from the early universe. Thus, in this section, we review these predictions from inflation.

We begin by going back to cosmological perturbation theory. During inflation, cosmological perturbations are created as a result of quantum fluctuations in the inflaton field and the background space-time. A slow-rolling scalar field acts like a perfect fluid with its potential energy dominating the energy. There exists two gauge invariant combinations of scalar perturbations in the inflaton and space-time metric. The first one is called the curvature perturbation on uniform density space-like hyper surfaces ζ defined as

$$-\zeta = \psi + \frac{H}{\dot{\rho}^0}\delta\rho \tag{B.14}$$

Its called so because the intrinsic curvature of the hyper surface is $R^{(3)} = 4\nabla^2\psi/a^2$. Under a gauge transformation $\psi \to \psi + (a'/a)\epsilon^0$ and $\delta\rho \to \delta\rho - \rho^{0'}\epsilon^0$ and so this combination is invariant. Similarly, there is another unique gauge invariant combination $\mathcal{R}$ defined as

$$\mathcal{R} = \psi + H\delta u^{ll} \tag{B.15}$$

where $\delta u_i = \partial_i\delta u^{ll} + \delta u_i^\perp$ is the perturbation in velocity field of the scalar fluid. The transformation law for δu^{ll} which is the just the scalar part of the velocity perturbation is $\delta u^{ll} \to \delta u^{ll} - a\epsilon^0$. Geometrically, $\mathcal{R}$ the spatial curvature of comoving (or constant $\delta\phi$) hyper surface. And we can see that because for one scalar perturbation $\delta\phi$ in the problem, we can keep it only in the inflaton (by gauge fixing), $\delta T_i^0 = \dot{\phi}\partial_i\delta\phi = \dot{\phi}^2\partial_i\delta u^{ll} \implies \mathcal{R} = \psi$ if $\delta\phi = 0$. Moreover, it turns out that using linearized Einstein's equations for scalar perturbations in fourier space, we can relate $\mathcal{R}$ and ζ as follows:

$$-\zeta = \mathcal{R} + \frac{k^2}{(aH)^2}\frac{2\rho^0}{3(\rho^0 + p^0)}\Psi \tag{B.16}$$

where $\Psi = \psi + a'(B - E')/a$ is the previously defined gauge invariant Bardeen variable. On scales which are much larger than the horizon which is size $1/(aH)$, $k \ll aH$, we see that $\zeta = -\mathcal{R}$ and this is all we will need because in what follows, we always work in this limit. Moreover, using the perturbation evolution equations, we find

$$\dot{\zeta} = -H\frac{\delta p_{en}}{\rho^0 + p^0} + \frac{k^2}{3a^2H}\left[\zeta - \Psi\left(1 - \frac{2\rho^0}{9(\rho^0 + p^0)}\frac{k^2}{a^2H^2}\right)\right] \tag{B.17}$$

where

$$\delta p_{en} = \delta p - \frac{\dot{p}^0}{\dot{\rho}^0} \delta \rho \tag{B.18}$$

δp_{en} is zero for adiabatic fluctuations i.e., when there is no entropy production, as is the case for single field slow-roll inflaton. And again for super-horizon scales where $k \ll aH$, we get a conservation law - *The curvature perturbation ζ is conserved on super-horizon scales.* This super horizon conservation is the linchpin for inflation generating primordial perturbations.

Although these fluctuations always exist in every field and every background, they typically die down in a time given by Heisenberg's uncertainty relation. However, a background deSitter expansion is different and can create long-lasting fluctuations. This is because fluctuations are created on all length scales - sub horizon ($k \gg aH$) and super horizon ($k \ll aH$). But during inflation they get stretched out (i.e., perturbations of every scale are stretched out by the scale factor) and eventually the sub horizon perturbations become super horizon. When they do so, their evolution stops and they get frozen in time. Another way to look at this non-evolution is to look at the behavior of the coming hubble radius which shrinks during inflation. Thus, the ends of a perturbation can't be in casual contact and so the evolution ceases. After inflation ends, the comoving hubble radius expands again and the perturbations come into the horizon and when they do, they start to evolve again as dictated by Einstein's equations. And these scalar fluctuations form the primordial seeds for inhomogeneities that lead to structure formation as over dense fluctuations that collapse gravitationally give rise to large scale structure of the universe. This behavior is shown in Figure (B.3) below.
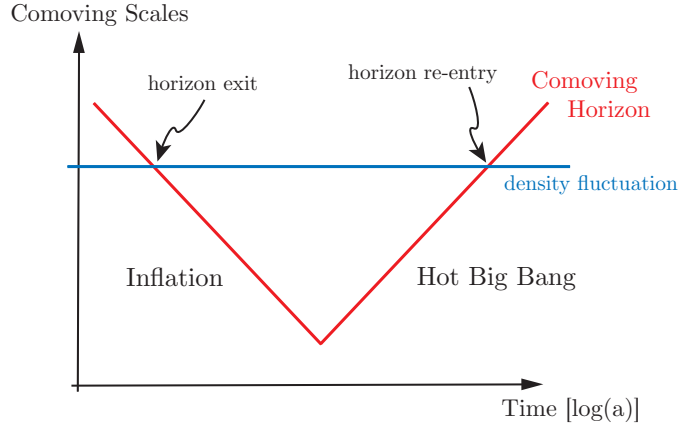
Since these fluctuations are created on all scales, a way to characterize them would be via their statistical properties. The simplest among them is the 2-point correlation function between any two scales k and k'. The fluctuations are inherently quantum mechanical in nature. Thus, for example a statistical measure like $\langle \mathcal{R}_k \mathcal{R}_{k'} \rangle$ is a quantum expectation value $\langle . \rangle$ of the $\mathcal{R}_k$ viewed as a quantum operator acting on its ground state.

Consider a slow-rolling scalar field ϕ in a FRW background. The action for the system is

$$S = \int d^4x \sqrt{-g} \left[R + \frac{1}{2}(\partial_\mu \phi)^2 - V(\phi) \right] \tag{B.19}$$

We consider perturbations about the FRW background. In this case we can characterize the background metric as

$$g_{ij} = a^2 \left[(1 - 2\mathcal{R})\delta_{ij} + h_{ij} \right] dx^i dx^j \tag{B.20}$$

where we have surpassed the vector perturbations (because they die as a^{-2} which is exponentially fast during inflation) and h_{ij} is traverse, traceless part of tensor perturbations. We work in a gauge (called the coming gauge) where there are no perturbations in the inflaton field i.e., $\delta\phi = \delta q = 0$ and $E = 0$. Moreover in this gauge using Einstein's equations we can express Φ and B solely in terms of $\mathcal{R}$ and $\delta\rho$. Using the ADM formalism we expand the action of gravity+inflaton to get a dynamical second order action for $\mathcal{R}$,

$$S_{\mathcal{R}}^{(2)} = \frac{1}{2} \int d^4x \; a^3 \frac{\dot{\phi}^2}{H^2} \left[\dot{\mathcal{R}}^2 - \frac{(\partial_i \mathcal{R})^2}{a^2} \right] \tag{B.21}$$

There exist higher order self-interaction terms which only contribute to the 2-point function for $\mathcal{R}$ at loop level and thus are suppressed. Moreover, they are also inherently suppressed by factors of the slow-roll parameter ϵ and even the 3-point function (contributing to non-gaussianities for example) is also surpassed for canonical slow roll inflation. Thus, one immediate prediction of inflation is small, almost negligible non-gaussianities in the scalar bispectrum. We use this action to compute the 2-point function in fourier space of $\mathcal{R}$ between two modes with different momenta k and k'. There is a subtlety about mode functions to be used in defining the vacuum state. This arises because we are working in a time dependent theory. Using the standard Bunch-Davies vacuum, we arrive at

$$\langle \mathcal{R}_{\mathbf{k}}(t_*)\mathcal{R}_{\mathbf{k}'}(t_*) \rangle = (2\pi)^3 P_{\mathcal{R}}(k)\delta^3(\mathbf{k}+\mathbf{k}') = (2\pi)^3 \delta^3(\mathbf{k}+\mathbf{k}') \frac{H_*^2}{2k^3} \frac{H_*^2}{\dot{\phi}_*^2} \tag{B.22}$$

where the 2-point function is evaluated at a certain time t_* such that $a(T_*)H(t_*) = k$ is the time at which a mode with coming wavenumber k crosses the hubble horizon. That is, we evaluate this 2-point function at a time of horizon crossing since we have already seen that this mode freezes (i.e., doesn't evolve) till it comes back into the horizon after inflation ends. Using $P_{\mathcal{R}}(k)$ we can define a dimensionless 2-point function called the power spectrum as

$$\Delta_{\mathcal{R}}^2(k) \equiv \frac{k^3}{2\pi^2} P_{\mathcal{R}}(k) = \frac{H_*^2}{(2\pi)^2} \frac{H_*^2}{\dot{\phi}_*^2} \tag{B.23}$$

One can immediately observe that this power spectrum is scale-invariant i.e., it doesn't explicitly depend on the wavenumber k. However, since inflation doesn't involve exact de Sitter expansion but rather quasi-deSitter, t_* does depend slightly on k and so the power spectrum is slightly shifted from perfect scale invariance.

In a similar manner, we can quantize tensor perturbations, h_{ij}. The second order action for fluctuations is given as

$$S_h^{(2)} = \frac{M_p^2}{8} \int d\eta d^3x \; a^2 \left[h_{ij}'^2 - (\partial_l h_{ij})^2 \right] \tag{B.24}$$

Here η is the conformal time and $'$ represents a derivative with respect to τ. We expand h_{ij} into fourier modes and using the transverse traceless polarization tensors $(\epsilon_{ii} = k^i \epsilon_{ij} = 0)$, we get two scalars $h_k^s(\eta)$, one for each polarization

$$h_{ij} = \int \frac{d^3k}{(2\pi)^3} \sum_{s=+,\times} \epsilon_{ij}^s(k) h_k^s(\eta) e^{i\mathbf{k}\cdot\mathbf{x}} \tag{B.25}$$

Substituting this back into the action, we get an action for $h_k^s(\eta)$ and thus we can calculate the 2-point function for tensor perturbations and from that extract the dimensionless power spectrum

$$\Delta_h^2(k) = \frac{4}{M_p^2} \left(\frac{H_*}{2\pi} \right)^2 \implies \Delta_t^2(k) = 2\Delta_h^2(k) \frac{2}{\pi^2} \left(\frac{H_*}{M_p} \right)^2 \tag{B.26}$$

where again H_* is evaluated at the time of horizon exit of mode k, i.e., $a(t_*)H_* = k$. The factor of 2 appears because there are two degrees of freedom in the tensor perturbation h_{ij} where each acts as its own scalar in fourier space. The tensor power spectrum also doesn't depend on the scale k explicitly. However, whats more interesting is that (i) inflation predicts a primordial tensor power spectrum and (ii) its scale invariant and only depends on the hubble scale during inflation. But the hubble scale immediately gives us the energy density or the scale of inflation from Friedmann's equation. Thus, the existence of primordial tensor perturbations is a non-trivial and robust (model independent) prediction from inflation that only depends on the energy scale of inflation.

The ratio of tensor-to-scalar power spectra as predicted from any one model is denoted as r and the energy scale of inflation V is related to r,

$$r = \frac{\Delta_t^2(k)}{\Delta_s^2(k)}, \quad V^{1/4} \sim \left(\frac{r}{0.01} \right)^{1/4} \times 10^{16} \text{ GeV} \tag{B.27}$$

Using the definition of the slow-roll parameter ϵ we can re-write $\Delta_s^2(k)$ as follows:

$$\Delta_s^2(k) = \Delta_{\mathcal{R}}^2(k) = \frac{1}{8\pi^2} \frac{H^2}{M_p^2} \frac{1}{\epsilon} \bigg|_{k=aH}$$

$$\Delta_t^2(k) = 2\Delta_h^2(k) = \frac{2}{\pi^2} \frac{H^2}{M_p^2} \bigg|_{k=aH} \tag{B.28}$$

143

where both H and ϵ are evaluated at horizon crossing. And r is given by

$$r = \frac{\Delta_t^2(k)}{\Delta_s^2(k)} = 16 \left. \epsilon \right|_{k=aH} \tag{B.29}$$

Finally, we also observe that since inflation involves expansion about a quasi deSitter background, the scalar and tensor power spectra aren't exactly scale invariant because the Hubble parameter is time dependent. Their scale dependence is quantified by spectral index,

$$n_s \equiv \frac{d\Delta_s^2}{d\ln k} = 1 + 2\eta_* - 4\epsilon_*$$
$$n_t \equiv \frac{d\Delta_t^2}{d\ln k} = -2\epsilon_* = -\frac{r}{8} \tag{B.30}$$

where again the slow-roll parameters are evaluated at horizon crossing (denoted by subscript *). Any deviation from perfect scale invariance is captured by $n_{s,t} - 1 \neq 0$.

In short, Δ_s^2, Δ_t^2, n_s, n_t and r are the observables predicted from inflation. They are evaluated when a particular mode crosses the horizon during inflation and freezes in thereafter (stops evolving). The mode comes back into the horizon during radiation domination and starts evolving according to Einstein's equations. Thus, inflation gives us a mechanism for generating primordial perturbations - as quantum fluctuations expanded to macroscopic scales. It 'stores' them by stretching them out to macroscopic scales and freezing them in. These primordial perturbations form the initial seeds of structure formation and give rise to all the matter over and under densities we see across the sky today in the form of large scale structure. Moreover, inflation generically predicts scale invariance of these matter densities on three largest scales, i.e., a very uniform sky with small inhomogeneities. And this is exactly what is observed in the CMB.

APPENDIX C

AXIONS

A relativistic quantum field theory is invariant under the combined set of discrete transformations - CPT. That is if we change all particles to anti-particles (C), flip all the coordinate system like a mirror would (P) and run the clock backwards (T) all the interactions and thus the dynamics of the theory would look exactly the same. So although the theory is allowed at least in principle to violate any combination of these transformations but not all three at once.

The Standard Model contains various sources of CP violation (which is the same as violation of T symmetry by CPT theorem). In the quark sector, there are non-removable phases in the CKM quark flavor mixing-matrix. This source of CP violation has been observed (which explains the observed CP violation in Kaons & B mesons). Similarly, in the lepton sector, neutrino flavor oscillations have been observed and they contain an unremovable phase that is the source of CP violation. However, both of these are violations caused by weak interactions. It turns out that the strong interactions have their own source of large CP violation but unlike those caused by weak force, these haven't been observed. In trying to understand this puzzle, we will come across a novel solution to the problem that posits the existence of a new light pseudo scalar particle called the axion. These axions could be cosmologically created in the early universe and could contribute to anisotropic stress, thus affecting propagation of primordial gravitational waves (tensor perturbations).

C.1   Introduction to the Strong-CP Problem

Consider a simple version of QCD with only two quark flavors, u and d [187]. In the limit that the quark masses $m_{u,d} \to 0$, the lagrangian has a $U(2)_L \times U(2)_R$ symmetry which is equivalent to $SU(2)_L \times SU(2)_R \times U(1)_V \times U(1)_A$. $SU(2)_L \times SU(2)_R$ is the chiral symmetry of QCD in the limit of vanishing quark masses. The $U(1)_V$ symmetry leads to the conservation of the quark current,

$$J_\mu^B = \bar{u}\gamma_\mu u + \bar{d}\gamma_\mu d \tag{C.1}$$

which physically manifests itself via baryon number conservation. On the other hand, the axial current $U(1)_A$ leads to the axial gauge invariant current,

$$J_\mu^5 = \bar{u}\gamma_\mu\gamma_5 u + \bar{d}\gamma_\mu\gamma_5 d \tag{C.2}$$

that doesn't correspond to any observed symmetry in hadrons. It is known that this theory with massless quarks has undergoes spontaneous symmetry breaking called chiral symmetry breaking when the quark doublet $\langle \bar{q}q \rangle \neq 0$ acquires a vacuum expectation value. The gauge group $SU(2)_l \times SU(2)_R$ breaks to $SU(2)$ of isospin. In the process, we get three broken generators that give rise to three goldstone bosons called the pions. Since the axial symmetry isn't realized in any interactions it is possible that the axial current also spontaneously breaks and leads to another goldstone boson. In the limit the quarks are massless, we expect all these goldstone modes to be massless. However, small quark masses explicitly break this symmetry and so pions are actually pseudo-goldstone bosons and are thus massive. For our $U(1)_A$ current then, we might expect the same fate - a pseudo scalar meson state with mass

comparable to pions. In fact such a pseudoscalar meson with the correct quantum number exists, called the η meson. Weinberg first calculated the relationship between masses as $m_\eta \leq \sqrt{3}m_\pi$. However, experimentally this bound is strongly violated, the η meson can't be the pseudoscalar from $U(1)_A$ breaking because it is too heavy. This problem was first dubbed by Weinberg as the $U(1)$ problem and it is also sometimes called the η-mass problem.

On first glance, this doesn't appear to be a problem in the standard model. This is because we already know that in QCD, the $U(1)_A$ current is anomalous even in the absence of quark masses. That is, although the action may be classically invariant under the transformation, its current conservation is violated by quantum loop effects. This is the famous Adler-Bell-Jackiw (ABJ) chiral anomaly. The general expression of the anomaly with N_f flavors is

$$\partial^\mu J_\mu^5 = 2N_f \frac{1}{16\pi^2}\text{Tr}(G_{\mu\nu}\tilde{G}^{\mu\nu}) + 2im_u\bar{u}\gamma^5 u + 2im_d\bar{d}\gamma^5 d \tag{C.3}$$

where $\tilde{G}^{\mu\nu}$ is the dual of $G^{\mu\nu}$. Thus, in the limit $m_{u,d} \to 0$, we see that the axial current is anomalous. However, it turns out that there still exists a conserved current. To derive it, first note that the right hand side can be written as a total divergence,

$$\partial^\mu K_\mu = 2N_f \frac{g^2}{16\pi^2}\text{Tr}(G_{\mu\nu}\tilde{G}^{\mu\nu}) \text{ where } K_\mu = 2N_f \frac{g^2}{16\pi^2}\epsilon_{\mu\nu\lambda\rho}\text{Tr}(G^{\nu\lambda}A^\rho) \tag{C.4}$$

And thus, $\tilde{J}_\mu^5 = J_\mu^5 - K_\mu$ is still conserved in the limit $m_{u,d} \to 0$ and there exists a conserved charge $\tilde{Q}_5 = \int \tilde{J}_0^5 d^3x$. However, $\tilde{J}_\mu^5$ and thus $\tilde{Q}_5$ are not gauge invariant. Nevertheless, it can be shown (Weinberg) using current-algebra techniques that there still should exist a pseudo-goldstone mode satisfying $m_\eta \leq \sqrt{3}m_\pi$. Thus, the fact that $U(1)_A$ is anomalous doesn't resolve the puzzle.

Before moving on to the resolution of the $U(1)_A$ puzzle, we first look at the structure of the vacuum for a non-abelian gauge theory like QCD. In QFT, vacuum is defined as the state of lowest possible energy, which is an integral of the hamiltonian density over all space. In the case of a non-abelian gauge field, we know that there are an infinite number of gauge field configurations which are equivalent physically. Specifically, under a gauge transformation (U), the gauge field transforms non-linearly as

$$A'_\mu = U^{-1}A_\mu U - \frac{i}{g}U^{-1}\partial_\mu U, \ A_\mu = t^a A_\mu^a \tag{C.5}$$

Vacuum being the lowest energy configuration requires that $G_{\mu\nu} = 0$. This means that field configurations be static and the gluon field A_μ be a pure gauge. It turns out that these various gauge field configurations can be labeled by an integer n called the winding number. This is because the gauge field which is now made entirely of the gauge transformation U now represents a mapping between the three sphere S^3 to the gauge group G and such mappings form a homotopy class where they can be uniformly deformed into one another. Each such mapping is labeled by n which

denotes how many times the mapping winds around the gauge group for each winding around S^3. The winding number n is a topological invariant given by

$$n = \frac{g^2}{16\pi^2} \int d^4x \ \text{Tr}(G_{\mu\nu}\tilde{G}_{\mu\nu}) = \frac{1}{2N_f} \int d^4x \ \partial_\mu K^\mu = \frac{1}{2N_f} \int d^3x \ K^0 \qquad \text{(C.6)}$$

where K^μ is given in Eqn (C.4) above. And so, we have an infinite number of vacuum states each labeled by its own integer $|n\rangle$. The true gauge-invariant vacuum state, denoted by $|\Theta\rangle$ is given by the coherent superposition,

$$|\Theta\rangle = \sum_n e^{-in\Theta} |n\rangle \qquad \text{(C.7)}$$

and this vacuum state is called the 'Θ-vacuum' [187]. These vacua with different winding numbers are separated by an energy barrier. A solution of field equations that interpolates between these vacua is called the instanton solution. It is a solution to the euclidean equation of motion of the gauge field and the corresponding euclidean action evaluated at this solution gives the tunneling probability at zero temperature between various vacua. Finite temperature effects can be incorporated easily using the finite temperature euclidean action.

In the path-integral formalism, we calculate the transition amplitude from vacuum-to-vacuum states. However, for a non-abelian gauge theory like QCD, this means having to sum over all possible initial and vacuum states with different winding numbers. It can be shown that this is equivalent to calculating usual Feynman rules from the ordinary path-integral but modifying the lagrangian by the following term,

$$\mathcal{L}_{QCD} \supset \Theta \frac{g^2}{16\pi^2}\text{Tr}(G_{\mu\nu}\tilde{G}^{\mu\nu}) \qquad \text{(C.8)}$$

What has all this got to do with the $U(1)_A$ problem? It turns out that under a gauge transformation labeled by the winding number n, the conserved gauge variant charge $\tilde{Q}_5$ transforms as $\tilde{Q}_5 \to \tilde{Q}_5 + 2N_f$. And so its effect on the gauge-invariant Θ-vacuum is,

$$e^{-i\alpha\tilde{Q}_5} |\Theta\rangle = |\Theta + 2\alpha N_f\rangle \qquad \text{(C.9)}$$

The non-gauge invariant but conserved current $\tilde{Q}_5$ transforms between disconnected vacua. And thus its presence simply means that the theory is invariant under transformation between vacuum states $|\Theta\rangle \to |\Theta'\rangle$. Choosing a specific Θ is like choosing a vacuum state i.e, the Θ-term spontaneously breaks the axial symmetry, $U(1)_A$. However unlike usual spontaneously broken theories with global symmetries, goldstone's theorem doesn't apply. This is because Θ is just a parameter of the lagrangian and different Θ correspond to different theories each with its own Hilbert space. Thus, by choosing one among infinitely many such theories, we are choosing a theory, not a field direction in one theory. There is no gapless mode and thus (when quark masses are turned on), no η or $U(1)_A$ problem.

Although the rich vacuum structure of QCD resolves the $U(1)_A$ problem, it gives rise to another big problem - CP violation! The Θ term is CP-odd and leads to a violation of CP in the strong sector. We can't set by hand $\Theta = 0$ because it would be generated radiatively. On the other hand, we can't impose CP invariance on the full lagrangian either, because we know that electroweak interactions that give mass to the quarks, violate CP. The Cabbibo-Kobayashi-Maskawa (CKM) matrix which mixes quark flavor and mass eigenstates has imaginary couplings. As we will see later in our study of baryogenesis, imaginary couplings in a lagrangian that can't be rotated away by field redefinitions violate CP invariance.

As we saw above, for massless quarks, a chiral transformation can take one Θ vacuum into another and thus it is possible to choose a specific rotation so that $\Theta = 0$. However, the quarks aren't massless and their mass mixing matrix, arising from the Yukawa couplings of quarks to higgs is in general complex. Because the weak interactions treat left and right handed quarks differently, transforming to mass eigenstates, on encounters a net $U(1)$ axial rotation which changes the Θ term (ϕ_L and ϕ_R are the phases of the rotation of the quart fields to mass eigenstates),

$$\Theta \to \bar{\Theta} = \Theta + 2N_f(\phi_L - \phi_R) = \Theta + \text{Arg}[\det M] \qquad (C.10)$$

where M is the original non-diagonal mass matrix for quarks. These two contributions are from widely different sources (QCD vacuum structure and weak mixing matrix) and in general we have no reason to expect they would cancel. And thus, the strong sector seems to have a residual source of CP violation. So, do we observe this violation experimentally?

One important consequence of the presence of the Θ-term is that it leads to an electric dipole moment (edm) for the neutron. EDM is calculated as an expectation value of the following operator,

$$\mathcal{O}_{EDM} = d_n \frac{i}{2} \bar{\psi} \sigma^{\mu\nu} \gamma^5 \psi \mathcal{F}_{\mu\nu} \qquad (C.11)$$

where ψ is the fermion field (here the neutron). In the non-relativistic limit, this operator reduces to

$$\text{NR}(\mathcal{O}_{EDM}) = -d_n(\vec{S}_N \cdot \vec{E}) \qquad (C.12)$$

and we know that the interaction hamiltonian for an object that carries a dipole moment, in the presence of an electric field is $-\vec{p} \cdot \vec{E}$. Since the only vectors that a quantum particle carries is spin and momenta, in the rest frame the dipole moment has to be proportional to spin. The EDM induced by the Θ-term can be calculated

$$4 \times 10^{-17} \bar{\Theta} \text{ e.cm.} < d_n < 2 \times 10^{-15} \bar{\Theta} \text{ e.cm.} \qquad (C.13)$$

which about 10 orders of magnitude larger than the present experimental limits of $|d_n| < 2.9 \times 10^{-26}$ e.cm [113]. Therefore,

$$\bar{\Theta} = \Theta + \text{Arg}[\det M] < 10^{-10} \qquad (C.14)$$

The strong CP problem is why Θ is so small and not $O(1)$. Peccei and Quinn proposed an ingenious solution to the strong CP problem which dynamically drives Θ to zero.

C.2 Peccei-Quinn Solution to Strong CP - Axions

Peccei and Quinn (PQ) [188, 189] realized that if the SM has another chiral global $U(1)$ symmetry, under which the left and right handed quarks are charged differently, this chiral symmetry would also be anomalously broken by quantum effects like $U(1)_A$. Maybe the effects of this broken global symmetry and the original axial SM symmetry could conspire to cancel the Θ term? Imposing an extra global $U(1)$ to the SM requires introduction of an extra complex scalar field charged under this new $U(1)_{PQ}$. When this field acquires a vacuum expectation value (vev), the PQ symmetry is spontaneously broken and we get a massless goldstone mode, dubbed the axion. However, since like $U(1)_A$, the $U(1)_{PQ}$ symmetry also suffers from the chiral anomaly, the axion isn't truly massless, but acquires a small mass. The chiral nature of the symmetry will introduce an anomaly term like Θ_{QCD}, given by

$$\mathcal{L}_{PQ} = \frac{a}{f_a} \xi \frac{g^2}{32\pi^2} G^a_{\mu\nu} \tilde{G}^{\mu\nu}_a \tag{C.15}$$

where $a(x)$ is now the axion field. Combined with the Θ term of QCD, this induces a tadpole for the axion, giving it a vev,

$$\langle a \rangle = \langle \bar{\Theta} | a | \bar{\Theta} \rangle = -\frac{\bar{\Theta}}{\xi} f_a \tag{C.16}$$

The physical excitation then is about this vev $a_{phys} = a - \langle a \rangle$ and thus the physical axion field eliminates the unwanted $\bar{\Theta}$ term driving it to zero, but trading in its place a spontaneously broken global symmetry giving rise to a physical pseudoscalar, CP conserving field called the axion which interacts via the anomaly term.

$$\mathcal{L}_a \supset \frac{1}{2}(\partial_\mu a_{phys})(\partial^\mu a_{phys}) + \frac{\xi a_{phys}}{f_a}\frac{g^2}{32\pi^2}G^a_{\mu\nu}\tilde{G}^{\mu\nu}_a \tag{C.17}$$

Since the axion is the NG boson of the global $U(1)_{PQ}$, it is derivatively coupled to itself and the SM fermions. For example, its effective interactions with nucleons, electrons and photons are

$$\mathcal{L}_{a,int} = \sum_{\psi=e,N} i\frac{g_{a\psi\psi}}{2m_N}\partial_\mu a(\bar{\psi}\gamma^\mu\gamma^5\psi) - \frac{g_{a\gamma\gamma}}{4}a(F_{\mu\nu}\tilde{F}^{\mu\nu}) \tag{C.18}$$

The coupling constants in these interaction terms are all inversely proportional to f_{PQ}, the Peccei-Quinn breaking scale, which is a completely free parameter in the PQ theory. Each of these interactions of the axion thus give us an independent way to probe the PQ scale from astrophysics.

The $\gamma + \gamma \rightarrow a$ process is called the Primakoff process and observations from the Sun - solar age, helioseismology and the solar neutrino flux all constrain $g_{a\gamma\gamma}$ independently. The CERN Solar Axion Telescope has looked for axions from the sun and has come with the most stringent limit (which is almost similar to that from solar neutrino flux) of $g_{a\gamma\gamma} \lesssim 1.16 \times 10^{-10}$ GeV. The axion electron interaction, on the

other hand affects the He ignition rate for RGB stars and also changes the cooling rate of White Dwarfs. Through these observations, the most stringent constraints are $g_{aee} < 3 \times 10^{-13}$. Finally, the interaction between nucleons and axions was very well constrained by the observations of supernova $1987A$ because the interaction leads to a new energy-loss mechanism for the supernova which gives a characteristic late-time signal of reduced neutrino burst duration. The overall best constraint on f_{PQ} from the various astrophysical searches comes from the supernova, $f_{PQ} \gtrsim 10^{10}$GeV.

Axions acquire a tiny mass due to the chiral axial and PQ anomalies, via mixing with the η and π^0 mesons. This mass has only one unknown parameter - the PQ scale, f_{PQ} and can be derived using chiral perturbation theory. Thus, knowing the symmetry breaking scale immediately tells us the mass of the axion,

$$m_a = \frac{\sqrt{m_u m_d}}{m_u + m_d} \frac{f_\pi m_\pi}{f_{PQ}} \sim \frac{\Lambda_{QCD}^2}{f_{PQ}} \simeq 6.3\text{eV} \left(\frac{10^6 \text{GeV}}{f_{PQ}} \right) \tag{C.19}$$

C.3 Axion Cosmology

Axions are phenomenologically interesting in cosmology because (i) their properties like f_{PQ} can be effectively probed and (ii) they are an ideal candidate for WIMP (Weakly Interacting Massive Particle) Dark Matter. In this thesis, we study a new cosmological signature of axions - their effect on primordial tensor perturbations.

Axions are also theoretically interesting in the cosmological context [190]. The cosmological history of axions begins with Peccei-Quinn breaking at energy scale f_{PQ}. The PQ symmetry is a global $U(1)$ symmetry and can be broken by a complex scalar field $\vec{\phi}$ with a potential,

$$V_{PQ} = \lambda \left(|\vec{\phi}|^2 - f_{PQ}^2/2 \right)^2 \tag{C.20}$$

The minima of the classical potential leaves the angular degree of freedom, i.e., the argument of $\langle \vec{\phi} \rangle$ undetermined and this is the goldstone boson of the symmetry breaking called the axion. As the universe cools, the axion remains massless. It acquires a mass around the QCD scale, $\Lambda_{QCD} \sim 200$MeV because of instanton effects, i.e., mixing with other QCD mesons as indicated above. Thus, between f_{PQ} and Λ_{QCD} the axion remains roughly massless after which it has a small mass. The temperature dependence of the axion mass is given by

$$m_a(T) = 0.1 m_a(T = 0) \left(\frac{\Lambda_{QCD}}{T} \right)^{3.7} \tag{C.21}$$

The axion self-interaction potential has to be computed using effective potential techniques that takes into account non-perturbative QCD. Since the axion couples to the topological charge, approximate analytical formula can be derived form the path integral using an approximation of QCD background made up of a dilute gas of instantons. The result is a periodic axion potential, a result that holds up well under Monte-Carlo simulations of the path integral,

$$V_{eff}(a) \supset m_a^2 f_{PQ}^2 [1 - \cos(a/f_{PQ})] \tag{C.22}$$

151

This potential above and the time (temperature and time can be exchanged using the scale factor in cosmology) dependence of axion mass in (C.21) are sufficient to analyze the cosmology of the axion.

If they exist, axions would be produced in the universe through three primary mechanisms -

- Thermal Axions
  We have seen that axions interact with quarks, gluons, electrons and photons. The decoupling or freeze-out temperature for axions thermally produced in the early universe via axion-quark-gluon interaction is given as

$$T_D = 5 \times 10^{11} \text{GeV} \left(\frac{f_a}{10^{12} \text{GeV}} \right)^2 \qquad \text{(C.23)}$$

  This is valid if the reheat temperature is above T_D. Otherwise inflation would wipe out this population of axions. But they can also be produced effectively, below Λ_{QCD} though pion-axion conversion, $\pi + N \rightarrow N + a$ or photo-production $\gamma + Q \rightarrow Q + a$ or the photon could also be a gluon or a Z-boson and the quark could be a lepton. The decoupling temperature for such process is

$$T_D \sim 2 \times 10^7 \text{GeV} \left(\frac{f_a}{10^{12} \text{GeV}} \right)^2 \qquad \text{(C.24)}$$

  All these interactions help thermalize axions in the early universe and when these reactions become inefficient, axions decouple and freeze out. Thus, either way we get a thermal relic of axions with a number density today which is

$$n_a(t_0) = 7.5 \text{cm}^{-3} \left(\frac{106.75}{N_D} \right) \qquad \text{(C.25)}$$

  where N_D is the number of relativistic species in the plasma at the time of axion decoupling. The axions produced thermally don't have enough energy to close the universe because their mass would have to be $\mathcal{O}(50\text{eV})$, which is already excluded.

- Θ-misalignment production
  The axion vev gives a CP conserving value of $\Theta = 0$ today. However, there is no reason to expect that in the early hot universe, this was the value of Θ. The axion mass comes form instanton processes and at high temperature, it is basically massless. Initially, it could be misaligned from the correct value of zero, instead stochastically set to some non-zero value after the PQ phase transition. If PQ happened after inflation, Θ would vary spatially and we could have domains in the universe where it is different from the value in our local patch.

  After the mass turns on, the axion field rolls down its potential (around the minima it is simply a quadratic potential because of mass) and oscillates. However, because of the time varying mass, the oscillations don't die down and the

axion forms a condensate i.e., cold coherent zero-momentum modes. This condensate of axions is highly non-thermal and interactions previously discussed can't thermalize these axions. This production mechanism of cold axions which can carry significant energy density makes them an ideal candidate for cold dark matter.

The equation of motion for the axion with temperature (or time) varying mass and close to its minima $\Theta = 0$ is [190],

$$\ddot{\Theta} + 3H\dot{\Theta} + m_a^2(T)\Theta = 0 \tag{C.26}$$

where we have traded the axion field a for the misalignment angle $\Theta = a/f_{PQ}$. At high temperatures when $T \gg \Lambda_{QCD}$, $m_a \approx 0$ and the solution is $\Theta = $ const. Once the mass becomes comparable to the Hubble term, the field starts to roll towards its minima. Under assumption of adiabatic evolution i.e., axion mass and hubble rate don't change much in one oscillation, it is easy to show that

$$\rho_a \propto \frac{m_a}{a^3} \tag{C.27}$$

where a is the scale factor. If T is the temperature when the axion density reaches this behavior, then the cosmological axion density created via this misalignment mechanism is given as

$$\Omega_a \approx 1.52 \left(\frac{f_{PQ}}{10^{12}\text{GeV}}\right)^{7/6} \left(\frac{\Theta_i}{\pi}\right)^2 \tag{C.28}$$

where Θ_i is the initial value of the misalignment angle. If PQ phase transition happens after Inflation, Θ_i would take on different values in different patches of the universe and we use the average values of $\langle\Theta_i^2\rangle$ in the range $[-\pi, \pi]$ and we get,

$$\Omega_a \approx 0.65 \left(\frac{f_{PQ}}{10^{12}\text{GeV}}\right)^{7/6} \tag{C.29}$$

If this density isn't to over-close the universe, the PQ scale has an upper bound,

$$f_{PQ} \leq 2.8 \times 10^{11}\text{GeV} \implies m_a \geq 21\mu eV \tag{C.30}$$

- Axions from PQ strings
  If the Peccei-Quinn symmetry breaks after Inflation, we will get topological defects like strings. This is because PQ is a $U(1)$ symmetry and the first homotopy group of $U(1)$, as in the group formed by mappings from $U(1)$ which has a topology of a circle to S^1 in space is non-trivial. For example we could go around the gauge group n times for every time we go around a circle in physical space. That is $\pi_1(G) = \mathcal{Z}_n$ where $G = U(1)$ and $\mathcal{Z}_n$ is the group of integers. In other words, we can have topological defects which can be enclosed by a circle

and go through entire space being infinite in extent - called topological strings. Essentially, these strings are peculiar field configurations that can arise as a result of the phase transition and which can't relax their energy because it is topologically impossible for them to do so.

However, it is possible for strings to loose energy through their own dynamics via gravitational radiation and emission of goldstone bosons of the symmetry. That is, the PQ strings formed after the phase transition will radiate axions and this is a novel new source of them. In fact, we will see that this can be the dominant source of the axion population in the universe. This is only true if PQ happens after inflation because inflation would wipe out any relic axions, if PQ happens before it.The spectrum of axions produced via this mechanism is again non-thermal but unlike those produced by misalignment mechanism, these axions can be relativistic and also have comparable energy density to the condensate produced by the misalignment mechanism.

We begin with the energy/length (μ) in a string, which is the hamiltonian for the PQ complex scalar evaluated on the string solution - a static field configuration which wraps around S^1 with a winding number n,

$$\phi = \eta e^{in\theta} \implies \mu = \int \left[(\partial\phi)^2 + \frac{\phi^2}{r^2} + V(\phi) \right] r dr \ d\phi \tag{C.31}$$

where $V(\phi)$ is the symmetry breaking potential and the field ϕ behaves like r inside the string and goes to f_{PQ} exponentially outside.

$$\mu = 2\pi f_{PQ}^2 \log\left(\frac{t}{\delta}\right) \tag{C.32}$$

where δ is the width of the string core and t is a long distance cut-off to make the energy finite. Davis' [191] derivation of the energy density in the axions radiated from PQ strings follows from the above formula. He considers t to be the length of size of cells the universe is divided into. He works in a radiation-dominated universe whose age is also t and he considers one string per length t cell. By computing the expansion of the cell in this universe and taking the difference in energies of the string to be exclusively lost as radiation in axions (they are radiated most effectively when kinks appear in strings as the universe expands), he is able to derive an expression for the energy density in them. This work also considered the effect of an axion mass turning on. The final result derived by Davis is

$$\rho_a(t) = \frac{4\pi f_{PQ}^2}{t^2} \int_{\Omega^{2/3}/\tilde{t}}^{\Omega^{5/6}/\sqrt{t*\tilde{t}}} \left(\frac{k^2 + (t/\tilde{t})m_a^2}{k^2 + \tilde{m}^2}\right)^{1/2} \left[\log\left(\frac{\Omega^{5/3}}{\tilde{t}k^2\delta}\right) - \frac{1}{2}\right] \frac{dk}{k} \tag{C.33}$$

where $\Omega = 2\pi$, $\tilde{t}$ is the time when the axion wavelength of a mode comes within the horizon and the axion mass at that time is $\tilde{m} = 1/\tilde{t}$. This is because

154

for times around $\tilde{t}$, the mass of the axion can be written approximately as $m(t) = t^2/\tilde{t}^3$ and $\delta = 1/f_{PQ}$. We will utilize this energy density to extract a distribution function and calculate the effect axions have on propagation of primordial tensor perturbations. Finally, for the energy-density in this kind of axions to not over-close the universe implies a bound on f_{PQ},

$$\rho_a < \rho_{cr} \implies f_{PQ} \lesssim 3 \times 10^{11} \text{GeV} \tag{C.34}$$

which is a bound similar to the one we derived from the axion energy density produced by the misalignment mechanism. Combining energy density from all sources and the astrophysical constraints (stingiest of which comes form supernova 1987A), we get that f_{PQ} can lie in a narrow window,

$$10^{10} \text{GeV} \lesssim f_{PQ} \lesssim 10^{11} \text{GeV} \tag{C.35}$$

which is a remarkably tight bound coming only from astrophysical and cosmological sources and no direct searches. There is some wiggle room in these, if for example the model for star cooling or supernova neutrino emission duration get theoretical corrections. But nonetheless it is expected to not change the bounds on the PQ scale, f_{PQ} much.

APPENDIX D

EFFECTIVE POTENTIAL

The effective potential is a very useful tool to study quantum effects in a theory by directly incorporating them as extra terms in the potential of the theory. That is we continue to view the theory with its classical lagrangian but with quantum effects that change the potential with terms proportional to powers of $\hbar$. The quantum loop effects get incorporated into the modified potential and thus when we calculate tree-level scattering from this potential, we have essentially done a loop calculation implicitly. We review the effective potential formalism, closely following [192] and its implicit assumptions below.

Consider a scalar field theory ϕ with the action

$$S[\phi] = \int d^4x \ \mathcal{L}\{\phi(x)\} \tag{D.1}$$

The generating functional in quantum field theory is the vacuum-to-vacuum amplitude given by the path integral in the presence of a source $\mathcal{J}(x)$

$$\mathcal{Z} = \langle 0_{in}|0_{out}\rangle_{\mathcal{J}} \equiv \int \mathcal{D}\phi \ \exp\{i(S[\phi] + \phi\mathcal{J})\}, \ \phi\mathcal{J} \equiv \int d^4x \ \phi(x)\mathcal{J}(x) \tag{D.2}$$

$\mathcal{J}$ is the generator of all diagrams, connected or not. On the other hand, $\mathcal{W}[\mathcal{J}]$, which is the generator of connected diagrams can be derived from $\mathcal{Z}[\mathcal{J}]$,

$$\mathcal{Z}[\mathcal{J}] = \exp\{i\mathcal{W}[\mathcal{J}]\} \tag{D.3}$$

that is functional derivatives of $\mathcal{W}$ with respect to $\mathcal{J}$ evaluated at $\mathcal{J} = 0$ give the expression for connected diagrams in the theory. Finally, the *effective action* $\Gamma[\bar{\phi}]$, which is the generator of 1-PI (1-particle irreducible) diagrams is derived as the legendre transform of $\mathcal{W}[\mathcal{J}]$,

$$\Gamma[\bar{\phi}] = \mathcal{W}[\mathcal{J}] - \int d^4x \frac{\delta\mathcal{W}[\mathcal{J}]}{\delta\mathcal{J}(x)}\mathcal{J}(x) \tag{D.4}$$

where the field $\bar{\phi}(x)$ is defined as

$$\bar{\phi}(x) = \frac{\delta\mathcal{W}[\mathcal{J}]}{\delta\mathcal{J}(x)} \tag{D.5}$$

$\Gamma[\phi]$ is also called the effective action of the theory for reasons that will be clear later. From these definitions it follows taking functional derivatives,

$$\frac{\delta\Gamma[\bar{\phi}]}{\delta\bar{\phi}} = \frac{\delta\mathcal{W}[\mathcal{J}]}{\delta\mathcal{J}}\frac{\delta\mathcal{J}}{\delta\bar{\phi}} - \mathcal{J} - \bar{\phi}\frac{\delta\mathcal{J}}{\delta\bar{\phi}} = -\mathcal{J} \tag{D.6}$$

And thus in the absence of sources $\mathcal{J} = 0$, there exists field configurations (called classical field ϕ_{cl}) such that

$$\left.\frac{\delta\Gamma[\bar{\phi}]}{\delta\bar{\phi}}\right|_{\mathcal{J}=0} = 0 \text{ for } \bar{\phi} = \phi_{cl} \text{ such that } \phi_{cl} = \langle 0|\bar{\phi}(x)|0\rangle_{\mathcal{J}=0} \tag{D.7}$$

and thus ϕ_c defines the true quantum vacuum of the theory because its the minima of the effective action. $\Gamma[\bar{\phi}]$ is the generator of 1-PI diagrams and thus $\Gamma[\bar{\phi}]$ in terms of the field $\bar{\phi}$ we get

$$\Gamma[\bar{\phi}] = \sum_{n=0}^{\infty} \frac{1}{n!} \int d^4x_1 d^4x_2...d^4x_n \; \bar{\phi}(x_1)\bar{\phi}(x_2)...\bar{\phi}(x_n)\Gamma^{(n)}(x_1, x_2..., x_n) \qquad (D.8)$$

where now $\Gamma^{(n)}$ are the one-particle irreducible (1PI) Green functions. Fourier transforming $\Gamma^{(n)}$ and $\bar{\phi}$ as

$$\Gamma^{(n)}(x) = \int \prod_{i=1}^{n} \left[\frac{d^4p_i}{(2\pi)^4}\exp\{ip_ix_i\} \right] (2\pi)^4\delta^{(4)}(p_1 + p_2 + ... + p_n)\Gamma^{(n)}(p)$$

$$\tilde{\phi}(p) = \int d^4x \; e^{-ipx}\bar{\phi}(x) \qquad (D.9)$$

Substituting into $\Gamma[\bar{\phi}]$ we obtain,

$$\Gamma[\bar{\phi}] = \sum_{n=0}^{\infty} \int \prod_{i=1}^{n} \left[\frac{d^4p_i}{(2\pi)^4}\tilde{\phi}(-p_i) \right] (2\pi)^4\delta^{(4)}(p_1 + p_2 + ... + p_n)\Gamma^{(n)}(p) \qquad (D.10)$$

In a theory with translational invariance we expect the true quantum vacuum expectation value of $\phi(x)$ to be translational invariant,

$$\bar{\phi}(x) = \phi_c \qquad (D.11)$$

and thus the effective potential should be a divergent integral over space-time volume of some function of ϕ_c. We call this function the effective potential $V_{eff}(\phi_c)$,

$$\Gamma[\phi_c] = - \int d^4x \; V_{eff}(\phi_c) \qquad (D.12)$$

Similarly, the fourier transform of ϕ_c has a divergent space-time volume,

$$\tilde{\phi}_c(p) = \int d^4x \; \phi_c e^{-ipx} = (2\pi)^4\phi_c\delta^{(4)}(p) \qquad (D.13)$$

Substituting into Eqn. (D.10), we get

$$\Gamma(\phi_c) = \sum_{n=0}^{\infty} \frac{1}{n!}\phi_c^n(2\pi)^4\delta^4(0)\Gamma^{(n)}(p_i = 0) = \sum_{n=0}^{\infty} \frac{1}{n!}\phi_c^n\Gamma^{(n)}(p_i = 0) \int d^4x \qquad (D.14)$$

And thus we get an expression for $V_{eff}(\phi_c)$,

$$\boxed{V_{eff}(\phi_c) = - \sum_{n=0}^{\infty} \frac{1}{n!}\phi_c^n\Gamma^{(n)}(p_i = 0)} \qquad (D.15)$$

This important formula states that the effective potential can be found by calculating the 1-PI connected green's function with the momenta on external legs set to zero. We use this formula to calculate both the tree-level and one loop effective potential for a scalar ϕ^4 theory as an example. This will also clarify the name "effective potential".

D.1 V_{eff} for ϕ^4-theory

Consider a scalar field theory of field ϕ with the lagrangian

$$\mathcal{L} = \frac{1}{2}(\partial_\mu \phi)(\partial^\mu \phi) - \frac{1}{2}m^2\phi^2 - \frac{\lambda}{4!}\phi^4 \tag{D.16}$$

To compute the tree level effective potential, we need to evaluate the 1-PI diagrams with no loops. But this is trivial since there is only one diagram with 4 external legs and one vertex giving the interaction term. The vertex brings a factor of $-i\lambda$ and there is an extra global factor of i from the definition of the generating functional. And thus to the lowest order we just get the classical potential back,

$$V_0(\phi_c) = -\frac{1}{2}m^2\phi_c^2 - \frac{\lambda}{4!}\phi_c^4 \tag{D.17}$$

To compute the effective action up to 1-loop, we consider all 1-PI one loop diagrams with arbitrary number of external legs as shown in FigD.1. Because of the quartic nature of the interaction, a diagram with $2n$ external legs has n vertices and n propagators. The n propagators contribute $i^n(p^2 - m^2 + i\epsilon)^{-n}$. Each vertex contributes $-i\lambda/2$ and there is a global symmetry factor $1/(2n)$ where n comes from the symmetry of the diagram under the discrete group of rotations $\mathbf{Z_n}$ and $1/2$ from the symmetry of the diagram under reflection. Since we evaluate the diagrams with external momenta $p_i = 0$, there is only one momentum in the loop, p which is integrated over. And again there is an extra global factor of i. Thus, the one loop contribution becomes
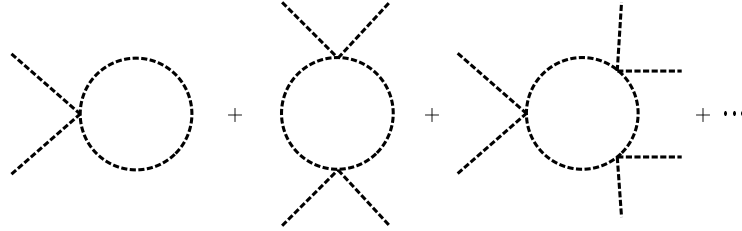
Figure D.1: Diagrams contributing to the effective action in ϕ^4 theory at 1-loop

$$V_1(\phi_c) = i\sum_{n=1}^{\infty} \int \frac{d^4p}{(2\pi)^4} \frac{1}{2n} \left[\frac{\lambda\phi_c^2/2}{p^2 - m^2 + i\epsilon}\right]^n \tag{D.18}$$

We can integrate by Wick rotating first,

$$p^0 = -ip_E^0, \ p_E = (-ip^0, \vec{p}), \ p^2 = (p^0)^2 - \vec{p}^2 = -p_E^2 \tag{D.19}$$

an so the integral becomes

$$V_1(\phi_c) = \frac{1}{2}\int \frac{d^4p_E}{(2\pi)^4} \log\left[1 + \frac{\lambda\phi_c^2/2}{p_E^2 + m^2}\right] \tag{D.20}$$

159

This motivates the definition of the shifted mass, $m(\phi_c)$,

$$m^2(\phi_c) = m^2 + \frac{1}{2}\lambda\phi_c^2 = \frac{d^2V_0(\phi_c)}{d\phi_c^2} \tag{D.21}$$

and in terms of the field dependent mass

$$V_1(\phi_c) = \frac{1}{2}\int\frac{d^4p}{(2\pi)^4}\log[p^2 + m^2(\phi_c)] \tag{D.22}$$

where the field independent term in the logarithm has been neglected because it doesn't change anything and can be absorbed in renormalization. To compute the integral, we first use dimensional regularization and compute a different integral V' which is simply the derivative of V_1 with respect to ϕ_c,

$$V' = \frac{1}{2}(\mu^2)^{2-n/2}\int\frac{d^np}{(2\pi)^n}\frac{1}{p^2 + m^2(\phi_c)} \tag{D.23}$$

The scale μ^2 has been included for correct mass dimensions of V' in $n \neq 4$ dimensions. Using the following identity,

$$\int d^np\frac{(p^2)^\alpha}{(p^2 + M^2)^\beta} = \pi^{n/2}(M^2)^{n/2+\alpha-\beta}\frac{\Gamma(\alpha + n/2)\Gamma(\beta - \alpha - n/2)}{\Gamma(n/2)\Gamma(\beta)} \tag{D.24}$$

we get

$$V_1(\phi_c) = -\frac{1}{32\pi^2}\frac{4}{n(n-2)}\left(\frac{m^2(\phi_c)}{4\pi\mu^2}\right)^{n/2-2}\Gamma\left(2 - \frac{n}{2}\right)m^4(\phi_c) \tag{D.25}$$

Taking the limit $n \to 4$ and using the $\overline{\text{MS}}$ renormalization scheme, we get

$$V_1(\phi_c) = \frac{1}{64\pi^2}m^4(\phi_c)\left\{\log\frac{m^2(\phi_c)}{\mu^2} - \frac{3}{2}\right\} \tag{D.26}$$

where μ is the renormalization scale or equivalently the energy scale at which we evaluate the 1-loop potential and the couplings have to be related by renormalization group flows to this scale. To absorb the divergent counter term

$$-\frac{m^4(\phi_c)}{64\pi^2}\left\{\frac{1}{2 - \frac{n}{2}} - \gamma_E + \log 4\pi\right\} \tag{D.27}$$

from the potential we need renormalization conditions. The typical conditions on renormalized field Z_R, mass m_R and coupling λ_R are (in evaluating the effective potential we keep external momenta zero, so we do the same for the renormalization conditions)

$$\begin{aligned}
m_R^2 = -\Gamma^{(2)}(p=0) &= \left.\frac{d^2V}{d\phi_c^2}\right|_{\phi_c=0} \\
\lambda_R = -\Gamma^{(4)}(p=0) &= \left.\frac{d^4V}{d\phi_c^4}\right|_{\phi_c=0} \\
Z_R &= 1
\end{aligned} \tag{D.28}$$

The second equity for m_R and λ_R follows from the fact that the effective action is the generator of 1-PI connected diagrams and at one loop the 1PI diagram with two external legs is the diagram that renormalizes mass and the one with four external legs renormalizes the coupling constant. So, the divergent counterterms in mass and coupling constant become

$$
\begin{aligned}
\delta m^2 &= 0 \\
\delta \lambda &= \frac{3\lambda^2}{32\pi^2} \left\{ \frac{1}{2 - \frac{n}{2}} - \gamma_E + \log 4\pi \right\}
\end{aligned}
\tag{D.29}
$$

Finally, the 1-loop effective potential i ϕ^4 theory becomes

$$
V_{eff}(\phi_c) = \frac{1}{2} m^2 \phi_c^2 + \frac{\lambda}{4!} m^2 \phi_c^4 + \frac{\lambda^2 \phi_c^4}{256\pi^2} \log \left(\frac{\lambda \phi_c^2}{2\mu^2} - \frac{3}{2} \right)
\tag{D.30}
$$

The higher loop function can be similarly computed. However, this process is quite cumbersome because an infinite number of Feynman diagrams need to be computed. There is however another method for deriving a general expression for the effective action by shifting the field about the classical field ϕ_c and using the shifted action to compute diagrams. We sketch out the method below. Start by defining the lagrangian

$$
\int d^4x \hat{\mathcal{L}}\{\phi_c; \phi(x)\} \equiv S[\phi_c + \phi] - S[\phi_c] - \phi \frac{\delta S[\phi_c]}{\delta \phi_c}
\tag{D.31}
$$

The propagator of the shifted theory is given in terms of the action of $\hat{S} = \int d^4x \hat{\mathcal{L}}$,

$$
i\mathcal{D}^{-1}\{\phi_c; x - y\} = \left. \frac{\delta^2 S[\phi]}{\delta \phi(x) \delta \phi(y)} \right|_{\phi = \phi_c}
\tag{D.32}
$$

and then it can be shown that the effective potential of the original theory is given as

$$
V_{eff}(\phi_c) = V_0(\phi_c) - \frac{i}{2} \int \frac{d^4p}{(2\pi)^4} \log \det i\mathcal{D}^{-1}\{\phi_c; p\} + i \left\langle \exp \left[\int d^4x \hat{\mathcal{L}}_I\{\phi_c; \phi(x)\} \right] \right\rangle
\tag{D.33}
$$

where $\hat{\mathcal{L}}_I$ is the interaction lagrangian of the shifted theory and $i\mathcal{D}^{-1}\{\phi_c; p\}$ is the propagator of Eqn (D.32) in fourier space.

D.2 Renormalization Group Improved Effective Potential

The effective action is the generator of 1PI connected green's functions. And these green's functions are directly to observables. Hence they satisfy the Callan-Symanzik equation which relates all the scale dependence in the green function to scale dependence in coupling constants and field strength.

$$
\left[\mu \frac{\partial}{\partial \mu} + \beta \frac{\partial}{\partial \lambda} - \gamma \phi_c \frac{\delta}{\delta \phi_c} \right] \Gamma[\phi_c] = 0
\tag{D.34}
$$

161

where β is the beta function for the coupling constant λ and γ is the anomalies dimension which gives the running of the field strength renormalization and μ is the scale at which we renormalize. From this it can be shown that

$$\left[\mu\frac{\partial}{\partial\mu} + \beta\frac{\partial}{\partial\lambda} - \gamma\phi_c\frac{\partial}{\partial\phi_c}\right] V_{eff} = 0 \tag{D.35}$$

This equation has a general solution

$$V_{eff}(\mu, \lambda, \phi_c) = V_{eff}(\mu(t), \lambda(t), \phi(t)) \tag{D.36}$$

where they all depend on the RG-flow parameter t,

$$
\begin{aligned}
\mu(t) &= \mu\exp(t) \\
\phi(t) &= \phi_c\xi(t) \\
\xi(t) &= \exp\left\{-\int_0^t \gamma(\lambda(t'))dt'\right\} \\
\beta(\lambda(t)) &= \frac{d\lambda(t)}{dt}
\end{aligned}
\tag{D.37}
$$

β gives the running of the coupling constant λ with respect to RG flow parameter t which is directly related to μ. In particular, we can fix the scale to be a ϕ_c dependent quantity using boundary conditions,

$$\mu(t) = f(\phi_c) \implies t = \log\{f(\phi_c)/\mu\} \tag{D.38}$$

Thus, we see that the solution of the RGE satisfied by V_{eff} implies using renormalized couplings and fields and the scale dependence can be reabsorbed in to RGE running. Fixing the scale, as a function of ϕ_c (i.e. giving different scales for different values of the field) is usually done to optimize the validity of the perturbative expansion, i.e. minimizing the value of radiative corrections to the effective potential around the minimum of the field. A very interesting general result is: *The RGE improved effective potential exact up to (next-to-leading) log order is obtained using the L-loop effective potential and the $(L+1)$-loop RGE β-functions.*

D.3   Standard Model Effective Potential

The Standard Model effective potential is calculated (i) to the one-loop order, (ii) working in the $\overline{\text{MS}}$ renormalization scheme with renormalization scale μ, and (iii) in the renormalizable class of gauges (R_ξ) as follows:

$$V_{\text{eff}}(\phi_c) = V^{(0)}(\phi_c) + V^{(1)}(\phi_c) \tag{D.39}$$

The tree-level potential is

$$V^{(0)}(\phi_c) = -\frac{1}{2}m^2\phi_c^2 + \frac{\lambda}{4}\phi_c^4 \tag{D.40}$$

And the one-loop correction is

$$V^{(1)}(\phi_c) = \sum_{f=t,b,c..} (-1)\frac{n_f}{4}\frac{\tilde{m}_f^4}{16\pi^2}\left(\ln\frac{\tilde{m}_f^2}{\mu^2}-\frac{3}{2}\right) + \frac{6}{4}\frac{\tilde{m}_W^4}{16\pi^2}\left(\ln\frac{\tilde{m}_W^2}{\mu^2}-\frac{5}{6}\right) \tag{D.41}$$

$$+\frac{3}{4}\frac{\tilde{m}_Z^4}{16\pi^2}\left(\ln\frac{\tilde{m}_Z^2}{\mu^2}-\frac{5}{6}\right) + \frac{1}{4}\frac{\tilde{m}_H^4}{16\pi^2}\left(\ln\frac{\tilde{m}_H^2}{\mu^2}-\frac{3}{2}\right) + \frac{1}{4}\frac{\tilde{m}_G^4}{16\pi^2}\left(\ln\frac{\tilde{m}_G^2}{\mu^2}-\frac{3}{2}\right)$$

$$+\frac{2}{4}\frac{\tilde{m}_{G^\pm}^4}{16\pi^2}\left(\ln\frac{\tilde{m}_{G^\pm}^2}{\mu^2}-\frac{3}{2}\right) - \frac{2}{4}\frac{\tilde{m}_{cW}^4}{16\pi^2}\left(\ln\frac{\tilde{m}_{cW}^2}{\mu^2}-\frac{3}{2}\right) - \frac{1}{4}\frac{\tilde{m}_{cZ}^4}{16\pi^2}\left(\ln\frac{\tilde{m}_{cZ}^2}{\mu^2}-\frac{3}{2}\right)$$

The sum over index f runs over all the SM fermion species with $n_f = 12$ for the quarks and $n_f = 4$ for the leptons. The effective masses are

$$
\begin{array}{lc}
\text{Fermions} & \tilde{m}_f^2 = \frac{y_f^2}{2}\phi_c^2 \\
\text{W-Bosons} & \tilde{m}_W^2 = \frac{g^2}{4}\phi_c^2 \\
\text{Z-Bosons} & \tilde{m}_Z^2 = \frac{g^2+g'^2}{4}\phi_c^2 \\
\text{Higgs Boson} & \tilde{m}_H^2 = -m^2 + 3\lambda\phi_c^2 \\
\text{Neutral Goldstones} & \tilde{m}_G^2 = -m^2 + \lambda\phi_c^2 + \tilde{m}_{cZ}^2 \\
\text{Charged Goldstones} & \tilde{m}_{G^\pm}^2 = -m^2 + \lambda\phi_c^2 + \tilde{m}_{cW}^2 \\
\text{Ghosts} & \tilde{m}_{cZ}^2 = \xi_Z\tilde{m}_{cZ}^2 \\
\text{Ghosts} & \tilde{m}_{cW}^2 = \xi_W\tilde{m}_{cW}^2
\end{array}
\tag{D.42}
$$

In writing down $\tilde{m}_f^2 = y_f^2\phi_c^2$ we have neglected mixing the quark mixing matrix which is assumed to be diagonal. One can also use $\tilde{m}_f^2 = m_f^2\phi_c^2/v^2$ where m_f is the fermion mass (eigenvalue of the mass matrix) and $v \simeq 246$ GeV is the Higgs VEV. The remaining Standard Model fields, the massless photon and gluons, do not enter the effective potential at the one-loop order.

In Eq. (D.41) we have distinguished the gauge fixing parameters, ξ_Z and ξ_W, for generality, but typically they are taken to be equal, $\xi_Z = \xi_W = \xi$. The common gauge choices are:

$$
\begin{array}{lc}
\text{Landau gauge} & \xi = 0 \\
\text{Feynman gauge} & \xi = 1 \\
\text{Unitary gauge} & \xi = \infty
\end{array}
\tag{D.43}
$$

Physically, the Goldstone bosons and ghosts decouple in the unitary gauge, but decoupling is not manifest in the $\overline{\text{MS}}$ renormalization scheme. Therefore, to implement the unitary gauge in the effective potential, one simply removes the would-be divergent terms by hand.

The renormalization scale μ should be chosen so as to optimize the validity of the perturbative expansion. At two-loop order, one finds terms of the form

$V^{(2)} \sim \tilde{m}^4 (\ln \tilde{m}^2/\mu^2)^2$ where $\tilde{m}^2$ is one of the field-dependent masses. If μ is chosen poorly, then the logarithm may be large, $\left| \ln \tilde{m}^2/\mu^2 \right| \gg 1$, and higher order terms in the $\hbar$ expansion can become significant. In the Standard Model, because there are multiple would-be large logarithms, it is not possible to find a single t_* at which all of the logarithms are vanishing. We must instead choose to minimize the potentially most dangerous logarithm. The heaviest field is the top quark, and this logarithm is minimized by determining the RG flow parameter t_* by solving

$$\left. \frac{y_t^2 \phi_c(t)^2}{2\mu(t)^2} \right|_{t=t_*} = 1 \implies t_* = \frac{1}{2} \ln \left[\frac{y_t(t_*)^2 e^{2\Gamma(t_*)} \phi_c^2}{2\mu_0^2} \right] \approx \frac{1}{2} \ln \left[\frac{y_0^2 \phi_c^2}{2\mu_0^2} \right] \tag{D.44}$$

where like before $\mu(t) = \mu_0 e^t$. Thus to the leading log order ($L = 1$) the RG-improved effective potential is given by Eqns. (D.39) and (D.41) where each parameter is replaced by the corresponding running parameter and evaluated at $t = t_*$. That is, we replace $\mu \to \mu(t_*)$, $y_f \to y_f(t_*)$. $m^2 \to m^2(t_*)$, $\phi_c \to \phi_c(t_*)$ and so on. To actually evaluate the effective potential, one must specify the scale μ_0 and the values of the parameters, y_{f0} etc., at that scale.

APPENDIX E

BARYOGENESIS

Andrei Sakharov laid out three conditions for successful generation of baryon asymmetry,

- Baryon Number Violation
  If we assume that at the big bang the universe started out with a new baryon number of zero and we see a net baryon asymmetry today, baryon number can't be a conserved symmetry of nature. It must be violated in the theory either in perturbative scattering or non-perturbative processes to create a net baryon asymmetry, $B \neq 0$.

- C & CP violation
  Charge conjugation operator exchanges particles and anti-particles. If this is a symmetry of the theory then the rate for a particle undergoing a process $i \to f$ which creates a baryon asymmetry $B_f - B_i = \Delta B$, there will be an analogous process $\bar{i} \to \bar{f}$ which creates the opposite asymmetry $B_{\bar{f}} - B_{\bar{i}} = -B_f + B_i = -\Delta B$ and thus the universe as a whole remains baryon symmetric. So, charge conjugation C can't be a symmetry of the interactions. Similarly, if the their is time symmetric, then its easy to see that, time averaged there can be no baryon asymmetry either. So the theory has to be asymmetric under time reversal operation i.e, T can't be a symmetry of the theory. But by CPT theorem, we know that non-invariance under T is the same as non-invariance under CP. Thus, for baryogenesis, a theory has be both C and CP violating.

We can illustrate how C and CP violation lead to a baryon asymmetry as follows. Consider a simple model [193] with two heavy bosons X and Y that can decay into two fermions each via the following lagragian,

$$\mathcal{L}_{int} = g_1 X f_2^\dagger f_1 + g_2 X f_4^\dagger f_3 + g_3 Y f_1^\dagger f_3 + g_4 Y f_2^\dagger f_4 + \text{h.c.} \qquad (E.1)$$

where $g_1, ..g_4$ are the coupling constant. The lagrangian can lead to following decays,

$$X \to \bar{f}_1 + f_2, \ \bar{f}_3 + f_4 \qquad (E.2)$$
$$T \to \bar{f}_3 + f_1, \ \bar{f}_4 + f_2 \qquad (E.3)$$
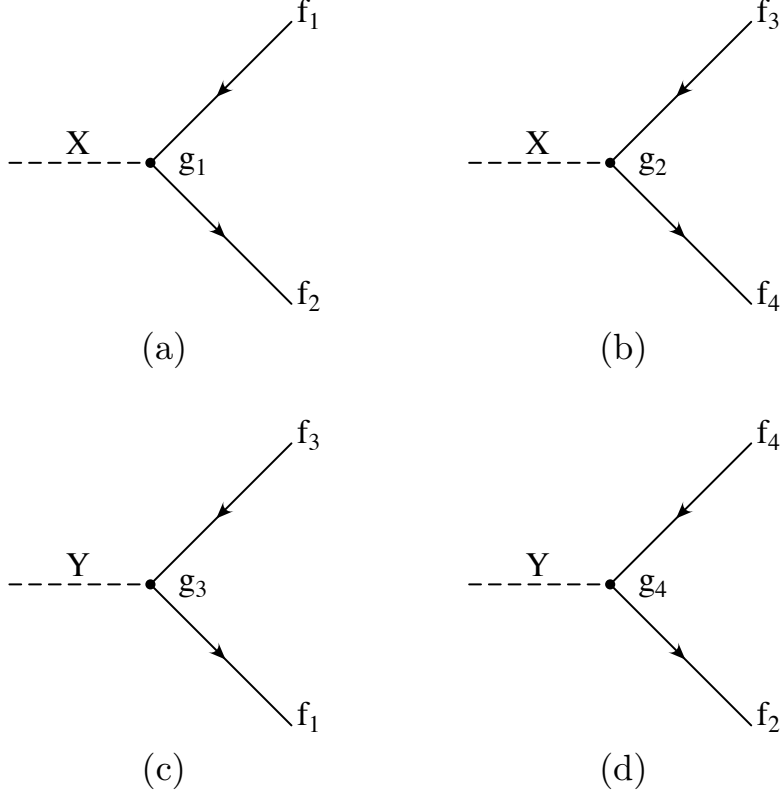
and the tree level diagrams of these decay processes are shown in Fig E.1 At the tree level, the decay rate of $X \to f_1 + f_2$ is proportional to $|g_1|^2$,

$$\Gamma(X \to \bar{f}_1 + f_2) = |g_1|^2 I_X \qquad (E.4)$$

where I_X is the phase space factor. For the conjugate process $\bar{X} \to f_1 + \bar{f}_2$, the decay rate is,

$$\Gamma(f_1 + \bar{f}_2) = |g_1^*|^2 I_{\bar{X}} \qquad (E.5)$$

At the tree level, no asymmetry is created because the phase space factors I_X and $I_{\bar{X}}$ are equal. However, at the one loop level, there are more diagrams via

Figure E.1: Tree level diagrams for the decays of the heavy scalar fields, X and Y.

loop process as shown in Fig E.2. The 1-loop amplitude interferes with the tree-level amplitude to give

$$\Gamma(X \to \bar{f}_1 + f_2) = g_1 g_2^* g_3 g_4^* I_{XY} + \text{h.c.}$$
$$\Gamma(\bar{X} \to f_1 + \bar{f}_2) = g_1^* g_2 g_3^* g_4 I_{XY} + \text{h.c.} \tag{E.6}$$

where I_{XY} is the overall phase space factor which is in general complex for on-shell fermions $f_{1,..4}$. Thus, we get that the difference between rates for particles in the final state vs anti-particles is

$$\Gamma(X \to \bar{f}_1 + f_2) - \Gamma(\bar{X} \to f_1 + \bar{f}_2) = 4\text{Im}(I_{XY})\text{Im}(g_1^* g_2 g_3^* g_4)$$
$$\Gamma(X \to \bar{f}_3 + f_4) - \Gamma(\bar{X} \to f_3 + \bar{f}_4) = -4\text{Im}(I_{XY})\text{Im}(g_1^* g_2 g_3^* g_4) \tag{E.7}$$

Thus, the total baryon number asymmetry due to X decays is thus given by,
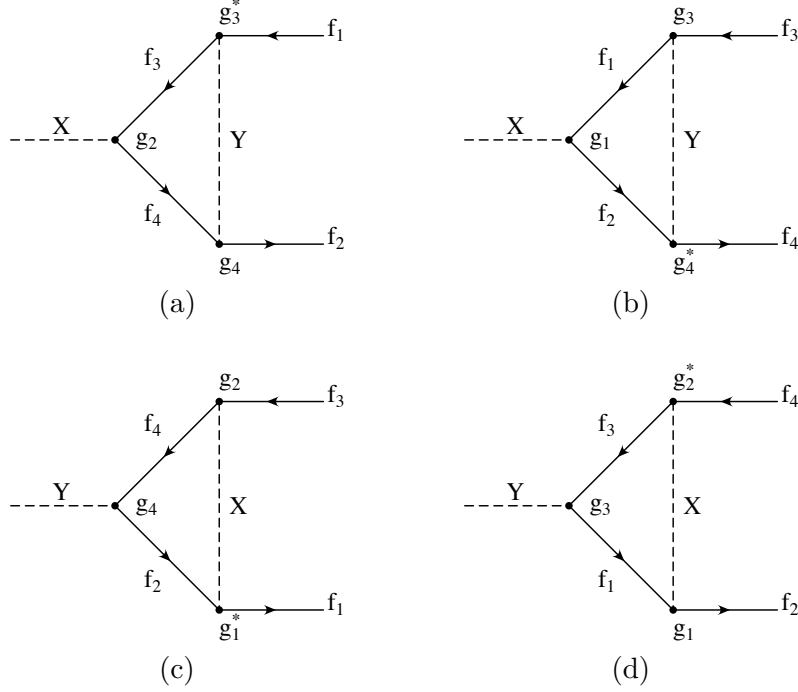
$$\epsilon_X = \frac{(B_1 - B_2)\Delta\Gamma(X \to \bar{f}_1 + f_2) + (B_4 - B_3)\Delta\Gamma(X \to \bar{f}_3 + f_4)}{\Gamma_X} \tag{E.8}$$

where B_i is the baryon number of the fermion f_i and Γ_X is the total decay width for X and

$$\Delta\Gamma(\bar{f}_1 + f_2) = \Gamma(X \to \bar{f}_1 + f_2) - \Gamma(\bar{X} \to f_1 + \bar{f}_2)$$
$$\Delta\Gamma(\bar{f}_3 + f_4) = \Gamma(X \to \bar{f}_3 + f_4) - \Gamma(\bar{X} \to f_3 + \bar{f}_4) \tag{E.9}$$

167

And similarly, we can find expressions for decays via Y. In fact using Eqn (E.7), we get

$$\epsilon_X = \frac{4}{\Gamma_X}\text{Im}(I_{XY})\text{Im}(g_1^* g_2 g_3^* g_4)\left[(B_4 - B_3) - (B_2 - B_1)\right]$$

$$\epsilon_Y = \frac{4}{\Gamma_Y}\text{Im}(I_{XY}')\text{Im}(g_1^* g_2 g_3^* g_4)\left[(B_2 - B_4) - (B_1 - B_3)\right] \qquad \text{(E.10)}$$

Figure E.2: One loop diagrams for the decays of the heavy scalar fields, X and Y.

The total asymmetry is then given by $\epsilon = \epsilon_X + \epsilon_Y$. Its clear however, that the coefficients have to be in general complex to get a asymmetry. That is, there should be at least one non-removable phase magnificent itself physically as violating CP. Moreover, there should be two different decay channels - typically a tree-level and loop diagram interfering to give the same baryon number violating decay products. We will look to this result as a guide in our work to generate the CP asymmetry needed in our baryogenesis model.

- Departure from thermal equilibrium In thermal equilibrium, the rate of forward and backward process are the same. So, any baryon asymmetry that could be created if the above two conditions are satisfied would be wiped out via thermal scatterings which allow the reverse process to occur at the same rate. This can be seen as follows. Using the fact that any relativistic theory is CPT invariant, the thermal equilibrium average of the baryon number B is

$$\langle B \rangle_T = \text{Tr}\left(e^{-\beta H}B\right) = \text{Tr}\left((CPT)(CPT)^{-1}e^{-\beta H}B\right) \qquad \text{(E.11)}$$

$$= \text{Tr}\left(e^{-\beta H}(CPT)^{-1}B(CPT)\right) = -\text{Tr}\left(e^{-\beta H}B\right) \implies \langle B \rangle_T = 0$$

168

The fourth equality comes from using the fact that baryon number B is PT-even but flips under charge conjugation, C. Thus, so long as we have thermal equilibrium in the universe, we can't create any baryon asymmetry. Therefore, whatever process leads to baryon asymmetry has to happen out-of-equilibrium. The decay of heavy particle can be one such process and in fact a number of theories of baryogenesis (including the oner studies in this work) employ this mechanism and so we take a closer look at it in the following section.

E.1   Out-of-Equilibrium Decays

Given enough time, all particles no matter how weakly they interact would achieve thermal equilibrium. However, this isn't so easy for particles in an expanding universe. This is because to achieve thermal equilibrium, particles have to interact with each other. However, in an expanding universe, particles get diluted away and thus the ability of a species to achieve equilibrium is diminished. If this interaction is a decay for a heavy particle X, the rate of decay Γ_X of the X particles eventually falls below the expansion rate H of the universe and the decays are unable to reduce the numbers of X particles to the levels required to stay in equilibrium.

Consider a heavy scalar boson that decays creating a net baryon number. At high enough temperatures $T \gg m_X$, the particle behaves like a relativistic species and the number densities of the X particles and their antiparticles are the same and we can assume thermal equilibrium with the plasma because the interaction rate is high at high temperatures,

$$n_X = n_{\bar{X}} = \frac{\zeta(3)}{\pi^2} T^3 \tag{E.12}$$

and thus

$$\frac{n_X}{n_\gamma} = \frac{1}{2} \tag{E.13}$$

As the universe expands and the particles X and $\tilde{X}$ need to continue to decay to maintain their thermal equilibrium densities and so long as they do that, net baryon number remains 0. However, as temperature keeps falling around $T \lesssim m_X$, the particle number densities are reduced compared to relativistic photons because the boltzmann suppression factor starts to become more relevant. Thus, the ratio of equilibrium densities of particle X to photons would become

$$\frac{n_{\bar{X}}^{eq}}{n_\gamma} = \frac{\pi^2}{2\zeta(3)} \left(\frac{m_X}{2\pi T}\right)^{3/2} e^{-m_X/T} \tag{E.14}$$

and the same for $n_{\bar{X}}$. For equilibrium densities to be maintained, the decay rate of X should remain higher than the expansion rate. On the other hand, for successful baryogenesis we want departure from thermal equilibrium. If the

decay rate for X falls below the Hubble rate when $T > m_X$, the species freezes out when its still relativistic. Then their density at a lower temperature doesn't have the Boltzmann suppression and thus they are out of equilibrium with the plasma because they are over abundant. So, if and when they do decay, it is an out of equilibrium process.

In the simple model of decay of a scalar X, this condition gives a constraint on the particles mass. We can derive it by noting that at high temperatures when the plasma is made of relativistic particles,

$$H^2 = \frac{\rho}{3M_p^2} = \left(\frac{4\pi^3 g_{*,T}}{45}\right) \frac{T^4}{M_p^2} \tag{E.15}$$

where $g_{*,T}$ is the effective number of relativistic species. Thus, the out-of-equilibrium condition becomes

$$\Gamma_X \lesssim H\bigg|_{T=m_X} \implies m_X^2 \gtrsim \frac{3}{2\pi}\left(\frac{5}{\pi g_{*,T}}\right)^{1/2} \Gamma_X M_p \tag{E.16}$$

To calculate an expression for the next baryon asymmetry, suppose that the X particle has decay channels $X \to f$ to a final state f producing baryon number B. Then the $\bar{X}$ has decay channels $\bar{X} \to \bar{f}$ producing baryon number $-B$, and the net baryon number produced by all of these decays is

$$\Delta B = \Gamma_X^{-1} \sum_n B \left[\Gamma(X \to f) - \Gamma(\bar{X} \to \bar{f})\right] \tag{E.17}$$

which gives a net baryon number density

$$n_B = n_X \Delta B \implies \eta \equiv \frac{n_B}{n_\gamma} = \frac{\Delta B}{2} \tag{E.18}$$

We can similarly calculate the baryon-to-entropy ratio except we have to be careful if there is any entropy injection happening as a result of the decays, which can also reheat the plasma. We will return to this point later in our work.

E.2   Models of Baryogenesis

E.2.1   Electroweak (EW) Baryogenesis

The electroweak theory of the standard model has all the ingredients necessary for baryogenesis. Lets first look at how they arise in the standard model and then we will discuss how in spite of this the electroweak theory can't explain the baryon asymmetry.

- Baryon number non-conservation in EW theory

  The standard model baryon fields are classically invariant under a $U(1)_B$ transformation. Thus, there is a conserved baryon current, $J_\mu^{(B)}$

$$J_\mu^{(B)} = \sum_\psi B_\psi (\bar\psi \gamma_\mu \psi), \text{ satisfies } \partial^\mu J_\mu^{(B)} = 0 \qquad (E.19)$$

where B_ψ is the baryon number of the ψ field. Similarly, there is also a classical global $U(1)_L$ symmetry for the lepton fields,

$$J_\mu^{(L)} = \sum_\psi L_\psi (\bar\psi \gamma_\mu \psi), \text{ satisfies } \partial^\mu J_\mu^{(L)} = 0 \qquad (E.20)$$

where L_ψ is the baryon number of the ψ field. However, classical symmetries such as these are generally not preserved at the quantum level. In particular, in a chiral theory, in which the left and right chiral fermion states are coupled differently, as occurs in electroweak theory, there are chiral anomalies resulting from the non-invariance of the field measure $\mathcal{D}\psi\mathcal{D}\bar\psi$ in the functional integral determining the generating function. The quantum anomaly arising from $U(1)_B$ non-conservation has the following RHS,

$$\partial^\mu J_\mu^{(B)} = -\frac{1}{32\pi^2}\text{Tr}\left[\{F_{\mu\nu}^L, \tilde{F}^{\mu\nu L}\}B - \{F_{\mu\nu}^R, \tilde{F}^{\mu\nu R}\}B\right] \qquad (E.21)$$

where $F_{\mu\nu}^L = T^a F_{\mu\nu}^{aL}$ is the gauge field strength couples to the left handed fermions and similarly for raw right handed one, and T^a are the generators of there relevant gauge group and $\tilde{F}_{\mu\nu}^L = \epsilon_{\mu\nu\rho\sigma}F^{\rho\sigma L}/2$ is the dual field strength tensor. The trace is over all the fermions and thus all the relevant gauge groups $SU(3)_c$ (contributes nothing) and $SU(2)_L$ and $U(1)_Y$. Denoting the $SU(2)_L$ field strength by $W_{\mu\nu}^a$ and $U(1)_Y$ by $B_{\mu\nu}$ and the relevant charge assignments for all fermions under these symmetries, we get

$$\langle\partial^\mu J_\mu^B\rangle = -\frac{N_G}{32\pi^2}\left[g_2^2 W_{\mu\nu}^a \tilde{W}^{\mu\nu a} - g_1^2 B_{\mu\nu}\tilde{B}^{\mu\nu}\right] \qquad (E.22)$$

where $N_G = 3$ is the number of fermion generations and $\langle.\rangle$ is the quantum average. It can be shown that the lepton current also satisfies a similar equality (recall that $SU(3)$ cancels out in the anomaly expression because left and right handed fermions are couples to gluons the same way).

$$\partial^\mu J_\mu^L = \frac{1}{N_G}\partial^\mu J_\mu^B, \ L \equiv \sum_l \left[\bar\nu_l\gamma_\mu\nu_l + \bar l\gamma_\mu l\right] \qquad (E.23)$$

and thus from this we see that $B - L$ is a conserved quantity, even quantum mechanically even though neither B nor L is. Here in lies our baryon number non-conservation we seek for baryogenesis. This non-conservation is bolstered at high temperatures by sphaleron inducing non-conservation of baryon number. This is because (just like with $U(1)_A$), the non-conservation of baryon number

171

is related to topologically distinct vacua of the electroweak theory, each labelled with its own baryon number. Dynamically, baryon number is violated when the field configurations jump from one vacua to another. Such a process requires energy and the higgs field configuration which interpolates between these vacua is called a sphaleron solution. This sphaleron transition rate is highly suppressed at low temperatures but is very active at high temperatures and this transition is accompanied by $\Delta B \neq 0$.

- CP Violation in the EW theory
  In the electroweak theory, the CKM matrix is a source of has CP violating phase in it. The CKM matrix mixes the quark flavors so that the quart mass and flavor eigenstates are different. However, it turns out that this CP violation in the standard model is too small. In fact, so much so that the dimensionless parameter that controls its $\delta < 10^{-25}$ and it can be shown that such a small parameter can't produce the baryon asymmetry. We would need new sources of CP violation in the SM, but that is severely constrained. Thus, CP violation alone rules out electroweak baryogenesis.

- Phase transition in the EW theory
  In spite of the fact that the EW theory has (sphaleron-induced) baryon violating process as well as CP-violation via the CKM matrix, there is a general argument that the sphaleron induced baryon non-conservation is suppressed unless the phase transition, as the Higgs acquires a vev is strongly first order. And this in turn puts a constraint on Higgs mass

$$m_H \lesssim 72 \text{ GeV} \tag{E.24}$$

  which is in clear contraction with the experimental measured value of $m_H = 125$ GeV. Its also in contraction with the constraints on higgs mass to avoid washout of the asymmetry created by sphaleron induced process, $m_H \lesssim 47 \text{GeV}$. So, even before measuring higgs mass, it was known that the electroweak theory can't produce the observed baryon asymmetry of the universe.

E.2.2   Leptogenesis

In general, leptogenesis is the generic name given to models of baryogenesis where we first create a lepton asymmetry which is then converted to a baryon asymmetry by the sphaleron process. A sphaleron is a field configuration that is a saddle point of the gauge-higgs system and interpolates between degenerate vacua. It is an instanton solution that gives the largest contribution to vacuum-to-vacuum transition amplitudes. For the sphaleron process to be effective however, the lepton asymmetry must be created by before the electroweak phase transition i.e, before this higgs acquires its vev (implying at temperatures above 246GeV).

We first give an overview of the sphaleron process [193] that coverts lepton asymmetry into a baryonic asymmetry. Next, we will study the most common leptogenesis example, that of a Majorana neutrino decay. Recall that $J_\mu^B - J_\mu^L$ is exactly conserved.

On the other hand, $J^B_\mu + J^L_\mu$ becomes

$$\partial^\mu(J^B_\mu + J^L_\mu) = 2N_f \partial_\mu K^\mu \tag{E.25}$$

where the current K^μ is given in terms of the $SU(2)_L$ field strength tensor $W^a_{\mu\nu}$ and the $U(1)_Y$ field B_μ (field strength, $B_{\mu\nu}$),

$$K^\mu = -\frac{g^2}{32\pi^2} 2\epsilon^{\mu\nu\rho\sigma} W^a_\nu \left(\partial_\rho W^a_\sigma + \frac{g}{3}\epsilon^{abc}W^b_\rho W^c_\sigma\right) + \frac{g'^2}{32\pi^2}\epsilon^{\mu\nu\sigma\rho}B_\nu B_{\rho\sigma} \tag{E.26}$$

This violation implies the existence in this non-abelian gauge theory of topologically distinct vacua labelled by an integer called the Chern-Simons number given as

$$N_{cs} = \frac{g^3}{96\pi^2}\int d^3x \epsilon_{ijk}\epsilon^{IJK}W^{Ii}W^{Jj}W^{Kk} \tag{E.27}$$

And thus a transition between vacua (either via quantum tunneling whose rate is exceptionally low or thermally at high temperatures whose rate can be significant) violates the baryon (lepton) number by ΔB (ΔL)

$$\Delta B = N_f \Delta N_{cs} \tag{E.28}$$

Since $B - L$ is conserved, any change in B must be accommodate by a change in L. In a plasma, the changing number of baryons or leptons is accommodated by using the grand canonical potential with non-zero chemical potential $\mu \neq 0$. Denoting by μ_{q_i} the chemical potential of the quark doublet, μ_{u,d_i} the chemical potential of the individual quark singlets and similarly μ_{l_i} the chemical potential of the lepton doublets and μ_{e_i} that of the singlet, we can write the baryon and lepton numbers as

$$B = \sum_i (2\mu_{q_i} + \mu_{u_i} + \mu_{d_i}$$
$$L = \sum_i (2\mu_{l_i} + \mu_{e_i}) \tag{E.29}$$

Assuming thermal equilibrium and the same chemical potential across generations, we get

$$B = -\frac{4}{3}N_f\mu_l, \ \ L = \frac{14N_f^2 + 9N_f}{6N_f + 3}\mu_l \implies L = -\left(\frac{9 + 14N_f}{4 + 8N_f}\right)B \tag{E.30}$$

Finally, we look at the most common example of leptogenesis via decay of a heavy Majorana neutrino which also gives the SM neutrinos a small mass, explaining two unrelated phenomenon. We begin by introducing a new Majorana (i.e., the fermion is the same as the anti-fermion) neutrino $N = \nu_R + \bar{\nu}^c_R$ and the interaction lagrangian is

$$\mathcal{L}_{int} = f_{ij}\bar{e}_{R_i}l_{L_j}H^\dagger + h_{ij}\bar{\nu}_{R_i}l_{L_j}H - \frac{1}{2}(M_R)_{ij}\bar{\nu}^c_{R_i}\nu_{R_j} + \text{h.c.} \tag{E.31}$$

Here H is the higgs doublet, l_{L_i} is the lepton doublet with $i = (e, \mu, \tau)$, e_{R_i} the right handed fermion and ν_{R_i} is the right handed neutrino which has a Majorana mass term M_R which is allowed because its a singlet under all SM gauge groups. Upon the electroweak symmetry breaking, the SM Higgs doublet gets a VEV, $\langle H \rangle = v$, and the charged leptons and the neutrino Dirac masses, which assumed to be much smaller than the RH neutrino Majorana masses, are generated,

$$m_l = fv, \ m_D = hv \ll M_R. \tag{E.32}$$

EWSB creates the Dirac mass which appears in the lagrangian as the following term for a fermion ψ

$$\mathcal{L}_D = -m_D \left(\bar{\psi}_L \psi_R + \text{h.c.} \right) \tag{E.33}$$

whereas if ψ was a Majorana particle the mass term would be

$$\mathcal{L}_M = -\frac{1}{2} m_L^M \left(\bar{\psi}_L \psi_R^C + \overline{\psi^C}_R \psi_L \right) - \frac{1}{2} m_R^M (L \leftrightarrow R) \tag{E.34}$$

In general then, if we have both type of mass terms, we like we do here, we can write the mass lagrangian as follows:

$$\mathcal{L}_{MD} = - \left(\bar{\psi}_L \ \overline{\psi^C}_L \right) \begin{pmatrix} m_L^M & m_D \\ m_D & m_R^M \end{pmatrix} \begin{pmatrix} \psi_R^C \\ \psi_R \end{pmatrix} + \text{h.c.} \tag{E.35}$$

Thus, our neutrino mass matrix as a see-saw form

$$\begin{pmatrix} 0 & m_D \\ m_D^T & M_R \end{pmatrix} \tag{E.36}$$

Diagonalizing this matrix,

The lepton asymmetry is created by the decay of the heavy Majorana state $N_i \to H + l_\alpha$ where $\alpha = (e, \mu\tau)$. The total width of this decay is,

$$\Gamma_{D_i} = \sum_\alpha \left[\Gamma(N_i \to H + l_\alpha) + \Gamma(N_i \to \bar{H} + \bar{l}_\alpha) \right] = \frac{1}{8\pi} (h^\dagger h)_{ii} M_i \tag{E.37}$$

The out-of-equilibrium condition requires that the total width for N_i decay, Γ_{D_i}, to be smaller compared to the expansion rate of the Universe (H) at temperature $T = M_i$ like we saw above.

$$\Gamma_{D_i} < H \Big|_{T=M_i} \tag{E.38}$$

CP violation happens due to the interference of tree and loop level vertex diagrams (a) and (b) in Fig (E.3) and the self-energy diagram in (c) and its characterized by

$$\epsilon_i = \frac{\sum_\alpha \left[\Gamma(N_i \to H + l_\alpha) - \Gamma(N_i \to \bar{H} + \bar{l}_\alpha) \right]}{\Gamma_{D_i}} \tag{E.39}$$

174
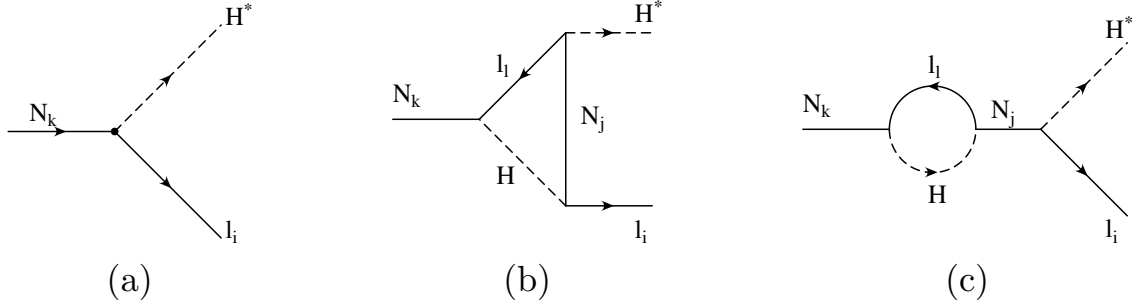
Figure E.3: Diagrams contributing to CP violation, each creating a lepton asymmetry by decay of a right handed neutrino into higgs and SM lepton. The asymmetry is generated due to the interference of the tree-level diagram (a) and the one-loop vertex correction (b) and self-energy (c) diagrams.

In this mechanism, we have to be careful with two other things. Since the same lagrangian also produces neutrino masses, we have to make sure that neutrino mass constraints are satisfied while creating the asymmetry. The out-of-equilibrium condition which translates to inverse process being suppressed has to be satisfied which is yet another constraint. We also have to ensure that scattering processes which change lepton number are also suppressed. Examples of the latter are given in Figs (E.4) and (E.5). Both of these further constraints will be relevant in our work, too and we will discuss them further in the relevant context later.
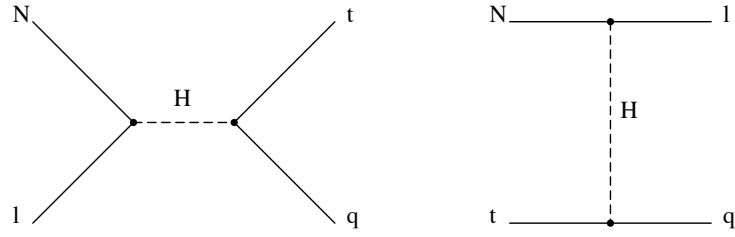
Figure E.4: $\Delta L = 1$ scattering process.
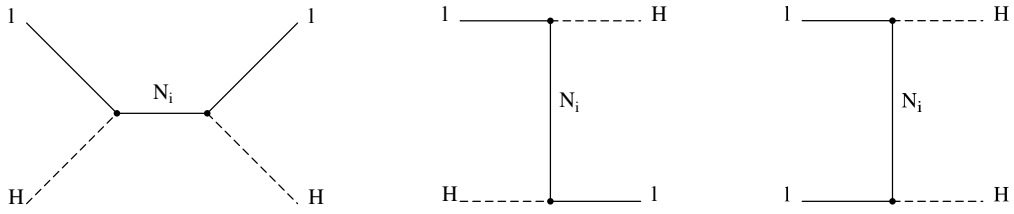
Figure E.5: $\Delta L = 2$ scattering process.

APPENDIX F

SUPERSYMMETRY

The Standard Model (SM) is incomplete. It doesn't unify the electroweak and strong nuclear force into one nor does it incorporate gravity. Further, it doesn't explain why the higgs mass is what it is. This is important because the higgs mass is the only dimensionful parameter in the SM. It receives large quadratic corrections and unless fine-tuned its mass should be $\mathcal{O}(M_{pl})$. Supersymmetry (SUSY) is a theory which doubles the particle content of the standard model. Essentially, it assigns a new boson (fermion) to every standard model fermion (boson) with the same quantum numbers. Although, it was born as a loophole to the Coleman-Mandula theorem, it was quickly realized that SUSY can solve the small higgs mass problem and it unifies all the coupling constants at a high scale.

We will first take a quick detour into the statement and consequences of the Coleman-Mandula theorem and then see how SUSY comes about as a loophole. Next, we will study the SUSY algebra and the superspace formalism which allows us to easily derive SUSY invariant actions. This will help us in constructing the Minimally Supersymmetric Standard Model (MSSM), introduce its particle content and see how the problems of unification and hierarchy (low higgs mass) are solved in the context of SUSY. Finally, we will briefly look at Supergravity (SUGRA) which arises by gauging global SUSY and study the gravitino in this context. The treatment in this appendix is adopted primarily from [194].

F.1   Coleman-Mandula & SUSY Algebra

Simply put, the Coleman-Mandula (CL) theorem states that any internal symmetry generator has to be a Lorentz scalar. More formally, consider the following algebra,

$$
\begin{aligned}
[\mathcal{P}_\mu, \mathcal{P}_\nu] &= 0 \\
[\mathcal{P}_\mu, \mathcal{M}_{\rho\sigma}] &= i(\eta_{\mu\rho}\mathcal{P}_\sigma - \eta_{\mu\sigma}\mathcal{P}_\rho) \\
[\mathcal{M}_{\mu\nu}, \mathcal{M}_{\rho\sigma}] &= i(\eta_{\nu\rho}\mathcal{M}_{\mu\sigma} - \eta_{\nu\sigma}\mathcal{M}_{\mu\rho} - \eta_{\mu\rho}\mathcal{M}_{\nu\sigma} + \eta_{\mu\sigma}\mathcal{M}_{\nu\rho}) \\
[T^a, T^b] &= iC^{abc}T^c
\end{aligned}
\tag{F.1}
$$

where $\mathcal{P}_\mu$ is the momentum and $\mathcal{M}_{\mu\nu}$ is the angular momentum operator for the Poincare group and T^a is the generator of whatever internal (non-spacetime) symmetry group the theory is charged under. Then the theorem states that T^a are Lorentz scalars, i.e.,

$$
[T^a, \mathcal{P}_\mu] = [T^a, \mathcal{M}_{\mu\nu}] = 0
\tag{F.2}
$$

However, imagine a transformation that would exchange a fermion with a boson. Heuristically, we could write this operator as

$$
Q = \sum_{ij} \int d^3k \, d^3k' \, f_{ij}(k, k') a^\dagger_{B_j}(k') a_{F_i}(k)
\tag{F.3}
$$

where $a_{F_i}(k)$ annihilates a fermion of type i with momentum k and $a^\dagger_{B_j}(k')$ creates a boson of type j with momentum k'. Because of the fermionic nature of this operator,

we expect it would have anti-commutation relations. Thus, it would be an internal symmetry generator that exchanges bosons and fermions in the theory but unlike T^a's above it enjoys anti-commutation relations. Such a lie algebra is called graded lie algebra. And with anti-commutation relations between Q's, it can be shown that CL can be evaded. Further, it has also been shown that this is the unique way out of this no-go theorem.

Since SUSY assigns a fermion to every boson and vice-versa, it must have an operator like Q which is the generator of this transformation. We have seen above that it must be fermionic in nature, thus evading the no-go theorem. However, its anti-commutator $\{Q, Q\}$ must be bosonic object like T^a and so must obey CL. Further in fact, because the anti-commutator is the symmetric combination of Lorentz spinors which are (say) $(1/2, 0)$ representations of the Lorentz algebra, the anti-commutator must be a Lorentz vector because $(1/2, 0) \otimes (1/2, 0) = 1$. The only vector it can be given CL is $\mathcal{P}_\mu$. We work with Majorana spinors and to have the spinor-vector structure work out correctly, we posit the following relations,

$$\boxed{\begin{aligned} \{Q_r, \bar{Q}_s\} &= 2\gamma^\mu_{rs}\mathcal{P}_\mu \\ [Q_r, \mathcal{P}^\mu] &= 0 \\ [Q_r, \mathcal{M}^{\mu\nu}] &= i\sigma^{\mu\nu}_{rs}Q_s \end{aligned}} \tag{F.4}$$

where

$$\bar{Q}_r = \left(Q^T\gamma^0\right)_r \tag{F.5}$$

The third relationship basically states that Q_r transforms as a spinor in spacetime. The second relationship is obvious because of the bosonic vector nature of the momentum operator and fermionic nature of Q_r. These relationships for $N = 1$ SUSY can be generalized by having N SUSY generators, Q^i_r, where a δ^{ij} appears on the right hand side in the first equation of (F.4). The SUSY generator Q acts on a boson and converts it into a fermion,

$$Q\ket{b} = \ket{f} \tag{F.6}$$

Applying $\mathcal{P}_\mu\mathcal{P}^\mu$ on both sides and noting that $\mathcal{P}_\mu\mathcal{P}^\mu$ commutes with Q_r,

$$\begin{aligned} \mathcal{P}_\mu\mathcal{P}^\mu\left(Q\ket{b}\right) &= \mathcal{P}_\mu\mathcal{P}^\mu\ket{f} = m_f^2 \tag{F.7} \\ &= Q\left(\mathcal{P}_\mu\mathcal{P}^\mu\ket{b}\right) = m_b^2 \tag{F.8} \end{aligned}$$

and thus the fermion and boson connected by a SUSY transformation have the same mass. Immediately, we can infer that if SUSY is a symmetry of our universe, it must be broken because we don't see a boson with the same mass as an electron. The SUSY algebra uniquely determines the hamiltonian ($\mathcal{H} = \mathcal{P}^0$) of the system. Use the first relation between the generators and multiply by γ^0 on both sides (sum over repeat matrix indices assumed),

$$\{Q_r, Q_t\}\gamma^0_{ts} = 2\gamma^\mu_{ts}\mathcal{P}_\mu \implies \{Q_r, Q_t\}(\gamma^{0^2})_{tr} = 2\text{Tr}(\gamma^0\gamma^\mu)\mathcal{P}_\mu \tag{F.9}$$

179

Next using $\gamma^{0^2} = 1$ and $\text{Tr}(\gamma^0 \gamma^\mu) = 4\eta^{0\mu}$, we get

$$\sum_r Q_r^2 = 4\mathcal{P}^0 \implies \mathcal{H} = \frac{1}{4} \sum_r Q_r^2 \tag{F.10}$$

and thus the hamiltonian is uniquely determined in terms of the SUSY generators. Moreover, its positive definite for theories invariant under global SUSY. This fact is significant for SUSY breaking - consider a vacuum state $|\Omega\rangle$ of a SUSY invariant theory,

$$\langle\Omega| \mathcal{H} |\Omega\rangle = \frac{1}{4} \sum_r ||Q_r |\Omega\rangle ||^2 \geq 0 \tag{F.11}$$

Thus, if the vacuum is invariant under SUSY then energy of the ground state is zero. On the other hand, if SUSY is spontaneously broken, that is, $Q_r |\Omega\rangle \neq 0$ then, $\langle\Omega| \mathcal{H} |\Omega\rangle \neq 0$ and thus the order parameter for this symmetry breaking is the vacuum energy, $\langle\Omega| \mathcal{H} |\Omega\rangle$. This is very different from gauge theories, where the order parameter is typically a scalar field ϕ, whose vacuum lies at $\langle\phi\rangle \neq 0$.

F.2   Superfields

Once we have the relations between the SUSY and Poincare generators as above, we intend to get at representations. To this end, we introduce the concept of *Superspace*, which is described by spacetime variables x^μ as well as the Grassmann variables θ^α, $\bar{\theta}_{\dot{\alpha}}$. Thus a function in superspace is now a function of $(x, \theta, \bar{\theta})$ and such function are called *Supefields*. The Grassmann variables are like the Majorana SUSY generators Q,

$$\{\theta^\alpha, \theta^\beta\} = \{\bar{\theta}_{\dot{\alpha}}, \bar{\theta}_{\dot{\beta}}\} = \{\theta^\alpha, \bar{\theta}_{\dot{\alpha}}\} = 0 \tag{F.12}$$

where $\alpha, \dot{\alpha} = 1, 2$ is the spinor index. Since we are working in the $2-$component notation, the algebra becomes,

$$\{Q_\alpha, \bar{Q}_{\dot{\alpha}}\} = 2\sigma^\mu_{\alpha\dot{\alpha}} \mathcal{P}_\mu, \ \{Q_\alpha, Q_\beta\} = \{\bar{Q}_{\dot{\alpha}}, \bar{Q}_{\dot{\beta}}\} = 0 \tag{F.13}$$

It can then be shown that the following then is a representation of the algebra,

$$\begin{aligned}
\mathcal{P}_\mu &= i\partial_\mu \\
Q_\alpha &= i\left[\frac{\partial}{\partial\theta^\alpha} + i\sigma^\mu_{\alpha\dot{\alpha}}\bar{\theta}^{\dot{\alpha}}\partial_\mu\right] \\
\bar{Q}_{\dot{\alpha}} &= -i\left[\frac{\partial}{\partial\bar{\theta}^{\dot{\alpha}}} + i\theta^\alpha\sigma^\mu_{\alpha\dot{\alpha}}\partial_\mu\right] \\
\bar{Q}^{\dot{\alpha}} &= i\left[\frac{\partial}{\partial\bar{\theta}_{\dot{\alpha}}} + i\bar{\sigma}^{\mu\dot{\alpha}\alpha}\theta^\alpha\partial_\mu\right]
\end{aligned} \tag{F.14}$$

A function in superspace $F(x, \theta, \bar{\theta})$, in general if a function of superspace coordinates x, θ and its complex conjugate $\bar{\theta}$. Using the anti-commutation property enjoyed by

the grassmann coordinates $\theta, \bar{\theta}$, we can expand F as

$$
\begin{aligned}
F(x, \theta, \bar{\theta}) &= f(x) + \theta \rho(x) + \bar{\theta} \bar{\chi}(x) + \theta^2 m(x) + \bar{\theta}^2 n(x) + (\theta \sigma^\mu \bar{\theta}) v_\mu(x) \\
&\quad + \theta^2 \bar{\theta} \bar{\lambda}(x) + \bar{\theta}^2 \theta \psi(x) + \theta^2 \bar{\theta}^2 d(x)
\end{aligned}
\tag{F.15}
$$

Recall that there are two grassmannian coordinates θ^α, $\alpha = 1, 2$ and its complex conjugate. The 2-component notation used above is: $\theta^2 \equiv \theta^\alpha \theta_\alpha = \theta^\alpha \epsilon_{\alpha\beta} \theta^\beta = \theta^2 \theta^1 \epsilon_{21} + \theta^1 \theta^2 \epsilon_{12} = \theta^2 \theta^1 - \theta^1 \theta^2 = 2\theta^2 \theta^1$. The functions f, m, n and d are complex scalars while ρ_α, $\bar{\chi}^{\dot\alpha}$, $\bar{\lambda}^{\dot\alpha}$ and ψ_α are (Weyl) spinor fields. A superspace translation δ_S acts on function F as (using the differential representation of operators and generalizing ordinary translations)

$$
F(x, \theta, \bar{\theta}) \rightarrow e^{i(y^\mu \mathcal{P}_\mu + \eta Q + \bar{\eta}\bar{Q})} F(x, \theta, \bar{\theta}) e^{-i(y^\mu \mathcal{P}_\mu + \eta Q + \bar{\eta}\bar{Q})}
\tag{F.16}
$$

where y^μ is an arbitrary $4-$vector and η, $\bar{\eta}$ are arbitrary (Weyl) spinor fields. Further, it can also be shown that

$$
\delta_S F = -iy^\mu \mathcal{P}_\mu F - i\eta Q F - i\bar{\eta}\bar{Q} F
\tag{F.17}
$$

As we see above, a general function of the superspace variables F is composed of complex scalars/spinors and complex vectors/spinors. However, it has too many d.o.f.'s to describe a single scalar/spinor and/or complex vector/spinor pair that would be relevant for SUSY. This can be reduced by introducing some constraint on a function Φ in superspace that would describe scalar/spinor fields which are connected by a SUSY transformation. This constraint should be SUSY-invariant and to this end, covariant derivatives $\mathcal{D}_\alpha$ and $\bar{\mathcal{D}}_{\dot\alpha}$ are introduced such that,

$$
\mathcal{D}_\alpha \delta_S F = \delta_S \mathcal{D}_\alpha F
\tag{F.18}
$$

Using the representation of the SUSY generators in Eqn. (F.14), it can be shown that $\mathcal{D}_\alpha$ and $\bar{\mathcal{D}}^{\dot\alpha}$ are:

$$
\begin{aligned}
\mathcal{D}_\alpha &= \frac{\partial}{\partial \theta^\alpha} - i\sigma^\mu_{\alpha\dot\alpha} \bar{\theta}^{\dot\alpha} \partial_\mu \\
\bar{\mathcal{D}}^{\dot\alpha} &= -\frac{\partial}{\partial \bar{\theta}_{\dot\alpha}} + i\sigma^{\mu\dot\alpha\alpha} \theta_\alpha \partial_\mu
\end{aligned}
\tag{F.19}
$$

A SUSY invariant restrictive condition on a function Φ in superspace is then,

$$
\bar{\mathcal{D}}^{\dot\alpha} \, \Phi(x^\mu, \theta, \bar{\theta}) = 0 \implies \Phi(x^\mu, \theta, \bar{\theta}) \equiv \Phi(x^\mu - i\theta\sigma^\mu\bar{\theta}, \theta)
\tag{F.20}
$$

Thus, our function in superspace now only depends on one of the grassmann coordinates and not its complex conjugate (in a sense we are restricting to holomorphic functions) and so using Eqn. (F.15), all the terms containing $\bar{\theta}$ drop out and so we can write Φ,

$$
\Phi(y, \theta) = \phi(y) + \sqrt{2}\theta^\alpha \psi_\alpha(y) + \theta^2 F(y)
\tag{F.21}
$$

Thus, our superfield now contains a complex scalar ϕ and a spinor ψ and in addition also contains another complex scalar F. We will see that F is only an auxiliary field

and thus Φ truly defines a scalar/spinor pair (supermultiplet) and such a field is called a *Chiral Superfield.*

On the other hand, the vector supermultiplet describes a real vector field and a spinor field. Just like the chiral superfield wad denoted by Φ, a vector superfield is denoted by V, and the spinor partner by $\lambda(x)$ and to describe a real vector field $A_\mu(x)$, we impose a reality condition,

$$V(x, \theta, \bar\theta) = V^\dagger(x, \theta, \bar\theta) \tag{F.22}$$

V can then be expanded as follows:

$$
\begin{aligned}
V(x, \theta, \bar\theta) =~ & C(x) + i\theta\chi(x) - i\bar\theta\bar\chi(x) + \frac{i}{2}\theta(x)^2 \left[M(x) + iN(x)\right] \\
& - \frac{i}{2}\bar\theta(x)^2 \left[M(x) - iN(x)\right] + \theta\sigma^\mu\bar\theta A_\mu(x) + \theta^2\bar\theta_{\dot\alpha}\left[\lambda^{\dot\alpha}(x) + \frac{1}{2}\left(\bar\sigma^\mu\partial_\mu\chi(x)\right)^{\dot\alpha}\right] \\
& + \bar\theta^2\theta^\alpha\left[\lambda_\alpha(x) - \frac{1}{2}\left(\sigma^\mu\partial_\mu\bar\chi(x)\right)_\alpha\right] - \frac{1}{2}\theta^2\bar\theta^2\left[D(x) + \frac{1}{2}\Box C(x)\right] \tag{F.23}
\end{aligned}
$$

It turns out that by a gauge transformation (abelian or non-abelian) that a vector field enjoys can eliminate all degrees of freedom except the gauge field $A_\mu(x)$, gaugino field $\lambda(x)$ which is the superpartner of the gauge field and $D(x)$ is the auxiliary field like for a chiral superfield. It turns out these components can be captured by a chiral superfield W_α,

$$W_\alpha = -\frac{1}{4}\bar{D}_{\dot\alpha}\bar{D}^{\dot\alpha}\bar{D}_\alpha V \implies \bar{D}_{\dot\beta}W_\alpha = 0 \tag{F.24}$$

It turns out that W_α can be expanded into component fields as below,

$$W_\alpha = \lambda_\alpha(y) - \left[\delta_\alpha^\beta D(y) + \frac{i}{2}(\sigma^\mu\bar\sigma^\nu)_\alpha^\beta F_{\mu\nu}(y)\right]\theta_\beta + i\theta^2\sigma^\mu_{\alpha\dot\alpha}\partial_\mu\bar\lambda^{\dot\alpha}(y) \tag{F.25}$$

F.2.1   Constructing SUSY Invariant Actions

We can construct a SUSY invariant action of the chiral superfield with any analytic, holomorphic function $W(\Phi)$ of the chiral superfield, Φ. In general, the full action for a SUSY invariant non-abelian gauge theory is (after integrating out the F term),

$$
\begin{aligned}
S = \int d^4x \Bigg\{ & D^\mu\phi^{i*}D_\mu\phi_i + i\psi_i\sigma^\mu D_\mu\bar\psi_i - \left|\frac{\partial W}{\partial\Phi}(\phi)\right|^2 - \left(\frac{1}{2}\frac{\partial^2 W}{\partial\Phi^2}(\phi)\psi\psi + \text{h.c.}\right) \\
& + g\left(\phi^{i*}D^a T_i^{aj}\phi_j + \sqrt{2}\phi^{i*}\lambda^a T_i^{aj}\psi_j + \sqrt{2}\bar\lambda^a\bar\psi^i T_i^{aj}\phi_j\right) \\
& + \left(-\frac{1}{8}\mathcal{F}_{\mu\nu}^a\mathcal{F}^{\mu\nu a} - \frac{i}{8}\mathcal{F}_{\mu\nu}^a\tilde{\mathcal{F}}^{\mu\nu a} + \frac{i}{2}\lambda^a\sigma^\mu D_\mu\bar\lambda^a + \frac{1}{4}D^a D^a\right) \Bigg\}
\end{aligned}
$$

where $\tilde{\mathcal{F}}$ is the dual of $\mathcal{F}$ given as

$$\tilde{\mathcal{F}}^a_{\mu\nu} = \frac{1}{2}\epsilon_{\mu\nu\rho\sigma}\mathcal{F}^{a\rho\sigma} \tag{F.26}$$

T^a are the generators of the non-abelian gauge group and g is the gauge coupling. The fields ϕ_i and ψ_i are in the (same) fundamental representation of the gauge group whereas the gauginos λ^a are in the adjoint representation of the gauge group, like the gauge bosons A^a_μ. That is,

$$\begin{aligned} D_\mu\lambda^a &= \partial_\mu\lambda^a + gC^{abc}A^b_\mu\lambda^c \\ D_\mu\phi_i &= \partial_\mu\phi_i - igA^a_\mu T^{aj}_i\phi_j \\ D_\mu\psi_i &= \partial_\mu\psi_i - igA^a_\mu T^{aj}_i\psi_j \end{aligned} \tag{F.27}$$

The auxiliary field D^a is a lagrange multiplier and can be integrated out. The index i denotes the number of different chiral superfields whereas a is the non-abelian gauge index denoting the number of generators of the Lie algebra.

F.3 Minimally Supersymmetric Standard Model (MSSM)

The MSSM has twice the number of fields of the Standard Model (counted as degrees of freedom before EWSB). For the quarks, there's spin-0 squarks, the leptons SUSY partner are scalar sleptons, the gauge bosons have spin-1/2 gauginos and there's one additional higgs field. The Standard Model Higgs is a linear combination of scalar degrees of freedom of the two MSSM higgs doublets.

The quark and lepton superfields may be expanded in flavor space as

$$\begin{aligned} \hat{Q}_i &= \{\hat{Q}_1, \hat{Q}_2, \hat{Q}_3\} \\ \hat{U}^c_i &= \{\hat{U}^c, \hat{C}^c, \hat{T}^c\} \\ \hat{D}^c_i &= \{\hat{D}^c, \hat{S}^c, \hat{B}^c\} \\ \hat{L}_i &= \{\hat{L}_1, \hat{L}_2, \hat{L}_3\} \\ \hat{E}^c_i &= \{\hat{e}^c, \hat{\mu}^c, \hat{\tau}^c\} \end{aligned} \tag{F.28}$$

The left-chiral superfields may be expanded in superspace as

$$\begin{aligned} \hat{Q}_1 &= (\tilde{q}_1, q_1) & \hat{Q}_2 &= (\tilde{q}_2, q_2) & \hat{Q}_3 &= (\tilde{q}_3, q_3) \\ \hat{U}^c &= (\tilde{u}^c, u^c) & \hat{C}^c &= (\tilde{c}^c, c^c) & \hat{T}^c &= (\tilde{t}^c, t^c) \\ \hat{D}^c &= (\tilde{d}^c, d^c) & \hat{S}^c &= (\tilde{s}^c, s^c) & \hat{B}^c &= (\tilde{b}^c, b^c) \\ \hat{L}_1 &= (\tilde{\ell}_1, \ell_1) & \hat{L}_2 &= (\tilde{\ell}_2, \ell_2) & \hat{L}_3 &= (\tilde{\ell}_3, \ell_3) \\ \hat{e}^c &= (\tilde{e}^c, e^c) & \hat{\mu}^c &= (\tilde{\mu}^c, \mu^c) & \hat{\tau}^c &= (\tilde{\tau}^c, \tau^c) \end{aligned} \tag{F.29}$$

$$\text{and} \quad \begin{aligned} \hat{H}_u &= (h_u, \tilde{h}_u) \\ \hat{H}_d &= (h_d, \tilde{h}_d) \end{aligned} \tag{F.30}$$

where the first entry is a complex scalar scalar field and the second is a left-chiral Weyl spinor. In the two-component spinor notation, χ_α transforms in the $(1/2, 0)$

representation of the Lorentz group while $\chi_{\dot{\alpha}}^{\dagger}$ transforms in the $(0, 1/2)$ representation. Each of the spinors is left-chiral, including those denoted with a "c" superscript. The three vector superfields are given by

$$
\begin{aligned}
\hat{g} &= (g\,,\,\tilde{g}) \\
\hat{W} &= (W\,,\,\tilde{W}) \\
\hat{B} &= (B\,,\,\tilde{B})
\end{aligned} \quad .
\tag{F.31}
$$

The charge assignments under the SM gauge groups of the various fields is given in Table F.1 below.

Field	$SU(3)_C$	$SU(2)_L$	$U(1)_Y$	$U(1)_R$	$U(1)_B$	$U(1)_L$
$\hat{Q}_i$	**3**	**2**	$1/6$	1	$1/3$	0
$\hat{U}_i^c$	$\bar{\mathbf{3}}$	**1**	$-2/3$	-1	$-1/3$	0
$\hat{D}_i^c$	$\bar{\mathbf{3}}$	**1**	$1/3$	-1	$-1/3$	0
$\hat{L}_i$	**1**	**2**	$-1/2$	-1	0	1
$\hat{E}_i^c$	**1**	**1**	1	1	0	-1
$\hat{H}_u$	**1**	**2**	$1/2$	0	0	0
$\hat{H}_d$	**1**	**2**	$-1/2$	0	0	0
$\hat{g}$	**8**	**1**	0	0	0	0
$\hat{W}$	**1**	**3**	0	0	0	0
$\hat{B}$	**1**	**1**	0	0	0	0

Table F.1: The MSSM field content and charges.

The supersymmetric lagrangian is described by a superpotential which is an analytic, holomorphic function of fields. Using the Higgs fields only, we get the quadratic potential,

$$
W^{(2)} = -\mu\ \hat{H}_u \cdot \hat{H}_d \equiv -\mu\ \epsilon_{ij}\hat{H}_u^i \cdot \hat{H}_d^j
\tag{F.32}
$$

The parameter μ is the only dimensionful parameter in the MSSM. Its value should be of the order of grand unification or Planck scale or some high scale where the theory breaks down. It turns out that EW higgs vev is related to μ and thus it can't be very large. This apparent smallness of the dimensionful parameter is called the μ-problem in SUSY.

At the cubic level, the superpotential has Yukawa couplings of the form,

$$
W^{(3)} = \lambda_d Q \cdot H_1 D^c + \lambda_u Q \cdot H_2 U^c + \lambda_e L \cdot H_1 E^c
\tag{F.33}
$$

After EWSB, the higgses acquire vevs and the Yukawa couplings are thus given by

$$
m_d = -\lambda_d \langle H_1^0 \rangle\,, \ m_u = \lambda_u \langle H_2^0 \rangle\,, \ m_e = -\lambda_e \langle H_1^0 \rangle
\tag{F.34}
$$

In addition, there are following baryon and lepton violating terms that are possible at the level of the superpotential,

$$
L \cdot L\ E^c,\ Q \cdot L\ D^c,\ U^c D^c D^c
\tag{F.35}
$$

The first two violate lepton number whereas the third one violates baryon number. These are dangerous interactions and to avoid that a symmetry called R-parity is imposed on the MSSM. The fields in the SM all have parity $+1$ (including both the higgs doublets) and its -1 for the superpartners. In general, the R-parity of a paprticle in the MSSM is given by $R = (-1)^{3B+L+2S}$ where B is the baryon number, L the lepton number and S the spin of the particle. The origin of R-parity is in the global continuous $U(1)$ symmetry that exists in $N = 1$ SUSY called R-symmetry. It basically arises whenever there is an internal symmetry group under which the SUSY generators transform non-trivially. It turns out that Q_α and $\bar{Q}_{\dot\alpha}$ transform under a $U(1)$ sub-group called R-symmetry and they have opposite charges under this symmetry.

F.4 Hierarchy Problem & Soft SUSY breaking

The Standard Model has one fundamental scalar particle - the higgs boson. Fundamental scalars suffer from self-energy divergences which modify their mass quadratically as a function of the energy scale. Specifically, in the case of the higgs, the three types of diagrams that contribute to its self-energy are shown in Fig. (F.1), thus modifying its mass in a quadratic manner:

$$\Delta M_H^2 \propto (\Lambda/M_W)^2 \left[3 \left(M_W^2 + M_Z^2 + M_H^2 \right)/4 - \sum m_f^2 \right] \tag{F.36}$$

Here Λ is the cut-off of the theory (or equivalently the regularized version of the momentum integrals), i.e., the energy scale to which we trust the theory. The higgs mass has been recently measured to be ~ 125 GeV. Since Λ can be as high as the cut-off of the theory, i.e., the Planck scale, $\Lambda \sim M_P \sim 10^{18}$GeV. Since $M_H^2 = M_0^2 + \Delta M_H^2$, where M_{0H}^2 is the bare higgs mass, this means that the squared bare mass and the self-energy corrections should cancel to 1 part in 10^{30}! This is called the Hierarchy Problem - why is the higgs mass so low in spite of the potentially large quadratic divergences (there are still smaller logarithmic corrections)? That is, why is the SM so fine-tuned? Alternatively, this is also called the naturalness problem where 't Hooft defines a theory as natural when sending its parameters to 0 enhances the symmetry of the system. The SM isn't natural because setting any of the masses doesn't enhance the symmetry of the theory.
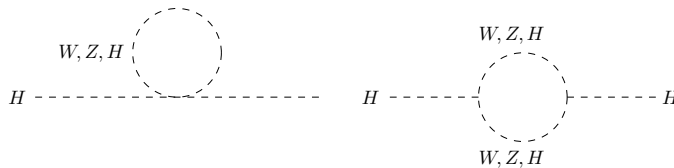
SUSY introduces a beautiful and most compelling solution to the hierarchy problem. We've already seen that SUSY imposes that for every fermion in the spectrum of the theory, there's also a boson with equal mass and charges and vice versa. Because of this, every bosonic contribution to the quadratic divergence is countered by a fermionic one (note the minus sign in Eqn. (F.36)). In fact, were as exact symmetry at the weak scale, then the quadratic divergences would be exactly zero and we would
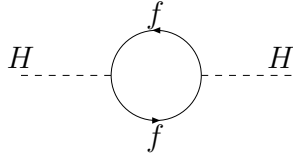
Figure F.1: Diagrams contributing to 1-loop corrections of the Higgs Mass in SM.

be left only with tamer (but expected) logarithmic divergences.

If we take cancellation of quadratic divergences to be the physical motivation behind SUSY (and not as a loophole to Coleman-Mandula), then it turns out that one can introduce more terms, modifying the MSSM. These terms are called soft SUSY breaking terms, which although explicitly break SUSY, still keep cancellation of quadratic divergences intact. In this sense, they break SUSY '*softly*'. There are three type of soft SUSY terms:

- Scalar mass terms introduce a gap between $Re(\phi)$ and $Im(\phi)$ where ϕ is the complex scalar,

$$\delta\mathcal{L}_{SB} = (\delta m^2 + \delta m'^2)(Re\ \phi)^2 + (\delta m^2 - \delta m'^2)(Im\ \phi)^2 \qquad (F.37)$$

- A-terms are cubic analytic functions (real part), if these are allowed by gauge symmetry,

$$\delta\mathcal{L}_{SB} = -\mathcal{A}\left(\phi^3 + \phi^{*3}\right) \qquad (F.38)$$

- Gaugino mass terms,

$$\delta\mathcal{L}_{SB} = -\frac{1}{2}M_\lambda\bar{\lambda}\lambda \qquad (F.39)$$

Soft SUSY breaking terms can in general have complex coefficients and together with R-parity violation play a pivotal role in leptogenesis studied in this thesis.

F.5   Supergravity

Consider finite SUSY transformations with parameters $\epsilon_1(x)$ and $\epsilon_2(x)$, which are Majorana spinors (and at the classical level grassmann variables). Then, the following can be shown using (F.4),

$$[\bar{\epsilon}_1(x)Q, \bar{\epsilon}_1(x)Q] = 2\bar{\epsilon}_1(x)\gamma^\mu\bar{\epsilon}_2(x)\mathcal{P}_\mu \qquad (F.40)$$

Note that since the parameters $\epsilon_1(x)$ and $\epsilon_2(x)$ are arbitrary, the RHS amounts to a spacetime dependent translation or a general coordinate transformation. So, if we try to make SUSY local, we can expect a theory invariant under local coordinate transformations, or in other Einstein's general relativity follows. We get a particle in

the spectrum that is spin 2, i.e., the graviton and also a spin 3/2 particle, called the gravitino. To see this, consider the Wess-Zumino model,

$$S_0 = \int d^4x \left[\partial^\mu \phi^* \partial_\mu \phi + \frac{i}{2} \bar{\Psi} \gamma^\mu \partial_\mu \Psi \right] \tag{F.41}$$

where ϕ is a complex scalar field and Ψ is a Majorana fermion. Writing $\phi = (A + iB)/\sqrt{2}$, this lagrangian is invariant under global SUSY transformation,

$$\begin{aligned} \delta A &= \bar{\epsilon}\Psi, \ \delta B = i\bar{\epsilon}\gamma^5\psi \\ \delta\Psi_r &= -i \left(\gamma^\mu \left[\partial_\mu (A + i\gamma^5 B) \right] \epsilon \right)_r \end{aligned} \tag{F.42}$$

The mass dimension of the parameter ϵ_r is $-1/2$. Under a local spacetime dependent transformation ϵ_r, the action is no longer invariant,

$$\delta S_0 = \int d^4x (\partial_\mu \bar{\epsilon}) \ \gamma^\rho \gamma^\mu \left[\partial_\rho (A + i\gamma^5 B) \right] \Psi \tag{F.43}$$

Just like the electromagnetic vector field arises by starting with the globally invariant Dirac lagrangian and imposing local invariance, we demand here the existence of a new field that carries both vector and spinor indices, $\psi_{\mu r}$, which has mass dimension of 3/2 (and lorentz spin of 3/2 as well) that introduces a new term in the action that counteracts Eqn. (F.43) as follows,

$$S_1 = -\frac{\kappa}{2} \int d^4x \ \bar{\psi}_\mu \gamma^\rho \gamma^\mu \left[\partial_\rho (A + i\gamma^5 B) \right] \Psi \tag{F.44}$$

and we impose that under the SUSY transformation, $\psi_{\mu r}$ changes as follows,

$$\delta\psi_{\mu r} = \frac{2}{\kappa} \partial_\mu \epsilon_r \tag{F.45}$$

This cancels the local SUSY variation in Eqn. (F.44) but now $S_0 + S_1$ is no longer invariant under local SUSY. S_1 itself transforms under $\epsilon_r(x)$ as

$$\delta S_1 = i\kappa \int d^4x \ \bar{\psi}_\mu(x) \gamma_\nu \epsilon(x) \left[\partial^\mu A \partial^\nu A - \frac{1}{2} g^{\mu\nu} \partial^\rho A \partial_\rho A + \cdots \right] \tag{F.46}$$

To make this combined action invariant again, first note that the term inside the square bracket is the energy momentum tensor of the A field. If the space-time metric is $g_{\mu\nu}$, then the energy-momentum tensor $\mathcal{T}_{\mu\nu}$ is given by the variation of the action with respect to the metric,

$$\delta S = \frac{1}{2} \int d^4x \ \delta g_{\mu\nu} \mathcal{T}^{\mu\nu} \tag{F.47}$$

Thus, we introduce the local metric field $g_{\mu\nu}$ which under SUSY transforms as

$$\delta g_{\mu\nu}(x) = -i\kappa \left(\bar{\psi}_\mu \gamma_\nu \epsilon(x) + \bar{\psi}_\nu \gamma_\mu \epsilon(x) \right) \tag{F.48}$$

Therefore, under local SUSY transformation, the spin-2 graviton field $g_{\mu\nu}$ transforms into the spin-3/2 field $\psi_{\mu r}$, which is called the gravitino. κ which has mass dimension of 1 and its nothing but the fundamental reduced Planck scale, $M_p/\sqrt{8\pi}$. We can continue this procedure and it can be shown that this infinite series of the graviton and gravitino can be summed up to the Ricci scalar plus a kinetic term for the gravitino,

$$S = \int d^4x \ \sqrt{-g} \left[-\frac{1}{2\kappa^2}\mathcal{R} - \frac{i}{2}\epsilon^{\mu\nu\rho\sigma}\bar{\psi}_\mu\gamma^5\gamma_\nu\partial_\rho\psi_\sigma \right] \tag{F.49}$$

and this action of Einstein gravity plus its superpartner is fually invariant under local SUSY. The second term for the gravitino is called the Schwinger-Rarita term. This can be generalized to include matter and the gravitino-matter interactions in the MSSM can thus be constructed. Being the superpartner of the graviton, the gravitino is a singlet under all SM gauge groups.

APPENDIX G

EFFECTIVE FIELD THEORY

It appears a basic fact of nature that phenomenon occurring at widely different energy scales don't impact each other much. There is a separation of scales where for example, we don't quite need to know what goes inside a nucleus to describe a ball (made up of atoms) in projectile motion. The knowledge of QCD would be quite irrelevant for physics described efficiently and accurately by Newton's laws. In other words, the corrections would be quite small. If that were not the case, we would need a full theory valid all the way up to the Planck scale to make any meaningful predictions. This simple fact is captured in quantum field theory by the idea of an Effective Field Theory (EFT). An EFT is a quantum field theory with the same or less number of degrees of freedom than the original theory and its non-renormalizable, valid only up to a certain heavy scale M which is greater than all other scales in the original problem. It is typically used in low-energy calculations when the effect of the heavy degree of freedom, not being important decouples leading to new effective interactions between the remaining low energy degrees of freedom.

To quantitatively understand how an EFT calculation works, consider [195] a renormalizable theory with a heavy scalar h with mass M and a light scalar l with mass m (the treatment here is adapted from the EFT review by C. Burgess) with a lagrangian $\mathcal{L}(h, l)$. We are only interested in processes involving the low energy modes of l, which have energies far less than the scale M. Recall that the effective action $\Gamma[\varphi]$ is the generator of the 1PI connected diagrams. It is calculated as the Legendre transform of the generator of connected diagrams, $W[\mathcal{J}]$ in the presence of a source $\mathcal{J}$ that couples linearly to the field, ϕ,

$$\exp\{iW[\mathcal{J}]\} = \int \mathcal{D}\phi \, \exp\left\{i \int d^4x \, [\mathcal{L}[\phi] + \mathcal{J}\phi]\right\} \tag{G.1}$$

The mean field φ is defined as the quantum expectation value of the field ϕ in the presence of $\mathcal{J}$,

$$\varphi = \frac{\delta W}{\delta \mathcal{J}} = \langle \phi(x) \rangle_{\mathcal{J}} \tag{G.2}$$

Then,

$$\Gamma[\varphi] = W[\mathcal{J}(\varphi)] - \int d^4x \, \varphi\mathcal{J} \implies \frac{\delta\Gamma[\varphi]}{\delta\varphi} + \mathcal{J} = 0. \tag{G.3}$$

In the absence of a source, $\mathcal{J} = 0$, the effective action, $\Gamma[\varphi]$ is minimized by the true quantum vacuum φ of the theory. However, solving for $\Gamma[\varphi]$ requires (G.2) be inverted to solve for $\mathcal{J}$ in terms of φ, which is possible in principle but maybe practically impossible. It turns out not to be needed. Writing the field $\phi = \hat{\phi} + \varphi$, we note that

$$\begin{aligned}
\exp\{i\Gamma[\varphi]\} &= \int \mathcal{D}\hat{\phi} \, \exp\left\{i \int d^4x \, \left[\mathcal{L}(\varphi + \hat{\phi}) + \mathcal{J}\hat{\phi}\right]\right\} \\
&= \int \mathcal{D}\hat{\phi} \, \exp\left\{i \int d^4x \, \left[\mathcal{L}(\varphi + \hat{\phi}) - \frac{\delta\Gamma[\varphi]}{\delta\varphi}\hat{\phi}\right]\right\}
\end{aligned} \tag{G.4}$$

This is an implicit equation for $\Gamma[\varphi]$ and it can be immediately solved perturbatively in terms of $\hbar$ or equivalently the loop expansion,

$$\Gamma[\varphi] = S[\varphi] + \frac{i}{2} \log \det \left[\frac{\delta^2 S}{\delta\phi(x)\delta\phi(y)} \right]_{\phi=\varphi} + \cdots \tag{G.5}$$

where $S[\varphi] = \int d^4x \, \mathcal{L}(\varphi)$ is simply the classical action. Thus, to the lowest order, the effective action is the same as the classical action evaluated at the mean field value φ.

In the case of a theory with two degrees of freedom, lighter l and heavier h, the EFT would consist of an effective action $\gamma[l]$ made up only of low-energy modes of l. $\gamma[l]$ would have tree level and loop pieces and we restrict our attention here only to the tree level low energy effective action. We begin with the full effective action $\Gamma[l, h]$ with two sources j and J which excite all the modes of the lighter and the heavier particles respectively. It can be explicitly derived using Eqn. (G.5). Now, if we don't want to excite the heavier modes h and the high energy modes of l, then we simply set $J = 0$ and $j(E \sim M) = 0$. Using Eqns. (G.3) and (G.5) thus, the tree-level low-energy effective action $\gamma^t[l]$ is given by solving the classical equations of motion for h and any high energy modes of l and putting them back into the action. This process is called *integrating out* the high energy modes. We thus get an action that only contains the low energy degree of freedom, l and the mass scale M, which would inevitably appear in the denominator. Such an action $\gamma[l]$ then defines an EFT with its validity only up to scale M or the lowest high energy modes integrated out.